VERSLAGEN EN VERHANDELINGEN

REPORTS AND TRANSACTIONS

NATIONAAL LUCHT- EN RUIMTEVAART-LABORATORIUM

NATIONAL AERO- AND ASTRONAUTICAL RESEARCH INSTITUTE

AMSTERDAM

XXIII — 1961

By joint decree of 13th April 1961 of the Ministers of Transport, Roads and Waterways, of Defence, of Economic Affairs, of Education, Arts and Sciences, and of Finance, the name of the "Stichting Nationaal Luchtvaartlaboratorium" (*shortened* N.L.L.) (= "*Foundation National Aeronautical Research* Institute"), was changed into "Stichting Nationaal Lucht- en Ruimtevaartlaboratorium" (abbreviated by N.L.R.) (= "Foundation National Aero- and Astronautical Research Institute").

PREFACE.

This volume of "Verslagen en Verhandelingen" (= "Reports and Transactions") of the "Nationaal Lucht- en Ruimtevaartlaboratorium" (N. L. R.) (= "National Aero- and Astronautical Research Institute") contains a selection of reports by the N. L. R., completed in recent years. As such, it is a logical continuation of the series up to Volume XXI of "Verslagen en Verhandelingen", which was published in the end of 1959, containing treatises on boundary layer theory, lifting surface theory and non-stationary aerodynamics. The preceding Volume XXII, published in the course of 1959, contained one comprehensive report, entitled "Boundary values in lifting surface theory", by E. van Spiegel, which served the author as a thesis for the degree of doctor of the technical sciences at the Technological University, Delft.

The printed reports of the N. L. R., which are collected at more or less regular intervals in the volumes of "Verslagen en Verhandelingen", form only a part of the publications issued by the N. L. R. A series of multigraphed reports and of publications in scientific and technical journals on research subjects studied by N. L. R. is continuously growing. Both the multigraphed reports and the preprints of the reports meant for bound volumes of "Verslagen en Verhandelingen" are distributed as soon as they become available.

A list of all printed and multigraphed papers, covering the period from 1956 up to the end of 1960 is included in this volume of "Verslagen en Verhandelingen". The complete list of publications issued between the years 1921 and 1956 is available upon request.

Amsterdam, July 1961.

A. J. Marx

Director of the

"Nationaal Lucht- en Ruimtevaartlaboratorium".

CONTENTS.

Report	Author(s)	Title	Completed	Pages
TR G. 1	van der Walle, F.	Theoretical determination of the power efficiency and overall flow behaviour of free jet wind tunnels with special emphasis on transsonic wind tunnels.	1957	1
TR S. 518	Zandbergen, P. J.	Determination of the stresses in a not shallow spherical shell with a hole, due to an axial force, a bending moment and a transverse force.	1958	13
TR S. 521	van der Neut, A.	Bending at the oblique end section of cylindrical shells.	1958	35
TR S. 539	Benthem, P. J.	The reduction in stiffness of combinations of rectangular plates in compression after exceeding the buckling load.	1959	51

List of printed or multigraphed reports published by the Nationaal Lucht- en Ruimtevaartlaboratorium between June 1956, 1st and December 1960, 31th.

(These reports are in English, unless indicated otherwise).

Report Nr.	Author(s)	Title
Aerodynamics Section.		
TM A. 1466	Slijkhuis, A. J.	Investigation of a valve system in the contraction nozzle to reduce velocity fluctuations in the small wind tunnel of the NLL. 1956. (In Dutch).
TM A. 1468	van Genderen, W.	The relationship between the intensity and the scale of turbulence and the critical Reynolds' number of spheres, especially at high Reynolds' numbers. 1958. (In Dutch).
TM A. 1475	Asbeek Brusse, B. J. G.	Literature study of the aerodynamic properties at low speeds. Delta wings. 1958. (In Dutch).
Section of Flutter and Aero-elasticity.		
TR F. 184	Zaat, J. A.	A simplified method for the calculation of three-dimensional laminar boundary layers. 1956.
TR F. 191	IJff, J.	The influence of wing bending and torsion flexibility on the gust response of aeroplanes. 1956.
TR F. 202	Zaat, J. A.	Checking of the simple method of calculation of three-dimensional laminar boundary layers with the aid of exact solutions. 1957. (In German).
TR F. 206 TR F. 206a	Eckhaus, W. de Jager, E. M.	Linearized theory of lifting sweptback wings at sonic speed. 1957.
TR F. 208	IJff, J.	The influence of non-stationary derivatives on the snaking motion at high subsonic speed. 1957.
TN F. 168	Bosschaart, A. C. A. van de Vooren, A. I.	Investigation of the effect of an improved strip theory for swept wings on the flutter speed. 1956.
TN F. 189	van Spiegel, E.	Theory of the circular wing in steady incompressible flow. 1957.
TN F. 192	van de Vooren, A. I. de Jager, E. M.	Calculation of aerodynamic forces on slowly oscillating rectangular wings in subsonic flow. 1956.
TN F. 193	Timman, R. Zaat, J. A. Burgerhout, Th. J.	Stability diagram for laminar boundary layer flow. 1956.
TN F. 197	van de Vooren, A. I. Schatz, O.	Comparative calculations of divergence speed for wings of not too large aspect ratio. 1957.
TN F. 200	Eckhaus, W.	A method for the asymptotic expansion of the integral equation of a lifting surface at near-sonic speeds. 1957.
TN F. 204	IJff, J.	An investigation on the influence of amplitude, sidewash effects and frequency on the aerodynamic derivatives of a model oscillating continuously in yaw. 1957.

TN F. 215	Zaat, J. A.	The behaviour of the three dimensional laminar boundary layer flow at increasing angles of incidence. 1958. (In German).
TM F. 164a	de Jager, E. M.	Lateral stability derivatives for a swept wing in supersonic flow. 1956. (In Dutch with English summary).
TM F. 178	de Kock, A. C. Hagedorn, A. C. F.	The NLL card catalogue of aerodynamic measurements. Manual. 1956.
TM F. 180	Burgerhout, Th. J.	The ZEBRA. Part II. Motivation of the choice. 1956. (In Dutch with English summary).
TM F. 181	Timman, R.	The aerodynamic forces on oscillating helicopter rotor blades. 1956.
TM F. 182	Bosschaart, A. C. A.	A criterion for aileron-springtab flutter. 1956.
TM F. 185	Zaat, J. A.	A revised integral equation method for the calculation of two-dimensional transsonic flows about symmetrical non-lifting aerofoil sections. 1956. (In Dutch with English summary).
TM F. 190	van Spiegel, E.	Method of calculation for heat regenerators of blowdown wind tunnels. 1956.
TM F. 194	Zaat, J. A.	Application of streamline coordinates for the calculation of the boundary layer on yawed cylinders. 1956. (In German with abstract in English).
TM F. 195	IJff, J.	Measurements of some low speed oscillatory stability derivatives of the AGARD wing model D. 1956.
TM F. 203	Hagedorn, A. C. F. de Kock, A. C.	Description of the NLL Hollerith card system catalogue of aerodynamic measurements. 1957.
TM F. 205	Bergh, H.	Experimental determination of the aerodynamic forces on an oscillating wing with an aerodynamically balanced flap in incompressible two-dimensional flow. 1957.
TM F. 211	IJff, J.	Gust loads on elastic swept wings. 1958. (In Dutch with English summary).
TM F. 213	Bosschaart, A. C. A.	Investigation of some semi-empirical methods for the instationary aerodynamic coefficients. 1958. (In Dutch with English summary).
TM F. 216	Bosschaart, A. C. A. IJff, J.	The influence of wing bending and torsional flexibility on the gust response of aeroplanes. 1959.
TM F. 217	Bergh, H.	Unsteady pressure measurements on a wing with an oscillating flap in two-dimensional, incompressible flow. 1958.
TM F. 220	de Jager, E. M.	Calculation of the pressure distribution on swept wings according to the so-called slender wing theory in the case of antisymmetric stationary flow. 1959. (In Dutch with English summary).

Gasdynamics Section.

TR G. 1	van der Walle, F.	Theoretical determination of the power-efficiency and overall flow behaviour of semi free-jet wind tunnels with special emphasis on transsonic wind tunnels 1958.
TR G. 3	van der Walle, F.	Determination of the influence of a fuselage on the characteristics of a general wing system and comparison between the properties of a ring wing and a plane wing. 1958.
TN G. 2	van der Walle, F.	Determination of the aerodynamic characteristics at supersonic speeds of ring wings combined with axially-symmetric fuselages. 1958.
TN G. 5	van der Walle, F.	Determination of the bending moment, tangential force and shear force in a cylindrical ring wing.
TM G. 17	Zandbergen, P. J.	Methods for the calculation of interference effects between fuselages and wings in the subsonic and transsonic speed range. 1959. (In Dutch).

Helicopter Section.

TM H. 1	Lucassen, L. R.	Calculation of the required power of helicopters in horizontal flight. 1955. (In Dutch with English summary).

Materials Section.

TR M. 1999	Schijve, J. Jacobs, F. A.	Research on cumulative damage in fatigue of riveted aluminum alloy joints. 1956.
TR M. 2070	Schijve, J. Jacobs, F. A.	Program-fatigue tests on notched light alloy specimens of 2024 and 7075 material. 1960.
TN M. 2009	Hartman, A.	Tensile strength and time to fracture tests on Redux-bonded 75 S-T clad single lap joints at temperatures from room temperatures to 80°C. 1956. (In Dutch with English summary).
TN M. 2010	Schijve, J.	Fatigue crack propagation in light alloys. 1956.
TN M. 2011	Hartman, A. Klaassen, W.	The fatigue strength at fluctuating tension of single lap joints of clad 24 S-T and 75 E-T aluminum alloy with 2 rows of 17 S rivets. 1956.
TN M. 2016	Hartman, A. Jacobs, F. A.	The fatigue strength at fluctuating tension ($R = 0.1$) of Redux-bonded 75 S-T clad simple lap joints from -45°C to $+80$°C. 1956.
TN M. 2024	Schijve, J. Jacobs, F. A.	The fatigue strength of aluminum alloy lugs. 1957.
TN M. 2033a	Hartman, A.	The influence of the thickness of the specimen on the mechanical properties in compression and in 3-point bending of glass fabric base plastic laminates at room temperature. 1957.
TN M. 2041	Hartman, A. Jacobs, F. A.	Research on the static and fatigue strengths of bonded and riveted single lap joints in clad 2024 and 7075 aluminum alloy at room and elevated temperatures. 1957.
TN M. 2045	Hartman, A.	The effect of the relative humidity of the air during fabrication on the mechanical properties of glass fabric reinforced plastics. 1958.
TN M. 2047	Hartman, A. de Rijk, P.	The effect on the static- and fatigue properties of riveted light alloy lap joints of reinforcing the critical section with thin adhesive bonded sheets. 1958.
TM M. 2000	Schijve, J.	Some remarks on the ultrasonic testing of glued metal joints in connection with a visit to the firm Dr. Lehfeldt and Co., GMBH at Heppenheim. 1956. (In Dutch with English summary).
TM M. 2008	Hartman, A.	Considerations on safety of aircraft against fatigue failures. 1956. (In Dutch with English summary).
TM M. 2019	van Leeuwen, H. P.	A survey of literature on the comparison of the mechanical properties at elevated temperatures and the technological properties of fourheat-resistant alloys. 1956. (In Dutch).
TM M. 2026	Hartman, A.	Literature search on the mechanical properties of glass base plastic laminates. 1957. (In Dutch with English summary).
TM M. 2039	de Vries, G.	Apparatus for the mechanical investigation of plastics. 1957. ((In Dutch).
TM M. 2044	Schijve, J.	Effect of curing on the internal damping of Redux metal adhesive. 1957. (In Dutch).
TM M. 2046	Schijve, J.	X-ray inspection of aircraft structures. 1958. (In Dutch with English summary).
TM M. 2051	Hartman, A.	Weathering tests of various wrought aluminum alloys on the roof of the NLL. 1958. (In Dutch with English summary).

TM M. 2057	Hartman, A.	Exploratory investigation on the effect of temperature on the mechanical properties of glass reinforced Araldite laminating resin No. 556. 1959. (In Dutch with English summary).
TM M. 2059	Schijve, J.	Fractographical investigation on a fatigue failure in an extrusion of a helicopter blade. 1959. (In Dutch).
TM M. 2064	Hartman, A. Jacobs, F. A.	Effect of friction on the fatigue strength of single row riveted double cover plate joints in clad 2024-T aluminum alloy. 1959.
TM M. 2065	Hartman, A. de Rijk, P. van der Vooren, J.	The effect of the thickness of the glue layer on the fatigue strength of light alloy specimens with adhesive bonded reinforcing plates on both sides. 1959.
TM M. 2068	Hartman, A.	Preliminary investigation of the influence of glue-line thickness and porosity on the peeling strength and shear strength of bonded light alloy specimens. 1960. (In Dutch with English summary).
TM M. 2071	Schijve, J.	Some remarks on random noise and fatigue. 1960. (In Dutch).
TM M. 2076	Hartman, A.	The effect of cell size and foil thickness of aluminum honeycomb on the peel strength and tensile strength of adhesive loaded light alloy sandwich specimens. 1960. (In Dutch with English summary).

Structures Section.

TR S. 476	Koiter, W. T.	Buckling and postbuckling behaviour of a cylindrical panel under axial compression. 1956.
TR S. 5158	Zandbergen, P. J.	Determination of the stresses in a not shallow spherical shell with a hole, due to an axial force, a bending moment and a transverse force. 1958.
TR S. 521	van der Neut, A.	Bending at the oblique end section of cylindrical shells. 1958.
TR S. 527	Benthem, J. P.	The buckling of flat panels that change in thickness across the bay. 1958.
TR S. 529	Hakkeling, B.	Airplane loads in pitching manoeuvres. 1958.
TR S. 539	Benthem, J. P.	The reduction in stiffness of combinations of rectangular plates in compression after exceeding the buckling load. 1959.
TR S. 542	Benthem, J. P.	A stress diffusion problem for a wedge-shaped plate with three stiffeners. 1959.
TN S. 478	Benthem, J. P.	The effect of airplane structural flexibility on landing gear loads. 1956.
TN S. 520	Benthem, J. P. van der Vooren, J.	Analysis of panels with bonded, hat-shaped stiffeners, loaded in shear. 1958.
TN S. 531	Benthem, J. P.	Note on the compressive and bending strength of fiberglass reinforced plastic plates. 1958.
TN S. 536	van Grol, H. J. Hakkeling, B. Schuerman, J. A.	Results of stress and deflection measurements performed on a swept-back box beam and their comparison with theoretical results. 1959.
TN S. 537	Benthem, J. P. van der Vooren, J.	On the stress problem of anisotropic wedges. 1959.
TN S. 541	Benthem, J. P. van der Vooren, J.	On the diffusion of a load from an edge stiffener into a wedge-shaped plate. 1959.
TN S. 558	Benthem, J. P. van der Vooren, J.	The reduction in stiffness after exceeding the buckling load of simply supported flat panels that change in thickness discontinuously. 1960.
TM S. 439	Floor, W. K. G.	Compressive tests on open-section columns. 1954. (In Dutch with English summary).

TM S. 463	Botman, M.	Ultimate compressive strength of panels. 1956. (In Dutch with English summary).
TM S. 467	Botman, M.	Electrical networks as models of shell structures. 1955. (In Dutch with English summary).
TM S. 483	Plantema, F. J. Klaassen, W.	Some preliminary fatigue tests of sandwich panels. 1956.
TM S. 484	Benthem, J. P.	Investigation of the root effect with swept beams. 1956. (In Dutch with English summary).
TM S. 504	Benthem, J. P.	Discussion of some information from literature on the number of gust loads on tailplanes. 1957. (In Dutch with English summary).
TM S. 519	Schijve, J.	Calculation of the bending moment diagram of a riveted single lap joint with and without reinforcing strips. 1958. (In Dutch with English summary).
TM S. 522	Benthem, J. P.	Experiments on the post-buckling behaviour of simply supported panels that change in thickness across the bay. 1958.
TM S. 530	van Leeuwen, H. P.	The effect of the shear stiffness of the flapping hinge on the bending moments in a helicopter rotorblade. 1958.
TM S. 532	Schijve, J.	Analysis of the fatigue strength data for asymmetrical bonded specimens. 1958. (In Dutch).
TM S. 534	Auer, Th. Hakkeling, B.	Strain measurements on polystyrene with electric resistance type strain gauges. 1958.
TM S. 547	Hakkeling, B.	Preliminary strain gage measurements on a simple plastic box beam. 1959. (In Dutch).

Transsonic Section.

TM T. 14	Cazemier, P. G.	Literature study of the base pressure and the effect of sting support on the base pressure in the case of transsonic and supersonic velocities. 1958. (In Dutch).

Flight Mechanics Section.

TN V. 1816	Overbeeke, J. L.	Measurements of the control force-time relations for sudden movements of the controls. 1958. (Translated from the Dutch by B. Hakkeling).
TM V. 1780	Kalkman, C. M.	The effect of transsonic and low supersonic velocities on the static longitudinal stability and control properties of aeroplanes with swept wings and delta wings. 1956. (In Dutch).
TM V. 1788	Marx, A. J.	Some results of comparison of model and full scale spinning tests. 1956.
TM V. 1795	Lucassen, L. R.	Assessment of the modified vertical rudder of the KNVvL-491 glider on 24th May 1956. 1956. (In Dutch with English summary).
TM V. 1797	van Oosterom, T.	Balloon contest for the Andries Blitz Coupe 1956 at Nijmegen (the Netherlands). Calculation and check of the gas filling and handicap ballast. 1956. (In Dutch).
TM V. 1865	Lucassen, L. R.	Circular turns in wind of constant velocity. 1960. (In Dutch).

Section Mathematical Problems and Numerical Computations.

TR W. 1	van Spiegel, E.	Boundary value problems in lifting surface theory. 1959.

Miscellation Publications.

MP. 131	Plantema, P. J.	Structural investigations for the development of the Fokker F-27 "Friendship", carried out at NLL. 1956. (In Dutch with English summary).

MP. 132	van de Vooren, A. I.	Unsteady airfoil theory. 1956.
MP. 133	Eckhaus, W.	Asymptotic solution of the two-dimensional oscillating aerofoil problem for high subsonic Mach numbers. 1956.
MP. 134	van Spiegel, E. Timman, R.	Linearized aerodynamic theory for wings of circular planform in steady and unsteady incompressible flow. 1956.
MP. 136	Benthem, J. P.	The enclosure of the flexibilities, the cross-flexibility included, of infinite hollow box beams with oblique ribs. 1956.
MP. 137	Buhrman, J.	Flight test instrumentation and data processing. 1956. (In Dutch).
MP. 139	Besseling, J. F.	Application of matrix calculus in adjusting stiffness and vibration properties of redundant strucures. 1956.
MP. 140	IJff, J.	The influence of wing bending and torsion flexibility on the gust response of aeroplanes. 1956.
MP. 141	van Asselt, B. J.	The NLL-transsonic tunnel. 1956.
MP. 143	Kalkman, C. M.	An investigation into the accuracy of an approximative method of calculation of the effect of aero-elastic wing distortion on the longitudinal static stability of aeroplanes with slender swept wings. 1956. (In Duch with English summary).
MP. 146	van de Vooren, A. I.	Flutter calculations for modern aeroplanes with many degrees of freedom. 1957. (In German).
MP. 147	Bergh, H.	Experimental determination of the aerodynamic coefficients of an oscillating flapped wing. 1957. (In German).
MP. 148	van Spiegel, E.	On singular solutions of the lifting surface problem. 1957. (In German).
MP. 149	Besseling, J. F.	Stress and vibration analyses of the NLL transsonic wind tunnel with the aid of electronic computers. 1957. (In Dutch with English summary).
MP. 150	Schijve, J.	Non-destructive testing of glued metal joints by the ultrasonic resonance method. 1957.
MP. 151	Bergh, H. van den Berg, B.	On the visualization of laminar boundary layer oscillations and the transition to turbulent flow. 1957.
MP. 152	Feis, N.	Investigations of smoke nuisance and soot deposit from stacks by the NLL. 1957. (In Dutch).
MP. 153	Schijve, J.	Discussion on the proposals for evaluating fatigue properties of airplane structures, published by B. Lundberg and S. Eggwertz. 1957.
MP. 154	Beerling, G. A.	List of periodicals. 1958. (In Dutch).
MP. 155	van der Walle, F.	The supersonic wind tunnel under construction at the NLL. 1957. (In Dutch).
MP. 157	Schijve, J.	Ultrasonic testing for fatigue cracks in compressor and turbine blades. 1958.
MP. 158	Zaat, J. A.	Numerical contributions to the stability theory of boundary layers. 1958. (In German).
MP. 159	van Oosterom, T.	Wind tunnel investigations and flight tests. 1958. (In Dutch).
MP. 160	Schijve, J.	Stress analysis and materials testing in aircraft design. 1958. (In Dutch).
MP. 161	van de Vooren, A. I.	General dynamic stability of systems with many degrees of freedom. 1958.
MP. 162	Hakkeling, B.	Airplane loads in pitching manoeuvres. 1958.

MP. 163	IJff, J.	The influence of non-stationary stability derivatives on the lateral motion at high supersonic speed. 1958.
MP. 164	Burgerhout, Th. J.	Some considerations concerning the electronic computer "ZEBRA" of the NLL. 1958. (In Dutch with English summary).
MP. 165	Bosman, D.	Semi-automatic 200-point scanner for static strain gauge measurements. 1958.
MP. 166	van Oosterom, T.	NLL flight test instrumentation for the Fokker F-27 "Friendship". 1958. (In Dutch with English summary).
MP. 167	van Oosterom, T.	Measurements during flight. 1959. (In Dutch with English summary).
MP. 168	Erdmann, S. F.	Aerodynamic aspects in the design of guided missiles and rockets. 1959. (In Dutch with English summary).
MP. 169	Fokkinga, G. Y.	Tests with flying models. 1959. (In Dutch with English summary).
MP. 170	van Oosterom, T.	Measurements on the relation between magnitude and duration and on the rate of application of the control forces achieved by pilots in simulated manoeuvres. 1959.
MP. 173	Fokkinga, G. Y.	Methods of telemetry. 1959. (In Dutch).
MP. 174	Bergh, H.	The flutter investigation for the helicopter "Kolibrie". 1959. (In Dutch with English summary).
MP. 175	Marx, A. J.	The National Aeronautical Research Institute, a short survey of its history, aims and facilities. 1959. (In Dutch with English summary).
MP. 176	van der Neut, A.	Structural design and analysis of the pressure shell of the NLL transsonic wind tunnel HST. 1959. (In Dutch with English summary).
MP. 177	van Leest, P.	Some constructions within the pressure liner of the wind tunnel HST of the NLL. 1959. (In Dutch with English summary).
MP. 178	Schijve, J.	The endurance under program-fatigue testing. 1959.
MP. 179	Boel, J. van der Zwaan, J. H.	The wind tunnel HST of the NLL as an aerodynamic tool. 1959. (In Dutch with English summary).
MP. 180	Benthem, J. P.	On the stress distribution in anisotropic wedges. 1959.
MP. 181	de Jager, E. H. van Spiegel, E.	Calculated tunnelwall corrections for two-dimensional high-lift wings. 1959.
MP. 182	Beerling, G. A.	Annual report 1958 of the library of the NLL in Amsterdam. 1959. (In Dutch).
MP. 183	Boel, J. Erdmann, S. F.	The NLL transsonic and supersonic wind tunnel facilities, with reference to their use for research and development testing. 1959.
MP. 184	Zwaaneveld, J.	The pilot tunnel of the NLL. 1959. (In Dutch).
MP. 185	Zwaaneveld, J.	Principal data of the NLL pilot tunnel. 1959.
MP. 186	van der Neut, A.	The construction of the transsonic wind tunnel HST of the NLL 1959. (In Dutch).
MP. 187	van Leeuwen, H. P.	Structural materials for supersonic aircraft and missiles. 1960. (In Dutch).
MP. 188	Boel, J. Erdmann, S. F.	The transsonic and supersonic experimental installations of the NLL in the light of their applicability for research and development. 1959. (In German).
MP. 189	Benthem, J. P.	On the affine transformation for orthotropic plane-stress and plane-strain problems. 1960.

MP. 190	Zaat, J.	Contributions to the theory of three-dimensional boundary layers. 1960. (In German).
MP. 191	Benthem, J. P.	Stress diffusion in wedge-shaped plates. 1960.
MP. 192	de Jager, E. M.	Oscillating rectangular wings in supersonic flow with arbitrary bending and torsion mode shapes. 1960.
MP. 193	Zandbergen, P. J. van der Walle, F.	The optimum shape of axi-symmetric configurations in supersonic flow, with a given base area, as derived by using the exact flow equations. 1960.
MP. 195	Schijve, J.	Fatigue crack propagation in light alloy sheet material and structures. 1960.
MP. 196	Benthem, J. P.	Some aspects of the stress analysis of swept wings. 1960.
MP. 197	Valk, H. van der Zwaan, J. H.	A review of measurements on AGARD calibration model B in the transsonic speed range. 1960.
MP. 198	Bergh, H.	Flutter in gliding structures. 1960.

C.C.L. Class. D 903 : D 901 : D 902 : D 911

REPORT NLL-TR G. 1.

Theoretical determination of the power efficiency and overall flow behaviour of free jet wind tunnels with special emphasis on transonic wind tunnels

by

F. VAN DER WALLE

Summary.

The power efficiency and the overall flow characteristics are theoretically derived for a free jet transonic wind tunnel. The derived formulae appear to be applicable to all types of wind tunnels (sub-, trans- and supersonic; with and without free jets).

It is found for the case of a transonic free jet wind tunnel that the results are in good accordance with experiments.

The theory given in this report is an extension and modification of the theory given by R. HERMANN in ref. 4 and 5. In contrast to the theory of HERMANN a loss factor λ is introduced which describes the combined influence of mixing losses in the free jet boundaries, tunnel wall friction drag, drag of model support and the re-entry losses of the air flowing through the permeable test section walls.

Because of the introduction of the factor λ it is possible to treat the cross section of the diffuser entry as an independent variable. As a consequence a blocking phenomenon with respect to this cross section is found that is analogous to the blocking phenomenon due to a too small diffuser throat in the case of closed wall wind tunnels.

In section 3.2 of this report a comparison is given of the measured and calculated power efficiencies for the transonic free jet wind tunnel of the N.L.L. together with an estimate of the permissible model drag coefficients.

Contents.

List of symbols.

1 Introduction.

2 Derivation of the equations.

- 2.1 Determination of M_2, $\dfrac{p_{2t}}{p_{1t}}$ and $\dfrac{\partial \dfrac{p_{2t}}{p_{1t}}}{\partial\delta}$ as a function of M_1, h, λ and δ.
- 2.2 Determination of the stability of the solutions.
- 2.3 Compatibility of the solutions with the second law of thermodynamics.

3 Discussion of the results.

- 3.1 Results for arbitrary values of M_1 and h.
- 3.2 Application to the N.L.L. transonic wind tunnel.

4 Conclusions.

5 Acknowledgments.

6 References.

Appendices:

A Derivation of the formulae for M_2, $\dfrac{p_{2t}}{p_{1t}}$ and $\dfrac{\partial \dfrac{p_{2t}}{p_{1t}}}{\partial\delta}$.

B Determination of the upper bound for $\dfrac{p_{2t}}{p_{1t}}$.

C Estimate of λ for the N.L.L. transonic wind tunnel.

12 figures.

List of symbols.

c_d	drag coefficient.
c_f	friction coefficient.
D	drag of model and model support.
D_m	drag of model alone.
D_s	drag of model support.
F	friction drag of the tunnel walls.
F_0	friction drag of the tunnel walls for $m_c = 0$.
h	$= \dfrac{S_2}{S_1}$
m_a	$= m_c + m_k$.
m_c	mass of air flowing through permeable test section walls.
m_k	$= \dfrac{D + F_0 + \int_{\text{jet}} \tau dS}{U_1}$.
p	= pressure.
R	gasconstant.
Re	Reynolds number.
S	area.
U	axial velocity.
δ	$= \dfrac{p_c - p_1}{p_1}$.
γ	ratio of specific heats.
ε	free-jet expansion angle.

λ $\quad \frac{m_a}{\rho_1 S_1 U_1}$ = "loss factor".
λ_T loss factor for tunnel with model support but without model.
λ_m loss factor for model alone.
ρ density.
μ $\quad \frac{\text{model frontal area}}{\text{test section area}}$ = model blockage coefficient.
ν kinematic viscosity.
τ shear stress along free-jet boundary.

Indices:

1	applies to	cross section just in front of test section.
2	,, ,,	cross section of constant-area diffuser intake-section.
c	,, ,,	plenum chamber around free-jet.
jet	,, ,,	free-jet boundary.
m	,, ,,	model.
mw	,, ,,	model wing.
s	,, ,,	model support.
t	,, ,,	stagnation condition.
td	,, ,,	diffuser throat.
tn	,, ,,	nozzle throat.
w	,, ,,	test section wall.

this way particular properties of free jet tunnels can be explained at least qualitatively. For instance HERMANN cites in ref. 4 page 34 that it was only possible to achieve pressure equilibrium in the Peenemünde tunnel, if the diffuser intake area was enlarged above the value mostly employed in free jet wind tunnels. This enlargement was necessary when large models at low Mach numbers were tested. This can be explained by the present analysis. The analysis shows also that the effect of the re-entry in the diffuser of the mass of air flowing through the permeable test-section walls is analogous to the effects of model drag, wall friction drag and shear stresses along the free jet boundaries. The influence of all these effects is described by one parameter λ, called the loss factor. As a consequence the application of the analysis is not limited to transonic wind tunnels but can also be extended to supersonic and subsonic wind tunnels with and without free jets.

The influence of the parameter λ is largest, however, for test section Mach numbers close to unity.

A schematic drawing of a free jet transonic wind tunnel, on which the analysis is based, is given in figure 1.

The characteristic properties of this type of tunnel are mainly determined by the flow-pheno-

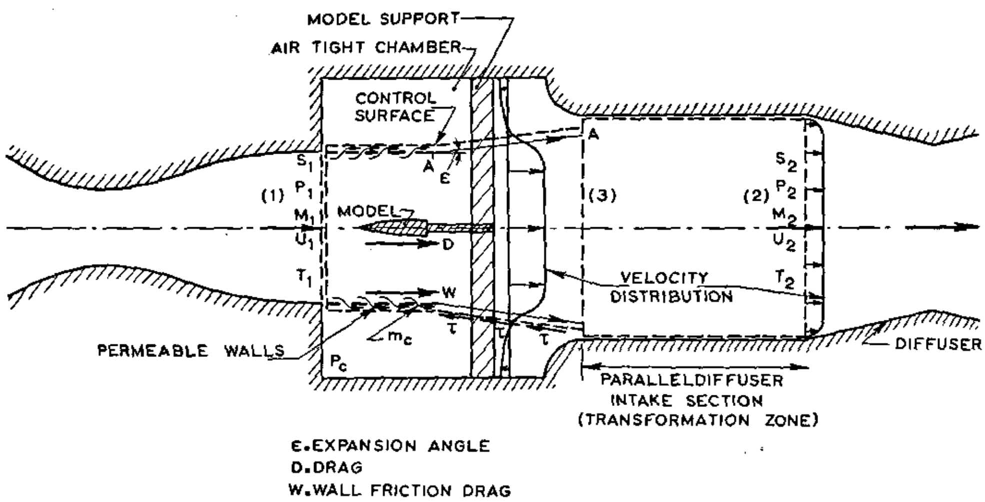

Fig. 1. Sketch of transonic semi free jet windtunnel.

1 Introduction.

The theory given by HERMANN in ref. 4 and 5 explains some fundamental properties of free jet supersonic wind tunnels. In a discussion on the applicability of the results of HERMANN to the N.L.L. transonic free jet wind tunnel, it became apparent, however, that in order to describe the special characteristics of this tunnel type some modifications and extensions would be necessary. A closer examination revealed that the fixed relationship between free jet length and diffuser intake cross section had to be revised and in addition that the effect of the re-entry in the diffuser of the mass of air flowing through the permeable test section walls had to be taken into account.

The subsequent analysis will show that in mena occurring between the cross sections 1 and 2 (see fig. 1).

The air flowing through the test section will be partly deflected outward and will flow through the permeable tunnel walls because of model blockage. This small mass flow of air will be denoted by m_c; from this air practically all kinetic energy will be transformed into heat. Experience with transonic test sections indicates that this mass of air will not flow back again through the test section walls behind the model but has to be induced in the flow again at the diffuser entry.

Along the free jet boundaries mixing takes place between the main flow and the air in the plenum chamber. Because of this mixing and its associated impuls losses in the main flow the free jet will expand. The expansion angle ε is dependent upon the pressure difference $p_c - p_1$ and the shape of the model support that will be located mostly in the free jet. In addition the angle ε varies slightly with Mach number (see ref. 2).

The first part of the diffuser consists of a parallel section. In this part the transition occurs from the non-homogeneous velocity distribution at the entrance to a homogeneous one at the end.

On the model, model support and the tunnel walls are acting respectively the drag D and the friction force F. Along the free jet boundaries work shearing stresses, denoted by τ.

In the next chapter the equations will be derived that govern the behaviour of the air within the dotted lined control surface in figure 1.

The total pressure ratio $\frac{p_{2t}}{p_{1t}}$, the Mach number M_2 in the diffuser intake and the stability of the solutions will be determined as a function of the test section Mach number M_1, the tunnel configuration, and the loss factor λ. Just as is done normally in the derivation of the normal shock wave equations, only the state of the homogeneous flow in cross section 2 will be determined. Apart from the introduction of the loss factor λ, the detailed flow phenomena between the cross sections 1 and 2 will not be considered.

In chapter 3 the results are discussed and applied to the case of the N.L.L. transonic wind tunnel.

2 Derivation of the equations.

2.1 *Determination of* M_2, $\frac{p_{2t}}{p_{1t}}$ *and* $\frac{\partial \frac{p_{2t}}{p_{1t}}}{\partial \delta}$.

The following conservation laws are valid:

a. Conservation of mass.

$$\rho_1 S_1 U_1 = \rho_2 S_2 U_2 \tag{1}$$

where ρ is density, S is the cross sectional area and U is the axial velocity. The indices 1 and 2 are related to the cross sections 1 and 2 in figure 1.

$$\delta = \frac{p_c - p_1}{p_1} = \frac{\text{pressure differential between pressure chamber and test-section}}{\text{test section pressure}}. \tag{7}$$

b. Conservation of impuls.

$$-D - F_0 - m_c U_1 - \int_{\text{jet}} \tau \, . \, dS + p_1 S_1 +$$
$$p_c(S_2 - S_1) + S_1 \rho_1 U_1^2 = p_2 S_2 + S_2 \rho_2 U_2^2 \tag{2}$$

where p is the static pressure.

The assumption is made that the wall friction force F is composed of the following parts:

1. The friction F_0 in case $m_c = 0$.
2. The additive friction force $m_c U_1$ in case a mass flow m_c is deflected through the permeable walls.

This assumption seems realistic as practically all kinetic energy of the mass flow m_c will be transformed in heat during passing through the permeable walls.

c. Conservation of energy.

$$\frac{\gamma}{\gamma - 1} \frac{p_1}{\rho_1} + \tfrac{1}{2} u_1^2 = \frac{\gamma}{\gamma - 1} \frac{p_2}{\rho_2} + \tfrac{1}{2} u_2^2. \tag{3}$$

The following assumptions have been made:

1. All changes of state are adiabatic.
2. All transverse velocities are neglected.

The righthand sides of the equations (1), (2) and (3) are identical to those of the normal shock equations. Because of this it can be expected that the equations (1), (2) and (3) will yield two solutions for the state of the flow in cross section 2; one with a subsonic and one with a supersonic Mach number. The two solutions are related to each other in the same way as the two solutions of the normal shock equations.

In appendix A it will be shown that from the equations (1), (2) and (3) the following expressions can be derived for the Mach number M_2 and the ratio $\frac{p_{2t}}{p_{1t}}$. (p_{1t} and p_{2t} are the stagnation pressures in the cross sections 1 and 2 respectively)

$$\frac{M_2 \left(1 + \frac{\gamma - 1}{2} M_2^2\right)^{1/2}}{1 + \gamma M_2^2} = \frac{M_1 \left(1 + \frac{\gamma - 1}{2} M_1^2\right)^{1/2}}{h + \delta(h - 1) + \gamma(1 - \lambda) M_1^2} \tag{4}$$

and

$$\frac{p_{2t}}{p_{1t}} = \frac{M_1}{h M_2} \left(\frac{1 + \frac{\gamma - 1}{2} M_2^2}{1 + \frac{\gamma - 1}{2} M_1^2} \right)^{\frac{\gamma + 1}{2(\gamma - 1)}}. \tag{5}$$

The symbols used are defined as follows:

$$h = \frac{S_2}{S_1} = \frac{\text{diffuser intake area}}{\text{test section exit area}}. \tag{6}$$

$$\lambda = \frac{m_a}{S_1 \rho_1 U_1}, \text{ with } m_a = m_c + \frac{D + F_0 + \int_{\text{jet}} \tau dS}{U_1} \tag{8}$$

λ will be called the "loss factor".

With equation (4) the two values of M_2 can be determined for given values of h, M_1, δ, γ and λ, where-after with equation (5) the two values of $\frac{p_{2t}}{p_{1t}}$ can be calculated.

2.2 *Determination of the stability of the solutions.*

It will be shown that the quantity $\frac{\partial \frac{p_{2t}}{p_{1t}}}{\partial \delta}$ directly determines the static stability of the solutions.

If in a certain tunnel set-up h and M_1 are fixed, the only parameter than can vary under the influence of disturbances is the parameter $\delta = \frac{p_c - p_1}{p_1}$. The influence of the disturbances on the parameter λ is assumed to be zero.

Suppose now that an equilibrium condition is disturbed in such a way that the plenum chamber pressure p_c is enlarged above its equilibrium value.

The equilibrium condition can only be restored in case more air escapes through the diffuser than enters through the test section. The ratio $\frac{\text{mass flow through diffuser}}{\text{mass flow through nozzle}}$ is equal to $\frac{p_{2t} \cdot S_{td}}{p_{1t} \cdot S_{tn}}$, where S_{td} = diffuser throat area and S_{tn} = nozzle throat area. Therefore, for a given tunnel geometry, a necessary condition for this to happen, is that the parameter $\frac{p_{2t}}{p_{1t}}$ must become larger because of the increase of p_c (and of δ).

The criterion for static stability is then:

$$\frac{\partial \frac{p_{2t}}{p_{2t}}}{\partial \delta} > 0. \tag{9}$$

In Appendix A the following expression will be derived:

$$\frac{\partial \frac{p_{2t}}{p_{1t}}}{\partial \delta} = \frac{p_{2t}}{p_{1t}} (h-1) \frac{M_2}{M_1} \left(\frac{1 + \frac{\gamma - 1}{2} M_2^2}{1 + \frac{\gamma - 1}{2} M_1^2} \right)^{1/2}. \tag{10}$$

From equation (10) it follows that the stability criterion is satisfied for every value of M_1 and M_2 if $h > 1$.

As this is normally the case in free-jet wind tunnels both solutions of the equations (4) and (5) will be stable in normal cases.

2.3 *Comptability of the solutions with the second law of thermodynamics.*

It may be possible that not all solutions of the equations (4) and (5) can be realized physically. The condition imposed by the second law of thermodynamics on the solutions is, that a decrease in entropy is forbidden. For the entropy S per unit mass the following expression is valid:

$$S = -R ln p_t + C \tag{11}$$

where R = gasconstant,

p_t = stagnation pressure,

C = integration constant.

From equation (11) and the second law of thermodynamics it follows that always the ratio $\frac{p_{1t}}{p_{1t}}$ should be smaller than 1.

It can be shown, however, that a more severe restriction is placed on the ratio $\frac{p_{2t}}{p_{1t}}$. A consideration of figure 1 reveals namely that several losses are introduced in the air flow before the transformation to a homogeneous velocity distribution takes place in the diffuser intake section.

All of these losses are accompanied by entropy increases and are related to the following phenomena:

a. The re-entry of the mass flow m_c in the diffuser intake.

b. The drag D of model and model support.

c. The friction force F on the tunnel walls.

d. The shearing stresses τ along the free-jet boundaries.

The entropy increase between the sections (1) and (3) is dependent upon the detailed flow distribution. When some crude assumptions are made, however, the following approximative criterion can be derived for the parameter $\frac{p_{2t}}{p_{1t}}$ (see appendix B):

$$\frac{p_{2t}}{p_{1t}} \leq \left(1 + \frac{\gamma - 1}{2} M_1^2\right)^{\frac{-\lambda\gamma}{\gamma - 1}}. \tag{12}$$

On the basis of the assumptions made in appendix B the upper bound $\left(\frac{p_{2t}}{p_{1t}}\right)_{\text{limit}}$ is completely determined by the Mach number M_1, the "loss factor" λ and γ.

3 Discussion of the results.

3.1 *Results for arbitrary values of M_1 and h.*

From equations (4) and (5) it can be seen that h and λ are the only parameters that take into account the free jet character of the wind tunnel, whereas also other factors contribute to the value of λ. The loss-factor λ is built up in the following way (see equation 8):

a. The influence of the re-entry of the mass flow m_c (characteristic of transonic wind tunnels).

b. The wall-friction force F_0 } (characteristic of any tunnel type).

c. The drag of model and model support } (characteristic of any tunnel type).

d. The shear stresses τ along the free jet boundaries (characteristic of free jet wind tunnels).

This means that the present analysis is valid for all types of wind tunnels; only in the calculation of λ and h the specific character of the tunnel has to be taken into account.

The parameter δ will be taken equal to zero in the remainder of this chapter, as pressure equilibrium will be prescribed for flexible wall transonic wind tunnels and is mostly desired for supersonic wind tunnels. The influence of δ has been described in detail by HERMANN in ref. 5.

In figure 2 the solutions for M_2 are given for $h = 1.25$ as a function of λ and M_1.

As remarked already, for most combinations of λ and M_1 two real solutions are found for M_2, a supersonic and a subsonic one. This stems from the fact that in equation (4) the quantity $\frac{M_2 \left(1 + \frac{\gamma - 1}{2} M_2^2\right)^{1/2}}{1 + \gamma M_2^2}$ has a maximum for $M_2 = 1$ (see figure 3).

There is an upper bound for λ above which no real solutions for M_2 are found (see figure 2). This maximum value λ_{max} is a function of the test section Mach number. The Mach number M_2 equals 1 for $\lambda = \lambda_{max}$. λ_{max} indicates the maximum allowable value for the drag, friction forces, etc., above which no real solutions for the tunnel flow will be found. The curves for M_2 shift to smaller values of λ when M_1 increases from $M_1 = 0$ and also when M_1 diminishes from $M_1 = \infty$. There is a Mach number $(M_1)_{crit}$ for which the curve lies most to the left.

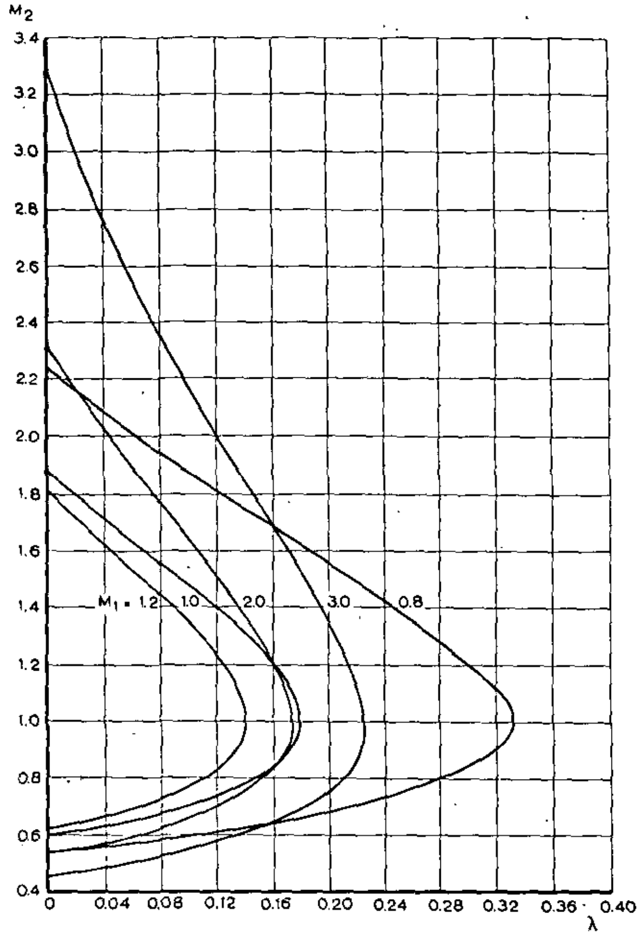

Fig. 2. The Mach number M_2 as a function of λ and M_1 for $h = 1.25$ and $\delta = 0$.

This Mach number is somewhat larger than 1 and it represents the most critical operating condition of the wind tunnel as for this Mach number the maximum allowable value for λ, λ_{max}, is the smallest. $(M_1)_{crit}$ is dependent upon the parameter $h = \dfrac{\text{diffuser intake area}}{\text{test section area}}$.

For $h = 1$ this critical Mach number also equals one and the associated value for λ is zero. This can be seen easily from equation (4) by introducing $M_2 = 1$ and $h = 1$. With increasing values of h, $(M_1)_{crit}$ and λ_{max} also increase (see figure 4).

Figure 2 shows that the influence of λ is largest at Mach numbers somewhat greater than 1. This is aggravated by the fact that λ will tend to become relatively large at these Mach numbers (high drag coefficients for model and model support in transonic flow).

In figure 4 λ_{max} is given as a function of Mach number for $\delta = 0$ (pressure equilibrium) and for some values of h.

From figure 4 the conclusion can be drawn that for a given value of λ a lower bound, h_{min}, for h exists. The parameter h (or the diffuser intake height) can only be decreased until λ_{max} equals the given value of λ. If the diffuser intake height is decreased to values below h_{min} no real solutions for M_2 for $\delta = 0$ will be obtained. This phenomenon is analogous to the blocking of the flow in closed-

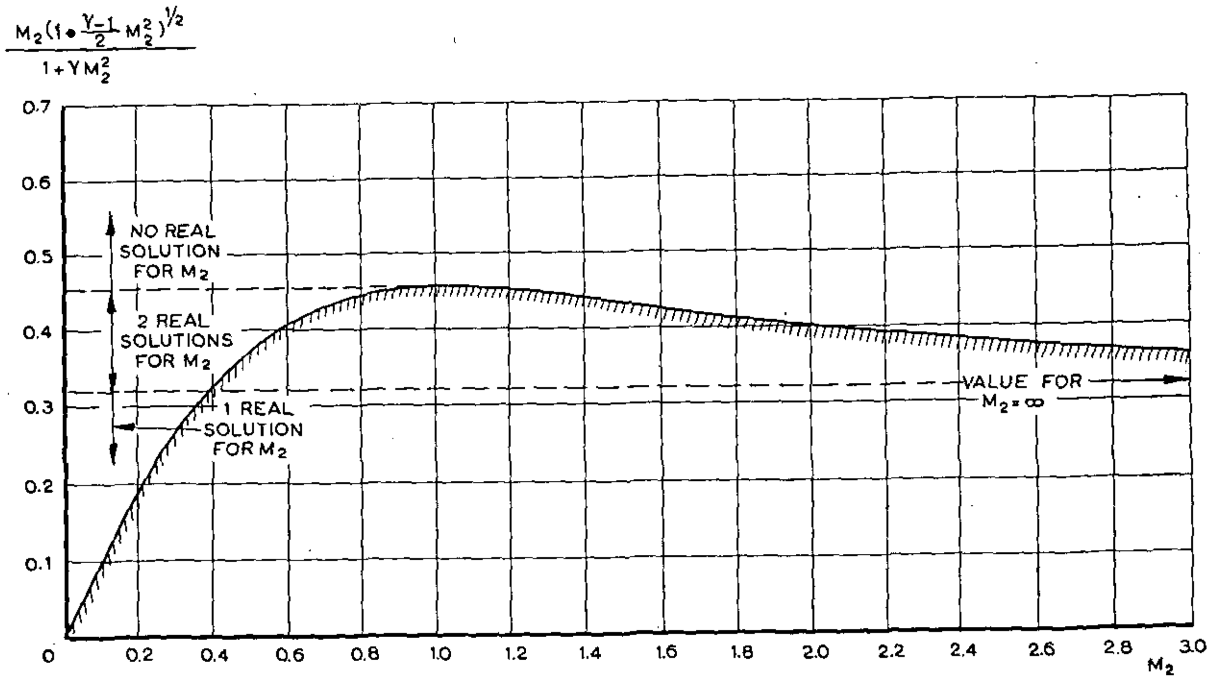

Fig. 3. The quantity $\dfrac{M_2\left(1+\dfrac{\gamma-1}{2}M_2^2\right)^{1/2}}{1+\gamma M_2^2}$ as a function of M_2.

wall wind tunnels when the diffuser throat area is decreased below a certain minimum value. In the case of free-jet wind tunnels, however, this blocking by the diffuser intake area does not lead to a complete flow bread-down but to an increase of the chamber pressure p_c. This can be seen in figure 5 where h_{min} is plotted against $\delta = \frac{p_c - p_1}{p_1}$ for $\lambda = .10$ and $M_1 = 1.2$.

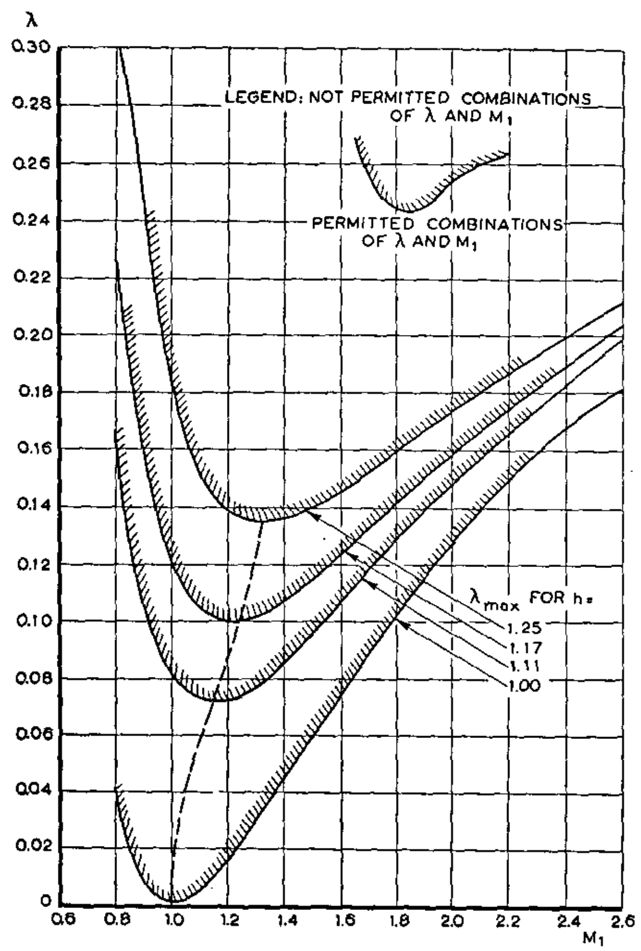

Fig. 4. The limiting value λ_{max} for λ as a function of M_1 and h, for $\delta = 0$.

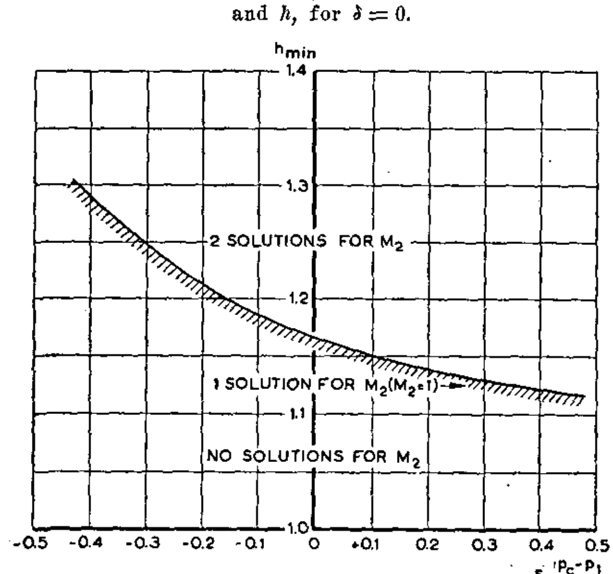

Fig. 5. The parameter h_{min} as a function of δ for $\lambda = .10$ and $M_1 = 1.2$.

The parameter h_{min} is decreasing steadily when δ is increased. This means, when h is decreased with constant values for λ and M_1, that the parameter δ will have to increase as soon as h becomes smaller than h_{min}.

This behaviour explains completely the phenomena mentioned by HERMANN in reference 4. According to HERMANN it was impossible in the Peenemünde wind tunnel to obtain pressure equilibrium with the original diffuser intake dimensions when large models at Mach numbers around 1.5 were tested. As the analysis predicts, pressure equilibrium could only be obtained in this wind tunnel when the diffuser intake height was enlarged. It is especially noteworthy that this phenomenon only occurred with large models (large λ) and at Mach numbers around 1.5. At these low Mach numbers the influence of λ is relatively large as is shown by figure 2.

The quantity $\frac{p_{2t}}{p_{1t}}$ is plotted in figure 6 against λ for some values of h and M_1.

Only those values of $\frac{p_{2t}}{p_{1t}}$ are plotted that are lower than the limiting value $\left(\frac{p_{2t}}{p_{1t}}\right)_{\text{limit}}$ (see section 2.3).

For each Mach number and diffuser intake height the curve of $\frac{p_{2t}}{p_{1t}}$ against λ consists of two branches; the upper branch is related to the supersonic solution ($M_2 > 1$); the lower branch to the subsonic one ($M_2 < 1$). The two branches have the point for $\lambda = \lambda_{max}$ in common. The following observations can be made:

a. Part of the supersonic solutions are permitted by the second law of thermodynamics. Experiments have to show, however, whether these supersonic solutions really occur. As shown in section 2.2 both solutions are stable. The supersonic solutions lead to a higher efficiency (greater $\frac{p_{2t}}{p_{1t}}$) of the transformation process than the subsonic ones.

This does not mean, however, that the overall flow efficiency is better for these supersonic solutions. The deceleration in the diffuser from the supersonic flow at Mach number M_2 to a subsonic flow will often have an efficiency that is somewhat lower than the efficiency of a normal shock at the supersonic Mach number M_2 so that normally the subsonic solution has the highest overall efficiency. This will probably cause the subsonic solutions to prevail in experiments.

b. The influence of λ is large for Mach numbers somewhat above 1 as λ_{max} is very small there (see also fig. 4).

c. The influence of h diminishes rapidly with increasing Mach number but is very high for small Mach numbers.

The influence of the diffuser geometry can be seen from figure 7. In this figure the

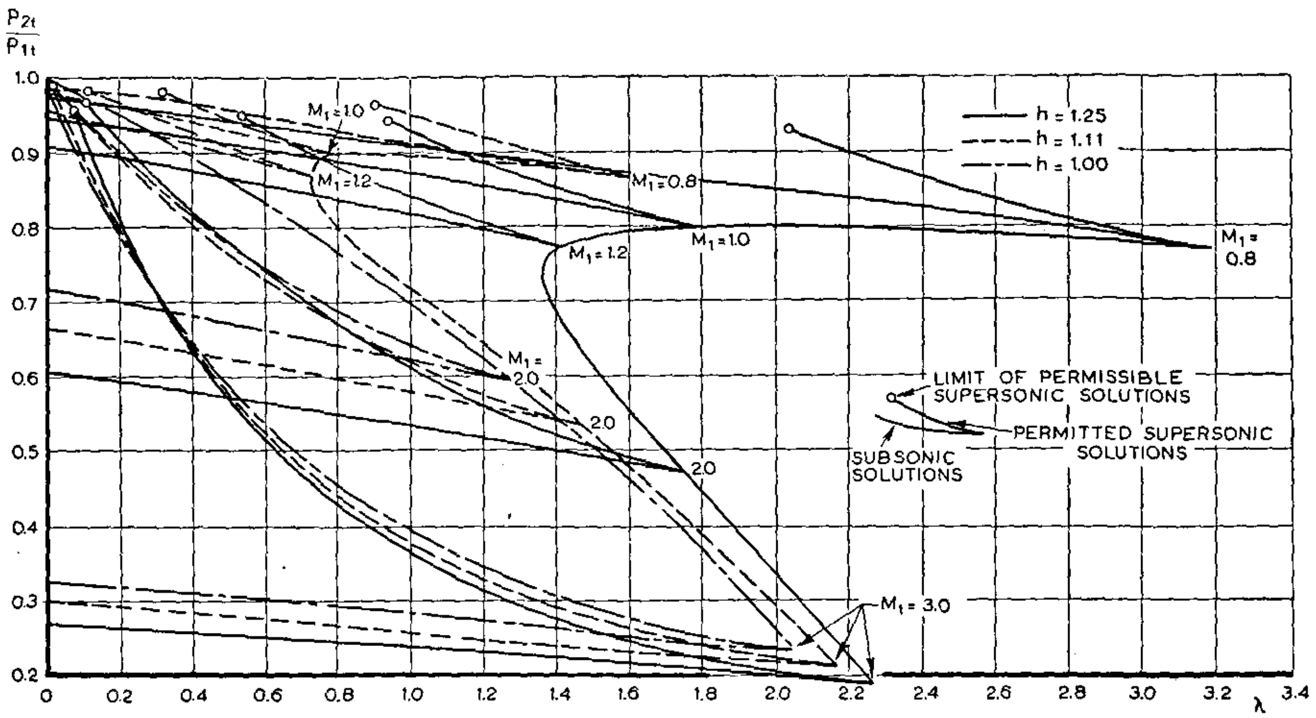

Fig. 6. The quantity $\frac{p_{2t}}{p_{1t}}$ as a function of λ with M_1 and h as parameters for $\delta = 0$.

pressure ratio $\frac{p_{2t}}{p_{1t}}$ is plotted against δ and h for $M_1 = 1.0$ and $\lambda = .04$.

The important diffuser dimensions are:

a. The diffuser intake area $S_2 \left(h = \frac{S_2}{S_1} \right)$

b. The diffuser throat area S_{td}.

The pressure ratio $\frac{p_{2t}}{p_{1t}}$ is determined by this throat area according to the equation:

$$\frac{p_{2t}}{p_{1t}} = \frac{\text{nozzle throat area}}{\text{diffuser throat area}} = \frac{S_{tn}}{S_{td}} \quad (13)$$

This relation stems from the fact that the massflows through nozzle and diffuser are equal and proportional to respectively $p_{1t} \cdot S_{tn}$ and $p_{2t} \cdot S_{td}$; the proportionality factors being the same in both cases, due to the constancy of the stagnation temperature.

From figure 7 it follows that at a fixed value of λ a decrease in $\frac{p_{2t}}{p_{1t}}$ (larger throat area) results in a decrease of δ (decrease in chamber pressure) and vice versa. An increase in h (increasing intake area) leads at a constant value of $\frac{p_{2t}}{p_{1t}}$ to a larger value of δ (increasing chamber pressure).

Thus the influence of the diffuser geometry can be summarized as follows:

a. A *decrease* in throat area leads to an *increase* in the chamber pressure.

b. A *decrease* in intake area leads to a *decrease* in chamber pressure.

A requisite is, however, that λ is essentially independent of δ. This theoretically predicted

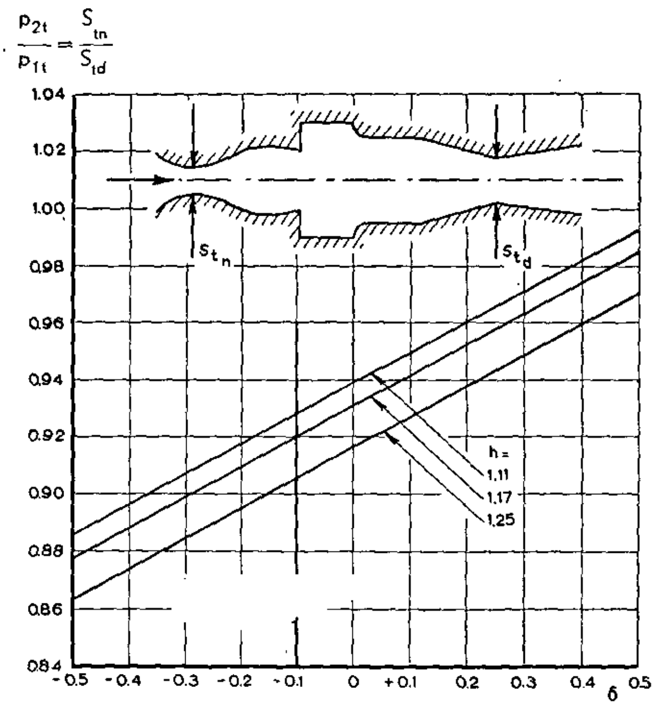

Fig. 7. The pressure ratio $\frac{p_{2t}}{p_{1t}}$ as a function of δ and h for $M_1 = 1.0$ and $\lambda = .04$.

behaviour of the chamber pressure p_c has been confirmed by some preliminary experiments at a Mach number of 1.5 in the 1″ × 1.5″ supersonic wind tunnel of the N.L.L. (National Aeronautical Research Institute).

3.2 *Application to the case of the N.L.L. transonic wind tunnel.*

The N.L.L. transonic wind tunnel, further denoted by H.S.T., is a continuous closed-circuit wind tunnel for Mach numbers up to 1.3. The test-section size is 2×1.6 m² (6.7×5.3 sq ft.). The value of h for the H.S.T. is 1.17.

As is seen from figure 4 the most critical operating Mach number with respect to λ_{max} for this value of h is 1.24.

In figures 8 and 9 plots are given of M_2 and $\frac{p_{2t}}{p_{1t}}$ respectively as a function of λ for some Mach numbers.

In the figures the limits imposed by the second law of thermodynamics upon M_2 and $\frac{p_{2t}}{p_{1t}}$ are indicated. In Appendix C an estimate is made of the value of λ for the H.S.T., as a function of the Mach number M_1.

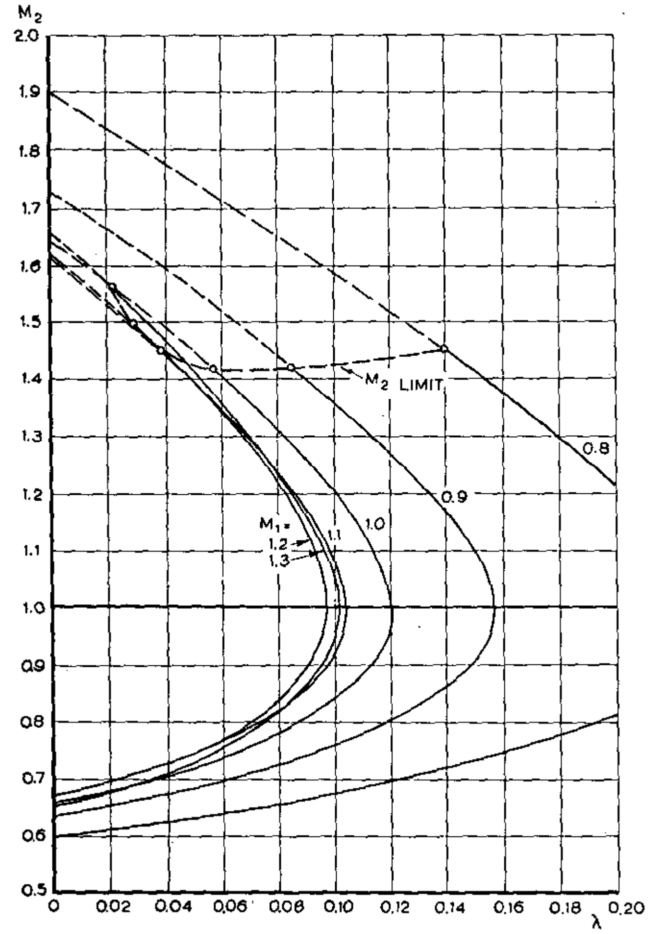

Fig. 8. The Mach number M_2 as a function of λ and M_1 for $h = 1.17$ and $\delta = 0$.

The following values of λ are considered:

a. The value for the wind tunnel without model but with model support, denoted by λ_T.

b. The additional value for the model alone, denoted by λ_m.

The value of λ_T is indicated by the dotted line in figure 9.

Without model there is ample margin between λ_T and λ_{max}, the most critical Mach number being about 1.24.

The largest permissible value for λ_m is limited for two reasons:

a. The value of λ_{max} is an upper limit for $\lambda_m + \lambda_T$.

b. The pressure ratio required to drive the wind tunnel is limited.

In figure 10 the pressure ratio $\frac{p_{1t}}{p_{2t}}$ is plotted against the Mach number . The following curves and data are given:

a. The calculated pressure ratio for $\lambda = \lambda_T$ (no model).

b. The pressure ratio as measured in the H.S.T. (no model).

c. The available pressure ratio across the driving fan corrected for the losses in the return-circuit.

d. The necessary pressure ratio as calculated for $\lambda = \lambda_{max}$.

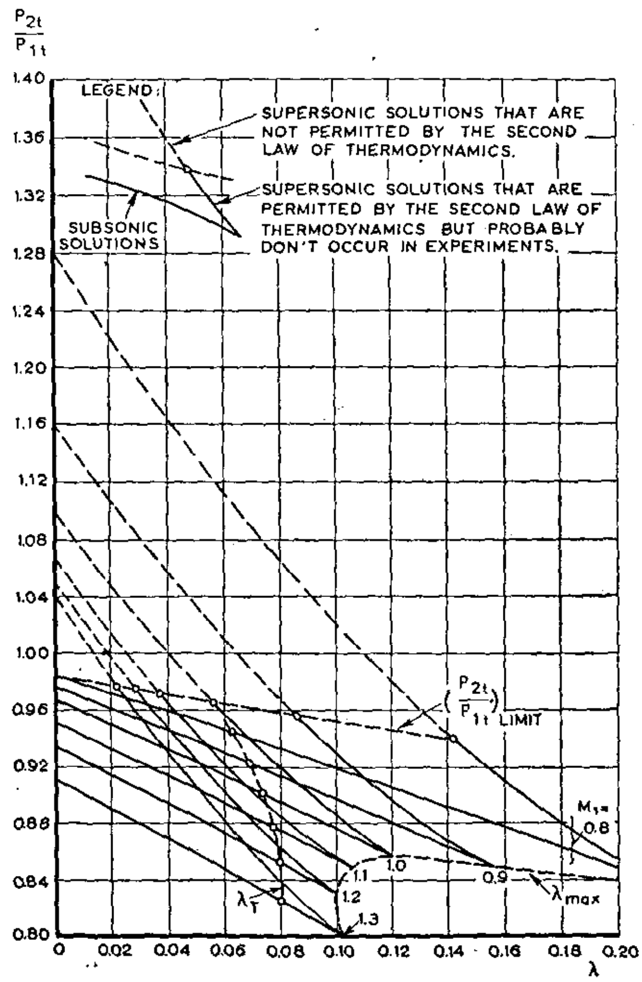

Fig. 9. The quantity $\frac{p_{2t}}{p_{1t}}$ as a function of λ and M_1 for $h = 1.17$ and $\delta = 0$.

The calculated pressure ratios agree with the measured ones within the measuring accuracy.

The curve for the required pressure ratio for $\lambda = \lambda_{max}$ and the curve for the available pressure ratio cross each other at a Mach number of 1.1 (see figure 10). This means that for Mach numbers below 1.1 the permissible model drag is limited by the available pressure ratio and for Mach numbers above 1.1 λ_{max} is the limiting factor.

In figure 11 the resulting maximum permissible value of λ_m is plotted against Mach number.

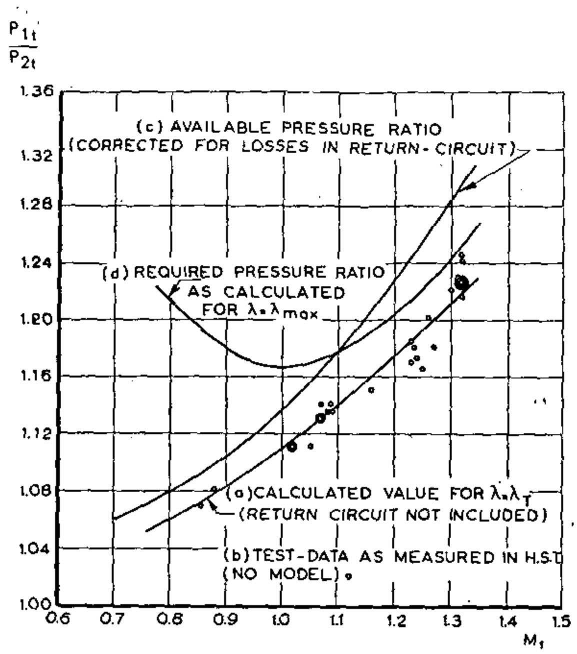

Fig. 10. Comparison of calculated, measured and available pressure ratio for the N.L.L. transonic windtunnel.

λ_m can be written as (see Appendix C):

$$\lambda_m = \frac{c_{D_{m_1}}}{2} + \mu = c_{D_{m_w}} \cdot \frac{S_W}{2\,S_1} + \mu$$

where $c_{D_{m_1}}$ = drag coefficient based on test section area

$c_{D_{m_w}}$ = drag coefficient based on wing area

μ = model blockage coefficient

S_W = model wing area.

Typical values for μ and $\frac{S_1}{S_W}$ are .005 and 20 respectively. For these values of μ and $\frac{S_1}{S_W}$ the maximum permissible value of $c_{D_{m_w}}$ is also plotted in figure 11.

The permissible value of $c_{D_{m_w}}$ seems to be well above the drag coefficients that can be expected.

This means that the available pressure ratio is larger than is necessary, which can lead to the following possibilities:

a. The Mach number can be increased above 1.3. The theory predicts a possible increase to $M = 1.5$ without a model.

b. At the high Mach numbers the stagnation pressure can be raised. A requisite is, however, that the fan can absorb the maximum horse-power at the lower pressure ratio.

It must be kept in mind, however, that the numerical results of the theory can not yet be checked sufficiently.

4 Conclusions.

With the theory derived in this report the overall flow characteristics of free jet wind tunnels can be analysed. The power efficiency of these wind tunnels can be calculated with a good degree of accuracy. In addition to the variation of the chamber pressure with the diffuser throat-area, that has been found first by R. Hermann in ref. 5, a variation of this chamber pressure with respect to the diffuser intake area has been predicted. This predicted behaviour has been confirmed by some preliminary experiments.

A blocking phenomenon with respect to the diffuser intake area has been found that is of special importance for transonic free jet wind tunnels.

5 Acknowledgements.

The author wishes to express his sincere thanks to Dr. S. F. Erdmann for his many helpful suggestions and to Messrs. B. van Asselt and W. Eckhaus for the informations they have given.

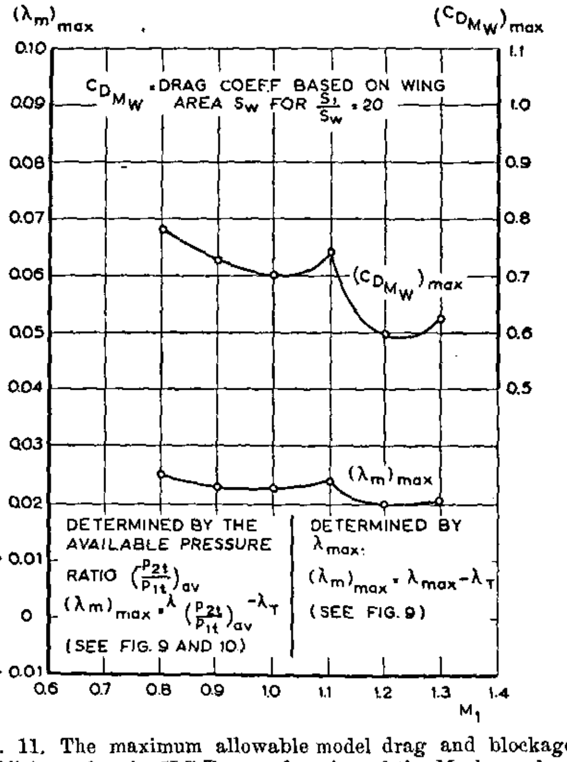

Fig. 11. The maximum allowable model drag and blockage coefficients for the H.S.T. as a function of the Mach number.

6 References.

1. Tollmien, W. Calculation of turbulent expansion processes. N.A.C.A. T. M. 1085, September 1945.
2. Gooderum, P. B. Investigation with an interferometer of the turbulent mixing of a free supersonic jet. N.A.C.A. T. R. 963, 1950.
3. Spreiter, J. R. On the application of transonic similarity rules to wings of finite span. N.A.C.A. T. R. 1153, 1953.
4. Hermann, R. Diffuser efficiency and flow process of supersonic wind tunnels with free jet test section. United States Air Force A. F. Technical report 6334, December 1950.
5. Hermann, R. Diffuser efficiency of free jet supersonic wind tunnels at variable test chamber pressure. Journal of the Aeronautical Sciences, June 1952, page 375—384.

APPENDIX A.

Derivation of the formulas for

$$M_2,\ \frac{p_{2t}}{p_{1t}}\ \text{and}\ \frac{\partial \dfrac{p_{2t}}{p_{1t}}}{\partial\delta}.$$

The basic equations are (see page 3)

$$\rho_1 S_1 U_1 = \rho_2 S_2 U_2\,. \tag{1}$$

$$-D - F_0 - m_c U_1 - \int_{\text{jet}} \tau\,.\,dS + p_1 S_1 + p_c(S_2 - S_1) + S_1\rho_1 U_1^2 = p_2 S_2 + S_2\rho_2 U_2^2. \tag{2}$$

$$\frac{\gamma}{\gamma-1}\ \frac{p_1}{\rho_1} + \tfrac{1}{2}U_1^2 = \frac{\gamma}{\gamma-1}\ \frac{p_2}{\rho_2} + \tfrac{1}{2}U_2^2. \tag{3}$$

The flow is assumed to be adiabatic.
The following parameters will be substituted.

$$h = \frac{S_2}{S_1}\,. \tag{4}$$

$$\delta = \frac{p_c - p_1}{p_1}. \tag{5}$$

$$m_a = m_c + \frac{D + F_0 + \int_{\text{jet}} \tau\,.\,dS}{U_1}\,. \tag{6}$$

$$\lambda = \frac{m_a}{\rho_1 S_1 U_1}. \tag{7}$$

$$M_1 = \frac{U_1}{\sqrt{\dfrac{\gamma\, p_1}{\rho_1}}} \tag{8}$$

$$M_2 = \frac{U_2}{\sqrt{\dfrac{\gamma\, p_2}{\rho_2}}}. \tag{9}$$

Equations (1); (4); (8) and (9) yield:

$$h\sqrt{\rho_2/\rho_1} = \frac{M_1}{M_2}\sqrt{\frac{p_1}{p_2}}. \tag{10}$$

Equations (2), (4), (5), (6), (7), (8) and (9) can be combined to:

$$\frac{p_1}{p_2}\left[\{h + \delta(h-1)\} + \gamma(1-\lambda)M_1^2\right] = h\,\{1 + \gamma M_2^2\}. \tag{11}$$

The substitution of (8), (9) and (10) in (3) gives:

$$\frac{p_2}{p_1} = \frac{1}{h}\ \frac{M_1}{M_2}\left(\frac{1 + \dfrac{\gamma-1}{2}M_1^2}{1 + \dfrac{\gamma-1}{2}M_2^2}\right)^{1/2}. \tag{12}$$

Elimination of $\dfrac{p_1}{p_2}$ from the equations (11) and (12) gives the following relationship between the Mach numbers M_1 and M_2.

$$\frac{M_2\left(1 + \dfrac{\gamma-1}{2}M_2^2\right)^{1/2}}{1 + \gamma M_2^2} = \frac{M_1\left(1 + \dfrac{\gamma-1}{2}M_1^2\right)^{1/2}}{h + \delta(h-1) + \gamma(1-\lambda)M_1^2}. \tag{13}$$

The ratio between the stagnation pressure p_t and the static pressure p in a stream with a Mach number M is:

$$\frac{p_t}{p} = \left(1 + \frac{\gamma-1}{2}\ M^2\right)^{\gamma/\gamma-1}; \tag{14}$$

From (14) and (12) it follows:

$$\frac{p_{2t}}{p_{1t}} = \frac{1}{h}\ \frac{M_1}{M_2}\left(\frac{1 + \dfrac{\gamma-1}{2}M_2^2}{1 + \dfrac{\gamma-1}{2}M_1^2}\right)^{\frac{\gamma+1}{2(\gamma-1)}}. \tag{15}$$

The quantity $\dfrac{\partial \dfrac{p_{2t}}{p_{1t}}}{\partial\delta}$ can be derived in the following way:

From eq. (15):

$$\frac{\partial\left(\dfrac{p_{2t}}{p_{1t}}\right)}{\partial M_2} = \frac{p_{2t}}{p_{1t}}\left[\frac{(\gamma+1)M_2}{2 + (\gamma-1)M_2^2} - \frac{1}{M_2}\right]. \tag{16}$$

From eq. (13):

$$\frac{\delta\partial}{\partial M_2} = \frac{M_1}{h-1}\left(\frac{1 + \dfrac{\gamma-1}{2}M_1^2}{1 + \dfrac{\gamma-1}{2}M_2^2}\right)^{1/2} \cdot \left[2\gamma - \frac{\dfrac{\gamma-1}{2}(1 + \gamma M_2^2)}{1 + \dfrac{\gamma-1}{2}M_2^2} - \frac{1 + \gamma M_2^2}{M_2^2}\right] \tag{17}$$

From equations (16) and (17) it follows:

$$\frac{\delta\,\dfrac{p_{2t}}{p_{1t}}}{\partial\delta} = \frac{\delta\,\dfrac{p_{2t}}{p_{1t}}}{\partial M_2}\cdot\frac{\partial M_2}{\partial\delta} = \frac{p_{2t}}{p_{1t}}\,(h-1)\,\frac{M_2}{M_1}\left[\frac{1 + \dfrac{\gamma-1}{2}M_2^2}{1 + \dfrac{\gamma-1}{2}M_1^2}\right]^{1/2}. \tag{18}$$

as can be shown with some simple algebra.

APPENDIX B.

Determination of the upper bound for $\frac{p_{2t}}{p_{1t}}$.

As remarked already in section 2.3 the following sources of losses are introduced in the flow between the cross-sections (1) and (2) (see figure 1).

a. The re-entry of the mass flow m_c in the diffuser intake.

b. The drag D of model and model support.

c. The friction force F_0 on the tunnel walls.

d. The shearing stresses τ along the free jet boundaries.

All these phenomena are the results of irreversible processes that are accompanied by entropy increases. The magnitude of the entropy increase is, however, not determined by the magnitude of the forces etc. alone, but also by the detailed velocity distribution in the flow.

In order to get an estimate of the order of magnitude, the entropy increase will be calculated for a schematized case.

Just as is the case with force (a) the forces (b), (c) and (d) are thought to result in a deceleration at constant pressure of a mass flow m_k at velocity U_1 to a negligible velocity. The total effect of the phenomena denoted above under (a) through (d) is thus that a mass flow of air $m_k + m_c$ is decelerated at constant pressure from the undisturbed stream velocity U_1 to a negligible velocity.

A simple impuls analysis shows that

$$m_k = \frac{D + F_0 + \int_{\text{jet}} \tau dS}{U_1}; \text{ i.e. } m_k + m_c = m_a.$$

The entropy S per unit mass can be calculated with

$S = -R \ln p_t + C$ where $p_t =$ stagnation pressure.

The increase in entropy ΔS between the cross-sections (1) and (3) is thus:

$$\Delta S = m_a R \{ \ln p_{1t} - \ln p_1 \}.$$

The second law of thermodynamics requires that

$$\rho_1 S_1 U_1 (-R \ln p_{2t}) \geq \rho_1 S_1 U_1 (-R \ln p_{1t}) + m_a \{ R \ln p_{1t} - R \ln p_1 \}$$

or:

$$-\ln p_{2t} \geq -\ln p_{1t} + \lambda (\ln p_{1t} - \ln p_1)$$

which leads to:

$$\ln \left(\frac{p_{2t}}{p_{1t}} \right) \leq \lambda \ln \left(\frac{p_1}{p_{1t}} \right)$$

or:

$$\underline{\underline{\frac{p_{2t}}{p_{1t}} \leq \left(1 + \frac{\gamma - 1}{2} M_1^2 \right)^{\frac{-\lambda\gamma}{\gamma - 1}}}}.$$

APPENDIX C.

Estimation of λ for the N.L.L. transonic wind tunnel.

The following data apply to the N.L.L. transonic wind tunnel.

Test section height	1.6 m (5.3 ft)
Test section width	2 m (6.7 ft)
Total slot area	5 m² (53.8 sq.ft)
Total length of test section wall	3 m (10 ft)
Free jet length	2.4 m (8 ft)
Diffuser intake width	2 m (6.7 ft)
Diffuser intake height	1.87 m (6.2 ft)
Shape of model support segment	see figure 12
Maximum Mach number	1.3
Maximum stagnation pressure at $M = 1$	1.1 ata
Maximum expected model blockage	1 %

The parameter λ is defined by

$$\lambda = \frac{D}{S_1 \rho_1 U_1^2} + \frac{m_c}{S_1 \rho_1 U_1} + \frac{\int_{\text{jet}} \tau . dS}{S_1 \rho_1 U_1^2} + \frac{F_0}{S_1 \rho_1 U_1^2}.$$

Two values for λ will be considered; one for the wind tunnel without model but with model support, denoted by λ_T, and an additional one for the model alone denoted by λ_m.

From the definition of λ it follows that:

$$\lambda_T = \frac{D_s}{S_1 \rho_1 U_1^2} + \frac{\int_{\text{jet}} \tau . dS.}{S_1 \rho_1 U_1^2} + \frac{F_0}{S_1 \rho_1 U_1^2}$$

and

$$\lambda_m = \frac{D_m}{S_1 \rho_1 U_1^2} + \frac{m_c}{S_1 \rho_1 U_1}$$

where $D_m =$ model drag and $D_s =$ model support drag.

C. 1 *Estimation of λ_T.*

$$\lambda_T = \frac{D_S}{S_1 \rho_1 U_1^2} + \frac{\int_{\text{jet}} \tau . dS}{S_1 \rho_1 U_1^2} + \frac{F_0}{S_1 \rho_1 U_1^2} = \\ = \frac{c_{D_S} . S_s}{2 S_1} + \frac{\overline{c_{f_{\text{jet}}}} . S_{\text{jet}}}{2 S_1} + \frac{\overline{c_{f_w}} . S_w}{2 S_1}$$

where

$$c_{D_s} = \frac{D_s}{\frac{1}{2}\rho_1 U_1^2 \,.\, S_s};$$

$$\overline{c}_{f\,\text{jet}} = \frac{\overline{\tau}}{\frac{1}{2}\rho_1 U_1^2}$$

$\overline{\tau}$ is mean value of shearing stress τ.

$$\overline{c}_{f_w} = \frac{F_0}{\frac{1}{2}\rho_1 U_1^2 \,.\, S_w}.$$

The total drag of the model support, consisting of segment and sting support, is assumed to be twice the drag of the front wedge of the model support segment (see figure 12).

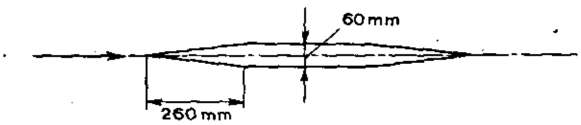

Fig. 12. Dimensions of model support segment.

The following drag coefficients for a wedge were taken from ref. 3.

M_1	$c_{D\,\text{wedge}}$	$\frac{c_{D_s} \,.\, S_s}{2\,S_1} = \frac{c_{D\,\text{wedge}} \,.\, S_{\text{wedge}}}{S_1}$
0.8	.0340	.00442
0.9	.0773	.0100
1.0	.1138	.0154
1.1	.1403	.0182
1.2	.1615	.0210
1.3	.1694	.0220

S_{wedge} is the area on which $c_{D\,\text{wedge}}$ is based; $S_{\text{wedge}} = .26 \times 1.6 = .416$ m².

As the quantity m_c is normally very small, the parameter $\overline{c}_{f_{\text{jet}}}$ in a first approximation is equal to the mean friction coefficient along the streamline A — A (see figure 1). From reference 1 it can be concluded that $\overline{c}_{f_{\text{jet}}}$ in an incompressible flow is independent of free jet length and is equal to .022.

The measurements from ref. 2 indicate that the mixing phenomena are quantitatively about equal for an incompressible flow and for a compressible flow at $M_1 = 2.9$.

As in general also the wall friction coefficients tend to vary only slightly with Mach number the value .022 is assumed to be valid in the whole Mach number range from .8 to 1.3.

The jet boundary is composed of:

a. The free jet boundary aft of the test section (9.6 m²).

b. The slot area.

The quantity $\frac{\overline{c}_{f_{\text{jet}}} \,.\, S_{\text{jet}}}{2\,S_1}$ becomes then:

$$\frac{\overline{c}_{f_{\text{jet}}} \,.\, S_{\text{jet}}}{2\,S_1} = \frac{.022 \times 14.6}{2 \times 3.2} = \underline{\underline{.0502}}$$

over the whole Mach number range.

The quantity $\overline{c}_{f_w}$ is evaluated for a flow at Mach number 1 along a flat plate of 3 m length at a stagnation pressure of 1 atmosphere absolute.

In a first approximation the wall friction coefficient can be taken equal to the incompressible one, so:

$$\overline{c}_{f_w} = .074\,(R_e)^{-.2}.$$

R_e is equal to

$$\frac{U_1 \,.\, l}{\nu} = \frac{310(\text{m/sec}) \,.\, 3(\text{m})}{22.10^{-6}\ (\text{m}^2/\text{sec})} = 4.09.10^7.$$

$$\overline{c}_{f_w} = .074.(4.09.10^7)^{-.2} = .00224.$$

The surface area S_w is composed of:

a. The side wall surface up to the diffuser intake about $2 \times 5.4 \times 1.6 = 17.3$ m².

b. The surface of lower and upper test section walls minus the slot area about $3.2.2 - 5 = 7$ m². The surface area of the diffuser walls has been neglected as the flow velocities are much smaller there.

From this it follows that:

$$\frac{\overline{c}_{f_w} \,.\, S_w}{2\,S_1} = \frac{.00224 \times 24.3}{2 \times 3.2} = .0085.$$

As this quantity results only in a small contribution to λ_T and as the friction coefficient will not vary much with Mach number this value of 0.0085 is assumed to be valid in the whole Mach number range.

In the next table the total value of λ_T is given as a function of the Mach number M_1.

M_1	$\frac{c_{D_s} \,.\, S_s}{2\,S_1}$	$\frac{\overline{c}_{f_{\text{jet}}} \,.\, S_{\text{jet}}}{2\,S_1}$	$\frac{\overline{c}_{f_w} \,.\, S_w}{2\,S_1}$	λ_T
.8	.0044	.0502	.0085	.0631
.9	.0100	.0502	.0085	.0687
1.0	.0154	.0502	.0085	.0741
1.1	.0182	.0502	.0085	.0769
1.2	.0210	.0502	.0085	.0797
1.3	.0220	.0502	.0085	.0807

C.2 *Estimation of* λ_m.

$$\lambda_m = \frac{D_m}{S_1 \rho_1 U_1^2} + \frac{m_c}{S_1 \rho_1 U_1}.$$

In near sonic flow the quantity $\frac{m_c}{S_1 \rho_1 U_1}$ is equal to the percentage model blockage μ in a good approximation.

D_m can be written as: $D_m = c_{d_{m_1}} \,.\, \frac{1}{2}\rho_1 U_1^2 \,.\, S_1$ where $c_{D_{m_1}}$ is the drag coefficient based on the test section area S_1.

So λ_m is equal to $\lambda_m = \frac{c_{D_{m_1}}}{2} + \mu$.

The value of $c_{D_{m_1}}$ depends to a large extent on the size and the shape of the model.

C.C.L. Class. C 270-0: C 35-0

NLL-TR S. 518

Determination of the stresses in a spherical shell with a hole, due to an axial force, a bending moment and a transverse force

by

P. J. ZANDBERGEN.

Summary.

In chapter 3 of this report, the stresses occurring at the edge of a hole in a sphere with a radius not small compared to the radius of the sphere are determined for the cases of introduction of an axial force, a bending moment and a transverse force. This is done by using an asymptotical bending theory, originally developed by A. HAVERS. This theory is reviewed in chapter 2. Numerical results for some cases are given in chapter 4.

Contents.

List of symbols.

1 Introduction.

2 Review of the solution of Havers.
   2.1 Derivation of the differential equations.
   2.2 Reduction of the differential equations.
   2.3 Solution of the differential equation.
   2.4 Determination of the displacements and the forces and moments.
   2.5 The arbitrary constants.
   2.6 Concluding remarks of chapter 2.

3 Application to the problems of an axial force, a transverse force and a bending moment.
   3.1 Introduction of an axial force.
   3.2 Introduction of a bending moment.
   3.3 Introduction of a transverse force.
   3.4 Concluding remarks of chapter 3.

4 Numerical solution for some cases.
   4.1 Introduction.
   4.2 Calculation for the case of axial load.
   4.3 Calculation for the case of a bending moment.
   4.4 Calculation for the case of a transverse force.
   4.5 Estimation of the error involved in the results.

5 Conclusions.

6 References.

Acknowledgement.

2 tables.

9 figures.

List of symbols.

a	= radius of the sphere.
a_r	= coefficient in the expansion of z_n.
b	= damping coefficient occurring in exponential functions.
b_i	= integration constants, to be determined from the edge conditions.
c_i	= integration constants, to be determined from the edge conditions.
h	= thickness of the shell.
$h = h_1$ or h_2	= see for definition eq. (2.41).
k	$= \frac{1}{12}\left(\frac{h}{a}\right)^2$
n	= quantity taking the values 1.2.3. ... — and so on.
r	= quantity taking the values 1.2.3. ... — and so on.
s_i	= separation constants.
u	= displacement of the shell in radial direction.
v	= displacement of the shell in tangential direction.
w	= displacement of the shell orthogonal to u and v.
x	= independent variable.
y	= solution of the differential equation given by eq. (2.22a).
y_n	= function of ϑ.
z_n	= hypergeometric function defined by eq. (2.27).
A	= constant, defining elastic properties of the shell.
$\overline{A}$	= factor of a particular integral of eq. (2.15).
B	= constant, defining elastic properties of the shell.
B_i	= integration constants.
$\overline{B}$	= factor of a particular integral of eq. (2.15).
C_i	= integration constants.
D	= transverse force.
E	= YOUNG's modulus.
H	= operator of the spherical functions.
$M_{\varphi\varphi}$, $M_{\vartheta\vartheta}$, $M_{\varphi\vartheta}$, $M_{\vartheta\varphi}$	moments occurring in the shell (fig. 3b).

$N_{\varphi\varphi}$, $N_{\vartheta\vartheta}$, $N_{\varphi\vartheta}$, $N_{\vartheta\varphi}$ membrane forces occurring in the shell (fig. 3a).

$Q_{\vartheta\xi}$, $Q_{\varphi\xi}$	shear forces occurring in the shell (fig. 3a).
S_{n_1}, S_{n_2}	solutions of the equation $H(y) = 0$.
T	$= V - u + \dfrac{\sin\vartheta}{2} \dfrac{\partial}{\partial\vartheta}\left(\dfrac{1}{\sin\vartheta} \dfrac{\partial\Omega}{\partial\vartheta}\right)$.
T_{n_1}, T_{n_2}, T_{n_3}, T_{n_4}	solutions of the equation $H(T) = sT$.
V	= defined by eq. (2.10a).
W	= defined by eq. (2.10b).
$\alpha(\xi)$	= function of ξ, which must be small compared to h.
$\overline{\alpha}$	= quantity taking the values 1, 2, 3 — and so on.
$\overline{\beta}$	= quantity taking the values 1, 2, 3 — and so on.
β	$= \dfrac{b}{\sqrt{2}}$
γ	= quantity taking the values 1, 2, 3 — and so on.
ϑ	= angular coordinate defined in fig. 2.
ε, ε_φ	= strains occurring in the shell.
ϑ_χ	= angle defined by eq. (2.44a).
λ	$= s_1$ or s_2.
σ_φ, τ_ϑ, resp. σ_a, σ_t	tangential and axial stresses occurring in the shell (fig. 6).
$\tau_{\varphi\vartheta}$	= shear stress occurring in the shell.
ρ	$= \dfrac{n^2}{b^2}$
ν	= POISSON's ratio.
Ψ	$= \dfrac{\pi}{2} - \vartheta$.
φ	= angular coordinate defined in fig. 2.
$\xi\ \overline{\xi}$	= functions of ϑ defined by eq. (2.44).
Λ, Λ_0	= function given by the first relation of eq. (2.44a).
Ω	= function defined by eq. (2.12).

1 Introduction.

It is well known that in spherical shells very high bending stresses due to local variations of stiffness or due to local loading may occur. These stresses decrease very rapidly as the distance from the disturbance increases. The problem which led to this investigation is the following one. Consider a pressure vessel, which consists of a cylinder closed by two half spheres. In one of these half spheres there is a hole which connects a pipe to the pressure vessel (see figure 1). The bending stresses which occur in the shell of the sphere due to an axial force N and a transverse force D, and due to a bending moment M exerted by the pipe on the sphere, form the subject of the present paper.

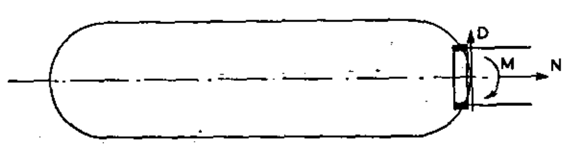

Fig. 1. The actual structure.

For a shallow sphere it is possible to make approximations which give rise to differential equations of BESSEL's type. By this method it is possible to find the stresses if the radius of the hole is small with respect to the radius of the sphere.

In 1935 A. HAVERS succeeded in finding the solution of the general problem of edge loading (ref. 1) *) by making use of an operation discovered by A. v. D. NEUT (ref. 2). However, it seems to the author that this work has not become generally known. It is therefore his intention to give a sketch of the work of HAVERS and thereupon to use the results for the solution of the above stated problems.

It is assumed that the pipe is attached to the sphere by means of a so-called "neutral hole" reinforcement. This is a heavy circular frame which makes the membrane stresses due to the pressure not to be disturbed by the hole. In general there will occur some bending stresses, but, as can be proved, these stresses always remain very small.

The report consists of three parts (chapters 2, 3 and 4). In the first part the theory of HAVERS will be reviewed. In the second part the application to the problems of an axial force, a transverse force and a bending moment will be given, while the third part is devoted to the numerical evaluation of stresses and displacements due to these loadings for the case of the pressure vessel and attached pipe of the supersonic wind tunnel to be built for the N.L.L.

2 Review of the solution of Havers.

2.1 *Derivation of the differential equations.*

Consider a part of the sphere as given in fig. 2 and denote by u, v and w the displacements of a point of the shell as indicated in

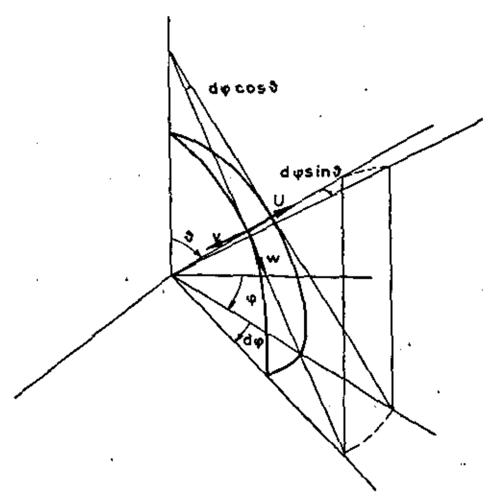

Fig. 2. Orientation of angles and displacements.

the figure. We now make the usual assumptions. Denoting by ξ the distance of a point above the

*) The author's attention was drawn to this paper by Prof. A. v. D. NEUT.

middle surface of the shell and by $\gamma_{\vartheta\xi}$, $\gamma_{\varphi\xi}$ and $\gamma_{\varphi\vartheta}$ the shear strain components, it is assumed that

$$\sigma_\xi = 0$$

$$\gamma_{\vartheta\xi} = \gamma_{\varphi\xi} = 0$$

and u, v and w are small compared to the thickness h of the shell.

According to ref. 3, p. 47

$$\varepsilon_\vartheta = \frac{1}{a+\xi}\frac{\partial w}{\partial \vartheta} + \frac{u}{a+\xi} \tag{2.1a}$$

$$\varepsilon_\varphi = \frac{1}{(a+\xi)\sin\vartheta}\frac{\partial v}{\partial\varphi} + \frac{u}{a+\xi} + \frac{w}{a+\xi}\operatorname{cotg}\vartheta \tag{2.1b}$$

$$\gamma_{\varphi\vartheta} = \gamma_{\vartheta\varphi} = \frac{1}{a+\xi}\frac{\partial v}{\partial\vartheta} = $$

$$= \frac{v}{a+\xi}\operatorname{cotg}\vartheta + \frac{1}{(a+\xi)\sin\vartheta}\frac{\partial w}{\partial\varphi}, \tag{2.1c}$$

where a denotes the radius of the middle surface of the shell. The assumption that $\gamma_{\vartheta\xi} = \gamma_{\varphi\xi} = 0$ implies that all points lying on a normal of the undeformed shell will remain on a normal of the deformed shell. If u_0, v_0 and w_0 are the displacements of the middle surface, a simple geometric investigation will learn that

$$u = u_0 \tag{2.2a}$$

$$v = \frac{\xi + a}{a} v_0 - \frac{\xi}{a\sin\vartheta}\frac{\partial u_0}{\partial\varphi} \tag{2.2b}$$

$$w = \frac{\xi + a}{a} w_0 - \frac{\xi}{a}\frac{\partial u_0}{\partial\vartheta}. \tag{2.2c}$$

On substituting these results in the eqs. (2.1a), (2.1b) and (2.1c) one obtains

$$\varepsilon_\vartheta = \frac{1}{a}\frac{\partial w_0}{\partial\vartheta} - \frac{\xi}{a(a+\xi)}\frac{\partial^2 u_0}{\partial\vartheta^2} + \frac{u_0}{a+\xi} \tag{2.3a}$$

$$\varepsilon_\varphi = \frac{1}{a\sin\vartheta}\frac{\partial v_0}{\partial\varphi} - \frac{\xi}{a(a+\xi)\sin^2\vartheta}\frac{\partial^2 u_0}{\partial\varphi^2} +$$

$$+ \frac{u_0}{a+\xi} + \frac{w_0}{a}\operatorname{cotg}\vartheta - \frac{\xi}{a(a+\xi)}\frac{\partial u_0}{\partial\vartheta}\operatorname{cotg}\vartheta \tag{2.3b}$$

$$\gamma_{\varphi\vartheta} = \frac{1}{a}\frac{\partial v_0}{\partial\vartheta} + \frac{2\xi\cos\vartheta}{a(a+\xi)\sin^2\vartheta}\frac{\partial u_0}{\partial\varphi} +$$

$$- \frac{2\xi}{a(a+\xi)\sin\vartheta}\frac{\partial^2 u_0}{\partial\varphi\partial\vartheta} - \frac{\vartheta_0}{a}\operatorname{cotg}\vartheta +$$

$$+ \frac{1}{a\sin\vartheta}\frac{\partial w_0}{\partial\varphi}. \tag{2.3c}$$

These strains are related to the stresses by means of Hooke's law

$$\sigma_\varphi = \frac{E}{1-\nu^2}(\varepsilon_\varphi + \nu\,\varepsilon_\vartheta) \tag{2.4a}$$

$$\sigma_\vartheta = \frac{E}{1-\nu^2}(\varepsilon_\vartheta + \nu\,\varepsilon_\varphi) \tag{2.4b}$$

$$\tau_{\varphi\vartheta} = \frac{E}{2(1+\nu)}\gamma_{\varphi\vartheta}. \tag{2.4c}$$

We will now calculate the forces and moments that occur in the shell and which are defined in figures 3a and 3b. We have

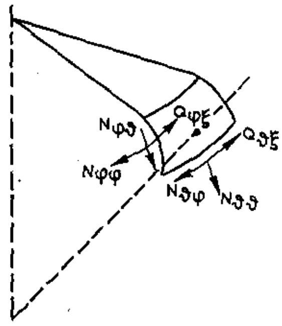

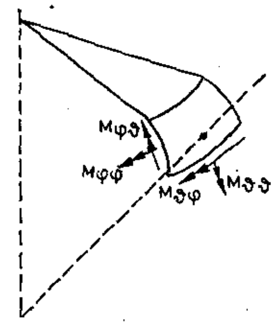

Fig. 3a. Fig. 3b.

Forces and moments acting on an element of the shell

$$N_{\varphi\varphi} = \int_{-\frac{h}{2}}^{+\frac{h}{2}} \sigma_\varphi \frac{a+\xi}{a}\,d\xi \tag{2.5a}$$

$$N_{\vartheta\vartheta} = \int_{-\frac{h}{2}}^{+\frac{h}{2}} \sigma_\vartheta \frac{a+\xi}{a}\,d\xi \tag{2.5b}$$

$$N_{\vartheta\varphi} = N_{\varphi\vartheta} = \int_{-\frac{h}{2}}^{+\frac{h}{2}} \tau_{\varphi\vartheta} \frac{a+\xi}{a}\,d\xi \tag{2.5c}$$

and

$$M_{\varphi\varphi} = -\int_{-\frac{h}{2}}^{+\frac{h}{2}} \tau_{\varphi\vartheta} \frac{a+\xi}{a}\,\xi\,d\xi = -M_{\vartheta\vartheta} \tag{2.6a}$$

$$M_{\vartheta\varphi} = \int_{-\frac{h}{2}}^{+\frac{h}{2}} \sigma_\vartheta \frac{a+\xi}{a}\,\xi\,d\xi \tag{2.6b}$$

$$M_{\varphi\vartheta} = \int_{-\frac{h}{2}}^{+\frac{h}{2}} \sigma_\varphi \frac{a+\xi}{a}\,\xi\,d\xi. \tag{2.6c}$$

By making use of the equations (2.4a), (2.4b), (2.4c) and (2.3a), (2.3b), (2.3c), we get, with

$$B = \frac{Eh}{1-\nu^2} \quad \text{and} \quad A = \frac{Eh^3}{12(1-\nu^2)}$$

$$N_{\varphi\varphi} = \frac{B}{a}\left\{\frac{1}{\sin\vartheta}\frac{\partial v_0}{\partial\varphi} + \right.$$

$$\left. + u_0 + w_0\operatorname{cotg}\vartheta + \nu\frac{\partial w_0}{\partial\vartheta} + \nu u_0 \right\} \tag{2.7a}$$

$$N_{\vartheta\vartheta} = \frac{B}{a}\left\{\frac{\partial w_0}{\partial\vartheta} + u_0 + \frac{\nu}{\sin\vartheta}\ \frac{\partial v_0}{\partial\varphi} + \nu u_0 + \nu w_0 \operatorname{cotg}\vartheta\right\} \tag{2.7b}$$

$$N_{\varphi\vartheta} = N_{\vartheta\varphi} = \frac{B}{a}\ \frac{1-\nu}{2}\left\{\frac{\partial v_0}{\partial\vartheta} - v_0\operatorname{cotg}\vartheta + \frac{1}{\sin\vartheta}\ \frac{\partial w_0}{\partial\varphi}\right\} \tag{2.7c}$$

$$M_{\varphi\varphi} = -\frac{A}{a^2}\ \frac{1-\nu}{2}\left\{\frac{\partial v_0}{\partial\vartheta} + \frac{2\cos\vartheta}{\sin^2\vartheta}\ \frac{\partial u_0}{\partial\varphi} - \frac{2}{\sin\vartheta}\ \frac{\partial^2 u_0}{\partial\varphi\partial\vartheta} - v_0\operatorname{cotg}\vartheta + \frac{1}{\sin\vartheta}\ \frac{\partial w_0}{\partial\varphi}\right\} = -M_{\vartheta\vartheta} \tag{2.7d}$$

$$M_{\varphi\vartheta} = -\frac{A}{a^2}\left\{\frac{1}{\sin\vartheta}\ \frac{\partial v_0}{\partial\varphi} - \frac{1}{\sin^2\vartheta}\ \frac{\partial^2 u_0}{\partial\varphi^2} + w_0\operatorname{cotg}\vartheta - \frac{\partial u_0}{\partial\vartheta}\operatorname{cotg}\vartheta + \frac{\partial w_0}{\partial\vartheta} - \nu\frac{\partial^2 u_0}{\partial\vartheta^2}\right\} \tag{2.7e}$$

$$M_{\vartheta\varphi} = -\frac{A}{a^2}\left\{\frac{\partial w_0}{\partial\vartheta} - \frac{\partial^2 u_0}{\partial\vartheta^2} + \frac{\nu}{\sin\vartheta}\ \frac{\partial^2 u_0}{\partial\varphi} - \frac{\nu}{\sin^2\vartheta}\ \frac{\partial^2 v_0}{\partial\varphi^2} + \nu\, w_0\operatorname{cotg}\vartheta - \nu\frac{\partial u_0}{\partial\vartheta}\operatorname{cotg}\vartheta\right\} \tag{2.7f}$$

It is our purpose to derive three differential equations for the unknown quantities u_0, v_0 and w_0. To obtain these equations we make use of the equilibrium of an element of the shell.
We find

$$a\ \frac{\partial N_{\varphi\varphi}}{\partial\varphi}\,d\varphi d\vartheta + a\,\frac{\partial(N_{\vartheta\varphi}\sin\vartheta)}{\partial\vartheta}\,d\varphi d\vartheta + a\,N_{\varphi\vartheta}\cos\vartheta\,d\varphi d\vartheta + a\,Q_{\varphi\xi}\sin\vartheta\,d\varphi d\vartheta = 0 \tag{2.8a}$$

$$a\ \frac{\partial(N_{\vartheta\vartheta}\sin\vartheta)}{\partial\vartheta}\,d\varphi d\vartheta + a\,\frac{\partial N_{\varphi\vartheta}}{\partial\varphi}\,d\varphi d\vartheta - a\,N_{\varphi\varphi}\cos\vartheta d\varphi d\vartheta + a\,Q_{\vartheta\xi}\sin\vartheta d\varphi d\vartheta = 0 \tag{2.8b}$$

$$a\ \frac{\partial(Q_{\vartheta\xi}\sin\vartheta)}{\partial\vartheta}\,d\varphi d\vartheta + a\,\frac{\partial Q_{\varphi\xi}}{\partial\varphi}\,d\varphi d\vartheta - a\,N_{\varphi\varphi}\sin\vartheta d\varphi d\vartheta - a\,N_{\vartheta\vartheta}\sin\vartheta d\varphi d\vartheta = 0 \tag{2.8c}$$

$$a\ \frac{\partial M_{\varphi\varphi}}{\partial\varphi}\,d\varphi d\vartheta + a\,\frac{\partial(M_{\vartheta\varphi}\sin\vartheta)}{\partial\vartheta}\,d\varphi d\vartheta - a\ M_{\varphi\vartheta}\cos\vartheta d\varphi d\vartheta + a\,Q_{\vartheta\xi}d\varphi d\vartheta\sin\vartheta = 0 \tag{2.8d}$$

$$a\ \frac{\partial(M_{\vartheta\vartheta}\sin\vartheta)}{\partial\vartheta}\,d\varphi d\vartheta - a\,\frac{\partial M_{\varphi\vartheta}}{\partial\varphi}\,d\varphi d\vartheta - a\,M_{\varphi\varphi}\cos\vartheta d\varphi d\vartheta - a\,Q_{\varphi\xi}d\varphi d\vartheta\sin\vartheta = 0 \tag{2.8e}$$

$$a\,M_{\vartheta\vartheta}\sin\vartheta d\varphi d\vartheta + a\,M_{\varphi\varphi}\sin\vartheta d\varphi d\vartheta - a\,N_{\vartheta\varphi}\sin\vartheta d\varphi d\vartheta + a\,N_{\varphi\vartheta}\sin\vartheta d\varphi d\vartheta = 0. \tag{2.8f}$$

Since $\tau_{\varphi\vartheta} = \tau_{\vartheta\varphi}$, *equation* (2.8f) *is satisfied identically. There remain five equations. If we eliminate* the quantities $Q_{\vartheta\xi}$ and $Q_{\varphi\xi}$ from the equations (2.8a), (2.8b) and (2.8c) by means of (2.8d) and (2.8e), three equations result. Now on substituting the equations (1.7) into these three equations we find the following differential equations, where k stands for $\frac{1}{12}\left(\frac{h}{a}\right)^2$.

$$(1+k)\left[\frac{1-\nu}{2}\left(\frac{\partial^2 v_0}{\partial\vartheta^2}\sin\vartheta + \frac{\partial v_0}{\partial\vartheta}\cos\vartheta + v_0\frac{\cos 2\vartheta}{\sin\vartheta}\right) + \frac{1}{\sin\vartheta}\ \frac{\partial^2 v_0}{\partial\varphi^2} + \frac{1+\nu}{2}\ \frac{\partial^2\omega_0}{\partial\varphi\partial\vartheta} + \right.$$
$$\left. + \frac{3-\nu}{2}\ \frac{\partial\omega_0}{\partial\varphi}\operatorname{cotg}\vartheta + (1+\nu)\frac{\partial u_0}{\partial\varphi}\right] - k\left[\frac{\partial^3 u_0}{\partial\vartheta^2\partial\varphi} + \frac{\partial^2 u_0}{\partial\varphi\partial\vartheta}\operatorname{cotg}\vartheta + 2\frac{\partial u_0}{\partial\varphi} + \frac{1}{\sin^2\vartheta}\ \frac{\partial^3 u_0}{\partial\varphi^3}\right] = 0 \tag{2.9a}$$

$$(1+k)\left[\frac{1+\nu}{2}\ \frac{\partial^2 v_0}{\partial\varphi\partial\vartheta} - \frac{3-\nu}{2}\ \frac{\partial v_0}{\partial\varphi}\operatorname{cotg}\vartheta + \frac{\partial^2\omega_0}{\partial\vartheta^2}\sin\vartheta + \frac{\partial\omega_0}{\partial\vartheta}\cos\vartheta - \omega_0\frac{\cos^2\vartheta + \nu\sin^2\vartheta}{\sin\vartheta} + \right.$$
$$\left. + \frac{1-\nu}{2}\ \frac{1}{\sin\vartheta}\ \frac{\partial^2\omega_0}{\partial\varphi^2} + (1+\nu)\sin\vartheta\,\frac{\partial u_0}{\partial\vartheta}\right] - k\left[\frac{\partial^3 u_0}{\partial\vartheta^3}\sin\vartheta + \frac{\partial^2 u_0}{\partial\vartheta^2}\cos\vartheta + \left(2 - \frac{1}{\sin^2\vartheta}\right)\frac{\partial u_0}{\partial\vartheta}\sin\vartheta + \right.$$
$$\left. + \frac{\partial^3 u_0}{\partial\varphi^2\partial\vartheta}\ \frac{1}{\sin\vartheta} - 2\,\frac{\partial^2 u_0}{\partial\varphi^2}\ \frac{\cos\vartheta}{\sin^2\vartheta}\right] = 0 \tag{2.9b}$$

$$-(1+k)\left[(1+\nu)\left(\frac{\partial v_0}{\partial\varphi} + \frac{\partial\omega_0}{\partial\vartheta}\sin\vartheta + \omega_0\cos\vartheta + 2\,u_0\sin\vartheta\right)\right] +$$
$$+ k\left[\frac{\partial^3 v_0}{\partial\varphi\partial\vartheta^2} - \frac{\partial^2 v_0}{\partial\varphi\partial\vartheta}\operatorname{cotg}\vartheta + \frac{\partial v_0}{\partial\varphi}\left(2 + \frac{1}{\sin^2\vartheta}\right) + \frac{1}{\sin^2\vartheta}\ \frac{\partial^3 v_0}{\partial\varphi^3} + \frac{\partial^3\omega_0}{\partial\vartheta^3}\sin\vartheta + 2\,\frac{\partial^2\omega_0}{\partial\vartheta^2}\cos\vartheta + \right.$$
$$\left. - \frac{\partial\omega_0}{\partial\vartheta}\ \frac{\cos^2\vartheta}{\sin\vartheta} + \omega_0\left(2 + \frac{1}{\sin^2\vartheta}\right)\cos\vartheta + \frac{1}{\sin\vartheta}\ \frac{\partial^3\omega_0}{\partial\varphi^2\partial\vartheta} + \frac{\partial^2\omega_0}{\partial\varphi^2}\ \frac{\cos\vartheta}{\sin^2\vartheta}\right] +$$
$$- k\left[\frac{\partial^4 u_0}{\partial\vartheta^4}\sin\vartheta + 2\,\frac{\partial^3 u_0}{\partial\vartheta^3}\cos\vartheta - (1 + \nu + \operatorname{cotg}^2\vartheta)\,\frac{\partial^2 u_0}{\partial\vartheta^2}\sin\vartheta + \left(1 - \nu + \frac{1}{\sin^2\vartheta}\right)\frac{\partial u_0}{\partial\vartheta}\cos\vartheta + \right.$$
$$-2\,(1+\nu)u_0\sin\vartheta + \frac{2}{\sin\vartheta}\ \frac{\partial^4 u_0}{\partial\varphi^2\partial\vartheta^2} - 2\,\frac{\partial^3 u}{\partial\varphi^2\partial\vartheta}\ \frac{\cos\vartheta}{\sin^2\vartheta} + \frac{(1+\nu)\cos^2\vartheta + 3 - \nu}{\sin^3\vartheta}\ \frac{\partial^2 u_0}{\partial\varphi^2} +$$
$$\left. + \frac{\partial^4 u_0}{\partial\varphi^4}\ \frac{1}{\sin^3\vartheta}\right] = 0. \tag{2.9c}$$

2.2 *Reduction of the differential equations.*

The problem has now been reduced to the solution of the three differential equations (2.9a, b, c). We will only give the main points of view that lead to the solution.

We introduce the following operations discovered by A. v. d. Neut (ref. 2):

$$v_0 = \frac{1}{\sin\vartheta}\,\frac{\partial V}{\partial\varphi} \qquad (2.10a)$$

and

$$w_0 = \frac{\partial W}{\partial\vartheta}. \qquad (2.10b)$$

Furthermore, we introduce the operator H of the spherical function

$$H(y) = \frac{\partial^2 y}{\partial\vartheta^2} + \frac{\partial y}{\partial\vartheta}\operatorname{cotg}\vartheta + 2y + \frac{1}{\sin^2\vartheta}\,\frac{\partial^2 y}{\partial\varphi^2} \qquad (2.11)$$

It is known that for a spherical function y_n of the n-th order

$$H(y_n) = -[n(n+1)-2]\,yn$$
$$n = 0,\ 1,\ 2,\ 3,\ \text{etc.}$$

On introducing now

$$V - W = \Omega \qquad (2.12)$$

the system of differential equations can be brought into the form

$$H\left(\frac{1}{\sin\vartheta}\,\frac{\partial\Omega}{\partial\vartheta}\right) = 0 \qquad (2.13)$$

$$HH(T) - 2H(T) + (1-\nu^2)\,\frac{1+k}{k}\,T = 0 \qquad (2.14)$$

where T is written for

$$V - u_0 + \frac{\sin\vartheta}{2}\,\frac{\partial}{\partial\vartheta}\left(\frac{1}{\sin\vartheta}\,\frac{\partial\Omega}{\partial\vartheta}\right)$$

and

$$H(u_0) = (1+k)\left[(1+\nu)T - H(T)\right]. \qquad (2.15)$$

Equation (2.14) can be split into two equations by writing

$$H(T) = sT. \qquad (2.16)$$

Inserting this in equation (2.14) one obtains

$$H(T) = s_1 T \quad \text{and} \quad H(T) = s_2 T \qquad (2.17)$$

where

$$s_1 = 1 + \sqrt{1 - (1-\nu^2)\,\frac{1+k}{k}}$$

and

$$s_2 = 1 - \sqrt{1 - (1-\nu^2)\,\frac{1+k}{k}}. \qquad (2.18)$$

Equation (2.15) can be reduced to the general equation $H(u_0) = 0$ by assuming a particular solution of the form

$$u_0 = \overline{A}\,H(T) + \overline{B}\,T. \qquad (2.19)$$

We then find by making use of eq. (2.14)

$$\overline{A} = -\frac{k}{1-\nu}, \quad \overline{B} = \frac{2k - (1-\nu)(1+k)}{1-\nu}. \qquad (2.20)$$

The solution of the problem has now been reduced to the solution of the equation

$$H(y) = \lambda\,y. \qquad (2.21)$$

2.3 *Solution of the differential equation.*

We have to solve the equation

$$\frac{\partial^2 y}{\partial\vartheta^2} + \frac{\partial y}{\partial\vartheta}\operatorname{cotg}\vartheta + 2y + \frac{1}{\sin^2\vartheta}\,\frac{\partial^2 y}{\partial\varphi^2} = \lambda\,y. \qquad (2.22)$$

We introduce

$$y = \sum_{0}^{\infty} y_n(\vartheta)\begin{Bmatrix}\cos n\varphi \\ \sin n\varphi\end{Bmatrix} \quad n = 1, 2, 3. \qquad (2.22a)$$

Inserting this in equation (2.22) we find the differential equation for $y_n(\vartheta)$

$$\frac{\partial^2 y_n}{\partial\vartheta^2} + \frac{\partial y_n}{\partial\vartheta}\operatorname{cotg}\vartheta + y_n\left(2 - \lambda - \frac{n^2}{\sin^2\vartheta}\right) = 0. \qquad (2.23)$$

Using the following transformations

$$x = \frac{1-\cos\vartheta}{2} \qquad z_n = y_n\left(\frac{1+\cos\vartheta}{1-\cos\vartheta}\right)^{\frac{n}{2}} \qquad (2.24)$$

$$x = \frac{1+\cos\vartheta}{2} \qquad z_n = y_n\left(\frac{1-\cos\vartheta}{1+\cos\vartheta}\right)^{\frac{n}{2}} \qquad (2.25)$$

equation (2.23) becomes a hypergeometric differential equation

$$x(x-1)\frac{\partial^2 z_n}{\partial x^2} + \left[(\overline{\alpha} + \overline{\beta} + 1)x - \gamma\right]\frac{\partial z_n}{\partial x} + \overline{\alpha}\,\overline{\beta}\,z_n = 0 \qquad (2.26)$$

with

$$2 - \lambda = \mu(\mu+1)$$

$$\overline{\alpha} = -\mu \qquad \overline{\beta} = \mu + 1 \qquad \gamma = 1 + n.$$

The solution of equation (2.26) is

$$z_n = F(\overline{\alpha}, \overline{\beta}, \gamma, x) = 1 + \sum_{r=1}^{\infty} a_r x^r \qquad (2.27)$$

with

$$a_r = \frac{\overline{\alpha}(\overline{\alpha}+1)\ldots(\overline{\alpha}+r-1).\,\overline{\beta}(\overline{\beta}+1)\ldots(\overline{\beta}+r-1)}{1.2.\ldots r.\,\gamma(\gamma+1)\ldots(\gamma+r-1).}. \qquad (2.28)$$

For $\lambda = 0 \rightarrow \mu = 1$ and

$$F(\overline{\alpha}, \overline{\beta}, \gamma, x) = 1 - \frac{2}{1+n}\,x. \qquad (2.29)$$

This gives with the equations (2.24) and (2.25)

$$y^*_{n_1} = \frac{n+\cos\vartheta}{n+1}\left(\frac{1-\cos\vartheta}{1+\cos\vartheta}\right)^{\frac{n}{2}} \qquad (2.30)$$

$$y^*_{n_2} = \frac{n-\cos\vartheta}{n+1}\left(\frac{1+\cos\vartheta}{1-\cos\vartheta}\right)^{\frac{n}{2}}. \qquad (2.31)$$

These solutions are independent for $n > 2$.

For $n=0$ and $n=1$ the solutions are dependent. For the independent solutions in this case, the reader is referred to the original paper by HAVERS. The whole system proves to be

$$n=0 \quad y^*_{01} = \cos\vartheta \tag{2.32a}$$

$$y^*_{02} = \cos\vartheta \ln \frac{1-\cos\vartheta}{1+\cos\vartheta} + 2. \tag{2.32b}$$

$$n=1 \quad y^*_{11} = \sin\vartheta \tag{2.33a}$$

$$y^*_{12} = \sin\vartheta \ln \frac{1-\cos\vartheta}{1+\cos\vartheta} - 2. \tag{2.33b}$$

The equations (2.30), (2.31), (2.32a), (2.32b), (2.33a) and (2.33b) give the solution of equation (2.23), except for constant factors, in the case that $\lambda = 0$.

We now turn our attention to the case that $\lambda = s_1$ or $\lambda = s_2$. Since s_1 and s_2 are complex numbers, computation of the coefficients a_r (see eq. 2.28) would be very cumbersome. There is, however, another fact that makes it impossible to use the expansion given by eq. (2.27). That is the fact that we have assumed the thickness of the shell to be small compared to the radius of the sphere. This causes, however, that s_1 and s_2 and thus μ too, are large. It is then to be expected that the convergence of the expansion is very slow. This would mean that a very complicated numerical analysis would be needed for every practical problem.

Therefore HAVERS followed another way, inspired by the work of BLUMENTHAL. He so succeeded in finding asymptotically correct solutions.

Notice that equation (2.23) can be written as

$$\frac{\partial^2 y_n}{\partial\vartheta^2} + \frac{\partial y_n}{\partial\vartheta}\cot\vartheta - y_n\left(\bar{h} + \frac{n^2}{\sin^2\vartheta}\right) = 0. \tag{2.34}$$

Here

$$\bar{h} = h_1 = -1 + i\sqrt{(1-\nu^2)\frac{1+k}{k} - 1} \quad \text{if } \lambda = s_1 \tag{2.35a}$$

$$\bar{h} = h_2 = -1 - i\sqrt{(1-\nu^2)\frac{1+k}{k} - 1} \quad \text{if } \lambda = s_2. \tag{2.35b}$$

In both cases

$$|h_1| = |h_2| = \left|\sqrt{(1-\nu^2)\frac{1+k}{k}}\right| \gg 1. \tag{2.36}$$

We will now try to bring eq. (2.34) in the following form

$$\frac{\partial^2\eta}{\partial\zeta^2} - [\,\bar{h} + \alpha(\xi)\,]\,\eta = 0. \tag{2.37}$$

If $\alpha(\xi)$ is small compared to h, the solution of eq. (2.37) will be approximately

$$\eta_1 = e^{\sqrt{\bar{h}}\xi} \quad \text{and} \quad \eta_2 = e^{-\sqrt{\bar{h}}\zeta}.$$

In order to transform eq. (2.34) into eq. (2.37) we introduce a new independent variable $\xi = f(\vartheta)$. This gives rise to

$$\left(\frac{\partial\xi}{\partial\vartheta}\right)^2 \frac{\partial^2 y_n}{\partial\xi^2} + \left(\frac{\partial^2\xi}{\partial\vartheta^2} + \frac{\partial\xi}{\partial\vartheta}\cot\vartheta\right)\frac{\partial y_n}{\partial\xi} + -\bar{h}\left(1 + \frac{n^2}{\bar{h}\sin^2\vartheta}\right) y_n = 0. \tag{2.38}$$

If we take

$$\frac{\partial\xi}{\partial\vartheta} = \frac{1}{\sin\vartheta}\sqrt{\sin^2\vartheta + \frac{n^2}{\bar{h}}}$$

eq. (2.38) gives

$$\frac{\partial^2 y_n}{\partial\xi^2} + \frac{\cos\vartheta\sin^2\vartheta}{\left(\sin^2\vartheta + \frac{n^2}{\bar{h}}\right)^{\frac{3}{2}}}\frac{\partial y_n}{\partial\xi} - \bar{h}\, y_n = 0. \tag{2.39}$$

On introducing a new dependent variable

$$y_n = \frac{\eta}{\sqrt[4]{\sin^2\vartheta + \frac{n^2}{\bar{h}}}} \tag{2.40}$$

the second term in eq. (2.34) vanishes and the result is eq. (2.37).

In our case we have to solve eq. (2.37) for two values of h. Remembering that k is assumed to be small compared to unity, we may write

$$h_1 = ib^2$$
$$b = \sqrt[4]{(1-\nu^2)\frac{1+k}{k}} \tag{2.41}$$
$$h_2 = -ib^2$$

On introducing $\frac{n^2}{b^2} = \rho$, and assuming that $|\alpha|$ may be neglected with respect to b^2, we obtain the following solutions (see eq. 2.40).

In the case that $h = h_1$

$$y_{n_1} = \frac{e^{\frac{1+i}{\sqrt{2}}b\xi}}{\sqrt[4]{\sin^2\vartheta - i\rho}}, \quad y_{n_2} = \frac{e^{-\frac{1+i}{\sqrt{2}}b\xi}}{\sqrt[4]{\sin^2\vartheta - i\rho}} \tag{2.42}$$

in the case that $h = h_2$

$$\bar{y}_{n_1} = \frac{e^{\frac{1-i}{\sqrt{2}}b\bar{\xi}}}{\sqrt{\sin^2\vartheta + i\rho}} \quad \bar{y}_{n_2} = \frac{e^{-\frac{1-i}{\sqrt{2}}b\bar{\xi}}}{\sqrt{\sin^2\vartheta + i\rho}}. \tag{2.43}$$

Here, the bar above ξ means the conjugate complex value of ξ. ξ as a function of ϑ can be calculated from the relation

$$\frac{\partial\xi}{\partial\vartheta} = \frac{1}{\sin\vartheta}\sqrt{\sin^2\vartheta - i\rho}. \tag{2.44}$$

Now, the eqs. (2.42), (2.43) and (2.22a) give the general solution of eq. (2.14) and therefore any linear combination of y_{n_1}, y_{n_2}, $\bar{y}_{n_1}$, and $\bar{y}_{n_2}$ is a solution of this equation too. We will use this to obtain a set of real functions. This can be done by taking

$$T_{n_1} = \frac{1}{2}(y_{n_2} + \bar{y}_{n_2})$$

$$T_{n_2} = \frac{i}{2}(y_{n_2} - \bar{y}_{n_2})$$

$$T_{n_3} = \frac{1}{2}(y_{n_1} + \bar{y}_{n_1}) \ ,$$

$$T_{n_4} = -\frac{i}{2}(y_{n_1} - \bar{y}_{n_1}).$$

By introducing the following notations

$$\Lambda^8 = \sin^4\vartheta + \rho^2,\ \mathrm{tg}\, 4\chi = \frac{\rho}{\sin^2\vartheta},\ \beta = \frac{b}{\sqrt{2}} \qquad (2.44a)$$

and

$$(1+i)\,\xi = \xi_1 + i\,\xi_2$$

one obtains:

$$T_{n_1} = \frac{e^{-\beta\xi_1}}{\Lambda}\cos(\beta\xi_2 - \chi) \qquad (2.45a)$$

$$T_{n_2} = \frac{e^{-\beta\xi_1}}{\Lambda}\sin(\beta\xi_2 - \chi) \qquad (2.45b)$$

$$T_{n_3} = \frac{e^{+\beta\xi_1}}{\Lambda}\cos(\beta\xi_2 + \chi) \qquad (2.46a)$$

$$T_{n_4} = \frac{e^{+\beta\xi_1}}{\Lambda}\sin(\beta\xi_2 + \chi). \qquad (2.46b)$$

As Havers has proved, this solution yields asymptotically correct results. Only if $\psi = \frac{\pi}{2} - \vartheta > 85°$ and at the same time $\rho < 0{,}5$, the error will be increasing rapidly.

The values of ξ_1 and ξ_2 as functions of ρ and ψ have been tabulated by Havers (see ref. 1) and are here reproduced in tables 1 and 2.

Having solved the differential equation we can now calculate the displacements and the moments and forces occurring in the shell.

2.4 *Determination of the displacements and the forces and moments.*

We start with the determination of u. From eqs. (2.15), (2.17) and (2.19) it follows that u is determined by the general solution of $H(u) = 0$, together with the solutions of $H(T) = s_1 T$ and $H(T) = s_2 T$. On expanding u in a Fourier series $u_0 = \Sigma\, u_n \left\{ \begin{matrix} \cos n\varphi \\ \sin n\varphi \end{matrix} \right\}$ we find for the coefficient u_n, using the equations (2.18), (2.19), (2.30) and (2.31):

$$u_n = B_1 y^*_{n_1} + B_2 y^*_{n_2} + (\bar{A}\,s_1 + \bar{B})\,\{C_1\, y_{n_1} + C_2\, y_{n_2}\} + (\bar{A}\,s_2 + \bar{B})\,\{C_3\,\bar{y}_{n_1} + C_4\,\bar{y}_{n_2}\}\,. \qquad (2.47)$$

Denoting $\frac{1}{\sin\vartheta}\frac{\partial\Omega}{\partial\vartheta}$ by ω, and recalling that $T = V - u_0 + \frac{\sin\vartheta}{2}\frac{\partial\omega}{\partial\vartheta}$ we have

$$V = T + u_0 - \frac{1}{2}\sin\vartheta\,\frac{\partial\omega}{\partial\vartheta}\,. \qquad (2.48)$$

By expanding v_0 in a Fourier series $v_0 = \Sigma\, v_n \left\{ \begin{matrix} \sin n\varphi \\ \cos n\varphi \end{matrix} \right\}$ we get (the upper sign refers to $\Sigma\, v_n \sin n\varphi$):

$$v_n = \mp n\,\frac{(\bar{A}\,s_1 + \bar{B} + 1)}{\sin\vartheta}\{C_1 y_{n_1} + C_2 y_{n_2}\} \mp n\,\frac{(A\,s_2 + \bar{B}_1 + 1)}{\sin\vartheta}\{C_3\bar{y}_{n_1} + C_4\bar{y}_{n_2}\} +$$
$$\mp \frac{n}{\sin\vartheta}\{B_1 y^*_{n_1} + B_2 y^*_{n_2}\} \pm \frac{1}{2}\,n \left\{ B_3\frac{\partial y^*_{n_1}}{\partial\vartheta} + B_4\frac{\partial y^*_{n_2}}{\partial\vartheta} \right\}. \qquad (2.49)$$

The displacement w_0 can be found from eq. (2.10b) and eq. (2.12)

$$w_0 = \frac{\partial W}{\partial\vartheta} = \frac{\partial V}{\partial\vartheta} - \omega\sin\vartheta. \qquad (2.50)$$

Introducing again the Fourier series $\omega_0 = \Sigma\omega_n \left\{ \begin{matrix} \cos n\vartheta \\ \sin n\vartheta \end{matrix} \right\}$ we get (using the equation $H(\omega) = 0$)

$$w_n = (\bar{A}s_1 + \bar{B} + 1)\left\{ C_1\frac{\partial y_{n_1}}{\partial\vartheta} + C_2\frac{\partial y_{n_2}}{\partial\vartheta} \right\} + (\bar{A}s_2 + \bar{B} + 1)\left\{ C_3\frac{\partial\bar{y}_{n_1}}{\partial\vartheta} + C_4\frac{\partial\bar{y}_{n_2}}{\partial\vartheta} \right\} +$$
$$+ B_1\frac{y^*_{n_1}}{\partial\vartheta} + B_2\frac{y^*_{n_2}}{\partial\vartheta} - \frac{n^2}{2\sin\vartheta}\,.\,\{B_3 y^*_{n_1} + B_4 y^*_{n_2}\}\,. \qquad (2.51)$$

It should be noted that in this way it is assumed that the solution of $H(u) = 0$ is

$$u = \sum_0^{\infty} (B_{1_n} y^*_{n_1} + B_{2_n} y^*_{n_2})\,\begin{matrix} \cos n\varphi \\ \sin n\varphi \end{matrix}$$

and the solution of $H(\omega) = 0$ is

$$\omega = \sum_0^{\infty} (B_{3_n} y^*_{n_1} + B_{4_n} y^*_{n_2})\,\begin{matrix} \cos n\varphi \\ \sin n\varphi \end{matrix}$$

For the sake of simplicity the suffix n has been omitted in the integration constants. With a view to obtaining a result which is in accordance with HAVERS' result we put

$$(\bar{A}\,s_1 + \bar{B} + 1)C_1 = \frac{1}{2(1-\nu)}\{c_3 - i\,c_4\}\;(\bar{A}\,s_2 + \bar{B} + 1)C_3 = \frac{1}{2(1-\nu)}\{c_3 + i\,c_4\}$$

$$(\bar{A}\,s_1 + \bar{B} + 1)C_2 = \frac{1}{2(1-\nu)}\{c_1 + i\,c_2\}\;(\bar{A}\,s_2 + B_1 + 1)C_4 = \frac{1}{2(1-\nu)}\{c_1 - i\,c_2\} \tag{2.52}$$

and

$$B_1 = \frac{b_1 - n\,b_3}{n(n-1)(1-\nu)},\; B_2 = \frac{b_2 + n\,b_4}{n(n-1)(1-\nu)},\; B_3 = \frac{-2\,b_3}{n(n-1)(1-\nu)},\; B_4 = \frac{-2\,b_4}{n(n-1)(1-\nu)} \tag{2.53}$$

Denoting $\frac{1}{n(n-1)}\,y^*_{n_1}$ by S_{n_1}, $\frac{1}{n(n-1)}\,y^*_{n_2}$ by S_{n_2} and differentiation with respect to ϑ by a dot, and introducing $\psi = \frac{\pi}{2} - \vartheta$, we obtain (this is done for $n \geqslant 2$; for $n < 2$, the definitions of S_{n_1} and S_{n_2} are given by eqs. (2.32a/b) and (2.33a/b) and $B_1 = b_1 - n\,b_3$, $B_2 = b_2 + n\,b_4$, $B_3 = -2\,b_3$ and $B_4 = -2\,b_4$)

$$w_n = \frac{1}{1-\nu}\{c_1\,\dot{T}_{n_1} + c_2\,\dot{T}_{n_2} + c_3\,\dot{T}_{n_3} + c_4\,\dot{T}_{n_4} + b_1\,\dot{S}_{n_1} + b\;\dot{S}_{n_2}\} + $$
$$+ \frac{n\,b_3}{1-\nu}\left\{\frac{n\,S_{n_1}}{\cos\psi} - \dot{S}_{n_1}\right\} + \frac{n\,b_4}{1-\nu}\left\{\frac{n\,S_{n_2}}{\cos\psi} + \dot{S}_{n_2}\right\} \tag{2.54}$$

$$v_n = \mp\frac{n}{(1-\nu)\cos\psi}\,[c_1\,T_{n_1} + c_2\,T_{n_2} + c_3\,T_{n_3} + c_4\,T_{n_4} + b_1\,S_{n_1} + b_2\,S_{n_2}] + $$
$$\mp\frac{n\,b_3}{1-\nu}\left\{\dot{S}_{n_1} - \frac{n}{\cos\psi}\,S_{n_1}\right\} \mp \frac{n\,b_4}{1-\nu}\left\{\dot{S}_{n_2} + \frac{n}{\cos\psi}S_{n_2}\right\} \tag{2.55}$$

$$u_n = \frac{b^2}{1-\nu^2}\{-c_1\,T_{n_2} + c_2\,T_{n_1} + c_3\,T_{n_4} - c_4\,T_{n_3}\} + $$
$$+ \frac{1}{1-\nu}\{b_1\,S_{n_1} + b_2\,S_{n_2} - b_3\,n\,S_{n_1} + b_4\,n\,S_{n_2}\}. \tag{2.56}$$

We will now establish the formulae which give the amplitude of the forces and moments occurring in the shell, as excited by the displacements

$$u_n\,\begin{matrix}\cos n\,\varphi\\ \sin n\,\varphi\end{matrix};\; v_n\,\begin{matrix}\sin n\,\varphi\\ \cos n\,\varphi\end{matrix}\;\text{and}\; w_n\,\begin{matrix}\cos n\,\varphi\\ \sin n\,\varphi\end{matrix}$$

Using the eq. (2.7a/f) and eq. (2.8d) and (2.8e) and neglecting k against unity we arrive at

$$N_{\varphi\varphi_n} = c_1\,\frac{B}{a}\left\{\operatorname{tg}\psi\,\dot{T}_{n_1} - \frac{n^2}{\cos^2\psi}\,T_{n_1} - b^2\,T_{n_2}\right\} + c_2\,\frac{B}{a}\left\{\operatorname{tg}\psi\,\dot{T}_{n_2} - \frac{n^2}{\cos^2\psi}\,T_{n_2} + b^2\,T_{n_1}\right\} + $$
$$+ c_3\,\frac{B}{a}\left\{\operatorname{tg}\psi\,\dot{T}_{n_3} - \frac{n^2}{\cos^2\psi}\,T_{n_3} + b^2\,T_{n_4}\right\} + c_4\,\frac{B}{a}\left\{\operatorname{tg}\psi\,\dot{T}_{n_4} - \frac{n^2}{\cos^2\psi}\,T_{n_4} - b^2\,T_{n_3}\right\} + $$
$$- b_1\,\frac{B}{a}\,(\ddot{S}_{n_1} + S_{n_1}) - b_2\,\frac{B}{a}\,(\ddot{S}_{n_2} + S_{n_2}) - b_4\,\frac{B}{a}\,n\left\{(\ddot{S}_{n_2} + S_{n_2}) + n\left(\frac{S_{n_2}}{\cos\psi}\right)^{\cdot}\right\} \tag{2.57}$$

$$N_{\vartheta\vartheta_n} = c_1\,\frac{B}{a}\left\{\frac{n^2}{\cos^2\psi}\,T_{n_1} - \operatorname{tg}\psi\,\dot{T}_{n_1}\right\} + c_2\,\frac{B}{a}\left\{\frac{n^2}{\cos^2\psi}\,T_{n_2} - \operatorname{tg}\psi\,\dot{T}_{n_2}\right\} + $$
$$+ c_3\,\frac{B}{a}\left\{\frac{n^2}{\cos^2\psi}\,T_{n_3} - \operatorname{tg}\psi\,\dot{T}_{n_3}\right\} + c_4\,\frac{B}{a}\left\{\frac{n^2}{\cos^2\psi}\,T_{n_4} - \operatorname{tg}\psi\,\dot{T}_{n_4}\right\} + $$
$$+ b_1\,\frac{B}{a}\,(\ddot{S}_{n_1} + S_{n_1}) + b_2\,\frac{B}{a}\,(\ddot{S}_{n_2} + S_{n_2}) + b_4\,\frac{B}{a}\,n\left\{(\ddot{S}_{n_2} + S_{n_2}) + n\left(\frac{S_{n_2}}{\cos\psi}\right)^{\cdot}\right\} \tag{2.58}$$

$$N_{\varphi\vartheta_n} = N_{\vartheta\varphi_n} = \mp n\,\frac{B}{a}\left\{c_1\left(\frac{T_{n_1}}{\cos\psi}\right)^{\cdot} + c_2\left(\frac{T_{n_2}}{\cos\psi}\right)^{\cdot} + c_3\left(\frac{T_{n_3}}{\cos\psi}\right)^{\cdot} + c_4\left(\frac{T_{n_4}}{\cos\psi}\right)^{\cdot} + b_1\left(\frac{S_{n_1}}{\cos\psi}\right)^{\cdot} + \right.$$
$$\left. + b_2\left(\frac{S_{n_2}}{\cos\psi}\right)^{\cdot} + b_4\left[(\ddot{S}_{n_2} + S_{n_2}) + n\left(\frac{S_{n_2}}{\cos\psi}\right)^{\cdot}\right]\right\} \tag{2.59}$$

$$M_{\varphi\vartheta n} = c_1 B \left\{ \nu T_{n_1} - \frac{1-\nu}{b^2} \left[\operatorname{tg}\psi \dot{T}_{n_2} - \left(\nu + \frac{n^2}{\cos^2\psi} \right) T_{n_2} \right] \right\} +$$
$$+ c_2 B \left\{ \nu T_{n_2} + \frac{1-\nu}{b^2} \left[\operatorname{tg}\psi \dot{T}_{n_1} - \left(\nu + \frac{n^2}{\cos^2\psi} \right) T_{n_1} \right] \right\} +$$
$$+ c_3 B \left\{ \nu T_{n_3} + \frac{1-\nu}{b^2} \left[\operatorname{tg}\psi \dot{T}_{n_4} - \left(\nu + \frac{n^2}{\cos^2\psi} \right) T_{n_4} \right] \right\} +$$
$$+ c_4 B \left\{ \nu T_{n_4} - \frac{1-\nu}{b^2} \left[\operatorname{tg}\psi \dot{T}_{n_3} - \left(\nu + \frac{n^2}{\cos^2\psi} \right) T_{n_3} \right] \right\} +$$
$$+ b_3 n^2 B k \left(\frac{S_{n_1}}{\cos\psi} \right)^{\cdot} + b_4 n^2 B k \left(\frac{S_{n_2}}{\cos\psi} \right)^{\cdot} \qquad (2.60)$$

$$M_{\vartheta\varphi n} = c_1 B \left\{ T_{n_1} + \frac{1-\nu}{b^2} \left[\operatorname{tg}\psi \dot{T}_{n_2} + \left(1 - \frac{n^2}{\cos^2\psi} \right) T_{n_2} \right] \right\} +$$
$$+ c_2 B \left\{ T_{n_2} - \frac{1-\nu}{b^2} \left[\operatorname{tg}\psi \dot{T}_{n_1} + \left(1 - \frac{n^2}{\cos^2\psi} \right) T_{n_1} \right] \right\} +$$
$$+ c_3 B \left\{ T_{n_3} - \frac{1-\nu}{b^2} \left[\operatorname{tg}\psi \dot{T}_{n_4} + \left(1 - \frac{n^2}{\cos^2\psi} \right) T_{n_4} \right] \right\} +$$
$$+ c_4 B \left\{ T_{n_4} + \frac{1-\nu}{b^2} \left[\operatorname{tg}\psi \dot{T}_{n_3} + \left(1 - \frac{n^2}{\cos^2\psi} \right) T_{n_3} \right] \right\} +$$
$$- b_3 n^2 B k \left(\frac{S_{n_1}}{\cos\psi} \right)^{\cdot} - b_4 n^2 B k \left(\frac{S_{n_2}}{\cos\psi} \right)^{\cdot} \qquad (2.61)$$

$$M_{\varphi\varphi} = - M_{\vartheta\vartheta_n} = \pm nB \left[c_1 \left\{ \frac{1-\nu}{b^2} \left(\frac{T_{n_2}}{\cos\psi} \right)^{\cdot} + k \left(\frac{T_{n_1}}{\cos\psi} \right)^{\cdot} \right\} + c_2 \left\{ - \frac{1-\nu}{b^2} \left(\frac{T_{n_1}}{\cos\psi} \right)^{\cdot} + k \left(\frac{T_{n_2}}{\cos\psi} \right)^{\cdot} \right\} + \right.$$
$$\left. + c_3 \left\{ - \frac{1-\nu}{b^2} \left(\frac{T_{n_4}}{\cos\psi} \right)^{\cdot} + k \left(\frac{T_{n_3}}{\cos\psi} \right)^{\cdot} \right\} + c_4 \left\{ \frac{1-\nu}{b^2} \left(\frac{T_n}{\cos\psi} \right)^{\cdot} + k \left(\frac{T_{n_4}}{\cos\psi} \right)^{\cdot} \right\} \right] +$$
$$\pm b_3 n k B (\ddot{S}_{n_1} + S_{n_1}) \pm b_4 n k B (\ddot{S}_{n_2} + S_{n_2}) \qquad (2.62)$$

$$Q_{\varphi\xi_n} = \pm \frac{B}{a} \frac{n}{\cos\psi} (c_1 T_{n_1} + c_2 T_{n_2} + c_3 T_{n_3} + c_4 T_{n_4}) \qquad (2.63)$$

$$Q_{\vartheta\xi_n} = - \frac{B}{a} (c_1 \dot{T}_{n_1} + c_2 \dot{T}_{n_2} + c_3 \dot{T}_{n_3} + c_4 \dot{T}_{n_4}). \qquad (2.64)$$

It should be observed that only b_1 and b_2 give rise to membrane stresses. The term with b_4 in $N_{\varphi\varphi_n}$, $N_{\vartheta\vartheta_n}$ and $N_{\varphi\vartheta n}$ vanishes except for $n = 1$.

2.5 *The arbitrary constants.*

As can be seen from the foregoing review, the solution is determined by eight constants. Now, in general, there are two edges where we can prescribe 4 independent edge conditions, viz. u_n, v_n, w_n and $\frac{\partial u_n}{\partial \vartheta}$. It is, however, possible to give the edge forces, as conditions to determine the constants. Since there are five edge forces at each edge, and we have only four constants, we replace the moment $M_{\vartheta\vartheta}$ by a system of forces tangential and normal to the shell.

Instead of the force $N_{\vartheta\varphi n}$ we find in this manner

$$N^*_{\varphi\vartheta n} = N_{\varphi\vartheta n} + \frac{1}{a} M_{\vartheta\vartheta n} \qquad (2.65)$$

and instead of $Q_{\vartheta\xi_n}$ we have

$$Q^*_{\vartheta\xi_n} = Q_{\vartheta\xi_n} + \frac{n}{a\cos\psi} M_{\vartheta\vartheta n}. \qquad (2.66)$$

2.6 *Concluding remarks of chapter 2.*

With the results derived here for the state of stress and strain in a not shallow spherical shell, we will analyse in chapter 3 of this report some technically important cases of sphere loading. It will be seen that the formulae derived here give rise to a very elegant analysis, which yields the results in a relatively simple way.

3 Application to the problem of an axial force, a transverse force and a bending moment.

3.1 *Introduction of an axial force.*

The actual structure is such as given in figure 1. For the sake of simplicity, however, we consider the structure given in figure 4. This simplification is perfectly acceptable, since we are mainly interested in the additional bending stresses occurring at the junction of pipe and sphere, and we may assume that the edges are located so far apart that they do not influence each other.

Having thus symmetrized the construction and its loading with respect to $\psi = 0$, it will be clear that the stresses and displacements will be given by symmetric functions.

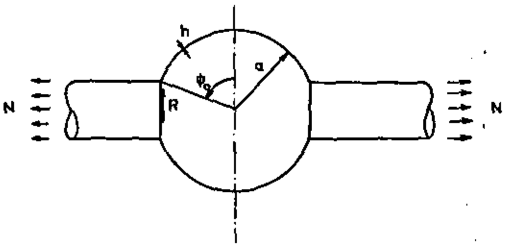

Fig. 4. Symmetrical loading by normal forces.

Now for $n = 0$, the case of rotational symmetry which we are considering here,

$$\xi_1 = \xi_2 = \psi \quad \text{and } \chi = 0 \quad \Lambda = \sqrt{\cos\psi} \tag{3.1}$$

$$S_{0_1} = \sin\psi \tag{3.2}$$

$$S_{0_2} = \sin\psi \ln \frac{1-\sin\psi}{1+\sin\psi} + 2.$$

Introducing this in eq. (2.55) for example and using the eqs. (2.45a/b), (2.46a/b), (3.1) and (3.2) we get

$$u_n = \frac{b^2}{1-v^2}\left\{ -c_1 \frac{e^{-\beta\psi}\sin\beta\psi}{\sqrt{\cos\psi}} + c_2 \frac{e^{-\beta\psi}\cos\beta\psi}{\sqrt{\cos\psi}} + c_3 \frac{e^{\beta\psi}\sin\beta\psi}{\sqrt{\cos\psi}} - c_4 \frac{e^{\beta\psi}\cos\beta\psi}{\sqrt{\cos\psi}} \right\} + \frac{1}{1-v}\left\{ b_1 \sin\psi + b_2 \left(\sin\psi \ln\frac{1-\sin\psi}{1+\sin\psi} + 2\right)\right\}. \tag{3.3}$$

To make u_n symmetric we have to choose

$$\left.\begin{array}{ll} c_4 = -c_2 & b_1 = 0 \\ c_3 = c_1 & \end{array}\right\}. \tag{3.4}$$

The constants b_3 and b_4 do not occur for $n = 0$.

We have thus reduced the problem to finding the three coefficients c_1, c_2 and b_2.

Now, as mentioned in the introduction, at the junction of pipe and sphere there is a heavy frame; the neutral hole reinforcement. We assume that this frame can be considered as rigid.

Denoting by ψ_0 the ψ-coordinate of the edge, we have the following edge conditions (see fig. 5):

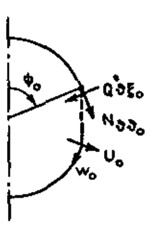

Fig. 5. Displacements and forces along the edge.

$$\left(\frac{\partial u_0}{\partial \vartheta}\right)_{\psi=\psi_0} = 0 \tag{3.5a}$$

$$(u_0)_{\psi_0} \cos\psi_0 + (\omega_0)_{\psi_0} \sin\psi_0 = 0 \tag{3.5b}$$

$$(N_{\vartheta\vartheta_0})_{\psi_0} \cos\psi_0 - (Q_{\vartheta_0})^*_{\psi_0} \sin\psi_0 = N \tag{3.5c}$$

where N is the load per unit of length of the circumference of the hole.

Using eq. (2.66), (2.58), (2.64) and (3.4), eq. (3.5c) becomes

$$b_2 \frac{B}{a} (\ddot{S}_{0_2} + S_{0_2}) \cos\psi_0 = N$$

or

$$b_2 = -\frac{N\cos\psi_0}{2}\,\frac{a}{B} \tag{3.6}$$

We introduce the abbreviations

$$\Lambda_0 = \sqrt{\cos\psi_0}$$

$$\alpha_1 = T_{0_1} + T_{0_3} = \frac{2}{\Lambda_0} \cosh\beta\psi_0 \cos\beta\psi_0$$

$$\alpha_2 = T_{0_2} - T_{0_4} = \frac{2}{\Lambda_0} \sinh\beta\psi_0 \sin\beta\psi_0$$

$$\alpha_3 = \dot{T}_{0_1} + \dot{T}_{0_3} = -\frac{2\beta}{\Lambda_0} \sinh\beta\psi_0 \cos\beta\psi_0 + \frac{2\beta}{\Lambda_0} \cosh\beta\psi_0 \sin\beta\psi_0 - \frac{\operatorname{tg}\psi_0}{\Lambda_0} \cosh\beta\psi_0 \cos\beta\psi_0$$

$$\alpha_4 = \dot{T}_{0_2} - \dot{T}_{0_4} = +\frac{2\beta}{\Lambda_0} \cosh\beta\psi_0 \sin\beta\psi_0 + \frac{2\beta}{\Lambda_0} \sinh\beta\psi_0 \cos\beta\psi_0 + \frac{\operatorname{tg}\psi_0}{\Lambda_0} \sinh\beta\psi_0 \sin\beta\psi_0 .$$

Then the solution of the eqs. (3.5a) and (3.5b) proves to be

$$c_2 = b_2 \frac{1+\nu}{b^2} \frac{\dot{S}_{0_2}\left(\alpha_2 \cos\psi_0 - \frac{1+\nu}{b^2}\alpha_3 \sin\psi_0\right) - \frac{2}{\cos\psi_0}\alpha_4}{(\alpha_1\alpha_4 - \alpha_2\alpha_3)\cos\psi_0 + \frac{1+\nu}{b^2}(\alpha_3^2 + \alpha_4^2)\sin\psi_0} \tag{3.7}$$

$$c_1 = b_2 \frac{1+\nu}{b^2} \frac{\dot{S}_{0_2}\left(\alpha_1 \cos\psi_0 + \frac{1+\nu}{b^2}\alpha_4 \sin\psi_0\right) - \frac{2}{\cos\psi_0}\alpha_3}{(\alpha_1\alpha_4 - \alpha_2\alpha_3)\cos\psi_0 + \frac{1+\nu}{b^2}(\alpha_3^2 + \alpha_4^2)\sin\psi_0} \tag{3.8}$$

where $\dot{S}_{0_2} = 2\operatorname{tg}\psi - \cos\psi \ln \dfrac{1-\sin\psi}{1+\sin\psi}$.

The forces and moments acting on the edge are given by eqs. (2.57), (2.58), (2.60) and (2.61). Using the above mentioned abbreviations they give

$$(N_{\varphi\varphi_0})_{\psi=\psi_0} = \frac{B}{a}\left[c_1(\alpha_3 \operatorname{tg}\psi_0 - b^2\alpha_2) + c_2(\alpha_4 \operatorname{tg}\psi_0 + b^2\alpha_1) + b_2 \frac{2}{\cos^2\psi_0}\right] \tag{3.9}$$

$$(N_{\vartheta\vartheta_0})_{\psi=\psi_0} = -\frac{B}{a}\left[c_1\alpha_3 \operatorname{tg}\psi_0 + c_2\alpha_4 \operatorname{tg}\psi_0 + b_2 \frac{2}{\cos^2\psi_0}\right] \tag{3.10}$$

$$(M_{\vartheta\varphi_0})_{\psi=\psi_0} = B\left[c_1\left\{\alpha_1 + \frac{1-\nu}{b^2}(\alpha_4 \operatorname{tg}\psi_0 + \alpha_2)\right\} + c_2\left\{\alpha_2 - \frac{1-\nu}{b^2}(\alpha_3 \operatorname{tg}\psi_0 + \alpha_1)\right\}\right] \tag{3.11}$$

$$(M_{\varphi\vartheta_0})_{\psi=\psi_0} = B\left[c_1\left\{\alpha_1 - \frac{1-\nu}{b^2}(\alpha_4 \operatorname{tg}\psi_0 - \alpha_2)\right\} + c_2\left\{\nu\alpha_2 + \frac{1-\nu}{b^2}(\alpha_3 \operatorname{tg}\psi_0 - \nu\alpha_1)\right\}\right]. \tag{3.12}$$

The stresses occurring in the shell at the edge are given by

$$\sigma_a = \frac{(N_{\vartheta\vartheta_0})_{\psi_0}}{h} \pm \frac{6}{h^2}(M_{\vartheta\varphi_0})_{\psi_0} \tag{3.13}$$

and

$$\sigma_t = \frac{1}{h}(N_{\varphi\varphi_0})_{\psi_0} \pm \frac{6}{h^2}(M_{\varphi\vartheta_0})_{\psi_0}. \tag{3.14}$$

The + sign refers to the inner side of the shell, the — sign to the outer side. The stresses are defined as in fig. 6.

We thus have solded the problem of finding the stresses due to an axial force $2\pi a \cos\psi_0 N$, introduced through a rigid pipe at the section $\psi = \psi_0$.

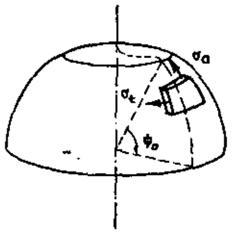

Fig. 6. Orientation of the stresses σ_a en σ_t.

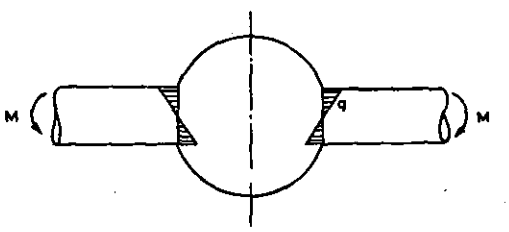

Fig. 7. Symmetrical loading by bending moment.

3.2 *Introduction of a bending moment.*

Here too, we symmetrize the construction and its load as shown in figure 7. We assume that the displacements can be expressed by:

$$u_0 = u_1 \cos\varphi \qquad v_0 = v_1 \sin\varphi \qquad w_0 = w_1 \cos\varphi. \tag{3.15}$$

This means that the bending moment is applied as a linearly varying load along the edge. This is the usual assumption in bending theory.

Since, for instance, v_1 must consist of symmetric functions, the coefficients c_1, c_2, c_3, c_4, b_1, b_2, b_3 and b_4 have to obey certain conditions. To find these conditions we make use of eqs. (2.55), (2.45a/b), ((2.46a/b), and of the fact that

$$S_{11} = \cos\psi \qquad \dot{S}_{11} = \sin\psi$$

$$S_{12} = \cos\psi \ln \frac{1-\sin\psi}{1+\sin\psi} - 2\,\mathrm{tg}\,\psi \qquad \dot{S}_{12} = \frac{2}{\cos^2\psi} + 2 + \sin\psi \ln \frac{1-\sin\psi}{1+\sin\psi}.$$

We get

$$\begin{aligned} v_1 = &-\frac{1}{1-\nu}\left[\frac{1}{\Lambda\cos\psi}\left\{c_1 e^{-\beta\xi_1}(\cos\beta\xi_2\cos\chi + \sin\beta\xi_2\sin\chi) + c_2 e^{-\beta\xi_1}(\sin\beta\xi_2\cos\chi + \right.\right.\\ &\left. - \cos\beta\xi_2\sin\chi) + c_3 e^{+\beta\xi_1}(\cos\beta\xi_2\cos\chi - \sin\beta\xi_2\sin\chi) + c_4 e^{+\beta\xi_1}(\sin\beta\xi_2\cos\chi + \cos\beta\xi_2\sin\chi)\right\} + \\ &+ \frac{1}{\cos\psi}\left\{b_1\cos\psi + b_2\left(\cos\psi\ln\frac{1-\sin\psi}{1+\sin\psi} - 2\,\mathrm{tg}\,\psi\right)\right\} + \\ &\left. + b_3\{\sin\psi - 1\} + b_4\left\{\left(\frac{2}{\cos^2\psi} + 2 + \sin\psi\ln\frac{1-\sin\psi}{1+\sin\psi}\right) + \frac{1}{\cos\psi}\left(\cos\psi\ln\frac{1-\sin\psi}{1+\sin\psi} - 2\,\mathrm{tg}\,\psi\right)\right\}\right]. \end{aligned} \tag{3.16a}$$

Since ξ_1 and ξ_2 are asymmetric and χ is symmetric, we find that

$$\left.\begin{aligned} c_1 &= c_3 \qquad & b_3 &= 0 \\ c_4 &= -c_2 \qquad & b_4 &= -b_2 \end{aligned}\right\}. \tag{3.16b}$$

Thus, we have reduced the problem to the determination of the four constants c_1, c_2, b_1 and b_2. To do this we use the edge conditions.

First we have the conditions that there is no displacement of the edge in its plane

$$(u_1)_{\psi_0}\cos\psi_0 + (w_1)_{\psi_0}\sin\psi_0 = 0 \tag{3.17a}$$

$$(v_1)_{\psi_0} = 0. \tag{3.17b}$$

Further we have the condition that the angle between the shell of the sphere and the pipe must remain the same after the deformation

$$\frac{1}{a}\left(\frac{\partial u_1}{\partial\psi}\right)_{\psi_0} = -\frac{(u_1)_{\psi_0}\sin\psi_0 - (w_1)_{\psi_0}\cos\psi_0}{a\cos\psi_0}. \tag{3.17c}$$

At last, we have the condition that the resultant of the forces and moments working along the edge must be equal to the applied moment M.

Denoting the amplitude of the linearly varying load by q, we have

$$M = \pi R^2 q \qquad R = a\cos\psi_0.$$

Now the resultant of the force $N_{\vartheta\vartheta} = N_{\vartheta\vartheta_1}\cos\varphi$ is $\pi R^2 N_{\vartheta\vartheta_1}\cos\psi_0$

the resultant of the force $Q^*_{\vartheta\xi} = Q^*_{\vartheta\xi_1}\cos\varphi$ is $-\pi R^2 Q_{\vartheta\xi_1}\sin\psi_0$

the resultant of the moment $M_{\vartheta\varphi} = M_{\vartheta\varphi_1}\cos\varphi$ is $-\pi R\, M_{\vartheta\varphi_1}$.

This gives for the last condition

$$N_{\vartheta\vartheta_1}\cos\psi_0 - Q^*_{\vartheta\xi_1}\sin\psi_0 - \frac{M\vartheta\varphi_1}{a\cos\psi_0} = q. \tag{3.17a}$$

Introduce the following abbreviations

$$\beta_1 = T_{11} + T_{13} = \frac{2}{\Lambda_1}\cosh\beta\xi_1\cos\beta\xi_2\cos\chi_1 - \frac{2}{\Lambda_1}\sinh\beta\xi_1\sin\beta\xi_2\sin\chi_1$$

$$\beta_2 = T_{12} - T_{14} = -\frac{2}{\Lambda_1}\sinh\beta\xi_1\sin\beta\xi_2\cos\chi_1 - \frac{2}{\Lambda_1}\cosh\beta\xi_1\cos\beta\xi_2\sin\chi_1$$

$$\begin{aligned} \beta_3 = \dot{T}_{11} + \dot{T}_{13} = &-\frac{2\,b\,\Lambda_1}{\cos\psi_0}\sinh\beta\xi_1\cos\beta\xi_2\cos\left(\chi_1 - \frac{\pi}{4}\right) - \frac{2\,b\,\Lambda_1}{\cos\psi_0}\cosh\beta\xi_1\sin\beta\xi_2\sin\left(\chi_1 - \frac{\pi}{4}\right) + \\ &- \frac{\sin 2\psi_0}{2\,\Lambda_1^{5}}\cosh\beta\xi_1\cos\beta\xi_2\cos 5\,\chi_1 + \frac{\sin 2\psi_0}{2\,\Lambda_1^{5}}\sinh\beta\xi_1\sin\beta\xi_2\sin 5\,\chi_1 \end{aligned}$$

$$\beta_4 = \dot{T}_{12} - \dot{T}_{34} = \frac{2\,b\,\Lambda_1}{\cos\psi_0}\cosh\beta\xi_1\sin\beta\xi_2\cos\left(\chi_1 - \frac{\pi}{4}\right) - \frac{2\,b\,\Lambda_1}{\cos\psi_0}\sinh\beta\xi_1\cos\beta\xi_2\sin\left(\chi_1 - \frac{\pi}{4}\right) +$$

$$+ \frac{\sin 2\,\psi_0}{2\,\Lambda_1^5}\sinh\beta\xi_1\sin\beta\xi_2\cos 5\,\chi_1 + \frac{\sin 2\,\psi_0}{2\,\Lambda_1^4}\cosh\beta\xi_1\cos\beta\xi_2\sin 5\,\chi_1$$

where $\Lambda_1^8 = \cos^4\psi_0 + \rho^2$, $\operatorname{tg} 4\,\chi_1 = \frac{\rho}{\cos^2\psi_0}$, $\rho = \frac{h}{2\,a\sqrt{3(1-\nu^2)}}$.

It is assumed that in the above abbreviations ξ_1 and ξ_2 have values belonging to ψ_0.

The eqs. (3.17a/d) become

$$c_1\left\{\beta_3\sin\psi_0 - \frac{b^2}{1+\nu}\beta_2\cos\psi_0\right\} + c_2\left\{\beta_4\sin\psi_0 + \frac{b^2}{1+\nu}\beta_1\cos\psi_0\right\} + b_1 - b_2 S_{12}\operatorname{tg}\psi_0 = 0 \tag{3.18a}$$

$$c_1\left\{-\beta_3\cos\psi_0 - \frac{b^2}{1+\nu}\beta_2\sin\psi_0 + \frac{b^2}{1+\nu}\beta_4\cos\psi_0\right\} + c_2\left\{-\beta_4\cos\psi_0 + \frac{b^2}{1+\nu}\beta_1\sin\psi_0 + \right.$$

$$\left. - \frac{b^2}{1+\nu}\beta_3\cos\psi_0\right\} - b_1\sin\psi_0\cos\psi_0 + b_2\dot{S}_{12} = 0 \tag{3.18b}$$

$$c_1\frac{\beta_1}{\cos\psi_0} + c_2\frac{\beta_2}{\cos\psi_0} + b_1 - b_2\dot{S}_{12} = 0 \tag{3.18c}$$

$$c_1 k\sin\psi_0\,(\beta_3 - \beta_1\operatorname{tg}\psi_0) + c_2 k\sin\psi_0\,(\beta_4 - \beta_2\operatorname{tg}\psi_0) - 4(1+k)b_2 = q\frac{a}{B}\cos^2\psi_0 = \frac{M}{\pi a B}. \tag{3.18d}$$

This system can now be simplified in a rather remarkable way.

Multiplying eq. (3.18a) with $\cos\psi_0$ and adding to it eq. (3.18b) multiplied with $\sin\psi_0$ and subtracting from the result eq. (3.18c) multiplied with $\cos^3\psi_0$ gives

$$c_1\left\{\frac{b^2}{1+\nu}(\beta_4\sin\psi_0\cos\psi_0 - \beta_2) - \beta_1\cos^2\psi_0\right\} - c_2\left\{\frac{b^2}{1+\nu}(\beta_3\cos\psi_0\sin\psi_0 - \beta_1) + \beta_2\cos^2\psi_0\right\} +$$

$$+ b_2\dot{S}_{12}\cos^3\psi_0 = 0. \tag{3.19a}$$

Multiplying eqs. (3.18a) and (3.18c) with $\cos\psi_0$ and subtracting yields

$$c_1\left\{(\beta_3\cos\psi_0\sin\psi_0 - \beta_1) - \frac{b^2}{1+\nu}\beta_2\cos^2\psi_0\right\} + c_2\left\{(\beta_4\sin\psi_0\cos\psi_0 - \beta_2) + \frac{b^2}{1+\nu}\beta_1\cos^2\psi_0\right\} +$$

$$+ \frac{4}{\cos\psi_0}b_2 = 0. \tag{3.19b}$$

The solution of the eqs. (3.19a) and (3.19b) is:

$$c_1 = -b_2\frac{\dot{S}_{12}\cos^3\psi_0\left[\overline{\beta}_2 + \frac{b^2}{1+\nu}\beta_1\cos^2\psi_0\right] + \frac{4}{\cos\psi_0}\left[\frac{b^2}{1+\nu}\overline{\beta}_1 + \beta_2\cos^2\psi_0\right]}{\left[\frac{b^2}{1+\nu}\overline{\beta}_2 - \beta_1\cos^2\psi_0\right]\left[\overline{\beta}_2 + \frac{b^2}{1+\nu}\beta_1\cos^2\psi_0\right] + \left[\frac{b^2}{1+\nu}\overline{\beta}_1 + \beta_2\cos^2\psi_0\right]\left[\overline{\beta}_1 - \frac{b^2}{1+\nu}\beta_2\cos^2\psi_0\right]} \tag{3.20a}$$

$$c_2 = +b_2\frac{\dot{S}_{12}\cos^3\psi_0\left[\overline{\beta}_1 - \frac{b^2}{1+\nu}\beta_2\cos^2\psi_0\right] - \frac{4}{\cos\psi_0}\left[\frac{b^2}{1+\nu}\overline{\beta}_2 - \beta_1\cos^2\psi_0\right]}{\left[\frac{b^2}{1+\nu}\overline{\beta}_2 - \beta_1\cos^2\psi_0\right]\left[\overline{\beta}_2 + \frac{b^2}{1+\nu}\beta_1\cos^2\psi_0\right] + \left[\frac{b^2}{1+\nu}\overline{\beta}_1 + \beta_2\cos^2\psi_0\right]\left[\overline{\beta}_1 - \frac{b^2}{1+\nu}\beta_2\cos^2\psi_0\right]} \tag{3.20b}$$

where $\overline{\beta}_1 = \beta_3\cos\psi_0\sin\psi_0 - \beta_1$, $\overline{\beta}_2 = \beta_4\cos\psi_0\sin\psi_0 - \beta_2$.

b_1 can be determined by using the following equation which is a result of adding eq. (3.18a) multiplied with $\cos\psi_0$ and eq. (3.18b) multiplied with $\sin\psi_0$.

$$\frac{b^2}{1+\nu}\overline{\beta}_2 c_1 - \frac{b^2}{1+\nu}\overline{\beta}_1 c_2 + b_1\cos^3\psi_0 = 0. \tag{3.20c}$$

b_2 follows from eq. (3.18d) which can be written as

$$\frac{c_1 k}{\cos\psi_0}[\overline{\beta}_1 + \beta_1\cos^2\psi_0] + \frac{c_2 k}{\cos\psi_0}[\overline{\beta}_2 + \beta_2\cos^2\psi_0] - 4(1+k)b_2 = \frac{M}{\pi a B}. \tag{3.20d}$$

Thus, the unknown quantities can be determined.

We will now give the forces and moments occurring in the shell at the edge, as derived from the eqs. (2.57)—(2.62).

$$N_{\varphi\varphi_1} = c_1 \frac{B}{a} \frac{1}{\cos^2\psi_0} [\overline{\beta}_1 - b^2\beta_2 \cos^2\psi_0] + c_2 \frac{B}{a} \frac{1}{\cos^2\psi_0} [\overline{\beta}_2 + b^2\beta_1 \cos^2\psi_0] + 4\, b_2 \frac{B}{a} \frac{1}{\cos^3\psi_0} \tag{3.21a}$$

$$N_{\vartheta\vartheta_1} = - c_1 \frac{B}{a} \frac{1}{\cos^2\psi_0} \overline{\beta}_1 - c_2 \frac{B}{a} \frac{1}{\cos^2\psi_0} \overline{\beta}_2 - 4\, b_2 \frac{B}{a} \frac{1}{\cos^3\psi_0} \tag{3.21b}$$

$$N_{\varphi\vartheta_1} = N_{\vartheta\varphi_1} = \frac{-c_1}{\sin\psi_0 \cos^2\psi_0} \frac{B}{a} [\overline{\beta}_1 + \beta_1 \cos^2\psi_0] - \frac{c_2}{\sin\psi_0 \cos^2\psi_0} \frac{B}{a} [\overline{\beta}_2 + \beta_2 \cos^2\psi_0] - 4\, b_2 \frac{B}{a} \frac{\sin\psi_0}{\cos^3\psi_0} \tag{3.21c}$$

$$M_{\varphi\vartheta_1} = \frac{c_1 B}{\cos^2\psi_0} \left[\nu\beta_1 \cos^2\psi_0 - \frac{1-\nu}{b^2} \{ \overline{\beta}_2 - \nu\beta_2 \cos^2\psi_0 \} \right] + \frac{c_2 B}{\cos^2\psi_0} \left[\beta_2 \cos^2\psi_0 + \frac{1-\nu}{b^2} \{ \overline{\beta}_1 - \nu\beta_1 \cos^2\psi_0 \} \right] +$$
$$- b_2 k B \frac{4}{\cos^3\psi} . \tag{3.21d}$$

$$M_{\vartheta\varphi_1} = \frac{c_1 B}{\cos^2\psi_0} \left[\beta_1 \cos^2\psi_0 + \frac{1-\nu}{b^2} \{ \overline{\beta}_2 + \beta_2 \cos^2\psi_0 \} \right] + \frac{c_2 B}{\cos^2\psi_0} \left[\beta_2 \cos^2\psi_0 - \frac{1-\nu}{b^2} \{ \overline{\beta}_1 + \beta_1 \cos^2\psi_0 \} \right] +$$
$$+ b_2 k B \frac{4}{\cos^3\psi_0} \tag{3.21e}$$

$$M_{\varphi\varphi_1} = - M_{\vartheta\vartheta_1} = \frac{c_1 B}{\sin\psi_0 \cos^2\psi_0} \left[\frac{1-\nu}{b^2} \{ \overline{\beta}_2 + \beta_2 \cos^2\psi_0 \} + k \{ \overline{\beta}_1 + \beta_1 \cos^2\psi_0 \} \right] +$$
$$+ \frac{c_2 B}{\sin\psi_0 \cos^2\psi_0} \left[- \frac{1-\nu}{b^2} \{ \overline{\beta}_1 + \beta_1 \cos^2\psi_0 \} + k \{ \overline{\beta}_2 + \beta_2 \cos^2\psi_0 \} \right] + b_2 k B \frac{4 \sin\psi_0}{\cos^3\psi_0} \tag{3.21f}$$

The highest bending stresses occurring in the shell at $\varphi = 0$ and $\varphi = 180°$ are given by

$$\sigma_a = \frac{N_{\vartheta\vartheta_1}}{h} \pm \frac{6}{h^2} M_{\vartheta\varphi_1} \tag{3.22}$$

$$\sigma_t = \frac{1}{h} N_{\varphi\varphi_1} \pm \frac{6}{h^2} M_{\varphi\vartheta_1} . \tag{3.23}$$

The highest shear stress occurring in the shell at $\varphi = -90°$ and $\varphi = 90°$ is given by

$$\tau = \frac{1}{h} N_{\varphi\vartheta_1} + \frac{1}{ah} M_{\vartheta\vartheta_1} . \tag{3.24}$$

To obtain the stiffness parameters of the sphere under this loading we will derive formulae for the displacement and rotation of the edge relative to the section $\psi = 0$.
This displacement is given by $(u_1)_{\psi=0}$. This yields per unit of moment

$$\overline{k}_M = \frac{(u_1)_{\psi=0}}{M} = \frac{b^2}{M(1-\nu^2)} \left\{ \frac{2 \sin\chi^*}{\sqrt[8]{1+\rho^2}} c_1 + \frac{2\cos\chi^*}{\sqrt[8]{1+\rho^2}} c_2 \right\} + \frac{1}{(1-\nu)M} b_1 \tag{3.25}$$

where

$$\operatorname{tg} 4\chi^* = \rho .$$

The rotation is given by $\dfrac{(u_1)_{\psi_0} \sin\psi_0 - (w_1)_{\psi_0} \cos\psi_0}{a \cos\psi_0}$. This gives per unit of moment

$$k_M = - \frac{1}{aM} \left(\frac{\partial u}{\partial \varphi} \right)_{\psi_0} = \frac{b^2}{aM(1-\nu^2)} [-c_1\beta_4 + c_2\beta_3] + \frac{b_1}{aM(1-\nu)} \sin\psi_0 . \tag{3.26}$$

3.3 *Introduction of a transverse force.*

In order to reduce the problem of the introduction of a transverse force to the simplified problem for the sphere, anti-symmetrically loaded, we have to add a bending moment at each edge (see fig. 8). Then we may conclude that, for instance, the function u will be antisymmetric with respect to $\psi = 0$.

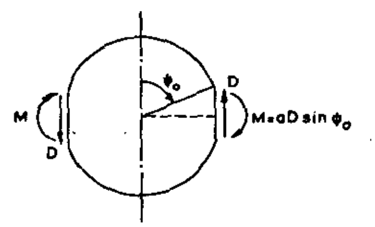

Fig. 8. Asymmetrical loading by transverse forces combined with bending moments.

We assume that the displacements can be expressed by

$$u = \bar{u}_1 \cos\varphi \qquad v = \bar{v}_1 \sin\varphi$$
$$w = \bar{w}_1 \cos\varphi. \tag{3.27}$$

To find the conditions for the coefficients c_1, c_2, c_3, c_4, b_1, b_2, b_3 and b_4 in order that e.g. $\bar{v}_1$ is antisymmetric, we make use of eqs. (2.55), (2.46a/b) and of the eqs. given for S_{11}, S_{12}, $\dot{S}_{11}$ and $\dot{S}_{12}$. The result has already been established as eq. (3.16a). We see that in order that v_1 be antisymmetrical with respect to $\psi = 0$,

$$\left.\begin{aligned} c_3 &= -c_1 \qquad & b_4 &= 0 \\ c_4 &= c_2 \qquad & b_3 &= b_1 \end{aligned}\right\} \tag{3.28}$$

To determine the four remaining constants, we use the edge conditions. Again assuming that the attached reinforcement is rigid, we have the displacement conditions (see e.g. eq. (3.17a), (3.17b) and (3.17c), which are similar)

$$(\bar{u}_1)_{\psi_0} \cos\psi_0 + (\bar{w}_1)_{\psi_0} \sin\psi_0 = 0 \tag{3.29a}$$

$$(\bar{v}_1)_{\psi_0} \qquad\qquad = 0 \tag{3.29b}$$

$$\left(\frac{1}{a}\right)\left(\frac{\partial \bar{w}_1}{\partial\psi}\right)_{\psi_0} = -\frac{(\bar{u}_1)_{\psi_0}\sin\psi_0 - (\bar{w}_1)_{\psi_0}\cos\psi_0}{a\cos\psi_0}. \tag{3.29c}$$

We assume that the distribution of the transverse force D along the edge is sinusoidal with amplitude $\bar{q}$. The resultant of the forces along the edge in transverse direction must be equal to D.

The resultant of the force $\bar{N}_{\vartheta\vartheta} = \bar{N}_{\vartheta\vartheta_1}\cos\varphi$ is $-\pi R \bar{N}_{\vartheta\vartheta}\sin\psi_0$.

The resultant of the force $\bar{Q}^*_{\vartheta\xi} = \bar{Q}^*_{\vartheta\xi_1}\cos\varphi$ is $-\pi R\,\bar{Q}^*_{\vartheta\xi_1}\cos\psi_0$.

The resultant of the force $\bar{N}^*_{\vartheta\varphi} = \bar{N}^*_{\vartheta\varphi_1}\sin\varphi$ is $\pi R\,\bar{N}^*_{\vartheta\varphi_1}$.

Thus we get

$$\bar{N}^*_{\vartheta\varphi_1} - \bar{Q}^*_{\vartheta\xi_1}\cos\psi_0 - \bar{N}_{\vartheta\vartheta_1}\sin\psi_0 = \bar{q} = \frac{D}{\pi R}. \tag{3.29d}$$

The equation giving the equilibrium of the moments is satisfied identically (except for terms of order k) by virtue of eqs. (3.28) and eqs. (3.29d) and (3.17d). To solve the system of equations (3.29a/d) we first introduce the following abbreviations

$$\beta_1^* = -\frac{2}{\Lambda_1}\sinh\beta\xi_1\cos\beta\xi_2\cos\chi_1 + \frac{2}{\Lambda_1}\cosh\beta\xi_1\sin\beta\xi_2\sin\chi_1 = T_{11} - T_{13}$$

$$\beta_2^* = \frac{2}{\Lambda_1}\cosh\beta\xi_1\sin\beta\xi_2\cos\chi_1 + \frac{2}{\Lambda_1}\sinh\beta\xi_1\cos\beta\xi_2\sin\chi_1 = T_{12} + T_{14}$$

$$\beta_3^* = \dot{T}_{11} - \dot{T}_{13} = \frac{2\,b\,\Lambda_1}{\cos\psi_0}\left\{\cosh\beta\xi_1\cos\beta\xi_2\cos\left(\chi_1 - \frac{\pi}{4}\right) + \sinh\beta\xi_1\sin\beta\xi_2\sin\left(\chi_1 - \frac{\pi}{4}\right)\right\} +$$
$$+ \frac{\sin 2\psi_0}{2\Lambda_1^5}\{\sinh\beta\xi_1\cos\beta\xi_2\cos 5\chi_1 - \cosh\beta\xi_1\sin\beta\xi_2\sin 5\chi_1\}$$

$$\beta_4^* = \dot{T}_{12} + \dot{T}_{14} = -\frac{2\,b\,\Lambda_1}{\cos\psi_0}\left\{\sinh\beta\xi_1\sin\beta\xi_2\cos\left(\chi_1 - \frac{\pi}{4}\right) - \cosh\beta\xi_1\cos\beta\xi_2\sin\left(\chi_1 - \frac{\pi}{4}\right)\right\} +$$
$$- \frac{\sin 2\psi_0}{2\Lambda_1^5}\{\cosh\beta\xi_1\sin\beta\xi_2\cos 5\chi_1 + \sinh\beta\xi_1\cos\beta\xi_2\sin 5\chi_1\}.$$

Here Λ_1, x_1 and ρ are the same as for β_1, β_2, β_3 and β_4.

The equations (3.29a/d) now become

$$c_1\left\{\beta_3^*\sin\psi_0 - \frac{b^2}{1+\nu}\,\beta_2^*\cos\psi_0\right\} + c_2\left\{\beta_4^*\sin\psi_0 + \frac{b^2}{1+\nu}\,\beta_1^*\cos\psi_0\right\} + b_1\sin\psi_0 +$$
$$+ b_2\{S_{12}\cos\psi_0 + \dot{S}_{12}\sin\psi_0\} = 0 \tag{3.30a}$$

$$c_1\frac{\beta_1^*}{\cos\psi_0} + c_2\frac{\beta_2^*}{\cos\psi_0} + b_1\sin\psi_0 + b_2\frac{S_{12}}{\cos\psi_0} = 0 \tag{3.30b}$$

$$c_1\left\{-\beta_3^*\cos\psi_0 - \frac{b^2}{1+\nu}\,\beta_2^*\sin\psi_0 + \frac{b^2}{1+\nu}\,\beta_4^*\cos\psi_0\right\} + c_2\left\{-\beta_4^*\cos\psi_0 + \frac{b^2}{1+\nu}\beta_1^*\sin\psi_0 +\right.$$
$$\left. - \frac{b^2}{1+\nu}\,\beta_3^*\cos\psi_0\right\} - b_1\cos\psi_0 + b_2\,\{S_{12}\sin\psi_0 - 2\,\dot{S}_{12}\cos\psi_0\} = 0 \tag{3.30c}$$

and

$$b_2 = -\frac{D}{4\pi R}\,\frac{a}{B}\cos\psi_0 = -\frac{D}{4\pi \bar{B}} \tag{3.30d}$$

Thus the value of b_2 is determined directly.

We will solve the three remaining constants c_1, c_2 and b_1 as a function of b_2 from the three equations (3.30a/c) by proceeding as follows.

Multiply eq. (3.30a) with ψ_0 and eq. (3.30c) with $\sin\psi_0$. Adding this together we find

$$C_1 \frac{b^2}{1+\nu} \bar{\beta}_2{}^* - c_2 \frac{b^2}{1+\nu} \bar{\beta}_1{}^* + b_2 \{ S_{12} - \dot{S}_{12} \sin\psi_0 \cos\psi_0 \} = 0 \tag{3.31a}$$

where

$$\bar{\beta}_1{}^* = \beta_3{}^* \cos\psi_0 \sin\psi_0 - \beta_1{}^* \qquad \bar{\beta}_2{}^* = \beta_4{}^* \cos\psi_0 \sin\psi_0 - \beta_2{}^*.$$

Multiplying eqs. (3.30a) and (3.30b) with $\cos\psi_0$ and subtracting we get

$$c_1 \left\} \bar{\beta}_1{}^* - \frac{b^2}{1+\nu} \beta_2{}^* \cos^2\psi_0 \right\{ + c_2 \left\} \bar{\beta}_2{}^* + \frac{b^2}{1+\nu} \beta_1{}^* \cos^2\psi_0 \right\{ + b_2 \{ S_{12} \cos^2\psi_0 + \dot{S}_{12} \sin\psi_0 \cos\psi_0 - S_{12} \} = 0. \tag{3.31b}$$

Now since

$$S_{12} - \dot{S}_{12} \sin\psi_0 \cos\psi_0 = \cos^2\psi_0 \, S_{12} - 4 \operatorname{tg}\psi_0$$

we have

$$S_{12} \sin^2\psi - \dot{S}_{12} \sin\psi_0 \cos\psi_0 = - 4 \operatorname{tg}\psi_0 .$$

The solution of the equations (3.31a) and (3.31b) is therefore

$$c_1 = - \frac{1+\nu}{b^2} b_2 \frac{\{ \cos^2\psi_0 \, S_{12} - 4 \operatorname{tg}\psi_0 \} \left\} \bar{\beta}_2{}^* + \frac{b^2}{1+\nu} \beta_1{}^* \cos^2\psi_0 \right\} + 4 \operatorname{tg}\psi_0 \frac{b^2}{1+\nu} \bar{\beta}_1{}^*}{\bar{\beta}_1{}^* \left\} \bar{\beta}_1{}^* - \frac{b^2}{1+\nu} \beta_2{}^* \cos^2\psi_0 \right\{ + \bar{\beta}_2{}^* \left\} \bar{\beta}_2{}^* + \frac{b^2}{1+\nu} \beta_1{}^* \cos^2\psi_0 \right\}} \tag{3.32a}$$

$$c_2 = + \frac{1+\nu}{b^2} b_2 \frac{\{ \cos^2\psi_0 \, S_{12} - 4 \operatorname{tg}\psi_0 \} \left\} \bar{\beta}_1{}^* - \frac{b^2}{1+\nu} \beta_2{}^* \cos^2\psi_0 \right\} - 4 \operatorname{tg}\psi_0 \frac{b^2}{1+\nu} \bar{\beta}_2{}^*}{\bar{\beta}_1{}^* \left\} \bar{\beta}_1{}^* - \frac{b^2}{1+\nu} \beta_2{}^* \cos^2\psi_0 \right\{ + \bar{\beta}_2{}^* \left\} \bar{\beta}_2{}^* + \frac{b^2}{1+\nu} \beta_1{}^* \cos^2\psi_0 \right\}} \tag{3.32b}$$

b_1 can now be determined by using eq. (3.30b).

We will now give the forces and moments occurring in the shell at the edge as derived from the eqs. (2.57)—(2.62).

$$\bar{N}_{\varphi\varphi_1} = c_1 \frac{B}{a} \frac{1}{\cos^2\psi_0} [\bar{\beta}_1{}^* - b^2 \beta_2{}^* \cos^2\psi_0] + c_2 \frac{B}{a} \frac{1}{\cos^2\psi_0} [\bar{\beta}_2 + b^2 \beta_1{}^* \cos^2\psi_0] + 4 b_2 \frac{B}{a} \frac{\sin\psi_0}{\cos^3\psi_0} . \tag{3.33a}$$

$$\bar{N}_{\vartheta\vartheta_1} = - c_1 \frac{B}{a} \frac{1}{\cos^2\psi_0} \bar{\beta}_1{}^* - c_2 \frac{B}{a} \frac{1}{\cos^2\psi_0} \bar{\beta}_2{}^* - 4 b_2 \frac{B}{a} \frac{\sin\psi_0}{\cos^3\psi_0} \tag{3.33b}$$

$$\bar{N}_{\varphi\vartheta_1} = \bar{N}_{\vartheta\varphi_1} = \frac{-c_1}{\sin\psi_0 \cos^2\psi_0} \frac{B}{a} [\bar{\beta}_1{}^* + \beta_1{}^* \cos^2\psi_0] - \frac{c_2}{\sin\psi_0 \cos^2\psi_0} \frac{B}{a} [\bar{\beta}_2{}^* + \beta_2{}^* \cos^2\psi_0] + $$
$$- 4 b_2 \frac{B}{a} \frac{1}{\cos^3\psi_0} \tag{3.33c}$$

$$\bar{M}_{\varphi\vartheta_1} = \frac{c_1 B}{\cos^2\psi_0} \left[\nu\beta_1{}^* \cos^2\psi_0 - \frac{1-\nu}{b^2} \{ \bar{\beta}_2{}^* - \nu\beta_2{}^* \cos^2\psi_0 \} \right] + \frac{c_2 B}{\cos^2\psi_0} \left[\nu\beta_2{}^* \cos^2\psi_0 + \frac{1-\nu}{b^2} \{ \bar{\beta}_1{}^* + \right.$$
$$\left. - \nu\beta_1{}^* \cos^2\psi_0 \} \right] \tag{3.33d}$$

$$\bar{M}_{\vartheta\varphi_1} = \frac{c_1 B}{\cos^2\psi_0} \left[\beta_1{}^* \cos^2\psi_0 + \frac{1-\nu}{b^2} \{ \bar{\beta}_2{}^* + \beta_2{}^* \cos^2\psi_0 \} \right] + \frac{c_2 B}{\cos^2\psi_0} \left[\beta_2{}^* \cos^2\psi_0 - \frac{1-\nu}{b^2} \{ \bar{\beta}_1{}^* + \beta_1{}^* \cos^2\psi_0 \} \right] \tag{3.33e}$$

$$\bar{M}_{\varphi\varphi_1} = - M_{\vartheta\vartheta_1} = \frac{c_1 B}{\sin\psi_0 \cos^2\psi_0} \left[\frac{1-\nu}{b^2} \{ \bar{\beta}_2{}^* + \beta_2{}^* \cos^2\psi_0 \} + k \{ \bar{\beta}_1{}^* + \beta_1{}^* \cos^2\psi_0 \} \right] +$$
$$+ \frac{c_2 B}{\sin\psi_0 \cos^2\psi_0} \left[- \frac{1-\nu}{b^2} \{ \bar{\beta}_1{}^* + \beta_1{}^* \cos^2\psi_0 \} + k \{ \bar{\beta}_2{}^* + \beta_2{}^* \cos^2\psi_0 \} \right] . \tag{3.33f}$$

The *highest stresses occurring* at the edge are given by

$$\sigma_a = \frac{N_{\vartheta\vartheta_1}}{h} \pm \frac{6}{h^2} \overline{M}_{\vartheta\varphi_1} \tag{3.34a}$$

$$\sigma_t = \frac{1}{h} N_{\varphi\varphi_1} \pm \frac{6}{h^2} \overline{M}_{\varphi\vartheta_1} \tag{3.34b}$$

$$\tau = \frac{1}{4} \overline{N}_{\varphi\vartheta_1} + \frac{1}{ah} \overline{M}_{\vartheta\vartheta_1}. \tag{3.34c}$$

To obtain the stiffness parameters of the sphere under this load, we determine the displacement and the rotation of the cross section $\psi = \psi_0$. Since the load is antisymmetrical, we have for $\psi = 0$: $u_1 = 0$ and $v_1 = 0$. Hence the displacement per unit of transverse force is given by

$$\overline{k}_D = \frac{(\overline{w}_1)_{\psi=0} \sin \psi_0}{D}$$

or

$$\overline{k} = \frac{1}{D} \frac{2 b \overline{\Lambda}_0}{1-\nu} \left[c_1 \cos\left(\chi^* - \frac{\pi}{4}\right) + c_2 \sin\left(\chi^* - \frac{\pi}{4}\right)\right] \sin \psi_0 + \frac{\sin \psi_0}{(1-\nu) D} [b_1 + 4 b_2]$$

where χ^* is given by $\operatorname{tg} 4 \chi^* = \rho$ and $\overline{\Lambda}_0$ by $\sqrt[4]{1+\rho^2}$. (3.35)

The rotation per unit of transverse force is given by

$$x_D = \frac{1}{D} \frac{(\overline{u}_1)_{\psi_0} \sin \psi_0 - (\overline{w}_1)_{\psi_0} \cos \psi_0}{a \cos \psi_0} + \frac{(\overline{w}_1)_{\psi=0}}{Da} = -\frac{1}{aD} \left(\frac{\partial \overline{u}_1}{\partial \psi}\right)_{\psi_0} - (\overline{w}_1)_{\psi=0}$$

or

$$k_D = \frac{b^2}{1-\nu^2} \cdot \frac{1}{aD} [c_1 \beta_4^* + c_2 \beta_3^*] + \frac{1}{aD(1-\nu)} b_2 \dot{S}_{12} +$$
$$+ \frac{1}{aD} \frac{2 b \overline{\Lambda}_0}{1-\nu} \left[c_1 \cos\left(\chi^* - \frac{\pi}{4}\right) + c_2 \sin\left(\chi^* - \frac{\pi}{4}\right)\right] + \frac{1}{aD(1-\nu)} [b_1 + 4 b_2]. \tag{3.36}$$

3.4 *Concluding remarks of chapter 3.*

As has been shown, the solution of the three problems given in this part, with the aid of HAVERS' theory, is exceedingly simple and elegant.

Closed expressions are obtained for all the displacements, moments and forces in terms of rather *simple functions. Once these expressions are established, the numerical work needed to calculate the stresses and stiffness parameters is not very elaborate. In chapter 4 of this report we will use* the solution of chapter 3 for some practical applications.

4 Numerical solution for some cases.

4.1 *Introduction.*

As already explained in the introduction, the problems investigated in chapters 2 and 3 originated from the question, what bending stresses occur in a sphere attached to a pipe if an axial- and a transverse force and a bending moment are applied. This question arose in connection with the design of the pressure vessel and attached pipe to be built at the National Aeronautical Research Institute (N. L. L.) as elements of a supersonic windtunnel. The numerical calculations given in this chapter are based on the actual dimensions of this construction. However, for the purpose of giving an idea about the influence of the radius of the hole (viz. the value of ψ_0) three cases are given.

The radius of the sphere $a = 200$ cm. The thickness of the shell $h = 2.2$ cm. The three cases to be calculated are $\cos \psi_0 = 0.3$; $\cos \psi_0 = 0.4$ and $\cos \psi_0 = 0.43511$ giving for the radius of the hole $R = 60$ cm; $R = 80$ cm; $R = 87.5$ cm, respectively. Here the value $R = 87.5$ cm refers to the actual construction.

4.2 *Calculation for the case of axial load.*

We will make these calculations for the cases specified above. It is assumed that the magnitude of the axial load is 1000 kg.

We get

1	$\cos \psi_0 = 0.3$	$R = 60$ cm
	$b_2 = -1.5184 \times 10^{-5}$	$c_1 = 2.1551 \times 10^{-13}$
		$c_2 = -4.8870 \times 10^{-14}$
	$\sigma_a^+ = -4.742$ kg/cm²	$\sigma_t^+ = -1.298$ kg/cm²
	$\sigma_a^- = +10.259$ kg/cm²	$\sigma_t^- = +2.842$ kg/cm²
2	$\cos \psi_0 = 0.4$	$R = 80$ cm
	$b_2 = -1.5184 \times 10^{-5}$	$c_1 = 2.7829 \times 10^{-13}$
		$c_2 = 4.8538 \times 10^{-13}$
	$\sigma_a^+ = -2.811$ kg/cm²	$\sigma_t^+ = -0.770$ kg/cm²
	$\sigma_a^- = +6.204$ kg/cm²	$\sigma_t^- = +1.720$ kg/cm²
3	$\cos \psi_0 = 0.4351$	$R = 87.5$ cm
	$b_2 = -1.5184 \times 10^{-5}$	$c_1 = 3.7547 \times 10^{-13}$
		$c_2 = 6.4264 \times 10^{-13}$
	$\sigma_a^+ = -2.411$ kg/cm²	$\sigma_t^+ = -0.661$ kg/cm²
	$\sigma_a^- = +5.344$ kg/cm²	$\sigma_t^- = +1.482$ kg/cm²

As will be seen from these results the stresses are very low, though increasing rapidly with decreasing radius.

It is seen that considerable normal forces can be withstood, without the occurrence of dangerously high stresses.

4.3 *Calculation for the case of a bending moment.*

It is assumed that the applied bending moment is $M = 10^5$ kgcm. Application of the formulae derived in part 2 of this report gives

1 $\cos\psi_0 = 0.3$ $\quad R = 60$ cm

$b_1 = -1.4844\times10^{-4}$ $\quad c_1 = \ \ 4.0934\times10^{-13}$
$b_2 = -7.8933\times10^{-6}$ $\quad c_2 = -2.2111\times10^{-13}$
$\sigma_a+ = -18.409$ kg/cm^2 $\quad \sigma_t+ = - \ \ 5.210$ kg/cm^2
$\sigma_a- = +36.241$ kg/cm^2 $\quad \sigma_t- = +10.203$ kg/cm^2
$\tau = 8.149$ kg/cm^2

$k_M = 9.4987\times10^{-11}$ radian/kgcm
$\overline{k}_M = -2.0616\times10^{-9}$ cm/kgcm

2 $\cos\psi_0 = 0.4$ $\quad R = 80$ cm

$b_1 = -8.6567\times10^{-5}$ $\quad c_1 = 6.6833\times10^{-13}$
$b_2 = -7.8935\times10^{-6}$ $\quad c_2 = 7.0504\times10^{-13}$
$\sigma_a+ = - \ \ 8.794$ kg/cm^2 $\quad \sigma_t+ = -2.487$ kg/cm^2
$\sigma_a- = +17.214$ kg/cm^2 $\quad \sigma_t- = +4.845$ kg/cm^2
$\tau = 3.643$ kg/cm^2

$k_M = 6.347\times10^{-11}$ radian/kgcm
$\overline{k}_M = -1.2023\times10^{-9}$ cm/kgcm

3 $\cos\psi_0 = 0.4351$ $\quad R = 87.5$ cm

$b_1 = -7.4429\times10^{-5}$ $\quad c_1 = 3.7913\times10^{-13}$
$b_2 = -7.8934\times10^{-6}$ $\quad c_2 = 1.2443\times10^{-12}$
$\sigma_a+ = - \ \ 6.825$ kg/cm^2 $\quad \sigma_t+ = -1.9305$ kg/cm^2
$\sigma_a- = +13.564$ kg/cm^2 $\quad \sigma_t- = +3.8177$ kg/cm^2
$\tau = 2.850$ kg/cm^2

$k_M = 4.6721\times10^{-11}$ radian/kgcm
$\overline{k}_M = -1.0337\times10^{-9}$ cm/kgcm

These stresses are fairly large, a moment of the order of 50×10^5 kgcm not being extraordinarily high, for the structure considered.

4.4 *Calculation for the case of a transverse force.*

It is assumed that the applied force is $D = 1000$ kg.

Using the formulae derived for this case in part 2 of this report, we get

1 $\cos\psi_0 = 0.3$ $\quad R = 60$ cm

$b_1 = -3.8268\times10^{-4}$ $\quad c_1 = -8.5908\times10^{-13}$
$b_2 = -1.5874\times10^{-5}$ $\quad c_2 = +4.0778\times10^{-13}$
$\sigma_a+ = -41.151$ kg/cm^2 $\quad \sigma_t+ = -11.166$ kg/cm^2
$\sigma_a- = +74.666$ kg/cm^2 $\quad \sigma_t- = +21.034$ kg/cm^2
$\tau = +17.676$ kg/cm^2

$k_D = +3.3883\times10^{-8}$ radian/kg
$\overline{k}_D = -5.9113\times10^{-7}$ cm/kg

2 $\cos\psi_0 = 0.4$ $\quad R = 80$ cm

$b_1 = -2.4186\times10^{-4}$ $\quad c_1 = -1.2306\times10^{-12}$
$b_2 = -1.5874\times10^{-5}$ $\quad c_2 = -1.3502\times10^{-12}$
$\sigma_a+ = -17.107$ kg/cm^2 $\quad \sigma_t+ = -4.711$ kg/cm^2
$\sigma_a- = +32.524$ kg/cm^2 $\quad \sigma_t- = +9.027$ kg/cm^2
$\tau = +8.459$ kg/cm^2

$k_D = 1.2452\times10^{-8}$ radian/kg
$\overline{k}_D = -3.8870\times10^{-7}$ cm/kg

3 $\cos\psi_0 = 0.4351$ $\quad R = 87.5$ cm

$b_1 = -2.1182\times10^{-4}$ $\quad c_1 = -6.5106\times10^{13}$
$b_2 = -1.5874\times10^{-5}$ $\quad c_2 = -2.3207\times10^{12}$
$\sigma_a+ = -13.151$ kg/cm^2 $\quad \sigma_t+ = -3.620$ kg/cm^2
$\sigma_a- = +25.273$ kg/cm^2 $\quad \sigma_t- = +7.015$ kg/cm^2
$\tau = +6.770$ kg/cm^2

$k_D = 9.0460\times10^{-9}$ radian/kg
$\overline{k}_D = -3.4430\times10^{-7}$ cm/kg

The stresses in this case are rather high too. As can be seen, however, by comparing these results with those for the case of a bending moment, the bending moment, applied together with the transverse force in order to give equilibrium, is the main cause of these stresses. This will be demonstrated by computing the stresses for the loading specified in fig. 9 and for the edge loaded

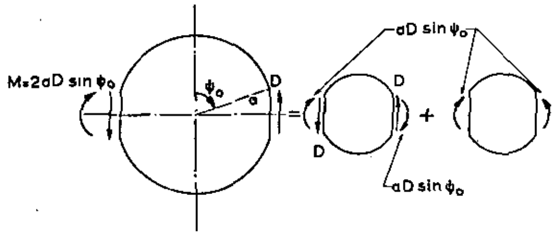

Fig. 9. Decomposition of the case of a transverse force along one edge into already considered cases.

by the transverse force only. We will limit ourselves to the case of $\cos\psi_0 = 0.4351$.

We then find

$\sigma_a+ = -0.793$ kg/cm^2 $\quad \sigma_t+ = -1.215$ kg/cm^2
$\sigma_a- = +0.713$ kg/cm^2 $\quad \sigma_t- = +2.114$ kg/cm^2
$\tau = 3.299$ kg/cm^2

As follows from these figures, the stresses resulting directly from a transverse force are very low indeed.

4.5 *Estimation of the error involved in the results.*

Due to the fact that the theory is only asymptotically correct, an error is involved in the results. In ref. 1 Havers has determined the order of this error for different angles ψ_0. For small values of ρ, as is the case here, he has found that the order of the error ranges from 0.5 % to 1 % for the angles ψ_0 considered here.

Another error is due to the fact that the values of ξ_1 and ξ_2 have been interpolated from the tables 1 and 2. Since these quantities have to be multiplied with the large quantity β to form the exponent of an exponential function, e.g. β_1, rather large differences can be expected in the numerical results, when only small differences occur in the values of ξ_1 and ξ_2.

In order to obtain a reliable impression about this error, a completely independent calculation was made for the cases presented by the "Instituut T. N. O. voor Werktuigkundige Constructies".

As a result of the comparison of the two calculations, it can be stated that the maximum error due to interpolating is of the order of 5 %.

The total error involved in the results, therefore, is of the order of 6 %.

5 Conclusions.

By using the asymptotic bending theory of HAVERS, which is reviewed in chapter 2 of this report, the stresses occurring at the edge of a circular hole in a sphere are determined in chapter 3 of this report for the following conditions.

The hole is reinforced by a heavy circular frame, which can be considered to be rigid.

The radius of the hole is not small compared to the radius of the sphere.

The thickness of the shell is small compared to the radius of the sphere.

The latter two assumptions are essential for the applicability of the theory of HAVERS.

The cases considered are:

Introduction of an axial force.
Introduction of a bending moment.
Introduction of a transverse force.

The analysis leads to very elegant expressions, which are in fact not much more complicated than the expressions occurring in the analysis of edge bending of a cylinder.

In chapter 4 of this report, the results of part 3 are used for the numerical evaluation of some cases. The case $\cos\psi_0 = 0.4351$ refers to the actual structure of a pressure vessel and attached pipe, to be built as an element of the supersonic windtunnel of the N. L. L. The numerical results indicate that rather high stresses occur in the case of a bending moment.

The stresses increase rapidly in all cases when the radius of the hole decreases.

To gain an insight in the stiffness of the shell, the stiffness parameters k_M, $\bar{k}_M$, k_D and $\bar{k}_D$ as defined in chapter 3, are also given in part 4.

These parameters can be useful for an analysis of a more complicated structure, where they enable the substitution of the sphere by a system of springs (see e.g. ref. 4).

6. References.

1. HAVERS, A. Asymptotische Biegetheorie der unbelasteten Kugelschale. Ingenieur-Archiv 1935, p. 282—312.
2. v. D. NEUT, A. De elastische stabiliteit van den dunwandigen bol. Dissertatie Delft, 1932.
3. BIEZENO, C. B. und GRAMMEL, R. Technische Dynamik. Verlag von Julius Springer, Berlin, 1939.
4. ZANDBERGEN, P. J. Statisch onbepaalde berekening van drukvat en verbindingsbuis van de S. S. T. N.L.L.-report ST. 28, 1958.

Acknowledgement.

Acknowledgement is made to the "Instituut T.N.O. voor Werktuigkundige Constructies" for checking the derivation of the equations given in this paper and performing the independent numerical calculations referred to in section 4.5.

Note.

After completion of this report the author's attention was drawn to the following publications of Russian origine in which some aspects of the elasticity theory of spherical shells are treated.

5. WLASSOW, W. S. Allgemeine Schalentheorie und ihre Anwendung in der Technik. Academie Verlag — Berlin 1958.
6. GOLDENWEISER, A. L. Theory of elastic thinwalled shells. (in Russian). Government Printing Office for technical-theoretical literature, Moscou, 1953.

TABLE 1.

ξ_1 as a function of ψ and ρ.

λ	ψ=10°	20°	30°	40°	50°	60°	65°	70°	75°	80°	85°
0.00	0.1745	0.3491	0.5236	0.6981	0.8727	1.0472	1.1345	1.223	1.309	1.396	1.484
0.01	0.1754	0.3509	0.5265	0.7024	0.8787	1.0559	1.1453	1.236	1.328	1.425	1.544
0.02	0.1763	0.3527	0.5294	0.7066	0.8847	1.0647	1.1563	1.250	1.347	1.455	1.604
0.03	0.1772	0.3546	0.5323	0.7109	0.8908	1.0736	1.1674	1.264	1.366	1.485	1.661
0.04	0.1781	0.3564	0.5353	0.7152	0.8969	1.0826	1.1786	1.278	1.385	1.516	1.716
0.05	0.1790	0.3583	0.5382	0.7195	0.9031	1.0916	1.1899	1.293	1.405	1.547	1.770
0.06	0.1799	0.3602	0.5412	0.7238	0.9092	1.1007	1.2012	1.308	1.425	1.578	1.821
0.07	0.1808	0.3620	0.5442	0.7281	0.9154	1.1099	1.2126	1.323	1.445	1.609	1.871
0.08	0.1817	0.3639	0.5472	0.7325	0.9217	1.1191	1.2241	1.338	1.465	1.639	1.918
0.09	0.1826	0.3658	0.5502	0.7369	0.9280	1.1283	1.2356	1.353	1.485	1.668	1.964
0.10	0.1836	0.3677	0.5532	0.7413	0.9343	1.1375	1.2471	1.368	1.505	1.697	2.009
0.15	0.1883	0.3773	0.5685	0.7636	0.9663	1.1847	1.3059	1.443	1.605	1.837	2.219
0.20	0.1930	0.3871	0.5841	0.7865	0.9990	1.2329	1.3657	1.519	1.702	1.969	2.409
0.25	0.1978	0.3970	0.5999	0.8098	1.0321	1.2816	1.4259	1.594	1.797	2.086	2.583
0.30	0.2027	0.4071	0.6159	0.8333	1.0656	1.3303	1.4858	1.667	1.888	2.202	2.746
0.35	0.2076	0.4173	0.6321	0.8569	1.0992	1.3787	1.5448	1.739	1.977	2.318	2.903
0.40	0.2125	0.4276	0.6484	0.8806	1.1329	1.4267	1.6026	1.810	2.063	2.431	3.054
0.45	0.2175	0.4379	0.6648	0.9043	1.1666	1.4742	1.6592	1.874	2.148	2.541	3.201
0.50	0.2225	0.4483	0.6813	0.9281	1.2002	1.5212	1.7148	1.946	2.230	2.649	3.342
0.55	0.2275	0.4586	0.6978	0.9519	1.2336	1.5677	1.7695	2.0123	2.3101	2.750	3.479
0.60	0.2325	0.4689	0.7143	0.9757	1.2667	1.6136	1.8234	2.0772	2.3881	2.848	3.611
0.65	0.2375	0.4791	0.7307	0.9994	1.2995	1.6589	1.8766	2.1408	2.4642	2.944	3.739
0.70	0.2424	0.4893	0.7470	1.0230	1.3320	1.7036	1.9291	2.2032	2.5386	3.037	3.862
0.75	0.2473	0.4995	0.7632	1.0464	1.3642	1.7477	1.9808	2.2643	2.6114	3.127	3.982
0.80	0.2522	0.5097	0.7793	1.0696	1.3961	1.7912	2.0318	2.3242	2.6826	3.215	4.097
0.85	0.2572	0.5199	0.7953	1.0925	1.4276	1.8341	2.0821	2.3830	2.7523	3.300	4.209
0.90	0.2622	0.5301	0.8112	1.1152	1.4588	1.8764	2.1317	2.4407	2.8206	3.384	4.318
0.95	0.2672	0.5403	0.8270	1.1376	1.4897	1.9181	2.1805	2.4974	2.8876	3.466	4.423
1.00	0.2722	0.5505	0.8426	1.1598	1.5203	1.9592	2.2286	2.5532	2.9532	3.5461	4.5268
1.05	0.2771	0.5605	0.8581	1.1818	1.5505	1.9997	2.2748	2.6081	3.0175	3.6249	4.6287
1.10	0.2819	0.5704	0.8735	1.2035	1.5804	2.0396	2.3204	2.6621	3.0806	3.7023	4.7291
1.15	0.2866	0.5801	0.8887	1.2250	1.6099	2.0789	2.3658	2.7152	3.1427	3.7784	4.8281
1.20	0.2913	0.5897	0.9038	1.2463	1.6390	2.1177	2.4103	2.7674	3.2039	3.8532	4.9257
1.25	0.2959	0.5992	0.9187	1.2574	1.6677	2.1559	2.4543	2.8198	3.2642	3.9268	5.0219
1.30	0.3005	0.6085	0.9335	1.2883	1.6959	2.1935	2.4978	2.8694	3.3237	3.9993	5.1167
1.35	0.3051	0.6179	0.9481	1.3090	1.7237	2.2306	2.5409	2.9192	3.3824	4.0707	5.2102
1.40	0.3096	0.6272	0.9626	1.3295	1.7511	2.2671	2.5835	2.9683	3.4403	4.1410	5.3023
1.45	0.3141	0.6364	0.9769	1.3498	1.7781	2.3030	2.6256	3.0167	3.4975	4.2103	5.3931
1.50	0.3185	0.6455	0.9911	1.3698	1.8047	2.3384	2.6672	3.0644	3.5539	4.2786	5.4825
1.55	0.3229	0.6545	1.0051	1.3896	1.8310	2.3733	2.7082	3.1115	3.6096	4.3460	5.5706
1.60	0.3272	0.6634	1.0190	1.4092	1.8570	2.4078	2.7486	3.1580	3.6654	4.4125	5.6574
1.65	0.3317	0.6723	1.0328	1.4286	1.8828	2.4419	2.7884	3.2039	3.7186	4.4781	5.7428
1.70	0.3360	0.6811	1.0464	1.4478	1.9084	2.4757	2.8276	3.2493	3.7719	4.5428	5.8268
1.75	0.3403	0.6898	1.0599	1.4668	1.9338	2.5092	2.8663	3.2941	3.8244	4.6066	5.9094
1.80	0.3445	0.6984	1.0733	1.4856	1.9590	2.5424	2.9044	3.3384	3.8761	4.6695	5.9907
1.85	0.3487	0.7069	1.0865	1.5042	1.9840	2.5753	2.9420	3.3821	3.9271	4.7315	6.0706
1.90	0.3527	0.7153	1.0996	1.5225	2.0088	2.6079	2.9791	3.4253	3.9773	4.7926	6.1492
1.95	0.3568	0.7237	1.1126	1.5406	2.0334	2.6403	3.0156	3.4680	4.0267	4.8528	6.2264
2.00	0.3609	0.7320	1.1255	1.5585	2.0578	2.6724	3.0516	3.5102	4.0753	4.9121	6.3022

TABLE 2.

ξ_2 as a function of ψ and ρ.

λ	$\psi=10°$	20°	30°	40°	50°	60°	65°	70°	75°	80°	85°	90°
0.00	0.1745	0.3491	0.5236	0.6981	0.8727	1.0472	1.1345	1.222	1.309	1.396	1.484	1.571
0.01	0.1736	0.3472	0.5207	0.6939	0.8667	1.039	1.124	1.208	1.292	1.369	1.430	1.468
0.02	0.1727	0.3454	0.5178	0.6898	0.8608	1.030	1.113	1.195	1.273	1.343	1.390	1.410
0.03	0.1719	0.3436	0.5150	0.8656	0.8550	1.022	1.103	1.182	1.256	1.320	1.357	1.374
0.04	0.1710	0.3419	0.5122	0.6815	0.8492	1.013	1.093	1.169	1.240	1.298	1.329	1.345
0.05	0.1701	0.3401	0.5094	0.6775	0.8434	1.005	1.083	1.157	1.224	1.277	1.306	1.320
0.06	0.1693	0.3383	0.5066	0.6734	0.8377	0.997	1.073	1.145	1.209	1.258	1.285	1.299
0.07	0.1684	0.3366	0.5038	0.6694	0.8321	0.989	1.063	1.133	1.196	1.240	1.266	1.279
0.08	0.1676	0.3348	0.5010	0.6654	0.8265	0.981	1.053	1.121	1.181	1.223	1.249	1.261
0.09	0.1667	0.3331	0.4983	0.6615	0.8209	0.973	1.044	1.110	1.168	1.208	1.233	1.244
0.10	0.1659	0.3314	0.4956	0.6575	0.8154	0.965	1.035	1.098	1.156	1.193	1.218	1.228
0.15	0.1618	0.3229	0.4822	0.6384	0.7887	0.928	0.991	1.046	1.096	1.126	1.148	1.155
0.20	0.1579	0.3147	0.4694	0.6199	0.7633	0.894	0.951	1.001	1.041	1.071	1.089	1.095
0.25	0.1541	0.3068	0.4571	0.6024	0.7393	0.862	0.914	0.959	0.994	1.025	1.039	1.045
0.30	0.1504	0.2992	0.4453	0.5857	0.7166	0.832	0.881	0.922	0.953	0.984	0.996	1.001
0.35	0.1469	0.2919	0.4339	0.5697	0.6952	0.804	0.850	0.888	0.918	0.946	0.957	0.962
0.40	0.1435	0.2849	0.4230	0.5544	0.6750	0.779	0.822	0.858	0.886	0.912	0.922	0.927
0.45	0.1402	0.2782	0.4125	0.5398	0.6560	0.755	0.797	0.831	0.858	0.880	0.891	0.895
0.50	0.1370	0.2718	0.4025	0.5260	0.6381	0.733	0.773	0.806	0.832	0.851	0.862	0.866
0.55	0.1340	0.2657	0.3929	0.5129	0.6213	0.7133	0.7507	0.783	0.808	0.824	0.835	0.839
0.60	0.1311	0.2598	0.3837	0.5005	0.6055	0.6945	0.7301	0.762	0.785	0.798	0.810	0.814
0.65	0.1283	0.2542	0.3750	0.4887	0.5906	0.6786	0.7108	0.742	0.764	0.775	0.788	0.791
0.70	0.1256	0.2488	0.3667	0.4775	0.5766	0.6601	0.6927	0.723	0.744	0.753	0.766	0.770
0.75	0.1230	0.2436	0.3588	0.4669	0.5634	0.6443	0.6757	0.705	0.725	0.734	0.747	0.750
0.80	0.1206	0.2387	0.3514	0.4568	0.5509	0.6293	0.6597	0.688	0.707	0.716	0.729	0.732
0.85	0.1183	0.2340	0.3444	0.4473	0.5390	0.6150	0.6446	0.672	0.691	0.699	0.712	0.715
0.90	0.1161	0.2296	0.3378	0.4383	0.5277	0.6014	0.6304	0.656	0.675	0.684	0.697	0.700
0.95	0.1140	0.2254	0.3316	0.4298	0.5169	0.5885	0.6171	0.642	0.660	0.671	0.682	0.685
1.00	0.1120	0.2214	0.3275	0.4218	0.5065	0.5762	0.6046	0.628	0.647	0.658	0.668	0.671
1.05	0.1100	0.2175	0.3201	0.4141	0.4966	0.5646	0.5928	0.615	0.634	0.646	0.655	0.658
1.10	0.1081	0.2138	0.3147	0.4066	0.4872	0.5536	0.5816	0.603	0.621	0.633	0.642	0.645
1.15	0.1063	0.2102	0.3095	0.3994	0.4783	0.5432	0.5709	0.591	0.601	0.621	0.630	0.633
1.20	0.1045	0.2067	0.3044	0.3925	0.4698	0.5334	0.5607	0.581	0.599	0.610	0.619	0.622
1.25	0.1028	0.2034	0.2995	0.3859	0.4617	0.5242	0.5510	0.570	0.588	0.599	0.608	0.611
1.30	0.1012	0.2002	0.2947	0.3796	0.4541	0.5157	0.5417	0.561	0.578	0.589	0.597	0.600
1.35	0.0996	0.1971	0.2901	0.3736	0.4469	0.5076	0.5328	0.552	0.569	0.580	0.588	0.590
1.40	0.0981	0.1942	0.2856	0.3679	0.4401	0.4998	0.5243	0.543	0.560	0.571	0.578	0.581
1.45	0.0967	0.1914	0.2812	0.3625	0.4337	0.4923	0.5161	0.535	0.551	0.562	0.569	0.571
1.50	0.0954	0.1888	0.2772	0.3575	0.4277	0.4851	0.5083	0.528	0.543	0.554	0.560	0.562
1.55	0.0942	0.1863	0.2732	0.3527	0.4220	0.4782	0.5008	0.520	0.535	0.546	0.552	0.554
1.60	0.0930	0.1839	0.2694	0.3481	0.4165	0.4716	0.4936	0.513	0.527	0.538	0.544	0.546
1.65	0.0918	0.1815	0.2657	0.3436	0.4112	0.4652	0.4868	0.506	0.520	0.531	0.536	0.538
1.70	0.0907	0.1792	0.2622	0.3392	0.4060	0.4590	0.4803	0.499	0.513	0.524	0.529	0.530
1.75	0.0896	0.1770	0.2588	0.3349	0.4009	0.4530	0.4739	0.493	0.507	0.517	0.521	0.523
1.80	0.0885	0.1748	0.2556	0.3306	0.3958	0.4472	0.4678	0.486	0.500	0.510	0.515	0.517
1.85	0.0874	0.1727	0.2525	0.3264	0.3907	0.4416	0.4618	0.480	0.494	0.504	0.508	0.510
1.90	0.0864	0.1706	0.2495	0.3223	0.3857	0.4361	0.4561	0.474	0.488	0.497	0.502	0.504
1.95	0.0854	0.1685	0.2466	0.3183	0.3807	0.4307	0.4507	0.468	0.481	0.491	0.496	0.498
2.00	0.0844	0.1665	0.2439	0.3144	0.3756	0.4254	0.4456	0.462	0.475	0.485	0.490	0.492

C.C.L. Class. C 260-0 : C 280-0 : C 35-0

REPORT NLL-TR S. 521.

Bending at the oblique end section of cylindrical shells

by

A. VAN DER NEUT. *)

Summary.

The investigation refers to the stress problem at the intersection of cylindrical shells, loaded by membrane stresses. The intersection is usually reinforced by an elliptic frame. The required compatibility of strains of cylinder walls and frame induces bending stresses over the thickness of the shell in the vicinity of the intersection. The paper establishes this bending effect near the oblique end section for edge loads consisting of bending moments m_0 and shear loads q_0 normal to the shell.

As a preliminary step the exact solution is given for the cylindrical shell bounded by an infinite helical edge under constant edge loads (Part I).

The fact that the stresses are negligibly small already at a short distance from the edge suggests that the stresses near the oblique end section and the stresses near the helical edge will differ only slightly, if the helix is tangent to the oblique edge in the region under consideration. It is shown in Part II that this concept is correct up to an error of the order $(h/a)^{1/2}$. A further result is that the edge load for which the stresses vanish at a short distance from the edge is *composed of the bending moments m_0 and the shear loads q_0 mentioned before and in addition of edge loads L, T,* proportional to q_0, in the plane tangential to the shell. The resultant of q_0, L, T lies in the oblique end section; its *reaction upon an oblique frame is equivalent to that of a frame flange with the cross section S. This quantity is* established. S represents the effective shell section which cooperates with the frame when it is being deformed.

Contents.

List of symbols.

1 Introduction.

Part I. The cylindrical shell loaded along its helical edge by constant bending moments and shear forces.

2 The differential equations.

3 The solution of the differential equation.

4 The stresses.

5 Summary and interpretation of results.

Part II. The oblique cylindrical shell loaded along its edge.

6 The approach to the problem.

7 The stresses.

8 The additional load system I.

9 The load system II.

10 The solution of the oblique cylinder problem.

11 Some characteristics of the edge load.

12 References.

Appendix A. Geometry of the oblique cylindrical shell.

Appendix B. Summary of formulae for use in applications.

16 figures.

---

*) Professor of Aircraft Structures at the Technological University of Delft.

List of symbols.

a	=	radius of the cylinder.
b	=	$a \tan \Phi$ (see fig. 1).
c	=	$\tan \Phi \sin \varphi = \tan \beta$.
h	=	wall thickness.
k	=	$\frac{1}{12} \frac{h^2}{a^2}$, wall thickness parameter, supposed to be of the order $\leqq 10^{-4}$.
m_{ij}	=	moment per unit length of the wall, acting upon a section normal to the axis i, its vector is in the direction of the axis j (fig. 5 and 6).
m_0	=	bending moment per unit length at the oblique edge.
q_{ij}	=	shear force per unit length of the wall, where i and j have the same meaning as with m_{ij} (fig. 5, 6).
q_0	=	shear force per unit length at the oblique edge (fig. 15, eq. 29).
r	=	radial coordinate.
s	=	coordinate along the oblique edge (fig. 1 and 8).
$\bar{s}$	=	curvilinear coordinate of an arbitrary point of the shell (fig. 8).
u	=	radial displacement component (fig. 3).
v, w	=	displacement components in the plane of the shell (fig. 3).
$\bar{v}, \bar{w}$	=	displacement components in the plane of the shell (fig. 7).
x, y	=	*coordinates in the normal section* (fig. 1).
$\bar{x}, \bar{y}$	=	„ „ „ oblique „ (fig. 1).

x $= \alpha \frac{\bar{z}}{a}$, dimensionless coordinate normal to the edge of the shell.
z = axial coordinate (fig. 1).
$\bar{z}$ = coordinate normal to the edge of the shell (fig. 2, 8).
D = shear force in the cross section of the oblique frame (fig. 16).
E = modulus of elasticity.
L = longitudinal edge load concurrent with q_0 (fig. 15, eq. 28a).
M = bending moment in the cross section of the oblique frame (fig. 16).
N = normal force in the cross section of the oblique frame (fig. 16, eq. 32).
Q = normal edge load, resulting from q_0 and L (fig. 15, 16, eq. 30).
R_1 = radius of the cylinder in the plane of the oblique edge (fig. 10).
R_2 = radius of the cylinder in the plane perpendicular to the oblique edge (fig. 12).
S = equivalent flange section (eq. 33).
T = tangential edge load concurrent with q_0 (fig. 15, 16, eq, 28b).
V, W = displacement potentials, defined by eq. 4.
α $= \left(\frac{1-\nu^2}{4k}\right)^{1/4} \cos \beta$.
β = angle between the tangent to the edge and the normal section of the cylinder (fig. 2).
γ = specific shear.
ε = specific strain.
φ = angular coordinate in the normal section (fig. 1).
ψ = angular coordinate in the oblique end section (fig. 1).
η $= \frac{s}{a}$ dimensionless coordinate along the edge (fig. 2 and 4).
ρ = radius of curvature of the edge (fig. 1).
σ = membrane normal stress.
τ = membrane shear stress.
ζ $= \frac{\bar{z}}{a}$, dimensionless coordinate normal to the edge (fig. 2 and 4).
Φ = angle between the oblique end section and the normal section (fig. 1).
θ = angle between the normal to the cylinder and the oblique end section (fig. 15).
$(\,)' = a \frac{\partial (\,)}{\partial z}$

1 Introduction.

The problem of shell bending at oblique end sections of cylindrical walls relates to the intersection of tubes of equal diameter. This investigation was carried out in connection with the design of the variable pressure windtunnel of the National Aeronautical Research Institute (N. L. L.), where the problem occurs at the rectangular corners ($\Phi = \pi/4$). This report deals with the problem of edge bending for an arbitrary value of Φ.

The total problem of the stress distribution near the intersection of tubes involves more than the problem of edge bending, since it includes the condition of the compatibility of the deformations of the two shells and of the frame in the plane of intersection. The deformations of the frame and those of the shell under its undisturbed membrane stresses do not fit together. As far as the edge strain of shell and frame is concerned, the compatibility of these strains is established by bending

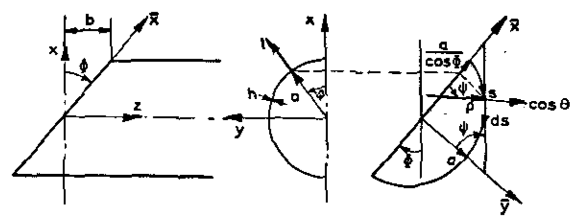

Fig. 1. Notations of the oblique cylinder.

moments m_0 and shear forces q_0 at the edge of the shell, which restrict their influence to the immediate vicinity of the edge. The problem, investigated in this report, is how to determine the stresses and deformations due to these edge loads.

The line of thought leading to the solution has been as follows. Edge bending restricts itself to a depth of shell, which is of the order $(ah)^{1/2}$ and therefore small of the order $\left(\frac{h}{a}\right)^{1/2}$ compared to the circumferential dimension. Geometrical conditions, e. g. curvature and edge angle β (fig. 2), change "slowly" along the oblique edge, since the derivatives of these functions to the edgewise

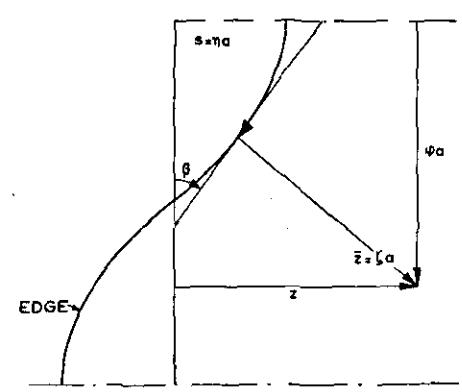

Fig. 2. The cylinder developed upon the flat plane.

coordinate $\eta = s/a$ are of the order of magnitude of these functions themselves. Then, if we confine ourselves to the case in which the edge loads (m_0, q_0) are changing slowly too along the edge, it may be concluded that the derivatives of displacements to the edgewise coordinate s will be small compared to the derivatives to the coordinate $\bar{z}$ normal to the edge. This statement suggests that in this case the strains and stresses in the point $(\eta, \bar{z})$ (fig. 2) will depend almost completely on the geometrical conditions and the edge load in the point η of the edge.

If this idea is correct the solution of the problem would be obtained by *solving the problem of* the edge effect of a cylindrical shell, where the *edge angle β is constant* and the edge loads m_0, q_0 are constant. This problem of the cylindrical shell bounded by a helix is solved rigorously in Part I; the usual assumption is made that $k^{1/2}$ is negligible to unity.

The applicability of this solution to the problem of the cylinder with oblique edge under edge loads, varying with η, is investigated in Part II. It appears *that its error is of the order* $k^{1/4}$. *An important* result of the investigation is that the edge load, pertaining to the solution, consists not only of m_0, q_0, but in addition of a membrane load, — normal to the edge the component L, tangential *to the edge the component* T, *(fig. 15)* —, which is proportional to q_0. The total load in any point of the edge is parallel to the plane of the oblique section. If the reaction of these edge loads is taken by a frame, it exerts upon the normal section of the frame a normal force N acting in the point of intersection of frame and shell.

The effect of the shell upon the frame is equivalent to that of a flange with the cross section S.

The *conclusions are indicated by marginal lines* in chapters 5, 10 and 11.

Appendices A and B contain the formulae relating to the geometry of the oblique cylindrical shell and a summary of formulae for use in applications respectively.

PART I.

The cylindrical shell loaded along its helical edge by constant bending moments and shear forces.

2 The differential equations.

The equation of the helical edge is, since $\frac{dz}{ad\varphi} = -\tan\beta = -c$ (fig. 3), $z + ca\varphi = A$ (see fig. 4).

The helix is infinitely long and every point is loaded in the same way. Hence, after rotating the

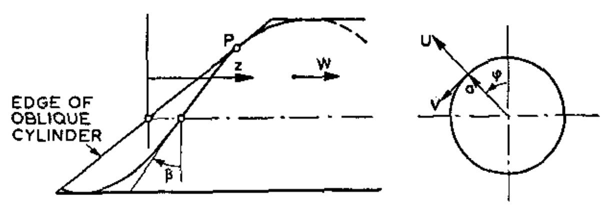

Fig. 3. Helical edge tangent to the edge of the oblique cylinder in P.

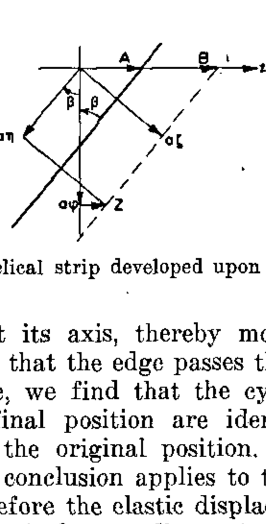

Fig. 4. The helical strip developed upon the flat plane.

cylinder about its axis, thereby moving it longitudinally such that the edge passes through a fixed point in space, we find that the cylinder and its load in the final position are identical to what they were in the original position. This involves that the same conclusion applies to the strains and stresses. Therefore the elastic displacements u, v, w are functions of the coordinate ζ only, they are constant along any helix parallel to the helical edge. The partial differential equations in z and φ as independent variables can be transformed into ordinary differential equations in ζ.

The equation of the helix $\zeta =$ constant is $z + ca\varphi = B$ (fig. 4).

The transformation formulae follow from fig. 4.

$$z = a\zeta\cos\beta - a\eta\sin\beta = a(\zeta - c\eta)\frac{1}{(1+c^2)^{1/2}}, \quad (1a)$$

$$a\varphi = a\zeta\sin\beta + a\eta\cos\beta = a(c\zeta + \eta)\frac{1}{(1+c^2)^{1/2}}. \quad (1b)$$

Since u, v, w are functions of ζ only

$$du = \frac{du}{d\zeta}d\zeta = \frac{\partial u}{\partial z}dz + \frac{\partial u}{\partial\varphi}d\varphi,$$

$$\frac{du}{d\eta} = 0 = \frac{\partial u}{\partial z}\left(\frac{dz}{d\eta}\right)_\zeta + \frac{\partial u}{d\varphi}\left(\frac{\partial\varphi}{d\eta}\right)_\zeta =$$
$$= \frac{\partial u}{\partial z}\cdot\frac{-ac}{(1+c^2)^{1/2}} + \frac{\partial u}{\partial\varphi}\frac{1}{(1+c^2)^{1/2}}.$$

Hence

$$\frac{\partial u}{\partial\varphi} = ac\frac{\partial u}{\partial z}.$$

Putting $a\frac{\partial u}{\partial z} = u'$ we have $\frac{\partial u}{\partial\varphi} = cu'$. (2a)

Then

$$\frac{\partial u}{d\zeta} = \frac{du}{dz}\left(\frac{\partial z}{d\zeta}\right)_\eta + \frac{\partial u}{d\varphi}\left(\frac{\partial\varphi}{d\zeta}\right)_\eta =$$
$$= \frac{1}{(1+c^2)^{1/2}}\left(a\frac{\partial u}{\partial z} + c\frac{\partial u}{\partial\varphi}\right) = (1+c^2)^{1/2}u'. \quad (2b)$$

The differential equations of the cylindrical shell are given in ref. 1, Chapt. VI, 21, eq. 10. After substitution of (2a) and without the external loads they become

$$u + cv' + \nu w' + k\left[(1+c^2)^2u'''' + 2c^2u'' + u - \right.$$
$$\left. - \frac{3-\nu}{2}cv''' + \left(\frac{1-\nu^2}{2}c^2 - 1\right)w'''\right] = 0 \quad (3a)$$

$$cu' + \left(c^2 + \frac{1-\nu}{2}\right)v'' + \frac{1+\nu}{2}cw'' +$$
$$+ k\left[-\frac{3-\nu}{2}cu''' + \frac{3}{2}(1-\nu)v''\right] = 0 \quad (3b)$$

$$\nu u' + \frac{1+\nu}{2}cv'' + \left(\frac{1-\nu}{2}c^2 + 1\right)w'' +$$
$$+ k\left[\left(\frac{1-\nu}{2}c^2 - 1\right)u''' + \frac{1-\nu}{2}c^2w''\right] = 0, \quad (3c)$$

where $k = \frac{h^2}{12a^2}$. Since k is negligibly small compared to unity ku can be neglected in (3a). Corresponding neglections apply to (3b, c).

We replace in these equations v and w by V and W, defined by

$$v = \frac{\partial V}{\partial\varphi} = cV' \qquad w = a\frac{\partial W}{\partial z} = W'. \quad (4)$$

Then integrating (3b, c) once, we obtain

$$u - k\frac{3-\nu}{2}u'' +$$
$$+ \left(c^2 + \frac{1-\nu}{2}\right)V'' + \frac{1+\nu}{2}W'' = C_1 \quad (5b)$$

$$\nu u + k\left(\frac{1-\nu}{2}c^2 - 1\right)u'' +$$
$$+ \frac{1+\nu}{2}c^2V'' + \left(\frac{1-\nu}{2}c^2 + 1\right)W'' = C_2, \quad (5c)$$

which yield

$$\frac{1}{1+c^2}\left[c^2(5\,b) + (5\,c)\right] \equiv \left(1 - \frac{1-\nu}{1+c^2}\right)u +$$
$$- ku'' + c^2V'' + W'' = \frac{1}{1+c^2}(c^2C_1 + C_2) = C_3 \quad (6b)$$

$$\frac{2}{1-\nu}\left[(5\,c) - \nu(5\,b)\right] \equiv k(c^2 - 2 + \nu)u'' +$$
$$+ (c^2 - \nu)V'' + (c^2 + 2 + \nu)W'' =$$
$$= \frac{2}{1-\nu}(C^2 - \nu C_1) = C_4. \quad (6c)$$

From (3a) and (4) follows

$$k(1+c^2)^2u'''' + 2\,kc^2u'' + u + c^2V'' -$$
$$- k\frac{3-\nu}{2}c^2V'''' + \nu W'' +$$
$$+ k\left(\frac{1-\nu}{2}c^2 - 1\right)W'''' = 0. \quad (7)$$

Solving (6b, c) for W'', V'' and substituting them in (7) we find

$$V'' = -\frac{c^2 + 2 + \nu}{(1+c^2)^2}u + \frac{2\,k}{1+c^2}u'' + C_5, \quad (8b)$$

where $C_5 = \dfrac{(c^2 + 2 + \nu)C_3 - C_4}{(c^2+\nu)(1+c^2)}$

$$W'' = \frac{c^2 - \nu}{(1+c^2)^2}u + k\frac{1-c^2}{1+c^2}u'' + C_6 \quad (8c)$$

where $C_6 = \dfrac{-(c^2-\nu)C_3 + c^2C_4}{(c^2+\nu)(1+c^2)}$

$$k(1+c^2)^2u'''' + 2\,ku''\left[2\,c^2 + \frac{(c^2+\nu)(1-c^2)}{1+c^2}\right] +$$
$$+ \frac{1-\nu^2}{(1+c^2)^2}u + c^2C_5 + \nu C_6 = 0. \quad (8a)$$

So far, the only assumption of this analysis is that the helical strip is uniformly loaded at its edge. Therefore the analysis applies not only to edge load, consisting of bending moment and shear force normal to the edge, but also to membrane loads: normal force $\sigma_\zeta h$ and shear force along the edge $\sigma_{\zeta\eta}h$. From now on we will restrict ourselves to load systems, which yield stresses in the vicinity of the edge only. So we put the condition that the stresses vanish for $\zeta = \infty$. Hence u, v, w and their derivatives must vanish at $\zeta = \infty$. Then (8b, c) yield $C_5 = C_6 = 0$ (consequently $C_3 = C_4 = C_1 = C_2 = 0$) and (8a) becomes

$$\frac{k(1+c^2)^4}{1-\nu^2}u'''' + \frac{2}{1-\nu^2}(1+c^2)\left[2\,c^2(1+c^2) +\right.$$
$$\left.+ (c^2+\nu)(1-c^2)\right]ku'' + u = 0.$$

After substitution of (2b) this equation becomes a differential equation in the independent variable ζ

$$\frac{k(1+c^2)^2}{1-\nu^2}\frac{d^4u}{d\zeta^4} + \frac{2}{1-\nu^2}\left[2\,c^2(1+c^2) +\right.$$
$$\left.+ (c^2+\nu)(1-c^2)\right]k\frac{d^2u}{d\zeta^2} + u = 0. \quad (9)$$

3 The solution of the differential equation.

The general solution of this equation is

$$u = e^{\mu\zeta},$$

yielding the characteristic equation

$$\mu^4 + \frac{2}{(1+c^2)^2}\left[2\,c^2(1+c^2) + (c^2+\nu)(1-c^2)\right]\mu^2 +$$
$$+ \frac{1-\nu^2}{(1+c^2)^2}\,\frac{1}{k} = 0.$$

This equation has the form

$$\mu^4 + 2\,A\mu^2 + \frac{B}{k} = 0,$$

where A and B are of the order of unity.

The roots are, when we neglect k against unity,

$$\mu = \pm\left(\frac{B}{4\,k}\right)^{1/4}\left\{1 - \left(\frac{A^2k}{4\,B}\right)^{1/2} \pm i\left[1 + \left(\frac{A^2k}{B}\right)^{1/2}\right]\right\}.$$

Since $k^{1/2} \ll 1$ we will neglect terms of the order of $k^{1/2}$. Hence

$$\mu = \pm\left(\frac{B}{4\,k}\right)^{1/4}(1 \pm i), \quad (10)$$

which are the roots of the characteristic equation

$$\mu^4 + \frac{1-\nu^2}{(1+c^2)^2}\,\frac{1}{k} = 0,$$

pertaining to the differential equation

$$\frac{k(1+c^2)^2}{1-\nu^2}\,\frac{d^4u}{d\zeta^2} + u = 0, \quad (11)$$

The term $2\,Ak\dfrac{d^2u}{d\zeta^2}$ of eq. (9), which is equal to $2\,Ak\mu^2u = \pm 2\,iAB^{1/2}k^{1/2}\,u$, is of the order $k^{1/2}$ compared to the other terms. Therefore it is negligible.

The solution of eq. (11) for which the strains vanish at $\zeta = \infty$ is

$$u = e^{-\alpha\zeta}(A_1\cos\alpha\zeta + A_2\sin\alpha\zeta), \quad (12a)$$

where

$$\alpha = [3(1-\nu^2)]^{1/4}\left(\frac{a}{(1+c^2)h}\right)^{1/2}. \quad (12b)$$

4 The stresses.

The membrane strain components relating to the normal coordinates are

$$\varepsilon_\varphi = \frac{1}{a}\,\frac{\partial v}{\partial\varphi} + \frac{u}{a} = \frac{1}{a}(c^2V'' + u)$$

$$\varepsilon_z = \frac{\partial W}{\partial Z} = aW''$$

$$\gamma = \frac{\partial v}{\partial z} + \frac{1}{a}\ \frac{\partial w}{\partial \varphi} = \frac{1}{a}\, c(V'' + W'').$$

The strain components relating to the ζ, η-axes are (ref. 1 Chapt. I, 10 eq. 3)

$$\varepsilon_\zeta = \varepsilon_z \cos^2\beta + \varepsilon_\varphi \sin^2\beta + \gamma \sin\beta\cos\beta =$$
$$= \frac{1}{a(1+c^2)}\,[c^2u + (1+c^2)(c^2V'' + W'')]$$
$$\varepsilon_\eta = \varepsilon_z \sin^2\beta + \varepsilon_\varphi \cos^2\beta - \gamma \sin\beta\cos\beta =$$
$$= \frac{1}{a(1+c^2)}\, u$$
$$\gamma_{\zeta\eta} = -2(\varepsilon_z - \varepsilon_\varphi)\sin\beta\cos\beta +$$
$$+ \gamma(\cos^2\beta - \sin\beta) =$$
$$= \frac{c}{a(1+c^2)}\,[2u + (1+c^2)(V'' - W'')].$$

Substituting from (8b, c) we find

$$\varepsilon_\zeta = \frac{1}{a(1+c^2)}\,[-\nu u + (1+c^2)ku'']$$
$$\varepsilon_\eta = \frac{1}{a(1+c^2)}\, u$$
$$\gamma_{\zeta\eta} = \frac{c}{a}\, ku''.$$

The stress components are

$$\sigma_\zeta = \frac{E}{a(1-\nu^2)}\, ku'',\ \sigma_\eta = \frac{E}{a}\left(\frac{u}{1+c^2} + \frac{\nu}{1-\nu^2}\, ku''\right),\ \tau_{\zeta\eta} = \frac{E}{2a(1+\nu)}\, cku''. \qquad (13)$$

Since ku'' is of the order $k^{1/2}.u$ the membrane stresses are composed of the first order stresses

$$\sigma_{\zeta_1} = 0,\ \sigma_{\eta_1} \doteq \frac{E\,.\,u}{a(1+c^2)},\ \tau_{\zeta\eta_1} = 0 \quad (13a)$$

and stresses of negligible magnitude

$$\sigma_{\zeta_2} = \frac{E}{a(1-\nu^2)}\, ku'',\ \sigma_{\eta_2} = \nu\sigma_{\zeta_2},\ \tau_{\zeta\eta_2} =$$
$$= \frac{1-\nu}{2}\, c\sigma_{\zeta_2}, \qquad (13b)$$

which are of the order $k^{1/2}$ as compared to the first order stresses.

The lateral load components are (ref. 1 Chapt. VI, 21 eqs. 6 and 9) (see fig. 5)

$$m_{zz} = \frac{Eh}{1-\nu^2}\, k(1-\nu)a\left(-\frac{\partial^2 u}{\partial\varphi\partial z} + \frac{\partial v}{\partial z}\right) = \frac{Eh}{1-\nu^2}\, k(1-\nu)c(-u'' + V'')$$

$$m_{z\varphi} = \frac{Eh}{1-\nu^2}\, k\left(\nu\frac{\partial^2 u}{\partial\varphi^2} + a^2\frac{\partial^2 u}{\partial z^2} - \nu\frac{\partial v}{\partial\varphi} - a\frac{\partial w}{\partial z}\right) = \frac{Eh}{1-\nu^2}\, k[(1+\nu c^2)u'' - \nu c^2V'' - W'']$$

$$m_{\varphi z} = -\frac{Eh}{1-\nu^2}\, k\left(\frac{\partial^2 u}{\partial\varphi^2} + \nu a\frac{2\,\partial^2 u}{\partial z^2} + u\right) = -\frac{Eh}{1-\nu^2}\, k[(\nu + c^2)u'' + u]$$

$$m_{\varphi\varphi} = \frac{Eh}{1-\nu^2}\, k\frac{1-\nu}{2}\left(2a\frac{\partial^2 u}{\partial\varphi\partial z} + \frac{\partial w}{\partial\varphi} - a\frac{\partial v}{\partial z}\right) = \frac{Eh}{1-\nu^2}\, k(1-\nu)c(u'' + \tfrac{1}{2}W'' - \tfrac{1}{2}V'')$$

$$aq_{zr} = -\frac{\partial m_{\varphi\varphi}}{\partial\varphi} - a\frac{\partial m_{z\varphi}}{\partial z} = -\frac{Eh}{1-\nu^2}\, k[(1+c^2)u''' - \frac{1+\nu}{2}\, c^2(V''' + W''')]$$

$$aq_{\varphi r} = \frac{\partial m_{\varphi z}}{\partial\varphi} + a\frac{\partial m_{zz}}{\partial z} = -\frac{Eh}{1-\nu^2}\, kc[(1+c^2)u''' + u' - (1-\nu)V'''].$$

As appears from (8b, c) V'' and W'' are of the order u, whereas u'' is of the order $k^{-1/2}\,u$. Since we neglect terms of the order $k^{1/2}$ the terms u,

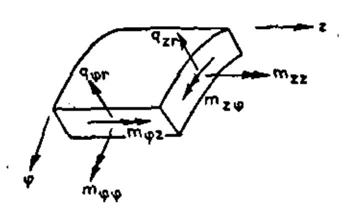

Fig. 5. The lateral load components with reference to th z-φ-axes.

V'' and W'' are negligible as compared with u''. Hence

$$\left.\begin{aligned}
m_{zz} &= -\frac{Eh}{1-\nu^2}\, k(1-\nu)cu'' \\
m_{z\varphi} &= \frac{Eh}{1-\nu^2}\, k(1+\nu c^2)u'' \\
m_{\varphi z} &= -\frac{Eh}{1-\nu^2}\, k(\nu + c^2)u'' \\
m_{\varphi\varphi} &= \frac{Eh}{1-\nu^2}\, k(1-\nu)cu'' \\
aq_{zr} &= -\frac{Eh}{1-\nu^2}\, k(1+c^2)u''' \\
aq_{\varphi r} &= -\frac{Eh}{1-\nu^2}\, kc(1+c^2)u'''.
\end{aligned}\right\} \qquad (14)$$

The lateral load components with respect to the ζ-η-axes can be computed from fig. 6.

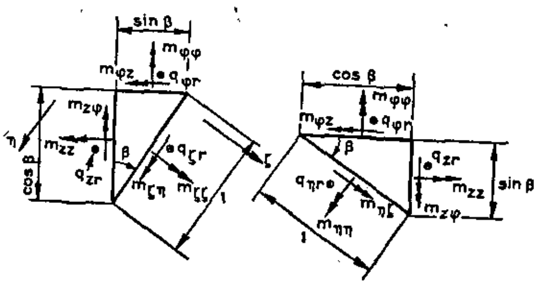

Fig. 6. The lateral load components with reference to the ζ-η-axes.

$$m_{\zeta\zeta} = m_{zz}\cos^2\beta + m_{z\varphi}\cos\beta\sin\beta + m_{\varphi z}\sin\beta\cos\beta + m_{\varphi\varphi}\sin^2\beta$$

$$m_{\zeta\eta} = -m_{zz}\cos\beta\sin\beta + m_{z\varphi}\cos^2\beta - m_{\varphi z}\sin^2\beta + m_{\varphi\varphi}\sin\beta\cos\beta$$

$$m_{\eta\zeta} = -m_{zz}\sin\beta\cos\beta - m_{z\varphi}\sin^2\beta + m_{\varphi z}\cos^2\beta + m_{\varphi\varphi}\cos\beta\sin\beta$$

$$m_{\eta\eta} = m_{zz}\sin^2\beta - m_{z\varphi}\sin\beta\cos\beta - m_{\varphi z}\cos\beta\sin\beta + m_{\varphi\varphi}\cos^2\beta$$

$$q_{\zeta r} = q_{zr}\cos\beta + q_{\varphi r}\sin\beta$$

$$q_{\eta r} = -q_{zr}\sin\beta + q_{\varphi r}\cos\beta.$$

Substitution of (14) yields

$$\left.\begin{aligned}
m_{\zeta\zeta} &= 0\\
m_{\zeta\eta} &= \frac{Eh}{1-\nu^2}k(1+c^2)u''\\
m_{\eta\zeta} &= -\frac{Eh}{1-\nu^2}k(1+c^2)\nu u''\\
m_{\eta\eta} &= 0\\
aq_{\zeta r} &= -\frac{Eh}{1-\nu^2}k(1+c^2)^{3/2}u'''\\
qa_{\eta r} &= 0
\end{aligned}\right\} \qquad (15)$$

5 Summary and interpretation of results.

The differential equation (11), its solution (12), the membrane stresses (13a) and the lateral load components (15) can be obtained in a straightforward manner by assuming that the strains and stresses in the cylinder bounded by a helix are identical to those in a straight edged cylinder having the radius equal to the radius of the cylinder in the plane through the tangent to the helix and through the normal to the cylinder. This radius is $R_1 = a(1+c^2)$ (see Appendix A). This conclusion can be obtained when we transform the derivatives to z into derivatives of the linear coordinate $\bar{z} = a\zeta$ by means of (2b) and when we replace a by $\dfrac{R_1}{1+c^2}$.

The differential equation (11) becomes

$$\frac{h^2R_1^{\,2}}{12(1-\nu^2)}\,\frac{d^4u}{d\bar{z}^4} + u = 0,. \qquad \text{(I)}$$

which corresponds to the differential equation of the straight edged cylinder with radius R_1 for axially symmetrical deformation (ref. 1, Chapt. VI, 19 eq. 9).

The membrane stress (13a) is

$$\sigma_{\eta_1} = E\,\frac{u}{R_1}.$$

(compare ref. 1, Chapt. VI, 19 eq. 1) (II)

The bending moments and shear force (15) are

$$m_{\zeta\eta} = \frac{Eh^3}{12(1-\nu^2)}\,\frac{d^2u}{d\bar{z}^2}$$

(compare ref. 1, Chapt. VI, 19 eq. 17) (III)

$$m_{\eta\zeta} = -\nu m_{\zeta\eta}$$

(compare ref. 1, Chapt. VI, 19 eq. 4) (IV)

$$q_{\zeta r} = -\frac{Eh^3}{12(1-\nu^2)}\,\frac{d^3u}{d\bar{z}^3}.$$

(compare ref. 1, Chapt. VI, 19 eq. 17) (V)

So far the correspondance between the straight cylinder concept and the helical theory is perfect. The straight cylinder concept fails to give an equivalent for the membrane stresses (13b). However, these stresses are of the order $k^{1/2}$ small compared to σ_{η_1} and to the bending stress following from $m_{\zeta\eta}$. The bending stresses are

$$\sigma_b = \frac{Eh}{2(1-\nu^2)}\,\frac{d^2u}{d\bar{z}^2}, \text{ whereas } \sigma_{\zeta_2} = \frac{h}{6R_1}\,\frac{Eh}{2(1-\nu^2)}\,\frac{d^2u}{d\bar{z}^2}.$$

Another discrepancy relates to the displacements v, w

$$\frac{dv}{d\bar{z}} = \frac{(1+c^2)^{1/2}}{a}v' = \frac{c(1+c^2)^{1/2}}{a}V'' \text{ and } \frac{dw}{d\bar{z}} = \frac{(1+c^2)^{1/2}}{a}W''.$$

The displacement components $\bar{v}$, $\bar{w}$ with respect to the ζ-η-axes are (see fig. 7)

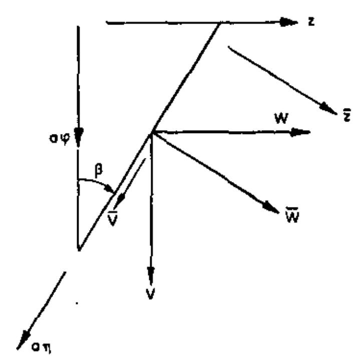

Fig. 7. Transformation of displacement components.

$$\bar{v} = +v\cos\beta - w\sin\beta,\quad \bar{w} = v\sin\beta + w\cos\beta.$$

Using 8b, c and neglecting thereby terms of the order $k^{1/2}$ we obtain

$$\frac{d\bar{v}}{d\bar{z}} = -\frac{2cu}{R_1},\quad \frac{d\bar{w}}{d\bar{z}} = -\frac{(c^2+\nu)u}{R_1} \qquad (16)$$

The straight cylinder yields

$$\frac{dv_R}{d\bar{z}} = 0,\ \frac{dw_R}{d\bar{z}} = -\frac{\nu u_R}{R}, \qquad (17)$$

which seems not to be in agreement with $\bar{v}$ and $\bar{w}$. However v_R, w_R are not physically identical to $\bar{v}$, $\bar{w}$, since the vectors $\bar{v} + \dfrac{d\bar{v}}{d\bar{z}}d\bar{z}$, $\bar{w} + \dfrac{d\bar{w}}{d\bar{z}}d\bar{z}$ are rotated through the angle $\dfrac{d\bar{z}\,.\,\sin\beta}{a}$ with respect to the vectors $\bar{v}$, $\bar{w}$, whereas $v_R + \frac{dv_R}{d\bar{z}} d\bar{z}$, $w_R + \frac{dw_R}{d\bar{z}} d\bar{z}$ are parallel to v_R, w_R. If we account for this fact the relation between u, $\bar{v}$, $\bar{w}$ and u_R, v_R, w_R must be

$$\frac{du_R}{d\bar{z}} = \frac{dv}{d\bar{z}} - \frac{\bar{v}}{a} \cos\beta \sin\beta - \frac{\bar{w}}{a} \sin^2\beta$$

$$\frac{dv_R}{d\bar{z}} = \frac{d\bar{v}}{d\bar{z}} + \frac{\bar{u}}{a} \sin\beta \cos\beta$$

$$\frac{dw_R}{d\bar{z}} = \frac{d\bar{w}}{d\bar{z}} + \frac{\bar{u}}{a} \sin^2\beta,$$

yielding, when we substitute from (16),

$$\frac{d^2u_R}{d\bar{z}^2} = \frac{d^2u}{d\bar{z}^2} + c^2(c^2 + 2 + \nu) \frac{u}{R^2}$$

$$\frac{dv_R}{d\bar{z}} = -\frac{cu}{R}.$$

$$\frac{dw_R}{d\bar{z}} = -\frac{\nu u}{R}.$$

Since $\frac{d^2u}{d\bar{z}^2}$ is of the order $k^{-1/4} \frac{u}{R^2}$ the second term in the first one of these equations is negligible. Hence

$$u_R = u, \quad \frac{dv_R}{d\bar{z}} = -\frac{cu_R}{R_1}, \quad \frac{dw_R}{d\bar{z}} = -\nu \frac{u_R}{R_1}.$$

We obtained from the straight cylinder concept the equations (17), which appear to be in error as far as v_R is concerned. This, however, is not a grave failure, since the displacement $\bar{v}$ is of the order $k^{1/4}$ small compared to u.

So we may conclude that the straight cylinder concept is correct apart from its description of the displacement component v_R. It yields the correct answer for the stress distribution.

The recipe for establishing the stresses in a cylinder with radius a and wall thickness h loaded by constant bending moments $m_{\zeta\eta}$ and shear forces $q_{\zeta r}$ along its helical edge, the pitch of the helix being $2\pi ac$, is:

The actual cylinder is replaced by a straight edged cylinder with radius $R_1 = a(1 + c^2)$ and wall thickness h; the loads $m_{\zeta\eta}$, $q_{\zeta r}$ are applied to the straight edge of this cylinder. Then the deflections u and the stresses established for the straight cylinder (formulae I through V) are identical to those for the cylinder bounded by the helix with the same edge load.

PART II.

The oblique cylindrical shell loaded along its edge.

6 The approach to the problem.

The edge of the cylinder is the line of intersection between the cylinder and a flat plane, which makes the angle Φ with the normal section (fig. 1).

The problem to be investigated is the stress distribution in and distortions of the shell near its edge for edge loads, consisting of bending moments and shear forces normal to the shell, together with other load components required for equilibrium.

It is known from bending theory of straight edged cylindrical shells that the deflections u due to these edge loads damp out very rapidly in axial direction, $\frac{du}{dz}$ being of the order $k^{-1/4}\frac{u}{a}$. We shall suppose that the edge loads are such that $\frac{\partial u}{\partial s}$ (s being the coordinate along the edge) is much smaller than $\frac{\partial u}{\partial z}$, $\frac{\partial u}{\partial s}$ will be of the order of $\frac{u}{a}$. This involves the restriction that the variation of *the edge loads shall be slow. So we assume that* the derivative of the edge load with respect to $\frac{s}{a}$ is of the order of the edge load, and we intend to solve the shell problem for this type of edge load.

Since $\frac{\partial u}{\partial s} \ll \frac{\partial u}{\partial z}$ the strains (and thereby the stresses)depend mainly on the derivatives of the displacements to z. This suggests that strains obtained for edge conditions, which do not vary with s, might be a good approximation for the strains occurring at edge conditions varying with φ.

Applying this approach to the oblique cylindrical shell we assume that the deflection u and the stresses in points along the line $s=$ constant, perpendicular to the edge, may be computed from the edge load in s by means of the theory for the cylinder bounded by a helix, developed in part I. The tangent to the edge in s is continued in a helix (fig. 3), this helix forming the edge of the substitute cylinder, and the helical edge is loaded by constant edge loads equal to those in s. In the edge points adjacent to s the actual edge loads are different and so is the angle β of the tangent helix. Thus there are two reasons by which the exact solution differs from the assumed approximate solution.

We will investigate the error of the approximation by establishing the additional loads which are required to maintain the assumed deformation and by estimating the effect of these additional loads.

7 The stresses.

An arbitrary point P of the shell is denoted by its coordinates $s=a\eta$ and $\bar{z}=a\zeta$, where s is the coordinate along the oblique section and $\bar{z}$ is the *distance to the edge. Developed upon the flat* plane, the cylindrical shell and its coordinate system is as indicated in fig. 8. In this way the point Q is adjungated to the point P of the edge, where on the developed cylinder the normal from Q to the edge cuts the edge.

It is assumed that the displacements u, $\bar{v}$, $\bar{w}$ in Q are equal to the displacements in Q, as excited by constant edge loads along a helical edge through P tangent to the curve s, the edge load being equal to the actual edge load in P. Then u is the solution of equation I, Chapter 5 and $\bar{v}$, $\bar{w}$ follow from eq. (16).

The membrane stresses occurring with these displacements can be computed from the specific deformations (see fig. 8).

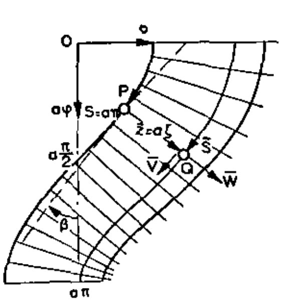

Fig. 8. Orthogonal coordinates η, ζ shown when the shell is developed upon a flat plane.

$$\left.\begin{aligned}\varepsilon_{\bar{z}} &= \frac{\partial \bar{w}}{\partial \bar{z}} + \frac{u}{a}\sin^2\beta\\ \varepsilon_{\bar{s}} &= \frac{\partial \bar{v}}{\partial \bar{s}} + \frac{u}{a}\cos^2\beta\\ \gamma_{\bar{z}\bar{s}} &= \frac{\partial \bar{v}}{\partial \bar{z}} + \frac{\partial \bar{w}}{\partial \bar{s}} + \frac{u}{a}2\sin\beta\cos\beta.\end{aligned}\right\} \quad (18)$$

These formulae follow from the general strain component formulae given in Part I, Chapter 3. The stresses thus established differ from the stresses occurring in the helical cylinder under constant edge load by an amount which is of the order $k^{1/4}$ small compared to those in the helical cylinder. This will be shown for the stress $\sigma_{\bar{s}}$.

Substituting (16) into (18), using (see fig. 8)

$$d\bar{s} = a d\eta \left(1 + \frac{d\beta}{d\eta}\zeta\right)$$

and taking into account that for $\bar{z} = \infty$ $\bar{v} = \bar{w} = 0$, we find

$$\sigma_{\bar{s}} = E\left[\frac{u}{a}\cos^2\beta + \frac{2}{1-\nu^2}\cdot\right.$$

$$\left.\cdot\frac{1}{a\left(1+\dfrac{d\beta}{d\eta}\zeta\right)}\frac{\partial}{\partial\eta}\left(\sin\beta\cos\beta\int_{\bar{z}}^{\infty}\frac{u}{a}\,d\bar{z}\right)\right].$$

The first term is identical to σ_{η_1} according to (13a), the second term is a consequence of the fact that u and β vary with η, which is not present with the problem investigated in Part I. Expressions of the same type apply to $\sigma_{\bar{z}}$ and $\tau_{\bar{z}\bar{s}}$.

u is given by (12)

$$u = e^{-x}\ (A_1\cos x + A_2\sin x),$$

where $x = \alpha\,\dfrac{\bar{z}}{a}$ and

$$\alpha = [3(1-\nu^2)]^{1/4}\left(\frac{a}{h}\right)^{1/2}\frac{1}{(1+c^2)^{1/2}} =$$

$$= \left(\frac{1-\nu^2}{4k}\right)^{1/4}\cos\beta.$$

A_1 and A_2 follow from the bending moment m_0 and the shear force q_0 at the edge, as given by form. III and V of Ch. 5.

$$A_1 = \frac{1}{Eh}\left(\frac{1-\nu^2}{k}\right)^{1/2}\frac{1}{\cos^2\beta}\left[m_0 + \right.$$

$$\left. - \left(\frac{4k}{1-\nu^2}\right)^{1/4}\frac{a}{\cos\beta}\,q_0\right]$$

$$A_2 = -\frac{1}{Eh}\left(\frac{1-\nu^2}{k}\right)^{1/2}\frac{1}{\cos^2\beta}\,m_0.$$

Then

$$u = \frac{1}{Eh}\left(\frac{1-\nu^2}{k}\right)^{1/2}\frac{1}{\cos^2\beta}\,e^{-x}\left[m_0(\cos x - \sin x) + \right.$$

$$\left. - \left(\frac{4k}{1-\nu^2}\right)^{1/4}\frac{a}{\cos\beta}\,q_0\cos x\right] \quad (19)$$

and

$$\int_{\bar{z}}^{\infty}\frac{u}{a}\,d\bar{z} = -\frac{1}{Eh}\left(\frac{1-\nu^2}{4k}\right)^{1/4}\frac{1}{\cos^3\beta}e^{-x}\left[2\,m_0\sin x + \right.$$

$$\left. + \left(\frac{4k}{1-\nu^2}\right)^{1/4}\frac{a}{\cos\beta}\,q_0\,(\cos x - \sin x)\right]. \quad (20)$$

When differentiating to η one should take into account that x is a function of η

$$\frac{dx}{d\eta} = \frac{\bar{z}}{a}\,\frac{d\alpha}{d\eta} = -\left(\frac{1-\nu^2}{4k}\right)^{1/4}\sin\beta\,\frac{d\beta}{d\eta}\,\frac{\bar{z}}{a} =$$

$$= -x\tan\Phi\sin\beta\cos^2\beta\cos\varphi.$$

Then

$$\frac{\partial}{\partial\eta}\left[\sin\beta\cos\beta\int_{\bar{z}}^{\infty}\frac{u}{a}\,d\bar{z}\right] =$$

$$= -\frac{1}{Eh}\left(\frac{1-\nu^2}{4k}\right)^{1/4}e^{-x}\left\{\left[2\frac{dm_0}{d\eta}\sin x + \right.\right.$$

$$\left. + \left(\frac{4k}{1-\nu^2}\right)^{1/4}\frac{a}{\cos\beta}\,\frac{dq_0}{d\eta}\,(\cos x - \sin x)\right]\frac{\sin\beta}{\cos^2\beta} +$$

$$+ 2\,m_0[(2-\cos^2\beta)\sin x - \sin^2\beta\,x(\cos x -$$

$$+ \sin x]\tan\Phi\cos\varphi +$$

$$+ \left(\frac{4k}{1-\nu^2}\right)^{1/4}\frac{a}{\cos\beta}\,q_0[(3-2\cos^2\beta)(\cos x +$$

$$- \sin x) + 2\sin^2\beta\,x\cos x]\tan\Phi\cos\varphi.$$

$\dfrac{dm_0}{d\eta}$, $\dfrac{dq_0}{d\eta}$ are of the order m_0, q_0. Then the second term in $\sigma_{\bar{s}}$ is of the order $\dfrac{1}{ahk^{1/4}}$ $(m_0 + k^{1/4} a\,q_0)$, whereas the first term is of the order $\dfrac{1}{ahk^{1/2}}$ $(m_0 + k^{1/4}\,aq_0)$. Therefore, when we put

$$\sigma_{\bar{s}} = \sigma_{\eta_1} = E\,\frac{u}{a}\cos^2\beta, \quad (21)$$

the error is of the order $k^{1/4}$.

A similar conclusion holds for the lateral load components.

Since $\bar{v}$, $\bar{w}$ are of the order $k^{1/4}u$ their contribution to the lateral load components is of the order $k^{1/2}$ compared to those of u. Then they are negligible and

$$m_{\bar{z}\bar{s}} = \frac{Eh^3}{12(1-\nu^2)}\left(\nu\,\frac{\partial^2 u}{\partial\bar{s}^2} + \frac{\partial^2 u}{\partial\bar{z}^2}\right)$$

$$m_{\bar{s}\bar{z}} = -\frac{Eh^3}{12(1-\nu^2)}\left(\frac{\partial^2 u}{\partial\bar{s}^2} + \nu\,\frac{\partial^2 u}{\partial\bar{z}^2}\right)$$

$$m_{\bar{s}\bar{s}} = -m_{\bar{z}\bar{z}} = \frac{Eh^3}{12(1-\nu^2)}\,(1-\nu)\,\frac{\partial^2 u}{\partial\bar{s}\partial\bar{z}}$$

$$q_{\bar{z}r} = -\frac{Eh^3}{12(1-\nu^2)}\left(\frac{\partial^3 u}{\partial\bar{s}^2\partial\bar{z}} + \frac{\partial^3 u}{\partial\bar{z}^3}\right)$$

$$q_{\bar{s}r} = -\frac{Eh^3}{12(1-\nu^2)}\left(\frac{\partial^3 u}{\partial\bar{s}^3} + \frac{\partial^3 u}{\partial\bar{s}\partial\bar{z}^2}\right).$$

Since $\dfrac{\partial u}{\partial\bar{s}} = \dfrac{1}{a\left(1+\dfrac{d\beta}{d\eta}\zeta\right)}\dfrac{\partial u}{\partial\eta}$ is of the order $\dfrac{u}{a}$ and $\dfrac{\partial u}{\partial\bar{z}}$ is of the order $k^{-1/4}\,\dfrac{u}{a}$ we find, neglecting again $k^{1/2}$ to unity,

$$m_{\bar{z}\bar{s}} = \frac{Eh^3}{12(1-\nu^2)}\,\frac{\partial^2 u}{\partial\bar{z}^2} \quad (22a)$$

$$m_{\bar{s}\bar{z}} = -\nu\,m_{\bar{z}\bar{s}} \quad (22b)$$

$m_{\bar{s}\bar{s}} = -m_{\bar{z}\bar{z}}$ is of the order $k^{1/4}m_{\bar{z}\bar{s}}$

$$q_{\bar{z}r} = -\frac{Eh^3}{12(1-\nu^2)}\frac{\partial^3 u}{\partial \bar{z}^3} \qquad (22c)$$

$q_{\bar{s}r}$ is of the order $k^{1/4}qzr$.

Therefore, when the stresses are taken from eq. II to V incl. of Ch. 5 the error is of the order $k^{1/4}$.

8 The additional load system I.

The element $d\bar{z}$, $d\bar{s}$ of the shell is not in equilibrium when the membrane stresses $\sigma_{\bar{s}}$, given by (21) and the lateral load components $m_{\bar{z}\bar{s}}$, $m_{\bar{s}\bar{z}}$, $q_{\bar{z}r}$, given by (22a, b, c) are applied, and $\sigma_{\bar{z}}$, $\tau_{\bar{z}\bar{s}}$, $m_{\bar{s}\bar{s}}$, $m_{\bar{z}\bar{z}}$, $q_{\bar{s}r}$ are assumed to vanish. The reason is that the coordinate system $\bar{z}$, $\bar{s}$ differs from the corresponding coordinate system $\bar{z}$, $a\eta$ used with the helical cylinder. We will establish the external load system, required for equilibrium at the assumed state of stress. This load system will be called "additional load system I".

This external load consists of (see fig. 9) forces

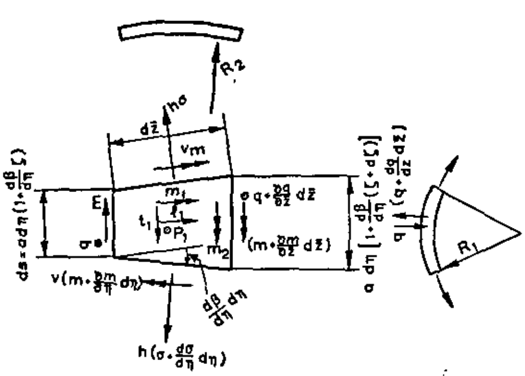

Fig. 9. Element $d\bar{z}$, $d\bar{s}$ with elastic stress components and additional loads $p_1 t_1 l_1 m_1$, m_2 per unit area.

l_1, t_1, p_1 and moments m_1, m_2 per unit area. They can be established by considering the equilibrium of an element of the shell.

For the sake of simplicity of notation we put $\sigma_{\bar{s}} = \sigma$, $m_{\bar{z}\bar{s}} = m$, $q_{\bar{z}r} = q$. The equations of equilibrium of the element are

$$h\sigma\frac{d\beta}{d\eta} - l_1 a\left(1+\frac{d\beta}{d\eta}\zeta\right) + \\ - q\left(1+\frac{d\beta}{d\eta}\zeta\right)\sin^2\beta = 0 \qquad (23a)$$

$$h\frac{\partial\sigma}{\partial\eta} + t_1 a\left(1+\frac{d\beta}{d\eta}\zeta\right) + \\ + q\left(1+\frac{d\beta}{d\eta}\zeta\right)\sin\beta\cos\beta = 0 \qquad (23b)$$

$$\frac{\sigma h}{R_1}\left(1+\frac{d\beta}{d\eta}\zeta\right) - \frac{q}{a}\frac{d\beta}{d\eta} - \frac{\partial q}{\partial \bar{z}} + \\ - p_1\left(1+\frac{d\beta}{d\eta}\zeta\right) = 0$$

$$-\nu\frac{\partial m}{\partial\eta} + m_1 a\left(1+\frac{d\beta}{d\eta}\zeta\right) = 0 \qquad (23d)$$

$$-\nu m\frac{d\beta}{d\eta} + a\frac{\partial m}{\partial \bar{z}} + m\frac{d\beta}{d\eta} + \\ + qa\left(1+\frac{d\beta}{d\eta}\zeta\right) + m_2 a\left(1+\frac{d\beta}{d\eta}\zeta\right) = 0.$$

Since σ, m and q are the exact solutions for the helical cylinder, where

$$\frac{d\beta}{d\eta} = \frac{d\sigma}{d\eta} = \frac{dm}{d\eta} = p_1 = m_2 = 0,$$

the third and the fifth equations yield in this case

$$\frac{\sigma h}{R_1} - \frac{\partial q}{\partial \bar{z}} = 0$$

$$a\frac{\partial m}{\partial \bar{z}} + qa = 0.$$

Subtracting these latter equations from those for the oblique cylinder and eliminating q we obtain:

$$\frac{d\beta}{d\eta}\left(\frac{\sigma h}{R_1}\zeta + \frac{1}{a}\frac{\partial m}{\partial \bar{z}} - p_1\left(1+\frac{d\beta}{d\eta}\zeta\right)\right) = 0 \qquad (23c)$$

$$\frac{d\beta}{d\eta}\left[(1-\nu)m - \frac{\partial m}{\partial \bar{z}}a\zeta\right] + m_2 a\left(1+\frac{d\beta}{d\eta}\zeta\right) = 0. \qquad (23e)$$

The equations (23a/e) establish the additional load required for equilibrium: forces l_1, t_1, p_1 and moments m_1, m_2 per unit area.

In order to simplify this system we decompose m_1, m_2 in statically equivalent forces. Adding these forces to l_1, n_1, p_1 we obtain a load system, consisting of forces per unit area l, t, p.

Fig. 10 shows how m_1 can be decomposed in

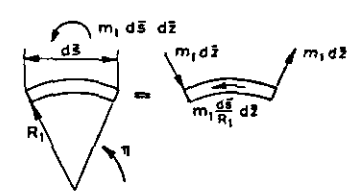

Fig. 10. Static equivalent of the moment m_1.

statically equivalent forces. Combining the edge loads of 2 consecutive elements $d\bar{s}$ (see fig. 11)

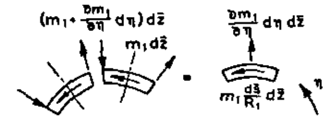

Fig. 11. Combined load upon 2 consecutive elements $d\bar{s}$.

we find that m_1 is equivalent to a tangential load t_2 and a normal load p_2 per unit area.

$$t_2 \; d\bar{s}\,d\bar{z} = \frac{m_1}{R_1}\,d\bar{s}\,d\bar{z}$$

$$p_2 \; d\bar{s}\,d\bar{z} = \frac{\partial m_1}{\partial\eta}\,d\eta\,d\bar{z}.$$

m_1 has been defined by (23d), hence

$$t_2\left(1+\frac{d\beta}{d\eta}\zeta\right)=\frac{\nu}{aR_1}\frac{\partial m}{\partial\eta} \tag{24a}$$

$$p_2\left(1+\frac{d\beta}{d\eta}\zeta\right)=\frac{\nu}{a_2}\frac{\partial}{\partial\eta}\left(\frac{1}{1+\frac{d\beta}{d\eta}\zeta}\frac{\partial m}{\partial\eta}\right) \tag{24b}$$

The same procedure is applied to m_2 in figs. 12 and 13; m_2 proves to be statically equivalent to a longitudinal load l_2 and a normal load p_3 par unit area.

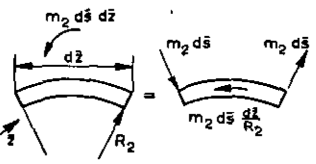

Fig. 12. Static equivalent of the moment m_2.

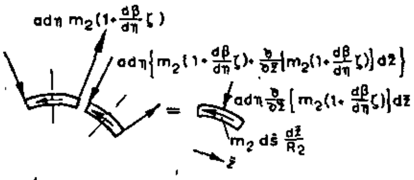

Fig. 13. Combined load upon 2 consecutive elements $d\bar{z}$.

$$l_2\,d\bar{s}\,d\bar{z}=-\frac{m_2}{R_2}\,d\bar{s}\,d\bar{z}$$

$$p_3\,d\bar{s}\,d\bar{z}=-\,ad\eta\frac{\partial}{\partial\bar{z}}\left[m_2\left(1+\frac{d\beta}{d\eta}\zeta\right)\right]d\bar{z}.$$

m_2 has been defined by (23e), hence

$$l_2\left(1+\frac{d\beta}{d\eta}\zeta\right)=\frac{1}{aR_2}\frac{d\beta}{d\eta}\left[(1-\nu)m-\frac{\partial m}{\partial\bar{z}}a\zeta\right] \tag{25a}$$

$$p_3\left(1+\frac{d\beta}{d\eta}\zeta\right)=\frac{-d\beta}{ad\eta}\left(\nu\frac{\partial m}{\partial\bar{z}}+\frac{\partial^2 m}{\partial\bar{z}^2}a\zeta\right) \tag{25b}$$

The total additional load components are

$$l=l_1+l_2,\quad t=t_1+t_2,\quad p=p_1+p_2+p_3$$

$$\left.\begin{aligned}
l\left(1+\frac{d\beta}{d\eta}\zeta\right)&=\frac{d\beta}{d\eta}\left\{\sigma\frac{h}{a}+\frac{1}{aR_2}\left[(1-\nu)m-\frac{\partial m}{\partial\bar{z}}a\zeta\right]\right\}-q\left(1+\frac{d\beta}{dq}\zeta\right)\frac{\sin^2\beta}{a}\\
t\left(1+\frac{d\beta}{d\eta}\zeta\right)&=-\frac{\partial\sigma}{\partial\eta}\frac{h}{a}+\frac{\nu}{aR_1}\frac{\partial m}{\partial\eta}+q\left(1+\frac{d\beta}{d\eta}\zeta\right)\frac{\sin\beta\cos\beta}{a}\\
p\left(1+\frac{d\beta}{d\eta}\zeta\right)&=\frac{d\beta}{d\eta}\left(\sigma\frac{h}{R_1}\zeta+\frac{(1-\nu)}{a}\frac{\partial m}{\partial\bar{z}}-\frac{\partial^2 m}{\partial\bar{z}^2}a\zeta\right)+\\
&\quad+\frac{\nu}{a^2\left(1+\frac{d\beta}{d\eta}\zeta\right)}\left(\frac{\partial^2 m}{\partial\eta^2}-\frac{\partial m}{d\eta}\frac{\frac{d^2\beta}{d\eta^2}\zeta}{1+\frac{d\beta}{d\eta}\zeta}\right).
\end{aligned}\right\} \tag{26}$$

Having thus established the load components l, t, p we will investigate their order of magnitude. Since we have already neglected stresses of the order $k^{1/4}\sigma$, we have to do so everywhere and hence to neglect loads which give rise to stresses of that order. After substraction of these negligible loads the remaining load system forms the load system I required for equilibrium.

We substitute σ and m from (21) and (22a), then l, t, p are expressed in u. So as to establish the order of magnitude of the additional loads it is useful to take instead of the variable $\bar{z}$

$$x=\alpha\frac{\bar{z}}{a}=\alpha\zeta.$$

Then $\frac{\partial u}{\partial\bar{z}}=\frac{a}{\alpha}\frac{\partial x}{\partial u}$, where $\frac{\partial u}{\partial x}$ is of the order of u as well as $\frac{\partial u}{\partial\eta}$.

Finally we introduce

$$R_1=\frac{a}{\cos^2\beta},\ R_2=\frac{a}{\sin^2\beta}.$$

Then we obtain

$$\begin{aligned}
l\left(1+\frac{d\beta}{d\eta}\zeta\right)&=\frac{Eh}{a^2}\left[\frac{d\beta}{d\eta}\left\{\cos^2\beta\,u+\tfrac{1}{2}\left(\frac{k}{1-\nu^2}\right)^{1/2}\sin^2\beta\cos^2\beta\left[(1-\nu)\frac{\partial^2 u}{\partial x^2}-x\frac{\partial^3 u}{\partial x^3}\right]\right\}+\right.\\
&\quad\left.+\frac{\cos^3\beta\sin^2\beta}{2^{3/2}}\left(1+\frac{d\beta}{d\eta}\zeta\right)\left(\frac{k}{1-\nu^2}\right)^{1/4}\frac{d^3u}{dx^3}\right]\\
t\left(1+\frac{d\beta}{d\eta}\zeta\right)&=\frac{Eh}{a^2}\left\{-\frac{\partial}{\partial\eta}(\cos^2\beta\,u)+\tfrac{1}{2}\left(\frac{k}{1-\nu^2}\right)^{1/2}\nu\cos^2\beta\frac{\partial}{\partial\eta}\left(\cos^2\beta\frac{\partial^2 u}{\partial x^2}\right)+\right.\\
&\quad\left.-\frac{\cos^4\beta\sin\beta}{2^{3/2}}\left(1+\frac{d\beta}{d\eta}\zeta\right)\left(\frac{k}{1-\nu^2}\right)^{1/4}\frac{d^3u}{dx^3}\right\}
\end{aligned}$$

$$p\left(1+\frac{d\beta}{d\eta}\,\zeta\right)=\left(\frac{4\,k}{1-\nu^2}\right)^{1/4}\frac{Eh}{4a^2}\left\{\frac{d\beta}{d\eta}\cos^3\beta\left[4\,xu+(1-\nu)\,\frac{\partial^3u}{\partial x^3}-x\,\frac{\partial^4u}{\partial x^4}\right]+\right.$$

$$\left.+\left(\frac{4\,k}{1-\nu^2}\right)^{1/4}\frac{\nu}{1+\dfrac{d\beta}{d\eta}\,\zeta}\,\frac{\partial^2}{\partial\eta^2}\left(\cos^2\beta\,\frac{\partial^2u}{\partial x^2}\right)-\left(\frac{4\,k}{1-\nu^2}\right)^{1/2}\frac{\nu\,\dfrac{d^2\beta}{d\eta^2}}{\left(1+\dfrac{d\beta}{d\eta}\,\zeta\right)^2}\,x\,\frac{\partial}{\partial\eta}\left(\cos\beta\,\frac{\partial^2u}{\partial x^2}\right)\right\}.$$

The functions of u and β occurring in these expressions are of the order u. Therefore neglecting terms of the order $k^{1/4}$ to unity, we find

$$l\left(1+\frac{d\beta}{d\eta}\,\zeta\right)=\frac{Eh}{a^2}\,\frac{d\beta}{d\eta}\cos^2\beta\,u$$

$$t\left(1+\frac{d\beta}{d\eta}\,\zeta\right)=-\,\frac{Eh}{a^2}\,\frac{\partial}{\partial\eta}\,(\cos^2\beta\,u)$$

$$p\left(1+\frac{d\beta}{d\eta}\,\zeta\right)=$$

$$=\left(\frac{4\,k}{1-\nu^2}\right)^{1/4}\frac{Eh}{4\,a^2}\,\frac{d\beta}{d\eta}\cos^3\beta\left[4\,xu+\right.$$

$$\left.+\;(1-\nu)\,\frac{\partial^3u}{\partial x^3}-x\frac{\partial^4u}{\partial x^4}\right].$$

The normal load p is of the order $k^{1/4}\dfrac{Eh}{a^2}\,u$. It causes membrane stress of the order $p\dfrac{a}{h}=k^{1/4}E\dfrac{u}{a}$, which is of the order $k^{1/4}\,\sigma$. As has already been observed we have to neglect stresses of this order of magnitude. This means that the additional load p is negligible. Then the remaining additional load components are just l and t and we conclude that the additional loads required for equilibrium in the assumed state of deformation are

$$l\left(1+\frac{d\beta}{d\eta}\,\zeta\right)=\frac{Eh}{a^2}\,\frac{d\beta}{d\eta}\cos^2\beta\,u \qquad (27a)$$

$$t\left(1+\frac{d\beta}{d\eta}\,\zeta\right)=-\,\frac{Eh}{a^2}\,\frac{\partial}{\partial\eta}\,(\cos^2\beta\,u) \quad (27b)$$

This load will be called "load I".

9 The load system II.

Since the shell is in fact not subjected to external load along its surface the load system I has to be compensated by an equal load system of opposite sign $(-l,\ -t)$. This load system forms part of "load II", which comprises in addition forces along the edge of the oblique cylinder. These edge forces L and T are chosen such, that the load system II it self equilibrated and restricts its influence to the vicinity of the edge. The distributed load l, t is important only in a narrow strip along the edge, since u damps out rapidly with increasing $\bar{z}$. Therefore, if the loads $-l$, $-t$ of the element $d\eta$, $0<\bar{z}<\infty$ find their reaction in $\bar{z}=0$ (fig. 14), the load system composed of $-l$, $-t$ and these edge forces will confine its influence on the shell to the vicinity of the edge.

Therefore we take (see fig. 14)

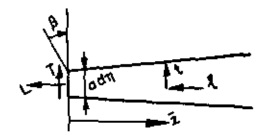

Fig. 14. Load system II.

$$L\,ad\eta+\int_0^\infty l\,a\,d\eta\left(1+\frac{d\beta}{d\eta}\,\zeta\right)d\bar{z}=0$$

$$T\,ad\eta+\int_0^\infty t\,a\,d\eta\left(1+\frac{d\beta}{d\eta}\,\zeta\right)d\bar{z}=0,$$

hence

$$L=-\,\frac{Eh}{a^2}\,\frac{d\beta}{d\eta}\cos^2\beta\int_0^\infty u\,d\bar{z}$$

$$T=\frac{Eh}{a^2}\,\frac{d}{d\eta}\left[\cos^2\beta\int_0^\infty u\,d\bar{z}\right].$$

From (20) follows that

$$\cos^2\beta\int_0^\infty\frac{u}{a}\,d\bar{z}=-\,\frac{u}{Eh\cos^2\beta}\,q_0=-\,\frac{R_1}{Eh}\,q_0\,,$$

yielding (see App. A eq. 8)

$$L=\frac{R_1}{a}\,\frac{d\beta}{d\eta}\,q_0=\tan\Phi\cos\beta\cos\varphi\,q_0 \qquad (28a)$$

$$T=-\,\frac{d(R_1\,q_0)}{a\,d\eta}\,. \qquad (28b)$$

The stresses imposed by the load system II are mainly membrane stresses since: 1° the width of the shell strip in which $-l$, $-t$ are not negligible is of the order $a\,k^{1/4}$ and the width is of the order $k^{1/4}$ small compared to the radius; 2° the load system consists merely of tangential components.

Then the membrane stresses are of the order of L/h and T/h, and according to (28) of the order of q_0/h.

(22c) yields

$$q_0/h=-\,\frac{E}{4\,a}\left(\frac{4\,k}{1-\nu^2}\right)^{1/4}\cos^3\beta\left(\frac{\partial^3u}{\partial x^3}\right)_0. \quad (29)$$

Therefore q_0/h is of the order $\dfrac{E}{a}\,k^{1/4}u$, which is (see 21) of the order $k^{1/4}\sigma_\eta$. So the membrane stresses by load system II are compared to those, pertaining to the edge load m_0, q_0 together with load system I, of the order $k^{1/4}$. Since we have neglected stresses of the order $k^{1/4}$ the stresses by load system II should be neglected likewise.

The membrane strains caused by load system II are of the order $k^{1/4}\,\frac{u}{a}$. Therefore they are likewise negligible to those pertaining to the edge loads m_0, q_0 plus the load system I, which are given by eq. (16).

We conclude that the effect of load system II can be neglected completely.

10 The solution of the oblique cylinder problem.

We found so far: 1° that the solution of the problem of an oblique cylinder under edge load $m_0(\eta)$, $q_0(\eta)$ together with the load system I, consisting of $l(\eta,\bar{z})$, $t(\eta,\bar{z})$ is given with an error $k^{1/4}$ by the solution for the helical cylinder under constant edge load $m_0(\eta)$, $q_0(\eta)$; 2° that the load system II, composed of $-l(\eta,\bar{z})$, $-t(\eta,\bar{z})$ and the edge load $L(\eta)$, $T(\eta)$, defined by eqs. (28), yield stresses which are of the order $k^{1/4}$ compared to those pertaining to m_0, q_0 plus load system I.

Adding m_0, q_0, load system I and load system II the resulting load consists merely of the edge loads $m_0(\eta)$, $q_0(\eta)$, $L(\eta)$, $T(\eta\mathrm{I})$. We call this the "total load".

For this total load the stresses are the sum of those for m_0, q_0 + load system I and those for load system II, which are with an error of the order $k^{1/4}$ equal to the stresses in the helical cylinder under constant edge load $m_0(\eta)$, $q_0(\eta)$. So we have obtained this important conclusion:

The solution for the oblique cylinder under edge loads $m_0(\eta)$, $q_0(\eta)$, $L(\eta) = \tan\Phi\cos\beta\cos\varphi\, q_0$, $T(\eta) = -\dfrac{d(q_0/\cos^2\beta)}{d\eta}$ is given with an error of the order $k^{1/4}$ by the solution of the differential equation (see Ch. 5 eq. I)

$$\frac{h^2a^2}{12(1-\nu^2)}\;\frac{1}{\cos^4\beta}\;\frac{d^4u}{d\bar{z}^4}+u=0$$

with the boundary conditions (see Ch. 5, aqs. III and V)

$$\bar{z}=0,\eta:\; m_0(\eta)=\frac{Eh^3}{12(1-\nu^2)}\left(\frac{d^2u}{d\bar{z}^2}\right)_0,$$

$$q_0(\eta)=\frac{-Eh^3}{12(1-\nu^2)}\left(\frac{d^3u}{d\bar{z}^3}\right)_0$$

$$\bar{z}=\infty\;:\; u=\frac{du}{d\bar{z}}=0,$$

which is (see eq. 19)

$$u(\bar{z},\eta)=\frac{1}{Eh}\left(\frac{1-\nu^2}{k}\right)^{3/4}\frac{1}{\cos^2\beta}\,e^{-x}\Big[m_0(\eta)(\cos x+$$
$$-\sin x)-\left(\frac{4k}{1-\nu^2}\right)^{1/4}\frac{a}{\cos\beta}\,q_0(\eta)\cos x\Big],$$

where

$$x=\left(\frac{1-\nu^2}{4k}\right)^{1/4}\cos\beta\,\frac{\bar{z}}{a}.$$

The displacement components in the plane of the shell are given by (see Ch. 5 eqs. 16)

$$\bar{v}=\sin 2\beta\int_{\bar{z}}^{\infty}\frac{u}{a}\,d\bar{z}$$

$$w=[1-(1-\nu)\cos^2\beta]\int_{\bar{z}}^{\infty}\frac{u}{a}\,d\bar{z}.$$

The membrane stresses are (see eq. 21)

$$\sigma_\eta=E\cos^2\beta\,\frac{u}{a},\quad \sigma_{\bar{z}}=0,\quad \tau_{\bar{z}\eta}=0.$$

The lateral elastic load components are (see eqs. 22)

$$m_{\bar{z}\eta}=\frac{Eh^3}{12(1-\nu^2)}\;\frac{\partial^2u}{\partial\bar{z}^2},\quad m_{\eta\bar{z}}=-\nu m_{\bar{z}\eta},$$

$$q_{\bar{z}r}=-\frac{Eh^3}{12(1-\nu^2)}\;\frac{\partial^3u}{\partial\bar{z}^3},\quad m_{\eta\eta}=m_{\bar{z}\bar{z}}=q_{\eta r}=0.$$

We can give this conclusion also in the wording:

The stresses and deflections of an oblique cylinder under edge loads

$$m_0(\eta),\; q_0(\eta),\; L(\eta)=$$
$$=\tan\Phi\cos\beta\cos\varphi\,q_0,\quad T(\eta)=-\frac{d(q_0/\cos^2\beta)}{d\eta}$$

are in the point $\eta,\bar{z}$ with an error of the order $k^{1/4}$ identical to those in the point $\bar{z}$ of a straight cylinder, with equal wall thickness and radius $a/\cos^2\beta$, under constant edge load $m_0(\eta)$, $q_0(\eta)$.

11 Some characteristics of the edge load.

The load components q_0, L_0 are situated in the plane normal to the edge (fig. 15). The angle θ

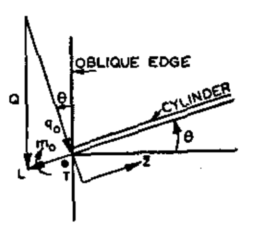

Fig. 15. The total edge load, seen in the plane perpendicular to the edge of the cylinder.

between q_0 and the plane through the edge is given by (see App. A, eq. 3)

$$\cos\theta=\frac{\cos\Phi}{\cos\beta},\;\sin\theta=\sin\Phi\cos\varphi.$$

Then the load normal to the oblique plane is

$$-q_0\sin\theta+\mathrm{L}\cos\theta=$$
$$=q_0\sin\Phi\,(-\cos\varphi+\cos\varphi)=0.$$

So the resultant of q_0 and L falls in the oblique plane along the normal to the edge and its magnitude is (see fig. 15 and App. A eqs. 1)

$$Q=q_0\cos\theta+L\sin\theta=$$
$$=\frac{q_0}{\cos\beta\cos\Phi}\,(\cos^2\Phi+\sin^2\Phi\cos^2\beta\cos^2\varphi)=q_0\frac{\cos\beta}{\cos\Phi}\qquad(30)$$

The load

$$T = -\frac{d(q_0/\cos^2\beta)}{d\eta}$$

is *tangential* to the edge.

When edge bending of the shell is caused by *an oblique frame the reactions of Q and T form* the load of this frame. The type of frame load shows the characteristic of being merely *normal* force upon the cross-section. This appears from the conditions of equilibrium of the element ds of the frame (fig. 16)

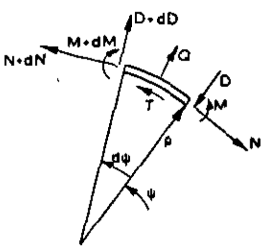

Fig. 16. Frame load by edge load of the oblique cylinder.

$$\left.\begin{aligned} &\frac{dN}{d\psi} + D + T\rho = 0 \\ &\frac{dD}{d\psi} - N + Q\rho = 0 \\ &\frac{dM}{d\psi} + D\rho = 0. \end{aligned}\right\} \qquad (31)$$

The first two equations yield

$$\frac{d^2D}{d\psi^2} + D + \frac{d(Q\rho)}{d\psi} + T\rho = 0.$$

Since (see App. A eq. 5, 6)

$$\frac{d(Q\rho)}{d\psi} + T\rho = \rho\left[\frac{d(Q\rho)}{a\,d\eta} + T\right] =$$

$$= \rho\left[\frac{d}{d\eta}\left(q_0\frac{\cos\beta}{\cos\Phi}\frac{\cos\Phi}{\cos^3\beta}\right) - \frac{d}{d\eta}\left(\frac{q_0}{\cos^2\beta}\right)\right] = 0$$

$$\left.\begin{aligned} &\text{is } D = 0,\ M = 0 \\ &N = q_0\frac{a}{\cos^2\beta} \end{aligned}\right\} \qquad (32)$$

a solution of the equations (31).

So the conclusion is:

The load applied to an oblique frame by edge bending of the cylindrical wall is a normal force upon the cross section of the frame tangent to the line of intersection of frame and cylinder and its magnitude is

$$N = q_0\frac{a}{\cos^2\beta}.$$

This effect of the shell upon the frame is equivalent to that of an inner flange, which is added to the frame, loaded by a compressive force N. Since the strain of this inner flange would be, due to the compatibility of strains of frame and shell, $\varepsilon_s = \frac{u_0}{a}\cos^2\beta$ (see eq. 18), the cross section of this equivalent flange is

$$S = \frac{-N}{E\varepsilon_s} = -\frac{q_0 a^2}{E u_0 \cos^4\beta}.$$

Using (29) and (19) we find

$$S = \frac{ah}{4\cos\beta}\left(\frac{4k}{1-\nu^2}\right)^{1/4}\left(\frac{\frac{\partial^3 u}{\partial x^3}}{u}\right)_0 =$$

$$= \frac{ah}{2\cos\beta}\left(\frac{4k}{1-\nu^2}\right)^{1/4}\cdot\frac{1}{1-\left(\frac{1-\nu^2}{4k}\right)^{1/4}\cos\beta\,\frac{m_0}{a\,q_0}} \qquad (33)$$

So the conclusion is:

The effect of the shell, to one side of an oblique frame, on the frame is equivalent to that of a flange having the cross section S, given by eq. (33).

Note

After completing this investigation the author got notice of a recent Polish paper

> Alexander Kornecki, The state of stress and strain in a thinwalled tube rigidly fixed in an oblique cross section.
> Rozprawy Inzynierskie LX—LXVI 1957,

which deals with the same subject.I The approach is different: oblique coordinates are used and an asymptotic solution is obtained, which again accepts errors of the order $k^{1/4}$. The results comply completely with those obtained in chap. 10. However, since terms of the order $k^{1/4}$ are neglected rigorously no mention is made of the membrane loads $L(\eta)$, $T(\eta)$, which have great importance for the frame load caused by edge bending. Therefore the paper does not include the conclusion of chapter 11.

12 References.

1. Biezeno, C. B. and Grammel, R. Technische Dynamik. Springer, Berlin, 1939.

APPENDIX A.

Geometry of the oblique cylindrical shell.

The equation of the edge of the cylinder is (fig. 1)

$$z_0 = b\cos\varphi = a\tan\Phi\cos\varphi,$$

where Φ is the angle between the oblique end section and the normal section of the cylinder.

The tangent to the edge makes the angle β with the normal section of the cylinder (fig. 2)

$$\tan\beta = \frac{-dz_0}{a\,d\varphi} = \tan\Phi\sin\varphi = c,\ \cos\beta =$$

$$= \frac{1}{(1+c^2)^{1/2}},\ \sin\beta = \frac{c}{(1+c^2)^{1/2}}. \qquad (A.1)$$

The radius of curvature of the cylinder in the *plane through the tangent to the edge and through* the normal to the cylinder is

$$R_1 = \frac{a}{\cos^2\beta} = a(1+c^2). \qquad (A.2a)$$

The radius of curvature of the cylinder in the *plane normal to the edge of the cylinder is*

$$R_2 = \frac{a}{\sin^2\beta} = \frac{a(1+c^2)}{c^2}\,. \qquad \text{(A. 2b)}$$

The angle θ between the normal to the cylinder and the plane through the edge is established by projecting a line element of the normal to the cylinder having unit length upon the plane through the edge. Its projected length is $\cos\theta$ (fig. 1). The ends 1 and 2 of the line element have the coordinates

$$x_1 = a\cos\varphi,\ y_1 = a\sin\varphi,\ z_1 = b\cos\varphi;$$

$$x_2 = (a+1)\cos\varphi,\ y_2 = (a+1)\sin\varphi,\ z_2 = b\cos\varphi.$$

The coordinates in the plane of the oblique section follow from (see fig. 1)

$$\bar{x} = x\cos\Phi + z\sin\Phi,\ \bar{y} = y.$$

Hence

$$\bar{x}_1 = a\,\frac{\cos\varphi}{\cos\Phi},\ \bar{y}_1 = a\sin\varphi;$$

$$\bar{x}_2 = \left(\frac{a}{\cos\Phi} + \cos\Phi\right)\cos\varphi,\ \bar{y}_2 = (a+1)\sin\varphi.$$

Then

$$\cos^2\theta = (\bar{x}_2 - \bar{x}_1)^2 + (\bar{y}_2 - \bar{y}_1)^2 =$$

$$= \cos^2\Phi\cos^2\varphi + \sin^2\varphi = \cos^2\Phi\,(1+c^2) = \frac{\cos^2\Phi}{\cos^2\beta},$$

$$\sin^2\theta = \sin^2\Phi\cos^2\varphi. \qquad \text{(A. 3)}$$

The equation of the elliptical edge is (fig. 1)

$$\cos^2\Phi\,\frac{\bar{x}^2}{a^2} + \frac{\bar{y}^2}{a^2} = 1,\ \bar{x} = a\,\frac{\cos\varphi}{\cos\Phi},\ \bar{y} = a\sin\varphi. \qquad \text{(A. 4)}$$

Hence

$$\tan\psi = -\frac{d\bar{x}}{d\bar{y}} = \frac{1}{\cos^2\Phi}\cdot\frac{\bar{y}}{\bar{x}} = \frac{\tan\varphi}{\cos\Phi} =$$

$$= \frac{c}{\sin\Phi\,(1 - c^2\cot^2\Phi)^{1/2}},$$

$$\sin\psi = \frac{c}{\sin\Phi\,(1+c^2)^{1/2}} = \frac{\sin\beta}{\sin\Phi},$$

$$\cos\psi = \left(\frac{1 - c^2\cot^2\Phi}{1+c^2}\right)^{1/2} = \cos\beta\cos\varphi. \qquad \text{(A. 4)}$$

The radius of curvature is

$$\rho = -\frac{[1 + (d\bar{y}/d\bar{x})^2]^{3/2}}{d^2\bar{y}/d\bar{x}^2} = a\cos\Phi\,(1+c^2)^{3/2} =$$

$$= a\,\frac{\cos\Phi}{\cos^3\beta} \qquad \text{(A. 5)}$$

The line-element ds of the edge is (fig. 2)

$$ds = a\,d\eta = \frac{a\,d\varphi}{\cos\beta} = a(1+c^2)^{1/2}\,d\varphi = \rho\,d\psi. \qquad \text{(A. 6)}$$

Then

$$\frac{d\psi}{d\varphi} = \frac{\cos^2\beta}{\cos\Phi} = \frac{1}{\cos\Phi\,(1+c^2)} \qquad \text{(A. 7)}$$

$$\frac{d\beta}{d\eta} = \frac{\cos\beta\,d\beta}{d\varphi} = \frac{d\sin\beta}{dc}\,\frac{dc}{d\varphi} = \tan\Phi\cos^3\beta\cos\varphi. \qquad \text{(A. 8)}$$

APPENDIX B.

Summary of formulae for use in application.

Geometry.

$$c = \tan\beta = \tan\Phi\sin\varphi,\ \cos\beta = \frac{1}{(1+c^2)^{1/2}},$$

$$\sin\beta = \frac{c}{(1+c^2)^{1/2}} \qquad \text{(A. 1)}$$

$$R_1 = \frac{a}{\cos^2\beta} \qquad \text{(A. 2a)}$$

$$\cos\theta = \frac{\cos\Phi}{\cos\beta},\ \sin\theta = \sin\Phi\cos\varphi \qquad \text{(A. 3)}$$

$$\sin\psi = \frac{\sin\beta}{\sin\Phi},$$

$$\cos\psi = \cos\beta\cos\varphi\ \frac{d\psi}{d\varphi} = \frac{\cos^2\beta}{\cos\Phi} \qquad \text{(A. 4, 7)}$$

$$\frac{d\beta}{d\eta} = \tan\Phi\cos^3\beta\cos\varphi \qquad \text{(A. 8)}$$

$$\rho = a\,\frac{\cos\Phi}{\cos^3\beta},\ ds = a\,d\eta = \rho\,d\psi = \frac{a\,d\varphi}{\cos\beta} \qquad \text{(A. 5, 6)}$$

Edge load.

$$m_0,\ q_0,\ L = \tan\Phi\cos\beta\cos\varphi\,q_0,$$

$$T = -\frac{d(q_0/\cos^2\beta)}{d\eta} \qquad (28)$$

Displacements.

$$u = \frac{1}{Eh}\left(\frac{1-\nu^2}{k}\right)^{1/2}\frac{1}{\cos^2\beta}\,e^{-x}\Big[m_0(\cos x - \sin x) +$$

$$-\left(\frac{4k}{1-\nu^2}\right)^{1/4}\frac{a}{\cos\beta}\,q_0\cos x\Big] \qquad (19)$$

$$\bar{v} = \sin 2\beta\int_{\bar{z}}^{\infty}\frac{u}{a}\,d\bar{z},$$

$$\bar{w} = [1 - (1-\nu)\cos^2\beta]\int_{\bar{z}}^{\infty}\frac{u}{a}\,d\bar{z}. \qquad (16)$$

$$x = \alpha\,\frac{\bar{z}}{a},\ \alpha = \left(\frac{1-\nu^2}{4k}\right)^{1/4}\cos\beta. \qquad (12)$$

Stresses.

$$\sigma_{\bar{z}} = 0,\ \sigma_{\bar{s}} = E\,\frac{u}{a}\cos^2\beta,\ \tau_{\bar{z}\bar{s}} = 0 \qquad \text{(13a, 21)}$$

$$m_{\bar{z}\bar{s}} = \frac{Eh^3}{12(1-\nu^2)}\,\frac{d^2u}{d\bar{z}^2},\ m_{\bar{s}\bar{z}} = -\nu m_{\bar{z}\bar{s}},$$

$$q_{\bar{z}r} = -\frac{Eh^3}{12(1-\tau^2)}\,\frac{d^3u}{d\bar{z}^3},\ m_{\bar{z}\bar{z}} = m_{\bar{s}\bar{s}} = q_{\bar{s}r} = 0 \qquad (22)$$

Frame load.

$$Q = q_0\,\frac{\cos\beta}{\cos\Phi},\ T \qquad (30)$$

$$N = q_0\,\frac{a}{\cos^2\beta} \qquad (32)$$

$$S = \frac{ah}{2\cos^2\beta}\left(\frac{4k}{1-\nu^2}\right)^{1/4}\frac{1}{1 - \left(\dfrac{1-\nu^2}{4k}\right)^{1/4}\cos\beta\,\dfrac{m_0}{a\,q_0}} \qquad (33)$$

C.C.L. Class. C 470-1: C 473-1

NLL-TR S. 539

The reduction in stiffness of combinations of rectangular plates in compression after exceeding the buckling load

by

J. P. BENTHEM.

Summary.

The combination may be a plate with stiffeners, a U-section member, panels that change in thickness discontinuously, etc. It is supposed that the buckling mode is already known (exactly or approximately). Formulas, based on the proper differential equation and well suited to numerical integration are derived for the reduction in stiffness (tangent modulus) for loads in small excess of the buckling load. Some numerical examples are given. These examples clearly show the influence of the boundary conditions for the membrane stresses which arise in the panels after buckling.

Contents.

List of symbols.
1 Introduction.
2 The von Karman equations for large deflections of plates and the expressions for the strain energy.
3 Application of the von Karman equations to a combination of rectangular panels.
 3.1 The combination.
 3.2 The buckling load and the mode of buckling.
 3.3 The membrane stresses.
4 Integration of the strain energy.
5 Stiffness after buckling.
6 Review of the final formulas.
7 Numerical examples.
 7.1 Calculations for a U-section member.
 7.2 Calculations for some other cases.
  7.2.1 Infinite sequence of panels supported by hinges.
  7.2.2 Sides of a compressed thinwalled square tube.
  7.2.3 Plate with one hinge and one end free.
8 Conclusions.
9 References.
 Appendix A. Refined analysis of the boundary conditions at a corner.
  A.1 More freedom for the varying displacements.
  A.2 The boundary conditions.
 Appendix B. Verification of the derived formula (4.27) for the strain energy.
 5 tables.
 5 figures.

This investigation was sponsored by the Netherlands Aircraft Development Board (N. I. V.).

List of symbols.

E	elasticity modulus.
ν	Poisson's ratio.
h	plate thickness.
b	width of the panel (strip).
D	bending stiffness $Eh^3/12(1-\nu^2)$.
w	deflections from the plane of the plate.
x, y, z	coordinate axes, x in longitudinal, y in transverse direction; z perpendicular to the plate (fig. 2). The x and y axes are taken in the middle plane of the plate.
σ_x, σ_y, τ	membrane stresses.
σ	compressive stress ($\sigma = -\sigma_x$).
e	mean shortening per unit of length.
ψ	stress function of Airy for the membrane stresses.
U	strain energy.
φ	parameter indicating the strength of the buckling mode and the membrane stresses due to buckling.
μ	indicates the wave length of the buckling mode, $w = \varphi f(y) \sin \mu x$. Wavelength is $2\pi/\mu$.
λ	half wave length, $\lambda = \pi/\mu$.
i, j	indices indicating panel number.
$\ldots\ldots_i$, $\ldots\ldots_j$, $\ldots\ldots_{,i}$, $\ldots\ldots_{,j}$	where 2 indices are used, sometimes separated by a comma, the second one refers to the panel number.
E^*	ratio between increment of mean compressive stress and mean shortening per unit of length, $E^* = d\sigma/de$.

1 Introduction.

TREFFTZ and MARGUERRE (ref. 1, 2) and KOITER (ref. 3), derived exact solutions for the membrane stresses that arise in a compressed panel immediately after excess of the buckling load, as well as expressions for the ratio between the increment of the load (beyond the buckling load) and the increment of the mean compressive strain. [1])

Such derivations are not yet available for combinations of rectangular panels. Such a combination may be a U-section member, a plate with stiffeners, panels that change in thickness discontinuously, etc.

At the start of the present analysis the buckling mode is supposed to be known, exactly or approximately. The membrane stresses which arise immediately after excess of the buckling load are derived with the aid of the proper differential equation. Hitherto, this was considered to be highly impracticable in view of the large number of (though elementary) integrals that would be met, especially in the determination of the strain energy corresponding to these stresses. However, if the function, describing the buckling mode, is used in tabulated form and all further necessary differentiations and integrations are carried out numerically, the procedure can very well be applied.

The procedure is illustrated by application to a U-section member, a square tube and some other examples. These examples clearly show the influence of the boundary conditions for the membrane stresses.

Calculations of the load at which buckling of some combinations of rectangular panels starts have already been performed in refs. 4, 5, 6 and 7. Experiments of the post buckling behaviour of panels that change in thickness discontinuously are described in ref. 8.

2 The von Karman equations for large deflections of plates and the expression for the strain energy.

These equations (see for example ref. 9, page 343) read for flat plates of constant thickness (external load perpendicular to the plate being absent)

$$\Delta\Delta w = \frac{h}{D}\left(\frac{\partial^2\psi}{\partial y^2}\;\frac{\partial^2 w}{\partial x^2} + \frac{\partial^2\psi}{\partial x^2}\;\frac{\partial^2 w}{\partial y^2} - 2\frac{\partial^2\psi}{\partial x\partial y}\;\frac{\partial^2 w}{\partial x\partial y}\right) \tag{2.1}$$

$$\Delta\Delta\psi = E\left\{\left(\frac{\partial^2 w}{\partial x\partial y}\right)^2 - \frac{\partial^2 w}{\partial x^2}\;\frac{\partial^2 w}{\partial y^2}\right\} \tag{2.2}$$

where the x and y axes are in the middle plane of the plate and

w = deflection of plate perpendicular to the plate
E = modulus of elasticity
D = bending stiffness of plate = $Eh^3/12(1-\nu^2)$
h = plate thickness
Δ = $\partial^2/\partial x^2 + \partial^2/\partial y^2$
ψ = Airy's stress function for the membrane stresses σ_x, σ_y and τ,

$$\sigma_x = \frac{\partial^2\psi}{\partial y^2}\;;\;\sigma_y = \frac{\partial^2\psi}{\partial x^2}\;;\;\tau = -\frac{\partial^2\psi}{\partial x\partial y}\,. \tag{2.3}$$

[1]) This ratio is often indicated with the aid of the notion "effective width".

If the plate is compressed in x direction by a uniform stress σ_x (σ_x has a negative sign, when compressive) a possible solution of (2.1), (2.2) is

$$w = A_1 y + A_2\,,\;\psi = \tfrac{1}{2}\,\sigma_x y^2 + B_1 y + B_2 \tag{2.4}$$

if the plate is free to expand in y direction and

$$w = A_1 y + A_2\,,\;\psi = \tfrac{1}{2}\,\sigma_x y^2 + \tfrac{1}{2}\,\nu\sigma_x x^2 + B_1 y + B_2 \tag{2.5}$$

if this expansion is completely suppressed. In (2.4) A_1, A_2, B_1 and B_2 are arbitrary integration constants which do not enter into the formulas (2.1) ... (2.3), but nevertheless it will prove to be convenient in the further work not to put B_1 and B_2 equal to zero (A_1 and A_2 describe a rigid body displacement).

At the onset of buckling, which starts for all panels of the combination at the same compressive strain, the solution (2.4) (or (2.5)) is no longer stable. Suppose the buckling mode for a panel is

$$w = \varphi w_1(x, y) \tag{2.6}$$

where φ is a parameter increasing from zero to a small value. Due to the smallness of the displacements w at the onset of buckling, the function w_1 may be determined from the differential equation (2.1) only ($\sigma_y = 0$)

$$\Delta\Delta w_1 = \frac{h}{D}\,\sigma_x\,\frac{\partial^2 w_1}{\partial x^2} \tag{2.7}$$

together with the appropriate boundary conditions for w_1. These conditions are coupled with the conditions for the deflections w_1 of other panels of the combination, which deflections are described with the aid of the same parameter φ.

For loads in small excess of the buckling load it may be assumed that the deflections w remain according to the function $w_1(x, y)$ of (2.6) [2]). Equation (2.7), which determines this function $w_1(x, y)$, is written in the form

$$\Delta\Delta w_1 = \frac{h}{D}\;\frac{\partial^2 F_{cr}}{\partial y^2}\;\frac{\partial^2 w_1}{\partial x^2} \tag{2.8}$$

where

$$F_{cr} = -\tfrac{1}{2}\,\sigma_c y^2 + B_1 y + B_2 \tag{2.9}$$

and σ_c is the compressive stress at buckling.

The membrane stresses must be a solution of (2.2).

$$\Delta\Delta\psi = \varphi^2 E\left\{\left(\frac{\partial^2 w_1}{\partial x\partial y}\right)^2 - \frac{\partial^2 w_1}{\partial x^2}\;\frac{\partial^2 w_1}{\partial y^2}\right\} \tag{2.10}$$

In (2.10) the stress function ψ is separated into

$$\psi = F + G \tag{2.11}$$

with

$$F = \tfrac{1}{2}\,C\,y^2 + B_1 y + B_2\,. \tag{2.12}$$

In (2.12) the constant C is chosen in such a way that the stress σ_x following from (2.3), i.e.

[2]) In the right-hand side of equation (2.1) the neglected terms are now of order φ^4 compared with the first term.

$\sigma_x = C$, equals the stress which would correspond to the compressive strain if buckling would not take place. If the shortening in x direction per unit length is e, this stress σ_x would be $\sigma_x = -eE$, hence $C = -eE$ (it is still supposed that the plate is free to expand in y direction). If one of the edges, parallel to the x direction, remains straight, the stress

$$\sigma_x = C = -eE \tag{2.13}$$

actually occurs and is called the edge stress.

If (2.11) is substituted into (2.10), the function F drops out and

$$\Delta\Delta G = \varphi^2 E \left\{ \left(\frac{\partial^2 w_1}{\partial x \partial y} \right)^2 - \frac{\partial^2 w_1}{\partial x^2} \frac{\partial^2 w_1}{\partial y^2} \right\}. \tag{2.14}$$

Substitution of

$$G = \varphi^2 G_2 \tag{2.15}$$

into (2.11) and (2.14) gives

$$\psi = F + \varphi^2 G_2 \tag{2.16}$$

$$\Delta\Delta G_2 = E \left\{ \left(\frac{\partial^2 w_1}{\partial x \partial y} \right)^2 - \frac{\partial^2 w_1}{\partial x^2} \frac{\partial^2 w_1}{\partial y^2} \right\} \tag{2.17}$$

together with the appropriate boundary conditions. The parameter φ still remains undetermined.

To find the load-compression relation the potential energy P (of all the panels of the combination) must be determined. Then the value of the parameter φ follows from the condition that P is a minimum, i. e.

$$\frac{\partial P}{\partial \varphi} = 0. \tag{2.18}$$

The potential energy P equals the strain energy U if the compression (overall shortening) is considered to be prescribed, i. e. if the differential quotient

$$\frac{1}{E} \frac{\partial^2 F}{\partial y^2} = \frac{C}{E}, \tag{2.20}$$

to be derived from (2.12), has a prescribed value (see (2.13)).

The equation (2.18) may thus be replaced by

$$\frac{\partial U}{\partial \varphi} = 0. \tag{2.21}$$

If U is the mean strain energy per unit length, and e the mean shortening per unit length, the compressive force K is

$$\frac{\partial U}{\partial e} = K. \tag{2.22}$$

The expression for the strain energy for one panel becomes

By putting $\partial U / \partial \varphi = 0$ it might seem that the theorem of the minimum potential energy is not used correctly, since the correct use of this theorem allows only a variation of displacements or compatible strains. Though a stress function ψ occurs in (2.23), all varying membrane stresses correspond with compatible strains, because they satisfy equation (2.2), which is in fact a compatibility equation. The only defect of these membrane stresses is, unless the parameter φ has the proper value of (2.21), that equilibrium in the direction perpendicular to the plate is not present.

It may thus be stated that the application of (2.21) implies that the displacements w, perpendicular to the plate and the displacements u and v, in the plane of the plate, are varied in such a way that the exact equation (2.2) is satisfied.

In principle, it would be possible to disregard eq. (2.2) and make independent assumptions for u, v and w. However, it is to be strongly recommended to use the procedure adopted here. It is relatively easy to choose a buckling mode (for the displacements w) by intuition (at least for a simple combination of a few panels), but it is much more difficult to do so for a mode of the displacements u and v (i. e. for the membrane stresses) which arise after buckling.

It may be noted that the equation (2.1) may be derived from the expression for U in (2.23) by the calculus of variations. In that case the functions w and ψ must be varied in such a way that the compatibility equation (2.2) is satisfied.

3 Application of the von Karman equations to a combination of rectangular panels.

3.1 *The combination.*

Figs. 1a ... 1e show cross sections of different combinations of long rectangular panels, or strips, which will be considered to be of infinite length. In fig. 1a two of the strips have a free edge. Figs. 1c and 1e may represent an infinite sequence of stiffeners on a flat plate.

The following different boundary conditions for a strip may be distinguished (fig. 1):

(1) *a corner*, i. e. a sharp bend between two adjacent strips.

(2) *a transition*. The two adjacent strips, unequal in thickness, lie in the same plane.

(3) *a free edge.*

(4) *a hinge.* Two adjacent strips in the same plane, equal or unequal in thickness, are supported by a hinge, or there is a hinged edge. A hinge may be either such that it cannot absorb shear stresses in longitudinal direction, or such that the compressive strain along the hinge is constant.

$$U = \iint \left[\frac{D}{2} \left\{ \left(\frac{\partial^2 w}{\partial x^2} \right)^2 + \left(\frac{\partial^2 w}{\partial y^2} \right)^2 + 2\nu \frac{\partial^2 w}{\partial x^2} \frac{\partial^2 w}{\partial y^2} + 2(1-\nu) \left(\frac{\partial^2 w}{\partial x \partial y} \right)^2 \right\} + \right.$$
$$\left. + \frac{h}{2E} \left\{ \left(\frac{\partial^2 \psi}{\partial x^2} \right)^2 + \left(\frac{\partial^2 \psi}{\partial y^2} \right)^2 - 2\nu \frac{\partial^2 \psi}{\partial x^2} \frac{\partial^2 \psi}{\partial y^2} + 2(1+\nu) \left(\frac{\partial^2 \psi}{\partial x \partial y} \right)^2 \right\} \right] dx dy. \tag{2.23}$$

(5) *a clamped edge.*

(6) *a branch point.*

(7) *an infinite repetition* of a configuration (figs. 1c and 1e).

In the analytical derivations of this paper only boundaries mentioned under (1), (2) and (3) will be considered. Thus, there is a finite number of strips linked in series, and the combination has two free edges, unless the first and the last strip are again linked together. In that case there are only corners and transitions. If the combination is compressed below the buckling load the strips are free to expand in transverse direction.

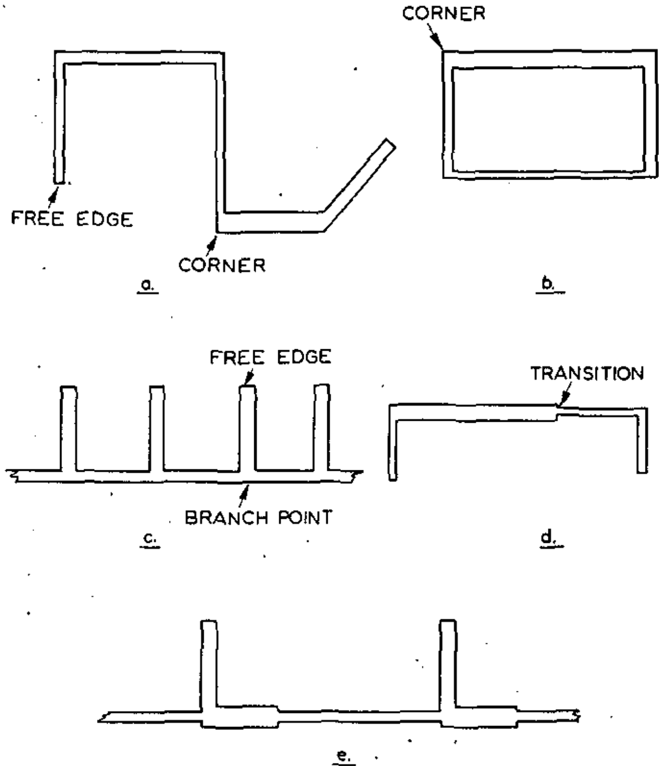

Fig. 1. Several combinations of strips.

It is not difficult to adapt the formulas of the present cases to the other boundaries mentioned under (4), (5), (6) and (7) if they would occur. The numerical example of section 7.2.1 contains a case meant under (7).

All panel widths, panel thicknesses and elasticity moduli must be of the same order of magnitude respectively. At a corner, the angle between two panels may not be almost 180°.

3.2. *The buckling load and the mode of buckling.*

The analysis of the buckling of combinations of strips like fig. 1 is closely connected with the well-established theories of buckling of single plates. Determination of the exact buckling load and mode of a uniform panel results in the solution of a homogeneous linear differential equation of the *fourth order* (2.7); *for combinations* like fig. 1 it results in the solution of a set of such equations with coupled boundary conditions. As mentioned, such calculations have been performed in refs. 4, 5, 6 and 7. Especially ref. 5 gives a practical procedure.

In the derivations it will be supposed that the buckling mode is known exactly. If only an approximate solution, obtained with the aid of the potential energy theorem, is available some minor alterations in the derivations are necessary. These alterations are indicated in the discussion of eq. (4.19), but all final formulas remain the same.

In order to obtain the boundary conditions in a proper form for each strip a coordinate system x_i, y_i, z_i is introduced. The subscript i refers to the i-th panel. The coordinate in longitudinal direction, x_i, is equal for all panels and hence $x_i = x$. The transverse coordinate y_i, in the middle plane of the plate, is directed from the $(i-1)$th towards the $(i+1)$th panel. The coordinates z_i are then determined by assuming that all systems are righthanded.

Fig. 2 shows such coordinate axes x_i, y_i, z_i for some adjacent strips. The boundary conditions for the deflections w at a corner between the i-th and the j-th strip are[1])

$$w_i = \text{constant} \tag{3.3}$$

$$w_j = \text{constant} \tag{3.4}$$

$$\frac{\partial w_i}{\partial y_i} = \frac{\partial w_j}{\partial y_j} \tag{3.5}$$

$$\left.\begin{aligned} &D_i\left(\frac{\partial^2 w_i}{\partial y_i^2} + \nu\,\frac{\partial^2 w_i}{\partial x^2}\right) = D_j\left(\frac{\partial^2 w_j}{\partial y_j^2} + \nu\,\frac{\partial^2 w_j}{\partial x^2}\right) \\ &\text{or} \\ &\qquad D_i\,\frac{\partial^2 w_i}{\partial y_i^2} = D_j\,\frac{\partial^2 w_j}{\partial y_j^2}\,. \end{aligned}\right\} \tag{3.6}$$

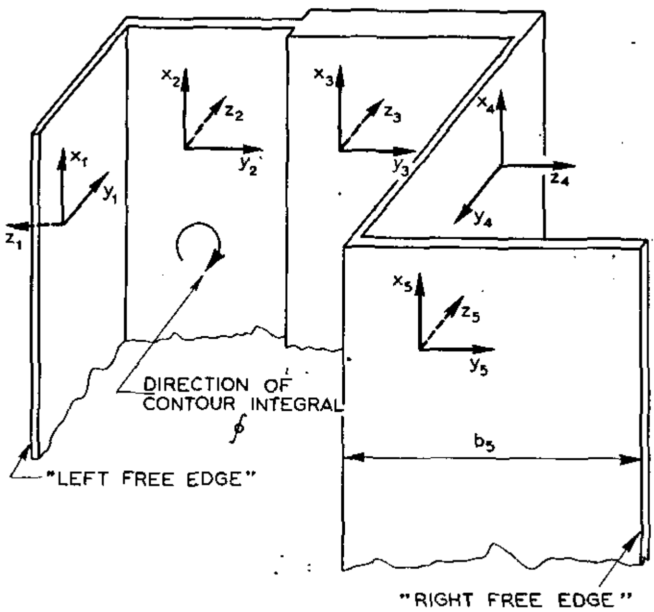

Fig. 2. Systems of coordinate axes in the strips of the *combination.*

Equations (3.3) and (3.4) express that the corners remain straight, equation (3.5) expresses

[1]) It is assumed that POISSON's ratio, ν, is the same for all strips.

the continuity of the geometry and equation (3.6) expresses the fact that the bending moments M_y at both sides of the corner are equal.

The boundary conditions at a transition (fig. 1d) are

$$w_i = w_j \tag{3.7}$$

$$\frac{\partial w_i}{\partial y_i} = \frac{\partial w_j}{\partial y_j} \tag{3.8}$$

$$D_i \left(\frac{\partial^2 w_i}{\partial y_i^2} + \nu \frac{\partial^2 w_i}{\partial x^2} \right) = D_j \left(\frac{\partial^2 w_j}{\partial y_j^2} + \nu \frac{\partial^2 w_j}{\partial x^2} \right) \tag{3.9}$$

$$D_i \left\{ \frac{\partial^3 w_i}{\partial y_i^3} + (2-\nu) \frac{\partial^3 w_i}{\partial x^2 \partial y_i} \right\} = $$

$$= D_j \left\{ \frac{\partial^3 w_j}{\partial y_j^3} + (2-\nu) \frac{\partial^3 w_j}{\partial x^2 \partial y_j} \right\}. \tag{3.10}$$

Equations (3.7) and (3.8) result from the requirement of geometrical continuity, (3.9) from the equality of bending moments M_y and the equation (3.10) from the continuity of the reduced shear force $Q_y - \partial\, M_{xy}/\partial x$ (Q_y shear force, M_{xy} twisting moment).

The (only two) boundary conditions at a free edge are

$$\frac{\partial^2 w_i}{\partial y_i^2} + \nu \frac{\partial^2 w_i}{\partial x^2} = 0 \tag{3.11}$$

$$\frac{\partial^3 w_i}{\partial y_i^3} + (2-\nu) \frac{\partial^3 w_i}{\partial x^2 \partial y_i} = 0. \tag{3.12}$$

The deflection surface of the i-th panel be (compare (2.6))

$$w_i = \varphi w_{1i} + \text{terms linear in } y \tag{3.13}$$

in which

$$w_{1i} = f_i(y) \sin \mu x \tag{3.14}$$

is the buckling mode for the i-th panel. The half wave length in x direction, which is the same for all strips, is of course π/μ. Each $f_i(y)$ is the sum of four (real or complex) exponential functions. Even if they are known exactly, these exponential functions will not be used, in spite of the fact that in the further work only elementary integrals would be met. Their huge number would lead to very laborious computations. The functions $f_i(y)$ will only be used in tabulated form.

If the buckling mode is known, the following formula for the compressive strain at buckling e_{cr} can be used (compare ref. 10, page 326, formula (211)),

$$e_{cr} = \frac{\Sigma D \iint \left\{ \left(\frac{\partial^2 w_1}{\partial x^2}\right)^2 + \left(\frac{\partial^2 w_1}{\partial y^2}\right)^2 + 2\nu \frac{\partial^2 w_1}{\partial x^2} \frac{\partial^2 w_1}{\partial y^2} + 2(1-\nu)\left(\frac{\partial^2 w_1}{\partial x \partial y}\right)^2 \right\} dxdy}{-\Sigma Eh \iint w_1 \frac{\partial^2 w_1}{\partial x^2}\, dxdy}$$

where the Σ sign refers to a summation over all panels.

With the substitution (3.14)

$$e_{cr} = \frac{\Sigma D \int \{ \mu^4 f^2 + (f'')^2 - 2\mu^2 \nu f f'' + 2(1-\nu)\mu^2 (f')^2 \}\, dy}{\mu^2 \Sigma Eh \int f^2 dy}. \tag{3.15}$$

3.3 *The membrane stresses.*

The stress function ψ for the membrane stresses in a strip is from (2.11), (2.12) and (2.15)

$$\psi = F + G \tag{3.16}$$

$$F = \tfrac{1}{2} C y^2 + B_1 y + B_2 \tag{3.17}$$

$$G = \varphi^2 G_2 . \tag{3.18}$$

The constant C for any strip is determined by its shortening, which has the same prescribed value for all strips. [1])

Into the differential equation for the stress function G_2, equation (2.17), the expression (3.14),

$$w_1 = f \sin \mu x,$$

is substituted (the linear terms of (3.13) do not play a role). The result becomes

$$\Delta\Delta G_2 = E\, \mu^2 (f'^2 \cos^2 \mu x + f f'' \sin^2 \mu x) \tag{3.19}$$

or

$$\Delta\Delta G_2 = \tfrac{1}{2} E\, \mu^2 \{ A(y) + H(y) \cos 2\mu x \} \tag{3.20}$$

where

$$A(y) = f'^2 + f f'' \tag{3.21}$$

$$H(y) = f'^2 - f f''. \tag{3.22}$$

The solution of (3.20) has the form

$$G_2 = \frac{E}{2} \mu^2 [\, Q(y) + K(y) \cos 2\mu x \,]. \tag{3.23}$$

In (3.23) $Q(y)$ is the solution of

$$\frac{d^4 Q}{\partial y^4} = A \tag{3.24}$$

and $K(y)$ the solution of

$$16\mu^4 K - 8\mu^2 \frac{d^2 K}{dy^2} + \frac{d^4 K}{dy^4} = H. \tag{3.25}$$

The solution of (3.24) is

$$Q = Q_p + U_0 + U_1 y + U_2 y^2 + U_3 y^3, \tag{3.26}$$

where Q_p is a particular solution and $U_0 \ldots U_3$ are integration constants.

The particular solutions Q_p will always be taken as

$$Q_p = \int \left(\int \tfrac{1}{2} f^2 dy \right) dy. \tag{3.27}$$

[1]) The strips may have different values for C if they have different elasticity moduli.

That (3.27) indeed is a particular solution of (3.24) is easily verified with the aid of (3.21).

The solution of (3.25) is

$$K = K_p + (T_1 + y\, T_2) \cosh 2\,\mu y + (T_3 + y\, T_4) \sinh 2\,\mu y \tag{3.28}$$

where K_p is a particular solution and $T_1 \dots T_4$ are integration constants in the complementary function.

The function K_p may be calculated from the following integral

$$K_p = \frac{1}{16\,\mu^3} \int_c^y H(\xi) \; \{ -\sinh 2\,\mu (y-\xi) + 2\,\mu (y-\xi) \cosh 2\,\mu (y - \xi) \} \, d\xi \tag{3.29}$$

where the lower boundary c, is an arbitrary constant. In (3.26) the integration constants U_0 and U_1 have of course no meaning for the derivation of the membrane stresses, as this is done by a two-fold differentiation. Nevertheless it will prove useful, see (4.5) ... (4.8), to give them special values. The integration constants U_2 and U_3 are determined from the requirement that the mean shortening, due to membrane stresses stemming from G_2 (eq. (3.23)) and the deflections w, is zero, this shortening being caused by stresses corresponding with F (eqs. (2.11), (2.12)) only. Thus, integration of the partial differential quotient

$$\frac{\partial u}{\partial x} = \varepsilon_x - \tfrac{1}{2} \left(\frac{\partial w}{\partial x} \right)^2 = \frac{\varphi^2}{E} \left(\frac{\partial^2 G_2}{\partial y^2} - \nu \frac{\partial^2 G_2}{\partial x^2} \right) - \tfrac{1}{2} \varphi^2 \left(\frac{\partial w_1}{\partial x} \right)^2 \tag{3.30}$$

over a wavelength must deliver zero for all values of y, i. e.

$$\int_0^{2\pi/u} \frac{\partial u}{\partial x}\, dx = 0. \tag{3.31}$$

The solutions of (3.23) and (3.14) are substituted into (3.30) and in its turn (3.30) into (3.31). If use is made of the fact that

$$\int_0^{2\pi/u} \cos 2\,\mu x\, dx = 0$$

the result is

$$\int_0^{\pi/u} \left\{ \tfrac{1}{2} \mu^2 \left(\frac{\partial^2 Q_p}{\partial y^2} + 2\, U_2 + 6\, U_3 y \right) - \tfrac{1}{2} \mu^2 f^2 \cos^2 \mu x \right\} dx = 0 \tag{3.32}$$

or

$$\frac{\partial^2 Q_p}{\partial y^2} + 2\, U_2 + 6\, U_3 y - \tfrac{1}{2} f^2 = 0. \tag{3.33}$$

Now, since from (3.27)

$$\frac{\partial^2 Q_p}{\partial y^2} = \tfrac{1}{2} f^2$$

the integration constants U_2 and U_3 are zero. Hence

$$\frac{\partial^2 Q}{\partial y^2} = \tfrac{1}{2} f^2 \tag{3.34}$$

where Q is the solution (3.26).

For each strip the integration constants $T_1 \dots T_4$ occurring in (3.28) are to be determined from the boundary conditions which are valid for the membrane stress functions ψ.

These boundary conditions at a corner between the i-th and the j-th strip are

$$\frac{\partial^2 \psi_i}{\partial x^2} = 0 \tag{3.35}$$

$$\frac{\partial^2 \psi_j}{\partial x^2} = 0 \tag{3.36}$$

$$h_i \frac{\partial^2 \psi_i}{\partial x \partial y_i} = h_j \frac{\partial^2 \psi_j}{\partial x \partial y_j} \tag{3.37}$$

$$\left.\begin{aligned} &\frac{1}{E_i} \left(\frac{\partial^2 \psi_i}{\partial y_i^2} - \nu \frac{\partial^2 \psi_i}{\partial x^2} \right) = \frac{1}{E_j} \left(\frac{\partial^2 \psi_j}{\partial y_j^2} - \nu \frac{\partial^2 \psi_j}{\partial x_j^2} \right) \\ &\text{or} \\ &\frac{1}{E_i} \frac{\partial^2 \psi_i}{\partial y_i^2} = \frac{1}{E_j} \frac{\partial^2 \psi_j}{\partial y_j^2} \end{aligned}\right\} \tag{3.38}$$

Equations (3.35) and (3.36) represent the requirements that the normal stresses perpendicular to the boundary are zero. Strictly taken these requirements are incompatible with the requirements (3.3) and (3.4) which express that corners remain straight. Thus it seems as if from a plate stresses and displacements normal to the boundary are prescribed, which is of course impossible. Although it can be reasoned by intuition that no significant error will arise from this incompatibility, a refined analysis of the boundary conditions at a corner has been made. This analysis, given in Appendix A, indeed leads to the conditions (3.3), (3.4) and (3.35), (3.36).

Equation (3.37) ensures equality of the shear flows at the boundary and equation (3.38) means that the normal strains in the direction of the boundary are equal.

The boundary conditions at a transition (fig. 1d) are

$$h_i \frac{\partial^2 \psi_i}{\partial x^2} = h_j \frac{\partial^2 \psi_j}{\partial x^2} \tag{3.39}$$

$$h_i \frac{\partial^2 \psi_i}{\partial x \partial y_i} = h_j \frac{\partial^2 \psi_j}{\partial x \partial y_j} \tag{3.40}$$

$$\frac{1}{E_i} \left(\frac{\partial^2 \psi_i}{\partial y_i^2} - \nu \frac{\partial^2 \psi_i}{\partial x^2} \right) = \frac{1}{E_j} \left(\frac{\partial^2 \psi_j}{\partial y_j^2} - \nu \frac{\partial^2 \psi_i}{\partial x^2} \right) \tag{3.41}$$

$$\frac{1}{E_i} \left\{ \frac{\partial^3 \psi_i}{\partial y_i^3} + (2+\nu) \frac{\partial^3 \psi_i}{\partial x^2 \partial y_i} \right\} = \frac{1}{E_j} \left\{ \frac{\partial^3 \psi_j}{\partial y_j^3} + (2+\nu) \frac{\partial^3 \psi_j}{\partial x^2 \partial y_j} \right\}. \tag{3.42}$$

The equations (3.39), (3.40), (3.41) and (3.42) ensure continuity of the normal stress flows perpendicular to the boundary, the shear flows, the normal strains in the direction of the boundary and the displacements perpendicular to the boundary respectively.

The (only two) boundary conditions at a free edge are

$$\frac{\partial^2 \psi_i}{\partial x^2} = 0 \tag{3.43}$$

$$\frac{\partial^2 \psi_i}{\partial x \partial y_i} = 0. \tag{3.44}$$

The part F of ψ automatically satisfies all the conditions (3.35) ... (3.44). Thus, all these formulas are also valid for the functions G and G_2. The partial differential quotients which then occur in (3.35) ... (3.44) become

$$\frac{\partial^2 G_2}{\partial x^2} = \frac{E}{2}\mu^2 \{ K_p + T_1 \cosh 2\mu y + T_2 y \cosh 2\mu y + T_3 \sinh 2\mu y + T_4 y \sinh 2\mu y \} (-4\mu^2 \cos 2\mu x) \tag{3.45}$$

$$\frac{\partial^2 G_2}{\partial y^2} = \frac{E}{2}\mu^2 \Big[\tfrac{1}{2} f^2 + \Big\{ \frac{\partial^2 K_p}{\partial y^2} + T_1 4\mu^2 \cosh 2\mu y + T_2 (4\mu^2 y \cosh 2\mu y + 4\mu \sinh 2\mu y) + T_3 4\mu^2 \sinh 2\mu y + $$
$$+ T_4 (4\mu^2 y \sinh 2\mu y + 4\mu \cosh 2\mu y) \Big\} \cos 2\mu x \Big] \tag{3.46}$$

$$\frac{\partial^2 G_2}{\partial x \partial y} = \frac{E}{2}\mu^2 \Big\{ \frac{\partial K_p}{\partial y} + T_1 2\mu \sinh 2\mu y + T_2 (2\mu y \sinh 2\mu y + \cosh 2\mu y) + T_3 2\mu \cosh 2\mu y + $$
$$+ T_4 (2\mu y \cosh 2\mu y + \sinh 2\mu y) \Big\} (-2\mu \sin 2\mu x) \tag{3.47}$$

$$\frac{\partial^3 G_2}{\partial y^3} = \frac{E}{2}\mu^2 \Big[f f' + \Big\{ \frac{\partial^3 K_p}{\partial y^3} + T_1 8\mu^3 \sinh 2\mu y + T_2 (12\mu^2 \cosh 2\mu y + 8\mu^3 y \sinh 2\mu y) + $$
$$+ T_3 8\mu^3 \cosh 2\mu y + T_4 (12\mu^2 \sinh 2\mu y + 8\mu^3 y \cosh 2\mu y) \Big\} \cos 2\mu x \Big] \tag{3.48}$$

$$\frac{\partial^3 G_2}{\partial x^2 \partial y} = \frac{E}{2}\mu^2 \Big\{ \frac{\partial K_p}{\partial y} + T_1 2\mu \sinh 2\mu y + T_2 (2\mu y \sinh 2\mu y + \cosh 2\mu y) + T_3 2\mu \cosh 2\mu y + $$
$$+ T_4 (2\mu y \cosh 2\mu y + \sinh 2\mu y) \Big\} (-4\mu^2 \cos 2\mu x). \tag{3.49}$$

Substitution of (3.45) ... (3.49) *into the conditions* (3.35) ... (3.44) gives the desired equations for the coefficients $T_1 \ldots T_4$ of the strips. In these equations the terms $\frac{1}{2} f^2$ of (3.46) and ff' of (3.48) will drop out in view of the boundary conditions for w, given in the formulas (3.3) ... (3.12).

The relations between the coefficients $T_{1,i} \ldots T_{4,i}$, $T_{1,j} \ldots T_{4,j}$ of two adjacent strips or between *the coefficients* $T_{1,i} \ldots T_{4,i}$ at a free edge are given in table 1.

4 Integration of the strain energy.

The formula for the strain energy (2.23) can be evaluated with the aid of the following formulas for each strip (see for example ref. 11, page 13)

$$\iint g \frac{\partial^2 f}{\partial x^2} dxdy = \iint f \frac{\partial^2 g}{\partial x^2} dxdy + \oint \left(g \frac{\partial f}{\partial x} - f \frac{\partial g}{\partial x} \right) dy \tag{4.1}$$

$$\iint g \frac{\partial^2 f}{\partial y^2} dxdy = \iint f \frac{\partial^2 g}{\partial y^2} dxdy - \oint \left(g \frac{\partial f}{\partial y} - f \frac{\partial g}{\partial y} \right) dx \tag{4.2}$$

$$\iint g \frac{\partial^2 f}{\partial x \partial y} dxdy = \iint f \frac{\partial^2 y}{\partial x \partial y} dxdy + \tfrac{1}{2} \oint \left(g \frac{\partial f}{\partial y} - f \frac{\partial g}{\partial y} \right) dy - \tfrac{1}{2} \oint \left(g \frac{\partial f}{\partial x} - f \frac{\partial g}{\partial x} \right) dx. \tag{4.3}$$

With the orientation of the x and y axes according to fig. 2, the contour integrals $\oint$ are to be taken clockwise. [1])

All integrations have been carried out for one wavelength and in view of the periodicity all contour integrals $\oint \ldots dy$ vanish.

The result then is

$$U = \Sigma \Big[\frac{D}{2} \iint w \Delta\Delta w \, dxdy + \frac{h}{2E} \iint \psi \Delta\Delta \psi \, dxdy + \frac{D}{2} \Big\{ - $$
$$- \oint \left(\frac{\partial^2 w}{\partial y^2} \frac{\partial w}{\partial y} - w \frac{\partial^3 w}{\partial y^3} \right) dx - \nu \oint \left(\frac{\partial^2 w}{\partial x^2} \frac{\partial w}{\partial y} - w \frac{\partial^3 w}{\partial x^2 \partial y} \right) dx + (1-\nu) \oint 2w \frac{\partial^3 w}{\partial x^2 \partial y} dx \Big\} + $$
$$+ \frac{h}{2E} \Big\{ - \oint \left(\frac{\partial^2 \psi}{\partial y^2} \frac{\partial \psi}{\partial y} - \psi \frac{\partial^3 \psi}{\partial y^3} \right) dx + \nu \oint \left(\frac{\partial^2 \psi}{\partial x^2} \frac{\partial \psi}{\partial y} - \psi \frac{\partial^3 \psi}{\partial x^2 \partial y} \right) dx + (1+\nu) \oint 2\psi \frac{\partial^3 \psi}{\partial x^2 \partial y} dx \Big\} \Big] \tag{4.4}$$

[1]) In (2.23) the terms $2\nu \frac{\partial^2 w}{\partial x^2} \frac{\partial^2 w}{\partial y^2}$ and $-2\nu \frac{\partial^2 \psi}{\partial x^2} \frac{\partial^2 \psi}{\partial y^2}$ are separated into $\nu \frac{\partial^2 w}{\partial x^2} \frac{\partial^2 w}{\partial y^2}$ and $\nu \frac{\partial^2 w}{\partial y^2} \frac{\partial^2 w}{\partial x^2}$, and $-\nu \frac{\partial^2 \psi}{\partial x^2} \frac{\partial^2 \psi}{\partial y^2}$ and $-\nu \frac{\partial^2 \psi}{\partial y^2} \frac{\partial^2 \psi}{\partial x^2}$ respectively.

The Σ sign refers to summation over all strips. It is seen from (3.13) and (3.14) that the "linear terms" mentioned in (3.13) drop out from the above formula, because of the periodicity of w_{1i}. From the boundary conditions (3.3) ... (3.12) it follows that, for all the strips, contour integrals, containing w vanish by periodicity or cancel each other.

There is a good reason now to choose the still undetermined integration constants of both parts of ψ, viz. the constants B_1 and B_2 in (3.17) and U_0 and U_1 in (3.26) in such a way that at a corner

$$G_{2i} = G_{2j} = 0 \text{ or } Q_i = Q_j = 0 \quad \text{and } F_i = F_j = 0 \tag{4.5}$$

and at each transition (fig. 1d)

$$h_i G_{2i} = h_j G_{2j} \text{ or } E_i h_i Q_i = E_j h_j Q_j \quad \text{and } h_i F_i = h_j F_j \tag{4.6}$$

$$h_i \frac{\partial G_{2i}}{\partial y_i} = h_j \frac{\partial G_{2j}}{\partial y_j} \text{ or } E_i h_i \frac{\partial Q_i}{\partial y_i} = = E_j h_j \frac{\partial Q_j}{\partial y_j} \text{ and } h_i \frac{\partial F_i}{\partial y_i} = h_j \frac{\partial F_j}{\partial y_j} \tag{4.7}$$

and at a free edge

$$G_{2i} = 0 \text{ or } Q_i = 0 \text{ and } F_i = 0. \tag{4.8}$$

At *corners* the functions

$$h_i \frac{\partial G_{2i}}{\partial y_i} - h_j \frac{\partial G_{2j}}{\partial y_j} = \frac{\mu^2}{2}\left(E_i h_i \frac{\partial Q_i}{\partial y_i} - E_j h_j \frac{\partial Q_j}{\partial y_j}\right) \tag{4.9}$$

and

$$h_i \frac{\partial F_i}{\partial y_i} - h_j \frac{\partial F_j}{\partial y_j} \tag{4.10}$$

are constants.

At free edges the functions

$$\frac{\partial G_{2i}}{\partial y_i} = \frac{E_i \mu^2}{2} \frac{\partial Q_i}{\partial y_i} \text{ and } \frac{\partial F_i}{\partial y_i} \tag{4.11}$$

are constants.

With (4.5) ... (4.11) and the boundary conditions (3.35) ... (3.44), and accounting for the fact that $\partial^2 G_2/\partial x^2$ is periodic, the expression (4.4) reduces to

$$U = \Sigma \left[\frac{D}{2} \iint w \Delta\Delta w \, dxdy + \frac{h}{2E} \iint \psi \Delta\Delta \psi \, dxdy - \frac{h}{2E} \oint \frac{\partial^2 \psi}{\partial y^2} \frac{\partial \psi}{\partial y} dx \right]. \tag{4.12}$$

In (4.12) the *contour integral is only to be taken along corners and free edges* (where $\partial^2\psi/\partial x^2 = 0$) *and not along transitions.* Note that the sum of a pair of integrals

$$-\frac{h}{2E} \oint \left(\frac{\partial^2 \psi}{\partial y^2} - \nu \frac{\partial^2 \psi}{\partial x^2}\right) \frac{\partial \psi}{\partial y}$$

along a transition is zero.

In (4.12) is substituted $w = \varphi w_1$ and $\psi = F + \varphi^2 G_2$. Then

$$\begin{aligned} U = \Sigma \Big[& \varphi^2 \frac{D}{2} \iint w_1 \Delta\Delta w_1 \, dxdy + \\ & + \varphi^2 \frac{h}{2E} \iint F \Delta\Delta G_2 dxdy \\ & + \varphi^4 \frac{h}{2E} \iint G_2 \Delta\Delta G_2 \, dxdy - \frac{h}{2E} \oint \frac{\partial^2 F}{\partial y^2} \frac{\partial F}{\partial y} dx \\ & - \varphi^2 \frac{h}{2E} \oint \frac{\partial^2 F}{\partial y^2} \frac{\partial G_2}{\partial y} dx - \varphi^2 \frac{h}{2E} \oint \frac{\partial^2 G_2}{\partial y^2} \frac{\partial F}{\partial y} dx \\ & - \varphi^4 \frac{h}{2E} \oint \frac{\partial^2 G_2}{\partial y^2} \frac{\partial G_2}{\partial y} dx \Big]. \end{aligned} \tag{4.13}$$

In the term $\varphi^2 \frac{h}{2E} \iint F \Delta\Delta G_2 \, dxdy$ is substituted the expression for $\Delta\Delta G_2$ of (2.17). This term then becomes

$$\varphi^2 \frac{h}{2} \iint \left\{ \left(F \frac{\partial^2 w_1}{\partial x \partial y}\right) \frac{\partial^2 w_1}{\partial x \partial y} - - \tfrac{1}{2} \left(F \frac{\partial^2 w_1}{\partial x^2}\right) \frac{\partial^2 w_1}{\partial y^2} - \tfrac{1}{2} \left(F \frac{\partial^2 w_1}{\partial y^2}\right) \frac{\partial^2 w_1}{\partial x^2} \right\} dxdy. \tag{4.14}$$

With the integration formulas (4.1) ... (4.3) the expression (4.14) is transformed into

$$\begin{aligned} & \varphi^2 \frac{h}{2E} \iint F \Delta\Delta G_2 \, dxdy = \\ & \varphi^2 \frac{h}{2} \Big[\iint w_1 \left(\frac{\partial F}{\partial y} \frac{\partial^3 w_1}{\partial x^2 \partial y} + F \frac{\partial^4 w_1}{\partial x^2 \partial y^2} + \frac{\partial F}{\partial x \partial y} \frac{\partial^2 w_1}{\partial x \partial y} + \frac{\partial F}{\partial x} \frac{\partial^3 w_1}{\partial x \partial y^3} \right) dxdy \\ & - \tfrac{1}{2} \iint w_1 \left(\frac{\partial^2 F}{\partial y^2} \frac{\partial^2 w_1}{\partial x^2} + F \frac{\partial^4 w_1}{\partial x^2 \partial y^2} + 2 \frac{\partial F}{\partial y} \frac{\partial^3 w_1}{\partial x^2 \partial y} \right) dxdy \\ & - \tfrac{1}{2} \iint w_1 \left(\frac{\partial^2 F}{\partial x^2} \frac{\partial^2 w_1}{\partial y^2} + F \frac{\partial^4 w_1}{\partial x^2 \partial y^2} + 2 \frac{\partial F}{\partial x} \frac{\partial^3 w_1}{\partial x \partial y^2} \right) dxdy \\ & - \tfrac{1}{2} \oint \left\{ F \frac{\partial^2 w_1}{\partial x \partial y} \frac{\partial w_1}{\partial x} - w_1 \left(\frac{\partial F}{\partial x} \frac{\partial^2 w_1}{\partial x \partial y} + F \frac{\partial^3 w_1}{\partial x^2 \partial y} \right) \right\} dx \\ & + \tfrac{1}{2} \oint \left\{ F \frac{\partial^2 w_1}{\partial x^2} \frac{\partial w_1}{\partial y} - w_1 \left(\frac{\partial F}{\partial y} \frac{\partial^2 w_1}{\partial x^2} + F \frac{\partial^3 w_1}{\partial x^2 \partial y} \right) \right\} dx \Big] = \\ & - \varphi^2 \frac{h}{4} \iint \frac{\partial^2 F}{\partial y^2} w_1 \frac{\partial^2 w_1}{\partial x^2} dxdy - \varphi^2 \frac{h}{4} \oint \frac{\partial F}{\partial y} w_1 \frac{\partial^2 w_1}{\partial x^2} dx. \end{aligned} \tag{4.15}$$

The contour integral of (4.15) only remains at free edges. With the substitution $w_1 = f \sin \mu x$ this contour integral becomes

$$\frac{\varphi^2 h}{8} \oint \frac{\partial F}{\partial y} \mu^2 f^2 \, dx. \tag{4.16}$$

The contour integral in (4.13)

$$-\varphi^2 \frac{h}{2E} \oint \frac{\partial^2 G_2}{\partial y^2} \frac{\partial F}{\partial y} dx \tag{4.17}$$

becomes with the substitution (see (3.23) and (3.34))

$$\frac{\partial^2 G_2}{\partial y^2} = \tfrac{1}{2} f^2 \frac{E}{2} \mu^2$$

(the periodic part need not be considered)

$$-\varphi^2 \frac{h}{8} \oint \frac{\partial F}{\partial y} \mu^2 f^2 dx \tag{4.18}$$

and the integrals (4.16) and (4.18) cancel each other.

In the term $\varphi^2 \frac{D}{2} \iint w_1 \Delta\Delta w_1 \, dxdy$ of (4.13) is substituted the expression for $\Delta\Delta w_1$ of (2.8), which gives

$$\varphi^2 \frac{h}{2} \iint \frac{\partial^2 F_c}{\partial y^2} w_1 \frac{\partial^2 w_1}{\partial x^2} dxdy. \tag{4.19}$$

If the deflection surface w_1 is an approximate solution obtained by means of the potential energy theorem, it may happen that the functions w_{1i} do not satisfy the boundary conditions (3.3) ... (3.12) as far as they ensure equilibrium. Not all contour integrals in (4.4) containing w will then vanish. In that case it is better not to apply the formulas (4.1) ... (4.3) to that part of the function (2.23) which contains w_1. Then the term

$$\varphi^2 \frac{D}{2} \iint w_1 \Delta\Delta w_1 \, dxdy$$

of (4.13) preserves its original form

$$\varphi^2 \frac{D}{2} \iint \left\{ \left(\frac{\partial^2 w_1}{\partial x^2}\right)^2 + \left(\frac{\partial^2 w_1}{\partial y^2}\right)^2 + 2\nu \frac{\partial^2 w_1}{\partial x^2} \frac{\partial^2 w_1}{\partial y^2} + 2(1-\nu)\left(\frac{\partial^2 w_1}{\partial x \partial y}\right)^2 \right\} dxdy.$$

Now, according to ref. 10, page 325, formula (2.10)

$$\Sigma \varphi^2 \frac{D}{2} \iint \left\{ \left(\frac{\partial^2 w_1}{\partial x^2}\right)^2 + \left(\frac{\partial^2 w_1}{\partial y^2}\right)^2 + 2\nu \frac{\partial^2 w_1}{\partial x^2} \frac{\partial^2 w_1}{\partial y^2} + 2(1-\nu)\left(\frac{\partial^2 w_1}{\partial x \partial y}\right)^2 \right\} dxdy =$$

$$-\Sigma \varphi^2 \frac{h}{2} \iint \frac{\partial^2 F_c}{\partial y^2} \left(\frac{\partial w_1}{\partial x}\right)^2 dxdy = \Sigma \varphi^2 \frac{h}{2} \iint \frac{\partial^2 F_c}{\partial y^2} w_1 \frac{\partial w_1}{\partial x} dxdy,$$

which is identical to (4.19).

The expression for the strain energy, for exact as well as approximate solutions w_1, now reads with (4.15) ... (4.19)

$$\begin{aligned} U = \Sigma \Bigg[& \varphi^2 \frac{h}{2} \frac{\partial^2 F_c}{\partial y^2} \iint w_1 \frac{\partial^2 w_1}{\partial x^2} dxdy - \varphi^2 \frac{h}{4} \frac{\partial^2 F}{\partial y^2} \iint w_1 \frac{\partial^2 w_1}{\partial x^2} dxdy \\ & + \varphi^4 \frac{h}{2E} \iint G_2 \Delta\Delta G_2 \, dxdy - \frac{h}{2E} \frac{\partial^2 F}{\partial y^2} \oint \frac{\partial F}{\partial y} dx \\ & - \varphi^2 \frac{h}{2E} \frac{\partial^2 F}{\partial y^2} \oint \frac{\partial G_2}{\partial y} dx - \varphi^4 \frac{h}{2E} \oint \frac{\partial^2 G_2}{\partial y^2} \frac{\partial G_2}{\partial y} dx \Bigg]. \end{aligned} \tag{4.20}$$

In (4.20)

$$\iint w_1 \frac{\partial^2 w_1}{\partial x^2} dxdy = -\mu^2 \iint_{x=0}^{x=2\pi/\mu} f^2 \sin^2 \mu x \, dx \, dy = -2\pi\mu \int \tfrac{1}{2} f^2 \, dy. \tag{4.21}$$

The three contour integrals of (4.20) must not be carried out along transitions (see (4.12)). Nevertheless two of them

$$h \oint \frac{\partial F}{\partial y} dx \quad \text{and} \quad h \oint \frac{\partial G_2}{\partial y} dx$$

may be carried out along all transitions since then they will drop out again, because at a transition

$$\left. \begin{aligned} h_i \frac{\partial F_i}{\partial y_i} &= h_j \frac{\partial F_j}{\partial y_j} \\ h_j \frac{\partial G_{2i}}{\partial y_i} &= h_j \frac{\partial G_{2j}}{\partial y_j} \end{aligned} \right\} \quad \text{see (4.7)}$$

$$\frac{1}{E_i} \frac{\partial^2 F_i}{\partial y_i^2} = \frac{1}{E_j} \frac{\partial^2 F_j}{\partial y_j^2}, \text{ see (2.20).}$$

Thus for every strip

$$\oint \frac{\partial F}{\partial y} dx = -\frac{2\pi}{\mu} \int \frac{\partial^2 F}{\partial y^2} dy = -\frac{2\pi}{\mu} \frac{\partial^2 F}{\partial y^2} b \tag{4.22}$$

if b is the width of the strip, and in view of (3.23) and (3.34).

$$\oint \frac{\partial G_2}{\partial y} dx = \frac{E}{2} \mu^2 \oint \frac{\partial Q}{\partial y} dx =$$

$$-\pi E \mu \int \frac{\partial^2 Q}{\partial y^2} dy = -\pi E \mu \int \tfrac{1}{2} f^2 \, dy. \tag{4.23}$$

Furthermore, from (3.17)

$$\frac{\partial^2 F_{cr}}{\partial y^2} = C_{cr}, \ \frac{\partial^2 F}{\partial y^2} = C. \tag{4.24}$$

Substitution of (4.21) ... (4.24) into (4.20) yields the expression

$$U = \Sigma\left[-\varphi^2 \frac{h}{2} C_{cr} 2\pi\mu \int \tfrac{1}{2} f^2 dy + \right.$$
$$+ \varphi^2 \frac{h}{4} C\, 2\pi\mu \int \tfrac{1}{2} f^2 dy$$
$$+ \varphi^4 \frac{h}{2E} \iint G_2 \Delta\Delta G_2\, dx dy + \frac{h}{2E} \frac{2\pi}{\mu} C^2 b$$
$$\left. + \varphi^2 \frac{h}{2} C \pi\mu \int \tfrac{1}{2} f^2 dy \quad - \varphi^4 \frac{h}{2E} \oint \frac{\partial^2 G_2}{\partial y^2} \frac{\partial G_2}{\partial y} dx\right] \tag{4.25}$$

which can be rewritten in the form

$$U = \Sigma\left[\frac{h}{E} \frac{\pi}{\mu} C^2 b + \varphi^2 h (C - C_{cr}) \pi\mu \int \tfrac{1}{2} f^2 dy \right.$$
$$\left. + \varphi^4 \frac{h}{2E} \iint G_2 \Delta\Delta G_2\, dx dy - \varphi^4 \frac{h}{2E} \oint \frac{\partial^2 G_2}{\partial y^2} \frac{\partial G_2}{\partial y} dx\right] \tag{4.26}$$

where it must be remembered that the contour integral is not to be taken along transitions.

At a corner (see (3.35) and (3.38))

$$\frac{1}{E_i} \frac{\partial^2 G_{2i}}{\partial y_i^2} = \frac{1}{E_j} \frac{\partial^2 G_{2j}}{\partial y_i^2}$$

and according to (4.9)

$$h_i \frac{\partial G_{2i}}{\partial y_i} - h_j \frac{\partial G_{2j}}{\partial y_j}$$

is a constant. At free edges (see (4.11)) $\frac{\partial G_{2i}}{\partial y_i}$ is constant. Hence, in the contour integral $\oint \frac{\partial^2 G_2}{\partial y^2} \frac{\partial G_2}{\partial y} dx$ the periodic part of $\frac{\partial^2 G_2}{\partial y^2}$ need not be considered.

Thus with (3.23) and (3.34)

$$\oint \frac{\partial^2 G_2}{\partial y^2} \frac{\partial G_2}{\partial y} dx = \frac{E}{2} \mu^2 \oint \tfrac{1}{2} f^2 \frac{\partial G_2}{\partial y} dx =$$
$$= \frac{E^2 \mu^4}{4} \oint \tfrac{1}{2} f^2 \frac{\partial Q}{\partial y} dx.$$

Since this contour integral vanishes at all corners ($f = 0$) it only remains at free edges.

Now

$$U = \Sigma\left[\frac{h}{E} \frac{\pi}{\mu} C^2 b + \varphi^2 h (C - C_{cr}) \pi\mu \int \tfrac{1}{2} f^2 dy + \right.$$
$$+ \varphi^4 \frac{h}{2E} \iint G_2 \Delta\Delta G_2\, dx dy -$$
$$\left. - \varphi^4 \frac{Eh}{8} \mu^4 \oint \tfrac{1}{2} f^2 \frac{\partial Q}{\partial y} dx\right]. \tag{4.27}$$

In appendix B a verification of this formula is given by means of Galerkin's principle.

For free edges the contour integral is further simplified into

$$\pm \varphi^4 \frac{Eh\, \mu^3 \pi}{8} \left(f^2 \frac{\partial Q}{\partial y}\right)_{\text{free edge}} \tag{4.28}$$

where the plus sign is to be chosen at a "right free edge" (fig. 2) and the minus sign at a "left free edge".

In order to evaluate the integral

$$\iint G_2 \Delta\Delta G_2\, dx dy$$

the expressions (3.20) and (3.23) are inserted

$$\iint G_2 \Delta\Delta G_2\, dx dy = \frac{E^2 \mu^3 \pi}{2} \int (AQ + \tfrac{1}{2} HK) dy \tag{4.29}$$

and

$$U = \Sigma\left[\frac{h}{E} \frac{\pi}{\mu} C^2 b + \frac{\varphi^2 h \pi\mu}{2} (C - C_{cr}) \int f^2 dy \right.$$
$$+ \frac{\varphi^4 E h \pi \mu^3}{4} \left\{\int (AQ + \right.$$
$$\left.\left. + \tfrac{1}{2} HK) dy \pm \tfrac{1}{2} \left(f^2 \frac{dQ}{dy}\right)_{\text{free edge}}\right\}\right]. \tag{4.30}$$

The mean shortening per unit length is e, the value of this shortening at the initial buckling load is e_{cr}. Thus, (see (2.13))

$$C = -eE, \; C_{cr} = -e_{cr} E. \tag{4.31}$$

The expression (4.30) gives the strain energy for one wave length $2\pi/\mu$. The mean strain energy per unit length becomes

$$U = \frac{e^2}{2} \Sigma Ehb + \frac{\varphi^2 \mu^2}{4} (e_{cr} - e) \Sigma Eh \int f^2 dy +$$
$$+ \frac{\varphi^4 \mu^4}{8} \Sigma R \tag{4.32}$$

with

$$R = Eh \left\{\int (AQ + \right.$$
$$\left. + \tfrac{1}{2} HK) dy \pm \tfrac{1}{2} \left(f^2 \frac{dQ}{dy}\right)_{\text{free edge}}\right\}. \tag{4.33}$$

5 Stiffness after buckling.

From the condition $\partial U / \partial \varphi = 0$ with U according to (4.32) the solutions for φ become $\varphi = 0$ and

$$\varphi^2 = \frac{(e - e_{cr}) \Sigma Eh \int f^2 dy}{\mu^2 \Sigma R}. \tag{5.1}$$

The compressive force acting on the configuration of strips is

$$K = \frac{\partial U}{\partial e} = e\, \Sigma\, Eh\, b - \frac{\varphi^2 \mu^2}{4} \Sigma\, Eh \int f^2 dy \tag{5.2}$$

or with the solution (5.1) for φ^2,

$$K = e\Sigma Ehb - \frac{e - e_{cr}}{4} \frac{(\Sigma Eh \int f^2 dy)^2}{\Sigma R}. \quad (5.3)$$

The mean compressive stress for all the strips is

$$\sigma = e\frac{\Sigma Ehb}{\Sigma hb} - \frac{e - e_{cr}}{4} \frac{(\Sigma Eh \int f^2 dy)^2}{\Sigma R(\Sigma hb)}. \quad (5.4)$$

The mean elasticity modulus is defined by $E_m = \Sigma Ehb/\Sigma hb$. The ratio between increment of mean compressive stress and mean shortening per unit of length is $E^* = d\sigma/de$. The ratio E^*/E_m becomes [1])

$$\frac{E^*}{E_m} = 1 - \frac{(\Sigma Eh \int f^2 dy)^2}{4(\Sigma R)(\Sigma Ehb)}. \quad (5.5)$$

The expressions (5.2), (5.3) for the force K may also be obtained by integration of the membrane stresses σ_x in the strips.

For a strip

$$\sigma_x = \frac{d^2\psi}{dy^2}.$$

With (2.11), (2.12), (2.13) and (2.16)

$$\sigma_x = -eE + \varphi^2 \frac{\partial^2 G_2}{\partial y^2},$$

with (3.23)

$$\sigma_x = -eE + \varphi^2 \frac{E\mu^2}{2}\left[\frac{d^2Q}{dy^2} + \frac{d^2K}{dy^2}\cos 2\mu x\right]$$

and with (3.34)

$$\sigma_x = -eE + \varphi^2 \frac{E\mu^2}{2}\left[\tfrac{1}{2}f^2 + \frac{d^2K}{dy^2}\cos 2\mu x\right].$$

The compressive force is

$$K = e\Sigma Ehb - \\ -\frac{\varphi^2\mu^2}{4}\Sigma Eh\int f^2 dy - \frac{\varphi^2\mu^2}{2}\cos 2\mu x \Sigma Eh \int \frac{d^2K}{dy^2}dy. \quad (5.6)$$

By partial integration of the integrals

$$Eh \int \frac{d^2K}{dy^2} dy$$

it will be observed that the sum of all these integrals vanishes since at all corners and transitions

$$E_i h_i \frac{dK_i}{dy_i} = E_j h_j \frac{dK_j}{dy_j}$$

and at free edges

$$\frac{dK_i}{dy_i} = 0.$$

Then indeed (5.6) is identical with (5.2).

The compressive force acting on the i-th strip is also obtained by integration of the membrane stresses σ_x, which delivers

$$K_i = eE_ih_ib_i - \frac{\varphi^2\mu^2}{4}E_ih_i\int f_i^2 dy - \\ -\frac{\varphi^2\mu^2}{2}\cos 2\mu x E_i h_i \int \frac{d^2K_i}{dy_i^2} dy_i. \quad (5.7)$$

In view of the last term this force is not constant in x-direction. The mean value is

$$K_i = eE_ih_ib_i - \frac{\varphi^2\mu^2}{4}E_ih_i \int f_i^2 dy \quad (5.8)$$

or with the solution (5.1) of φ^2

$$K_i = eE_ih_ib_i - \frac{e - e_{cr}}{4}\frac{E_ih_i\int f_i^2 dy \Sigma Eh \int f^2 dy}{\Sigma R} \quad (5.9)$$

The mean compressive stress in the i-th strip becomes

$$\sigma_i = eE_i - \frac{e - e_{cr}}{4}\frac{E_i \int f_i^2 dy \Sigma Ehf_i^2 dy}{b_i \Sigma R}. \quad (5.10)$$

The ratio between increment of mean compressive stress and mean shortening per unit of length of any strip is $E_i^* = d\sigma_i/de$ and the expression for the ratio E_i^*/E_i becomes

$$\frac{E_i^*}{E_i} = \frac{1}{E_i}\frac{d\sigma_i}{de} = 1 - \frac{\int f_i^2 dy}{4 b_i}\frac{\Sigma Eh\int f^2 dy}{\Sigma R}. \quad (5.11)$$

It must be emphasized that if the buckling mode (i. e. the function f) or its wavelength (i. e. the quantity μ) is varied in the region where the buckling load has its minimum value, the ratio E^*/E_m of (5.5) does not take an extreme value [2]) like the expression for e_{cr} in (3.15). Thus, an error in the buckling mode, though of little influence on the buckling load, can have a relatively large influence on the ratio E^*/E_m. If an approximate solution for the deflections w of the buckling mode is used, it is necessary to be only content with a very good approximation.

6 Review of the final formulas.

The final formulas are (5.11), giving the ratio E_i^*/E_i for the i-th strip of the combination, and (5.5), giving this ratio for the combination as a whole. The Σ-sign refers to summation over all strips. Under the Σ-sign the index i has been omitted.

In (5.11) and (5.5) f is defined by (3.14). R follows from (4.33) where

- A is given in (3.21).
- Q is given in (3.26) and (3.27), where $U_2 = U_3 = 0$ and U_1 and U_2 are such that at all corners and free edges $Q = 0$. At transitions (fig. 1d) the functions Q must satisfy the expressions given in (4.6) and (4.7).
- H is given in (3.22).
- K is the solution (3.28) of (3.25) where K_p may be calculated from (3.29) and where the constants $T_1 \ldots T_4$ are such that they satisfy the equations of table 1.

For the $\pm$ sign in the expression for R of

[1]) This ratio is identical with the ratio b'_m/b of ref. 12, b'_m being defined in (5.8) of ref. 12.

[2]) This will be demonstrated in the numerical example of section 7.2.1.

(4.33), the + sign is to be chosen at a "right free edge" (fig. 2) and the — sign at a "left free edge".

The value for the strain at which buckling starts does not occur in the final formulas, only knowledge of the (exact or approximate) buckling mode is necessary. If desired, formula (3.15) offers an expression for the strain at buckling.

7 Numerical examples.

7.1 *Calculations for a U-section member* (fig. 3).

The width of the web is a, the width b of the flanges 0.35767a. The thickness of the web and flanges is h. Poisson's ratio $\nu = 0.3$. Coordinate

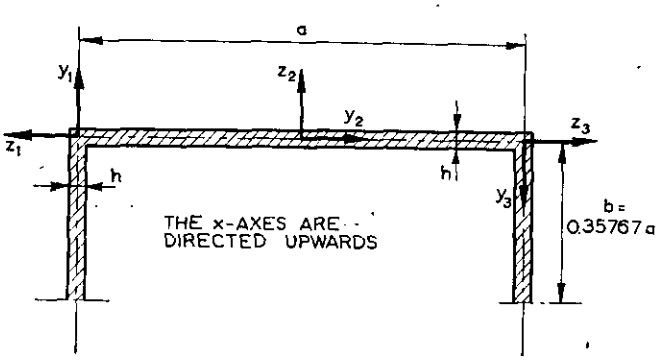

Fig. 3. Dimensions and coordinate axes of the U-profile of section 6.1.

axes are chosen as indicated in fig. 3. The exact buckling mode in the three parts is

$$\begin{aligned} w_{1,1}(y_1) &= f_1(y_1)\sin\mu x \\ w_{1,2}(y_2) &= f_2(y_2)\sin\mu x \\ w_{1,3}(y_3) &= f_3(y_3)\sin\mu x. \end{aligned} \tag{7.1}$$

The half wave length $\lambda = \pi/\mu = 1.1410\ a$ ($\mu = 2.7534/a$). It was supposed that the wavelength had the freedom to take any desired value to make the potential energy a minimum.

The critical buckling stress is

$$\sigma_{cr} = 4.0701\ \frac{\pi^2 D}{a^2 h} \tag{7.2}$$

$$= 40.710\ \frac{D}{a^2 h} \tag{7.3}$$

$$= k_a E\ \frac{h^2}{a^2}\text{, with } k_a = 3.6786. \tag{7.4}$$

The flange width/web width-ratio $\omega = 0.35767$ has been chosen in such a way that, at buckling, no moments occur at the corners between the flanges and the web.[1]

Due to the symmetry of the U-section member and of its buckling mode, the calculations need only be performed for the web $y_2 > 0$ and the flange $y_3 > 0$.

The functions $f_2(y_2)$ and $f_3(y_3)$ are

$$f_2(y_2) = -1.236336\ a\cos\frac{\pi y_2}{a}$$

$$f_3(y_3) = 0.16537\ a\sinh 5.0032\frac{y_3}{a} + a\sin\pi\frac{y_3}{a}.$$

For the web the functions f_2, f_2^2 as well as the functions A_2, H_2, $Q_{p,2}$ and $K_{p,2}$ from (3.21), (3.22), (3.24) and (3.25) are given in table 2. The same functions for the flange are given in table 3. $K_{p,3}$ was computed from (3.29), but $K_{p,2}$ was not.

The particular solutions $Q_{p,2}$ and $Q_{p,3}$ are augmented with the complementary functions of (3.26) so that (3.34) and (4.5) ... (4.8) are satisfied. The particular solutions $K_{p,2}$ and $K_{p,3}$ are augmented with the complementary functions of (3.28), where the constants $T_{1,2}$, $T_{2,2}$, $T_{3,2}$, $T_{4,2}$, $T_{1,3}$, $T_{2,3}$, $T_{3,3}$ and $T_{4,3}$ are such that the equations of table 1 are satisfied. From symmetry it follows that $T_{2,2} = T_{3,2} = 0$. The equations and their solutions are presented in table 4. Numerical values of the right-hand sides of these equations were calculated by numerical differentiation (see for example ref. 13) of the functions $K_{p,2}$ and $K_{p,3}$.

The result, the functions Q_2, K_2 and Q_3, K_3 are given in table 2 and 3 as well as some other functions which are necessary in the final formulas.

From tables 2 and 3 have been calculated, by numerical integration and differentiation,

$$A_2 = \int_0^{1/2} f_2^2 dy = 0.39902\ a^3$$

$$B_2 = \int_0^{1/2} A_2 Q_2 dy = 0.11942\ a^5$$

$$C_2 = \tfrac{1}{2}\int_0^{1/2} H_2 K_2 dy = 0.02412\ a^5$$

$$K_2 = B_2 + C_2 = 0.14353\ a^5$$

$$A_3 = \int_0^{0.35767} f_3^2 dy = 0.23044\ a^3$$

$$B_3 = \int_0^{0.35767} A_3 Q_3 dy = -0.01625\ a^5$$

$$C_3 = \tfrac{1}{2}\int_0^{0.35767} H_3 K_3 dy = -0.00019\ a^5$$

$$D_3 = \tfrac{1}{2}\left(f_3^2\ \frac{dQ_3}{dy}\right)_{y=0.35767} = 0.08236\ a^5$$

$$K_3 = B_3 + C_3 + D_3 = 0.06592\ a^5$$

[1]) KIMM (ref. 4) computed buckling loads for U-section members with different ratios ω. Indeed, in fig. 10 of ref. 4, the point $k_a = 3.6786$, $\omega = 0.35767$ lies on the curve c for exact solutions. The present author provisionally chose the values $\omega = 0.375$, $k_a = 3.615$ (or in (6.2) $\sigma_{cr} = 4\,\pi^2 D/a^2 h$), for which solution KIMM states that the buckling mode is such that no moments occur at the corners (page 163, ref. 4). Obviously, this is the solution where the half wave length would be $\lambda = a = 2.67\ b$. Prof. KOITER drew the attention of the author to the fact that the latter solution cannot be the proper one if the half wave length λ has the freedom to take any desired value, which is also assumed in ref. 4.

The final result for the web is from (5.11)

$$\frac{E_2^*}{E} = 1 - \frac{A_2(A_2 + A_3)}{4 \times 0.5\, a(R_2 + R_3)} = 0.4004. \quad (7.5)$$

The final result for the flange is from (5.11)

$$\frac{E_3^*}{E} = 1 - \frac{A_3(A_2 + A_3)}{4\, b(R_2 + R_3)} = 0.5159. \quad (7.6)$$

The final result for the complete member is from (5.5)

$$\frac{E^*}{E} = 1 - \frac{(A_2 + A_3)^2}{4(0.5\, a + b)(R_2 + R_3)} = 0.4486. \quad (7.7)$$

7.2 *Calculation for some other cases.* [1]

7.2.1 *Infinite sequence of panels supported by hinges.*

Also for the sake of comparison with the results (7.5) and (7.6) some simple cases are dealt with.

It is obvious that the present formulas may be applied to one panel of an infinite sequence of equal panels supported by hinges in longitudinal direction at distances a. The hinges are such that they cannot absorb shear stresses. The panels are free to expand in transverse direction, but at the hinges there may be transverse membrane stresses σ_y, whose resultant is zero. The boundary conditions for the membrane stresses at a hinge are those of a transition (3.39) ... (3.42).

It is well known (ref. 1, 2, 3) that for the half wave length $\lambda = a$

$$\sigma_{cr} = \frac{k\pi^2 D}{a^2 h}, \; k = 4, \quad (7.8)$$

while the ratio E^*/E then becomes

$$E^*/E = 0.5. \quad (7.9)$$

If the wavelength is forced to have another value the deflection surface of the buckling mode becomes $(-\tfrac{1}{2} a < y < \tfrac{1}{2} a)$

$$w_1 = f(y) \sin \mu x, \; \mu = \pi/\lambda,$$
$$f(y) = a \cos \pi y/a.$$

The functions A, H, Q and K of (3.21), (3.22), (3.26) and (3.28) respectively become

$$A = -\pi^2 \cos 2\pi y/a$$

$$H = \pi^2$$

$$Q = a^2 \left\{ \frac{1}{8} y^2 - \frac{a^2}{16\pi^2} \cos \frac{2\pi y}{a} + (U_0 + U_1 y) \right\}. \quad (7.10)$$

In (7.10) the integration constants U_0 and U_1 of the panels require no further attention, because they drop out again of (7.11).

$$K = \pi^2/16\, \mu^4.$$

[1]) In the cases of this section the buckling modes are simple and the integrations have been carried out analytically.

Further

$$\left. \begin{aligned} &\int_0^{\frac{1}{2}a} AQ\, dy = \frac{3}{64}\, a^5 \\ &\frac{1}{2} \int_0^{\frac{1}{2}a} HK\, dy = \frac{1}{64}\, a\lambda^4 \\ &\left(\int_0^{\frac{1}{2}a} f^2\, dy \right)^2 = \frac{1}{16}\, a^6 \end{aligned} \right\} \quad (7.11)$$

Application of (5.5) and (4.33) gives

$$\frac{E^*}{E} = 1 - \frac{\frac{1}{16}}{4\left(\frac{3}{64} + \frac{1}{64}\, \frac{\lambda^4}{a^4}\right)\frac{1}{2}} = 1 - \frac{2}{3 + \frac{\lambda^4}{a^4}}.$$

Indeed at $\lambda = a$, $E^*/E = 0.5$. If the wavelength is forced to have the value $\lambda = 1.1410\, a$, i. e. the value for the web of the U-section member of section 7.1, then

$$\frac{E^*}{E} = 0.574. \quad (7.12)$$

The buckling stress for $\lambda = 1.1410\, a$ is

$$\sigma_{cr} = \frac{k\, \pi^2\, D}{a^2 h}, \; k = 4.070. \quad (7.13)$$

The fact that the result (7.12) is so remarkably different from the result (7.5) can be explained by the fact that for the web of the U-section member at the corners all membrane stresses σ_y must be zero (compare appendix A on the boundary conditions at a corner).

Note that a change in wavelength from $\lambda = a$ to $\lambda = 1.1410\, a$, only changes k from $k = 4$ in (7.8) to $k = 4.070$ in (7.13). The value of the ratio E^*/E is, however, changed much more, viz. from $E^*/E = 0.5$ to $E^*/E = 0.574$. This is due to the fact that the ratio E^*/E, in contrast to the buckling load, does not show an extreme value at $\lambda = a$ (compare discussion at the end of section 5).

Also for changes in the function $f(y)$, indicating the buckling mode in y direction, the ratio E^*/E does not take an extreme value. Take for example $\lambda = a$, $\mu = \pi/a$ and add to $f(y)$ the deviation $c \cos 3\pi y/a$, thus

$$f(y) = a \cos \pi y/a + c \cos 3\pi y/a.$$

Application of the proper formulas delivers

$$\frac{E^*}{E} = 1 - \frac{\left\{1 + \left(\frac{c}{a}\right)^2\right\}^2}{2 + 2\frac{c}{a} + \frac{476}{25}\left(\frac{c}{a}\right)^2 + 42\left(\frac{c}{a}\right)^4}$$

which result does not take an extreme value at $c = 0$.

7.2.2 *Sides of a compressed thinwalled square tube.*

The sides have the width a ($-\frac{1}{2}a < y < \frac{1}{2}a$) (fig. 4). Poisson's ratio $\nu = 0.3$. The buckling mode is

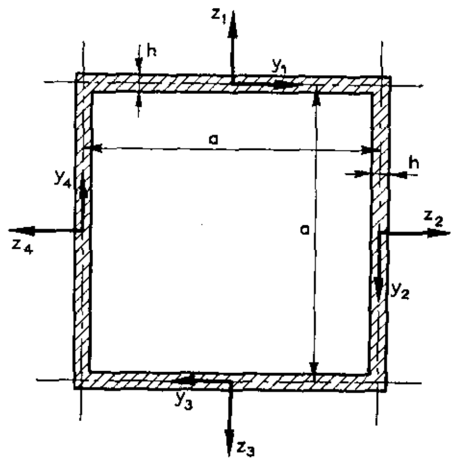

Fig. 4. Coordinate axes of the square tube of section 7.2.2.

$$w_{1,1} = f_1(y) \sin \mu x$$
$$w_{1,2} = f_2(y) \sin \mu x, \text{ etc.}, \mu = \pi/\lambda, \ \lambda = a$$
$$f_1(y) = a \cos \pi y_1/a$$
$$f_2(y) = - a \cos \pi y_2/a, \text{ etc.}$$

The functions A, H, Q and K_p of (3.21), (3.22), (3.26) and (3.25) respectively become

$$A_1 = A_2 = -\pi^2 \cos 2\pi y/a$$
$$H_1 = H_2 = \pi^2$$
$$Q_1 = Q_2 = a^2 \left\{ \frac{1}{8} y^2 - \frac{a^2}{16\pi^2} \cos \frac{2\pi y}{a} - - a^2 \left(\frac{1}{32} + \frac{1}{16\pi^2} \right) \right\}$$
$$K_{p,1} = K_{p,2} = a^4/16\pi^2$$

$$\int_0^{\frac{1}{2}a} A_1 Q_1 dy = \int_0^{\frac{1}{2}a} A_2 Q_2 dy = \frac{3}{64} a^5$$

$$\frac{1}{2} \int_0^{\frac{1}{2}a} H_1 K_{p,1} \, dy = \frac{1}{2} \int_0^{\frac{1}{2}a} H_2 K_{p,2} dy = \frac{1}{64} a^5$$

$$\left(\int_0^{\frac{1}{2}a} f_1^2 dy \right)^2 = \left(\int_0^{\frac{1}{2}a} f_2^2 dy \right)^2 = \frac{1}{16} a^6.$$

From symmetry considerations it follows that of the constants T of (3.28) $T_{2,1} = T_{3,1} = T_{2,2} = T_{3,2} = 0$.

For the remaining constants $T_{1,1}$, $T_{4,1}$, $T_{1,2}$ and $T_{4,2}$ the equations (1), (2), (3) and (4) of table 1 are valid. It proves that these equations can be reduced to

$$T_{1,1} = T_{1,2}$$
$$T_{4,1} = T_{4,2}$$
$$T_{1,1} \cosh \pi + T_{4,1} \frac{a}{2} \sinh \pi = - 0.00633257 \, a^4$$
$$T_{1,1} \, 2\pi \sinh \pi + T_{4,1} \, a(\pi \cosh \pi + \sinh \pi) = 0.$$

From the latter equation it follows that there are no shear stresses τ at the corners.

The solutions are

$$T_{1,1} = - 0.0022169 \, a^4$$
$$T_{4,1} = 0.0033537 \, a^3$$

and

$$K_1 = K_{p,1} + T_{1,1} \cosh 2\pi \frac{y_1}{a} + T_{4,1} \, y_1 \sinh 2\pi \frac{y_1}{a}$$

$$\frac{1}{2} \int_0^{\frac{1}{2}a} H_1 K_1 dy = 0.0059427 \, a^5.$$

Application of (5.5) and (4.33) gives

$$\frac{E_1^*}{E} = 1 - \frac{\frac{1}{16}}{4 \left(\frac{3}{64} + 0.0059427 \right) \frac{1}{2}} = 0.4083. \tag{7.14}$$

Cox, ref. 15 also obtained this result (plate with at the boundaries $w = 0$, $\sigma_y = 0$, $\tau = 0$, $\lambda = a$, $\nu = 0.3$). The fact that the result (7.14) remains about 20 % below 0.5 must again be explained by the fact that the membrane stresses σ_y are zero at the corners (compare appendix A on the boundary conditions at a corner).

7.2.3 *Plate with one hinge and one free edge.*

The width of the plate is b. It is supposed that both at the hinge and at the free edge the membrane stresses σ_y and τ vanish. It is further supposed that the half wave length λ is forced to have the value,

$$\lambda = \frac{\pi}{\mu} = 3.19009 \, b,$$
$$\mu = 0.98480/b,$$

of the flange of the U-section member of section 7.1.

For the deflection surface of the buckling mode is now taken the approximate solution

$$w_1 = f(y) \sin \mu x.$$
$$f(y) = y.$$

The functions A, H, Q and K_p of (3.21), (3.22), (3.26) and (3.25) respectively become

$$A = 1$$
$$H = 1$$
$$Q = \frac{y^4}{24} - \frac{yb^3}{24}$$
$$K_p = \frac{1}{16\mu^4}.$$

The equations for T_1, T_2, T_3, T_4 of table 1 and their solutions are given in table 5.

$$K = K_p + (T_1 + yT_2)\cosh 2\mu y + (T_3 + yT_4)\sinh 2\mu y$$

$$\int_0^b f^2 dy = \tfrac{1}{3} b^3$$

$$\frac{1}{2}\left(f^2 \frac{dQ}{dy}\right)_{y=b} = \frac{1}{16} b^5$$

$$\int_0^b AQ\,dy = -\frac{1}{80} b^5$$

$$\frac{1}{2}\int_0^b HK\,dy = \frac{1}{2}\int_0^b K dy = 0.0005725\, b^5$$

$$\frac{E^*}{E} = 1 - \frac{\frac{1}{9}}{4\left(-\frac{1}{80} + 0.0005725 + \frac{1}{16}\right)} = 0.4507. \tag{7.15}$$

The result (7.15) is less than the result (7.6) for the flange of the U-section member. The reason is that in the latter the shear stress τ at the corner is not zero.

8 Conclusions.

The present method to determine the reduction in stiffness of combinations of rectangular plates in compression at loads slightly above the buckling load, could be very well applied to numerical examples.

For complex configurations, though the method remains straightforward, the aid of an electronic digital computer may be desirable, but only routine-programmes (solution of linear equations, numerical integration) will be necessary.

If the exact solution for the buckling mode is used in the calculations, the results are also exact, apart from errors due to numerical integration and differentiation, but these errors can easily be made as small as desired.

Since the minimum theorem of the potential energy is used, solutions for the load derived, for a given compression, from the present formulas will be too large if an approximate solution for the buckling mode is used. [1]) This is also the case if the exact mode of buckling is used and the present formulas are applied for loads in large excess of the buckling load.

The numerical examples clearly demonstrate the influence of the wavelength of the buckling mode and, especially, the great influence of the boundary conditions of the membrane stresses. One of the remarkable results was that the sides of an infinitely long, thinwalled square tube showed a ratio $E^*/E = 0.4083$ in stead of the value of 0.5 obtained for the well-known case of an infinite sequence of simply-supported panels, which have the same buckling mode.

In view of the great influence of the membrane stresses on the final result, it is desirable that they are derived from the deflections of the buckling mode with the aid of the proper differential equation, as is done in the present work, the more so, since it is much more difficult to choose a pattern for these stresses by intuition than to do so for a buckling mode.

Furthermore, it should be emphasized that if the buckling mode in transverse direction or its wavelength is varied in the region where the buckling load has its minimum value, the ratio E^*/E does not take an extreme value. Hence, if an exact buckling mode is not used, one should only be content with a very good approximation of the buckling mode.

[1]) Strictly, this is only true for the work done during the compression.

9 References.

1. TREFFTZ, E. und MARGUERRE, K. Ueber die Tragfähigkeit eines längsbelasteten Plattenstreifens nach Ueberschreiten der Beullast. Zeitschr. f. angew. Math. u. Mech. Bd. 17, p. 85 (1937).
2. MARGUERRE, K. Die mittragende Breite der gedrückten Platte. Luftfahrtforschung, Bd. 14, p. 121 (1937).
3. KOITER, W. T. On the stability of the elastic equilibrium. (in Dutch). Doctor Thesis Techn. University Delft, 1945.
4. KIMM, G. Beitrag zur Stabilität dünnwandiger U-Profile mit konstanter Wandstärke im elastischen Bereich. Luftfahrtforschung, Bd 18, S. 155, 1941.
5. VAN DER NEUT, A. The local instability of compression members built up from flat plates. Techn. Univ. Delft. Aero. Dept. V. T. H. - 47, Aug. 1952. Also: Anniversary Volume on Applied Mechanics dedicated to C. B. Biezeno. Stam, Haarlem, 1953.
6. CAPEY, E. C. The buckling under longitudinal compression of a simply supported panel that changes in thickness across the width. Ministry of Supply, Aeronautical Research Council, C. P. No. 235, London 1956.
7. BENTHEM, J. P. The buckling load of flat panels that change in thickness across the bay. N.L.L. - Techn. Rep. S. 527, 1958.
8. BENTHEM, J. P. Experiments on the post buckling behaviour of simply supported panels that change in thickness across the bay. N.L.L.-Techn. Memo. S. 522, 1958.
9. TIMOSHENKO, S. Theory of plates and shells. McGraw-Hill Book Company. New York and London, 1940.
10. TIMOSHENKO, S. Theory of elastic stability. MGraw-Hill Book Company, New York, 1936.
11. WEINSTOCK, R. Calculus of variations. McGraw-Hill Book Company, New York, 1952.
12. BOTMAN, M. and BESSELING, J. F. The effective width in the plastic range of flat plates under compression. N.L.L. Report S. 445, Amsterdam, 1954. Also N.L.L. Reports and Transactions Vol. XIX, 1954.
13. Interpolation and allied tables. London, Her Majesty's Stationary Office, 1956.
14. BIEZENO, C. B. and GRAMMEL, R. Technische Dynamik. Julius Springer, Berlin, 1939.
15. COX, H. L. The buckling of a flat rectangular plate under axial compression and its behaviour after buckling. Min. of Aircraft Production, R and M No. 2041, London, 1945.

APPENDIX A.

Refined analysis of the boundary conditions at a corner.

A.1. *More freedom for the varying membrane stresses.*

In the main text of this paper the boundary conditions at any corner have been given as eqs. (3.3) ... (3.6) and (3.35 ... (3.38). Hence, eight boundary conditions are available for the displacements w and the membrane stresses, derived from the functions ψ.

Strictly, four of them, viz. (3.3), (3.4), (3.35) and (3.36),

$$\left.\begin{aligned} w_i &= \text{constant} \\ w_j &= \text{constant} \\ \sigma_{y,i} &= 0 \\ \sigma_{y,j} &= 0 \end{aligned}\right\} \qquad (A.1)$$

are incompatible, since it is impossible to prescribe, along the boundary of a plate, displacements as well as stresses normal to the boundary.

In order to perform a refined analysis of these boundary conditions it is necessary to allow for more freedom in the variations of the displacements w and the membrane stresses, stemming from ψ. Suppose, in stead of (2.6),

$$w(x,y,\varphi) = \frac{\varphi}{1!}\left(\frac{\partial w}{\partial\varphi}\right)_{\varphi=0} + \frac{\varphi^2}{2!}\left(\frac{\partial^2 w}{\partial\varphi^2}\right)_{\varphi=0} + \ldots$$

$$w = \varphi w_1 + \varphi^2 w_2 + \varphi^3 w_3 + \ldots\ldots \qquad (A.2)$$

In (A.2) the functions w_1, w_2, w_3 ...... are of the order b, where b is the order of the panel width. An n-th derivative is of the order b^{1-n}, for example

$$w_1 = b\,(\sin \pi y/b)(\sin \pi x/b).$$

Suppose, in stead of (2.16)

$$\psi = F + G(x,y,\varphi)$$

where

$$G(x,y,\varphi) = \varphi G_1 + \varphi^2 G_2 + \varphi^3 G_3 + \varphi^4 G_4 + \ldots \qquad (A.3)$$

The compatibility-relation (2.2) between ψ and w is written in the form

$$\Delta\Delta\psi = J[w.w], \qquad (A.4)$$

where $J[p.q]$ means

$$J[p.q] = E\left(\frac{\partial^2 p}{\partial x\partial y}\,\frac{\partial^2 q}{\partial x\partial y} - \frac{1}{2}\,\frac{\partial^2 p}{\partial x^2}\,\frac{\partial^2 q}{\partial y^2} - \frac{1}{2}\,\frac{\partial^2 q}{\partial x^2}\,\frac{\partial^2 p}{\partial y^2}\right) \qquad (A.5)$$

From (A.2) ... (A.5) it follows by equating terms of the same power of φ that

$$\Delta\Delta G_1 = 0 \qquad (A.6)$$

$$\Delta\Delta G_2 = J[w_1 . w_1] \qquad (A.7)$$

$$\Delta\Delta G_3 = 2\,J[w_1 . w_2] \qquad (A.8)$$

$$\Delta\Delta G_4 = 2\,J[w_1 . w_3] + J[w_2 . w_2]. \qquad (A.9)$$

From (A.7) ... (A.9) it follows that the order of G_2, G_3, G_4 is

$$\begin{aligned} G_2 &= \text{Ord}\,(Eb^2) \\ G_3 &= \text{Ord}\,(Eb^2) \\ G_4 &= \text{Ord}\,(Eb^2) \end{aligned} \qquad (A.10)$$

if E denotes the order of elasticity moduli and b the order of panel widths.

The expression for the strain energy (2.23) is written in the form

$$U = \Sigma(I_1[w.w] + I_2[\psi.\psi]) \qquad (A.11)$$

where

$$I_1[p.q] = \frac{D}{2}\iint\left(\frac{\partial^2 p}{\partial x^2}\,\frac{\partial^2 q}{\partial x^2} + \frac{\partial^2 p}{\partial y^2}\,\frac{\partial^2 q}{\partial y^2} + \nu\,\frac{\partial^2 p}{\partial x^2}\,\frac{\partial^2 q}{\partial y^2} + \nu\,\frac{\partial^2 p}{\partial y^2}\,\frac{\partial^2 q}{\partial x^2} + 2(1-\nu)\,\frac{\partial^2 p}{\partial x\partial y}\,\frac{\partial^2 q}{\partial x\partial y}\right) dxdy \qquad (A.12)$$

$$I_2[p.q] = \frac{h}{2E}\iint\left(\frac{\partial^2 p}{\partial x^2}\,\frac{\partial^2 q}{\partial x^2} + \frac{\partial^2 p}{\partial y^2}\,\frac{\partial^2 q}{\partial y^2} - \nu\,\frac{\partial^2 p}{\partial x^2}\,\frac{\partial^2 q}{\partial y^2} - \nu\,\frac{\partial^2 p}{\partial y^2}\,\frac{\partial^2 q}{\partial x^2} + 2(1+\nu)\,\frac{\partial^2 p}{\partial x\partial y}\,\frac{\partial^2 q}{\partial x\partial y}\right) dxdy. \qquad (A.13)$$

After substitution of (A.2) and (A.3) into (A.11) the result is

$$U = \Sigma(U_0 + \varphi U_1 + \varphi^2 U_2 + \varphi^3 U_3 + \varphi^4 U_4 + \ldots\ldots) \qquad (A.14)$$

where

$$U_0 = I_2[F.F] \qquad (A.15)$$

$$U_1 = 2\,I_2[F.G_1] \qquad (A.16)$$

$$U_2 = I_1[w_1 . w_1] + I_2[G_1 . G_1] + 2\,I_2[F.G_2] \qquad (A.17)$$

$$U_3 = 2\,I_1[w_1 . w_2] + 2\,I_2[G_1 . G_2] + 2\,I_2[F.G_3] \qquad (A.18)$$

$$U_4 = 2\,I_1[w_1 . w_3] + I_1[w_2 . w_2] + I_2[G_2 . G_2] + 2\,I_2[G_1 . G_3] + 2\,I_2[F.G_4]. \qquad (A.19)$$

For an infinitely long configuration, reversal of the sign in φ cannot change the strain energy and thus (A.14) reduces to

$$U = \Sigma(U_0 + \varphi^2 U_2 + \varphi^4 U_4 + \ldots\ldots). \qquad (A.20)$$

The parameter φ must obey the conditions

$$\frac{\partial U}{\partial\varphi} = \Sigma(2\,\varphi U_2 + 4\,\varphi^3 U_4 + \ldots\ldots). \qquad (A.21)$$

There is always a solution $\varphi = 0$, which is not stable beyond the buckling load.

If the configuration is not infinitely long it may behave if it were infinitely long. But if, for example, a short U-profile is compressed such that at the ends the displacements in the y directions are suppressed, curvature of the elements of the U profile will occur at all loads. Then in (A.14) the coefficients of the uneven powers of φ are not zero and the U-profile has not a well defined buckling load.

A.2 *The boundary conditions.*

For the sake of convenience, it is supposed that the panels bounding the corner are at a right angle. The final conclusions, however, are also valid for other angles.

The boundary conditions (A.1) are now replaced by the proper ones (fig. 5)

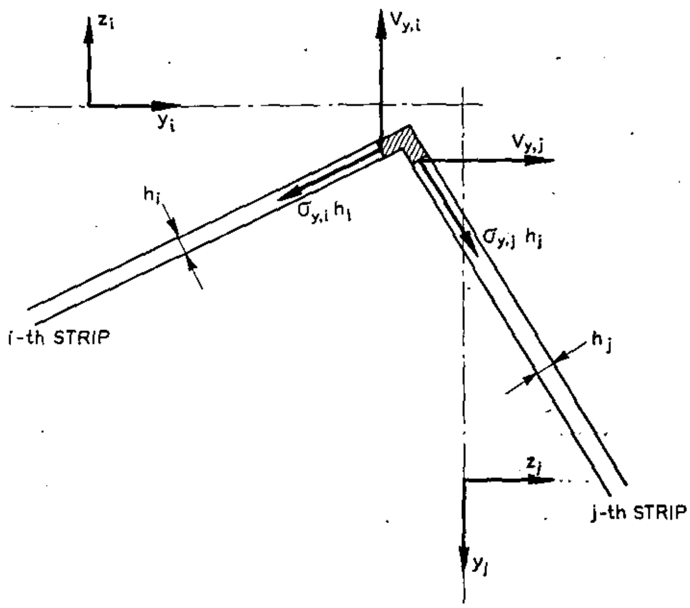

Fig. 5. Forces acting on an element at the corner.

$$w_i = -v_j \tag{A.22}$$

$$w_j = v_i \tag{A.23}$$

$$-\sigma_{y,i}h_i + \sigma_{y,j}h_j \frac{\partial w_j}{\partial y_j} = -V_{y,j} \tag{A.24}$$

$$-\sigma_{y,j}h_j - \sigma_{y,i}h_i \frac{\partial w_i}{\partial y_i} = -V_{y,i}\,. \tag{A.25}$$

In (A.24), $V_{y,j}$ is the reduced shear force $(Q_y - \partial M_{xy}/\partial x)$ in the j-th strip at the corner. Equation (A.22) is reduced to a relation between ψ_j, w_i and w_j in the following way

$$\frac{\partial^2 w_i}{\partial x^2} = -\frac{\partial^2 v_j}{\partial x^2}, \text{ see eq. (A.22)}$$

$$\gamma_j = \frac{\partial u_j}{\partial y_j} + \frac{\partial v_j}{\partial x} + \frac{\partial w_j}{\partial x}\,\frac{\partial w_j}{\partial y_j} \tag{A.26}$$

$$\frac{\partial \gamma_j}{\partial x} = \frac{\partial^2 u_j}{\partial x \partial y_j} + \frac{\partial^2 v_j}{\partial x^2} + \frac{\partial^2 w_j}{\partial x^2}\,\frac{\partial w_j}{\partial y_j} + \frac{\partial w_j}{\partial x}\,\frac{\partial^2 w_j}{\partial x \partial y_j} \tag{A.27}$$

$$\varepsilon_{x,j} = \frac{\partial u_j}{\partial x} + \tfrac{1}{2}\left(\frac{\partial w_j}{\partial x}\right)^2 \tag{A.28}$$

$$\frac{\partial \varepsilon_{x,j}}{\partial y_j} = \frac{\partial^2 u_j}{\partial x \partial y_j} + \frac{\partial w_j}{\partial x}\,\frac{\partial^2 w_j}{\partial x \partial y_j}\,. \tag{A.29}$$

From (A.27) and (A.29) follows

$$\frac{\partial^2 v_j}{\partial x^2} = \frac{\partial \gamma_j}{\partial x} - \frac{\partial \varepsilon_{x,j}}{\partial y_j} - \frac{\partial^2 w_j}{\partial x^2}\,\frac{\partial w_j}{\partial y_j}\,. \tag{A.30}$$

With the substitution

$$\gamma_j = \frac{-2(1+\nu)}{E_j}\,\frac{\partial^2 \psi_j}{\partial x \partial y_j}$$

$$\varepsilon_{x,j} = \frac{1}{E_j}\left(\frac{\partial^2 \psi_j}{\partial y^2_j} - \nu\,\frac{\partial^2 \psi_j}{\partial x^2}\right)$$

eq. (A.30) becomes

$$\frac{\partial^2 v_j}{\partial x^2} = -\frac{1}{E_j}\left\{\frac{\partial^3 \psi_j}{\partial y_j^3} + (2+\nu)\,\frac{\partial^3 \psi_j}{\partial x^2 \partial y_j}\right\} - \frac{\partial^3 w_j}{\partial x^2}\,\frac{\partial w_j}{\partial y_j}\,.$$

Thus boundary condition (A.22) becomes,

$$\frac{\partial^2 w_i}{\partial x^2} = \frac{1}{E_j}\left\{\frac{\partial^3 \psi_j}{\partial y^3_j} + (2+\nu)\,\frac{\partial^3 \psi_j}{\partial x^2 \partial y_j}\right\} + \frac{\partial^2 w_j}{\partial x^2}\,\frac{\partial w_j}{\partial y_j}\,. \tag{A.31}$$

In condition (A.24) is substituted

$$\sigma_{y,i} = \frac{\partial^2 \psi_i}{\partial x^2}\,,\quad \sigma_{y,j} = \frac{\partial \psi_j}{\partial x^2}\,,$$

$$V_{y,j} = -D_j\left\{\frac{\partial^3 w_j}{\partial y_j^3} + (2-\nu)\,\frac{\partial^3 w_j}{\partial x^2 \partial y_j}\right\}$$

which results in

$$-h_i\,\frac{\partial^2 \psi_i}{\partial x^2} + h_j\,\frac{\partial^2 \psi_j}{\partial x^2}\,\frac{\partial w_j}{\partial y_j} = D_j\left\{\frac{\partial^3 w_j}{\partial y_j^3} + (2-\nu)\,\frac{\partial^3 w_j}{\partial x^2 \partial y_j}\right\}. \tag{A.32}$$

With the aid of

$$\psi_i = F_i + G_i\,,\quad \psi_j = F_j + G_j$$

the boundary conditions (A.31), (A.32), and along the same lines (A.23), (A.25), become

$$\frac{\partial^2 w_i}{\partial x^2} = \frac{1}{E_j}\left\{\frac{\partial^3 G_j}{\partial y_j^3} + (2+\nu)\frac{\partial^3 G_j}{\partial x^2 \partial y_j}\right\} + \frac{\partial^2 w_j}{\partial x^2}\frac{\partial w_j}{\partial y_j} \tag{A.33}$$

$$\frac{\partial^2 w_j}{\partial x^2} = -\frac{1}{E_i}\left\{\frac{\partial^3 G_i}{\partial y_i^3} + (2+\nu)\frac{\partial^3 G_i}{\partial x^2 \partial y_i}\right\} - \frac{\partial^2 w_i}{\partial x^2}\frac{\partial w_i}{\partial y_i} \tag{A.34}$$

$$h_i\frac{\partial^2 G_i}{\partial x^2} = -D_j\left\{\frac{\partial^3 w_j}{\partial y_j^3} + (2-\nu)\frac{\partial^3 w_j}{\partial x^2 \partial y_j}\right\} + h_j\frac{\partial^2 G_j}{\partial x^2}\frac{\partial w_j}{\partial y_j} \tag{A.35}$$

$$h_j\frac{\partial^2 G_j}{\partial x^2} = D_i\left\{\frac{\partial^3 w_i}{\partial y_i^3} + (2-\nu)\frac{\partial^3 w_i}{\partial x^2 \partial y_i}\right\} - h_i\frac{\partial^3 G_i}{\partial x^2}\frac{\partial w_i}{\partial y_i} \tag{A.36}$$

where

$$\frac{\partial w_i}{\partial y_i} = \frac{\partial w_j}{\partial y_j}.$$

Substitute in (A.33) and (A.35) the expressions (A.2) and (A.3),

$$w = \varphi w_1 + \varphi^2 w_2 + \ldots\ldots$$

$$G = \varphi G_1 + \varphi^2 G_2 + \ldots\ldots$$

Separate the obtained equations into parts of equal powers of φ. Some results, to be used further, are

$$\frac{\partial^2 w_{1i}}{\partial x^2} = \frac{1}{E_j}\left\{\frac{\partial^3 G_{1j}}{\partial y_j^3} + (2+\nu)\frac{\partial^3 G_{1j}}{\partial x^2 \partial y_j}\right\}, \tag{A.37}$$

$$h_i\frac{\partial^2 G_{1i}}{\partial x^2} = -D_j\left\{\frac{\partial^3 w_{1j}}{\partial y_j^3} + (2-\nu)\frac{\partial^3 w_{1j}}{\partial x^2 \partial y_j}\right\} \tag{A.38}$$

and

$$h_i\frac{\partial^2 G_{2i}}{\partial x^2} = -D_j\left\{\frac{\partial^3 w_{2j}}{\partial y_j^3} + (2-\nu)\frac{\partial^3 w_{2j}}{\partial x^2 \partial y_j}\right\} + h_j\frac{\partial^2 G_{1j}}{\partial x^2}\frac{\partial w_{1j}}{\partial y_j}. \tag{A.39}$$

From (A.6) did not follow an order of G_1, but from (A.38) follows the order of G_{1i} for the whole panel,

$$G_{1i} = \text{Ord}\,(Eh^2), \tag{A.40}$$

if h denotes the order of panel thicknesses.

But then, see (A.37), at a corner

$$\frac{\partial^2 w_{1i}}{\partial x^2} = \text{Ord}\left(\frac{h^2}{b^3}\right)$$

while the normal order for a second derivative of w_{1i} is $1/b$. It is thus allowable, in view of the smallness of the ratio h/b, to put as boundary condition for w_1

$$\frac{\partial^2 w_{1i}}{\partial x^2} = 0. \tag{A.41}$$

From (A.39) it follows

$$\frac{\partial^2 G_{2i}}{\partial x^2} = \text{Ord}\left(E\,\frac{h^2}{b^2}\right)$$

while from (A.10) it is obvious that the normal order of a second derivative of G_{2i} is E. It is thus allowable, in view of the smallness of the ratio $\frac{h}{b}$, to put as boundary condition for G_{2i}

$$\frac{\partial^2 G_{2i}}{\partial x^2} = 0. \tag{A.42}$$

In the expressions U_0, U_2, U_4 of (A.15) ... (A.19) terms, which are an order h^2/b^2 lower than the others, are neglected and (A.20) becomes (F is of order Eh^2)

$$U = \Sigma\,\{\,I_2[F\,.\,F] + \varphi^2(I_1[w_1\,.\,w_1] + 2\,I_2[F\,.\,G_2] + \varphi^4\,I_2[G_2\,.\,G_2] + \ldots\,\} \tag{A.43}$$

The fact, that in (A.43) only w_1, F and G_2 remain, justifies the supposition, made in (2.6), (2.11) and (2.15), namely

$$w(x, y, \varphi) = \varphi w_1 \tag{A.44}$$

$$\psi = F + G(x, y, \varphi) = F + \varphi^2 G_2. \tag{A.45}$$

Thus (A.43) is the expression used in the calculations of section 4.

Since, as boundary conditions, (A.41) and (A.42) were already accepted, it is allowable to put

$$\frac{\partial^2 w_i}{\partial x^2} = 0$$

$$\frac{\partial^2 \psi_i}{\partial x^2} = 0$$

and likewise

$$\frac{\partial^2 w_j}{\partial x^2} = 0$$

$$\frac{\partial^2 \psi_j}{\partial x^2} = 0$$

which was to be proved.

APPENDIX B.

Verification of the derived formula (4.27) for the strain energy.

In section 5 a solution for the parameter φ has been obtained by integrating the strain energy U, and the proper value of φ has been determined by putting

$$\frac{\partial U}{\partial \varphi} = 0.$$

The solution of φ can also be obtained by following Galerkin's method (see e. g. ref. 14, page 137). With this method also displacements are varied which, of course, (the proper solution excluded) do not satisfy equilibrium conditions. However, the equilibrium conditions can be satisfied if additional surface and mass forces are introduced. Galerkin's method requires that the work, done by these additional forces through their displacements, vanishes. In the present case these additional forces consist only of forces perpendicular to the plate. Per unit of surface area the expression for these forces reads

$$q = D\Delta\Delta w - h\left(\frac{\partial^2\psi}{\partial y^2}\,\frac{\partial^2 w}{\partial x^2} + \frac{\partial^2\psi}{\partial x^2}\,\frac{\partial^2 w}{\partial y^2} - 2\,\frac{\partial^2\psi}{\partial x\partial y}\,\frac{\partial^2 w}{\partial x\partial y}\right). \tag{B.1}$$

After substitution of

$$w = \varphi w_1\,,$$

$$\psi = F + \varphi^2 G_2\,,$$

and

$$\Delta\Delta w_1 = \frac{h}{D}\,\frac{\partial^2 F_{cr}}{\partial y^2}\,\frac{\partial^2 w_1}{\partial x^2}$$

$$q = \varphi h\,\frac{\partial^2 F_{cr}}{\partial y^2}\,\frac{\partial^2 w_1}{\partial x^2} - h\varphi^3\left(\frac{\partial^2 G_2}{\partial y^2}\,\frac{\partial^2 w_1}{\partial x^2} + \frac{\partial^2 G_2}{\partial x^2}\,\frac{\partial^2 w_1}{\partial y^2} - 2\,\frac{\partial^2 G_2}{\partial x\partial y}\,\frac{\partial^2 w_1}{\partial x\partial y}\right) - \varphi h\,\frac{\partial^2 F}{\partial y^2}\,\frac{\partial^2 w_1}{\partial x^2}. \tag{B.2}$$

According to Galerkin's principle (the Σ-sign refers to integration over all panels)

$$\Sigma \iint q w_1\, dxdy = 0$$

and together with

$$\frac{\partial^2 F_{cr}}{\partial y^2} = C_{cr}\,,\quad \frac{\partial^2 F}{\partial y^2} = C$$

$$\varphi_2 = \frac{\Sigma h(C_{cr} - C)\displaystyle\iint w_1\,\frac{\partial^2 w_1}{\partial x^2}\,dxdy}{\Sigma h\displaystyle\iint w_1\left(\frac{\partial^2 G_2}{\partial y^2}\cdot\frac{\partial^2 w_1}{\partial x^2} + \frac{\partial^2 G_2}{\partial x^2}\,\frac{\partial^2 w_1}{\partial y^2} - 2\,\frac{\partial^2 G_2}{\partial x\partial y}\,\frac{\partial^2 w_1}{\partial x\partial y}\right)dxdy}$$

and with (4.21)

$$\varphi_2 = \frac{\Sigma h\pi\mu(C - C_{cr})\displaystyle\int f^2 dy}{\Sigma h\displaystyle\iint w_1\left(\frac{\partial^2 G_2}{\partial y^2}\,\frac{\partial^2 w_1}{\partial x^2} + \frac{\partial^2 G_2}{\partial x^2}\,\frac{\partial^2 w_1}{\partial y^2} - 2\,\frac{\partial^2 G_2}{\partial x\partial y}\,\frac{\partial^2 w_1}{\partial x\partial y}\right)dxdy} \tag{B.3}$$

The result (B.3) can also be obtained from (4.26) by following another line. In the form $G_2\Delta\Delta G_2$ is substituted the expression for $\Delta\Delta G_2$ in (2.17)

$$\Sigma\,\frac{h}{E}\iint G_2\Delta\Delta G_2 dxdy = \Sigma h\iint\left\{\left(G_2\,\frac{\partial^2 w_1}{\partial x\partial y}\right)\frac{\partial^2 w_1}{\partial x\partial y} - \tfrac{1}{2}\left(G_2\,\frac{\partial^2 w_1}{\partial x^2}\right)\frac{\partial^2 w_1}{\partial y^2} - \tfrac{1}{2}\left(G_2\,\frac{\partial^2 w_1}{\partial y^2}\right)\frac{\partial^2 w_1}{\partial x^2}\right\}dxdy \tag{B.4}$$

To (B.4) the integration formulas (4.1)...(4.3) are applied. The result is

$$\begin{aligned}
\Sigma\,\frac{h}{E}\iint G_2\Delta\Delta G_2 dxdy = \Sigma h\Bigg[&\iint w_1\left(\frac{\partial G_2}{\partial y}\,\frac{\partial^3 w_1}{\partial x^2\partial y} + G_2\,\frac{\partial^4 w_1}{\partial x^2\partial y^2} + \frac{\partial^2 G_2}{\partial x\partial y}\,\frac{\partial^2 w_1}{\partial x\partial y} + \frac{\partial G_2}{\partial x}\,\frac{\partial^3 w_1}{\partial x\partial y^2}\right)dxdy \\
&- \tfrac{1}{2}\iint w_1\left(\frac{\partial^2 G_2}{\partial y^2}\,\frac{\partial^2 w_1}{\partial x^2} + G_2\,\frac{\partial^4 w_1}{\partial x^2\partial y^2} + 2\,\frac{\partial G_2}{\partial y}\,\frac{\partial^3 w_1}{\partial x^2\partial y}\right)dxdy \\
&- \tfrac{1}{2}\iint w_1\left(\frac{\partial^2 G_2}{\partial x^2}\,\frac{\partial^2 w_1}{\partial y^2} + G_2\,\frac{\partial^4 w_1}{\partial x^2\partial y^2} + 2\,\frac{\partial G_2}{\partial x}\,\frac{\partial^3 w_1}{\partial x\partial y^2}\right)\mathrm{dxdy} \\
&- \tfrac{1}{2}\oint\left\{G_2\,\frac{\partial^2 w_1}{\partial x\partial y}\,\frac{\partial w_1}{\partial x} - w_1\left(\frac{\partial G_2}{\partial x}\,\frac{\partial^2 w_1}{\partial x\partial y} + G_2\,\frac{\partial^3 w_1}{\partial x^2\partial y}\right)\right\}dx \\
&+ \tfrac{1}{2}\oint\left\{G_2\,\frac{\partial^2 w_1}{\partial x^2}\,\frac{\partial w_1}{\partial y} - w_1\left(\frac{\partial G_2}{\partial y}\,\frac{\partial^2 w_1}{\partial x^2} + G_2\,\frac{\partial^3 w_1}{\partial x^2\partial y}\right)\right\}dx\Bigg] = \\
= \Sigma\Bigg[h\iint w_1\Bigg(&\frac{\partial^2 G_2}{\partial x\partial y}\,\frac{\partial^2 w_1}{\partial x\partial y} - \tfrac{1}{2}\,\frac{\partial^2 G_2}{\partial y^2}\,\frac{\partial^2 w_1}{\partial x^2} - \tfrac{1}{2}\,\frac{\partial^2 G_2}{\partial x^2}\,\frac{\partial^2 w_1}{\partial y^2}\Bigg)dxdy \\
+ h\Bigg\{&-\tfrac{1}{2}\oint\left(G_2\,\frac{\partial^2 w_1}{\partial x\partial y}\,\frac{\partial w_1}{\partial x} - w_2\,\frac{\partial G_2}{\partial x}\,\frac{\partial^2 w_1}{\partial x\partial y}\right)dx \\
&+ \tfrac{1}{2}\oint\left(G_2\,\frac{\partial^2 w_1}{\partial x^2}\,\frac{\partial w_1}{\partial y} - w_1\,\frac{\partial G_2}{\partial y}\,\frac{\partial^2 w_1}{\partial x^2}\right)dx\Bigg\}\Bigg].
\end{aligned} \tag{B.5}$$

Now at all corners $G_2 = 0$, $w_1 = 0$. At the free edges $G_2 = 0$. At transitions (fig. 1d) (see (4.6), (4.7), (3.7) and (3.8))

$$\begin{aligned}
h_i\,G_{2i} &= h_j\,G_{2j} \\
h_i\,\frac{\partial G_{2i}}{\partial y_i} &= h_j\,\frac{\partial G_{2j}}{\partial y_j} \\
w_{1i} &= w_{1j} \\
\frac{\partial w_{1i}}{\partial y_i} &= \frac{\partial w_{1j}}{\partial y_j}\,.
\end{aligned} \tag{B.6}$$

From the four contour integrals in (B.5) only the last one remains at free edges, and thus

$$\Sigma \frac{h}{E} \iint G_2 \Delta\Delta G_2 dxdy = \Sigma \left[h \iint w_1 \left(\frac{\partial^2 G_2}{\partial x \partial y} \frac{\partial^2 w_1}{\partial x \partial y} - \tfrac{1}{2} \frac{\partial^2 G_2}{\partial y^2} \frac{\partial^2 w_1}{\partial x^2} - \tfrac{1}{2} \frac{\partial^2 G_2}{\partial x^2} \frac{\partial^2 w_1}{\partial y^2} \right) dxdy \right.$$

$$\left. - \tfrac{1}{2} h \oint w_1 \frac{\partial G_2}{\partial y} \frac{\partial^2 w_1}{\partial^2 x^2} dx \right]. \tag{B.7}$$

For the contour integral in (B.7) holds the equality

$$- \tfrac{1}{2} h \oint w_1 \frac{\partial G_2}{\partial y} \frac{\partial^2 w_1}{\partial x^2} dx = \tfrac{1}{8} E h \mu^4 \oint f^2 \frac{\partial Q}{\partial y} dx. \tag{B.8}$$

The substitution of (B.7) and (B.8) into equation (4.27) delivers

$$U = \Sigma \left[\frac{h}{E} \frac{\pi}{\mu} C^2 b + \varphi^2 h (C - C_{cr}) \pi \mu \int \tfrac{1}{2} f^2 dy \right.$$

$$\left. + \frac{\varphi^4 h}{2} \iint w_1 \left(\frac{\partial^2 G_2}{\partial x \partial y} \frac{\partial^2 w_1}{\partial x \partial y} - \tfrac{1}{2} \frac{\partial^2 G_2}{\partial y^2} \frac{\partial^2 w_1}{\partial x^2} - \tfrac{1}{2} \frac{\partial^2 G_2}{\partial x^2} \frac{\partial^2 w_1}{\partial y^2} \right) dxdy \right]. \tag{B.9}$$

Putting $\dfrac{\partial U}{\partial \varphi} = 0$ gives

$$\Sigma\, 2 \varphi h (C - C_{cr}) \pi \mu \int \tfrac{1}{2} f^2 dy =$$

$$\Sigma \frac{-4 \varphi^3 h}{2} \iint w_0 \left(\frac{\partial^2 G_2}{\partial x \partial y} \frac{\partial^2 w_1}{\partial x \partial y} - \tfrac{1}{2} \frac{\partial^2 G_2}{\partial y^2} \frac{\partial^2 w_1}{\partial x^2} - \tfrac{1}{2} \frac{\partial^2 G_2}{\partial x^2} \frac{\partial^2 w_1}{\partial y^2} \right) dxdy$$

from which is again found

$$\varphi^2 = \frac{\Sigma h \pi \mu (C - C_{cr}) \int f^2 dy}{\Sigma h \iint w_1 \left(\frac{\partial^2 G_2}{\partial y^2} \frac{\partial^2 w_1}{\partial x^2} + \frac{\partial^2 G_2}{\partial x^2} \frac{\partial^2 w_1}{\partial y^2} - 2 \frac{\partial^2 G_2}{\partial x \partial y} \frac{\partial^2 w_1}{\partial x \partial y} \right) dxdy} \tag{B.10}$$

The reason that in the present calculations no use is made of the Galerkin method lies in the fact that the form

$$\iint G_2 \Delta\Delta G_2\, dxdy$$

was easier to integrate numerically than the form

$$\iint w_1 \left(\frac{\partial^2 G_2}{\partial y^2} \frac{\partial^2 w_1}{\partial x^2} + \frac{\partial^2 G_2}{\partial x^2} \frac{\partial^2 w_1}{\partial y^2} - 2 \frac{\partial^2 G_2}{\partial x \partial y} \frac{\partial^2 w_1}{\partial x \partial y} \right) dxdy.$$

TABLE 2.

Functions which refer to the web of the U-section member of section 7.1 and fig. 3.

$\pm\, y_2/a$	f_2/a	f_2^2/a^2	A_2	H_2	$100\, Q_{p,2}/a^4$	$100\, K_{p,2}/a^4$	$100\, Q_2/a^4$	$100\, K_2/a^4$	$100\, A_2Q_2/a^4$	$50\, H_2K_2/a^4$
0.00	−1.26336	1.59608	−15.7527	15.7527	−1.01073	1.71299	−7.00921	1.00862	110.41398	7.94424
0.05	−1.24781	1.55703	−14.9818	15.7527	−0.91138	1.71299	−6.90986	0.99544	103.52214	7.84044
0.10	−1.20153	1.44367	−12.7442	15.7527	−0.61819	1.71299	−6.61667	0.95594	84.32417	7.52933
0.15	−1.12567	1.26713	−9.2593	15.7527	−0.14520	1.71299	−6.14368	0.89032	56.88618	7.01246
0.20	−1.02208	1.04465	−4.8679	15.7527	0.48570	1.71299	−5.51278	0.79920	26.83566	6.29475
0.25	−0.89333	0.79804	0	15.7527	1.24694	1.71299	−4.75154	0.68409	0.0	5.38812
0.30	−0.74259	0.55144	4.8679	15.7527	2.10793	1.71299	−3.89055	0.54817	−18.93881	4.31761
0.35	−0.57355	0.32896	9.2593	15.7527	3.03810	1.71299	−2.96038	0.39744	−27.41105	3.13039
0.40	−0.39040	0.15241	12.7442	15.7527	4.00986	1.71299	−1.98862	0.24240	−25.34337	1.90923
0.45	−0.19763	0.03906	14.9818	15.7527	5.00134	1.71299	−0.99714	0.10056	−14.93895	0.79203
0.50	−0	0	15.7527	15.7527	5.99848	1.71299	0	0	0	0

TABLE 3.

Functions which refer to the flanges of the U-section member of section 7.1 and fig. 3.

$-y_1/b = y_3/b$	$-y_1/a = y_3/a$	$f_1/a = f_3/a$	$f_1^2/a^2 = f_3^2/a^2$	$A_1 = A_3$	$H_1 = H_3$	$100\, Q_{p,1}/a^4 = 100\, Q_{p,3}/a^4$	$100\, K_{p,1}/a^4 = 100\, K_{p,3}/a^4$	$100\, Q_1/a^4 = 100\, Q_3/a^4$	$100\, K_1/a^4 = 100\, K_3/a^4$	$100\, A_1Q_1/a^4 = 100\, A_3Q_3/a^4$	$50\, H_1Q_1/a^4 = 50\, H_3K_3/a^4$
0.00	0	0	0	15.75271	15.7527	0	0	0	0	0	0
0.10	0.035767	0.1418800	0.0201299	15.64957	15.7523	0.00010737	0.00010770	−0.103925	−0.0296810	−1.62638	−0.23377
0.20	0.071534	0.2833010	0.0802594	15.35707	15.7458	0.00171567	0.00173652	−0.206349	−0.0334935	−3.16892	−0.26369
0.30	0.107301	0.4238525	0.1796509	14.92578	15.7173	0.00866705	0.00890494	−0.303431	−0.0239661	−4.52894	−0.18834
0.40	0.143068	0.5632218	0.3172188	14.43968	15.6399	0.02731314	0.02865300	−0.388817	−0.0099452	−5.61439	−0.07777
0.50	0.178835	0.7012450	0.4917445	14.01605	15.4741	0.06644674	0.07157398	−0.453716	+ 0.0026964	−6.35931	+ 0.02086
0.60	0.214602	0.8379596	0.7021762	13.80629	15.1673	0.13722549	0.15259527	−0.486970	+ 0.0105673	−6.72325	+ 0.08014
0.70	0.250369	0.9736619	0.9480175	13.99863	14.6511	0.25310665	0.29204651	−0.475121	+ 0.0124458	−6.65105	+ 0.09117
0.80	0.286136	1.1089678	1.2298095	14.82420	13.8401	0.42981791	0.51706690	−0.402442	+ 0.0091201	−5.96589	+ 0.06311
0.90	0.321903	1.2448796	1.5497253	16.56848	12.6293	0.68539519	0.86341911	−0.250898	+ 0.0033598	−4.15699	+ 0.02122
1.00	0.35767	1.3828608	1.9123040	19.59115	10.8916	1.04032550	1.37779569	0	0	0	0

TABLE 4.

Equations of table 1 for the U-section member of section 7.1 and fig. 3.

Coefficients of the unknowns						known right hand sides	From (...) of table 1
$T_{1,2}$	$aT_{4,2}$	$T_{1,3}$	$aT_{2,3}$	$T_{3,3}$	$aT_{4,3}$		
$\cosh \mu a$	$\frac{1}{2} \sinh \mu a$	0	0	0	0	$-K_{p,2}\left(\frac{a}{2}\right)$	(1)
$2\, \mu a \sinh \mu a$	$\mu a \cosh \mu a + \sinh \mu a$	0	-1	$-2\, \mu a$	0	$-aK'_{p,2}\left(\frac{a}{2}\right) + aK'_{p,3}(0)$	(3)
$4\, \mu^2 a^2 \cosh \mu a$	$2\, \mu^2 a^2 \sinh \mu a + 4\, \mu a \cosh \mu a$	$-4\, \mu^2 a^2$	0	0	$-4\, \mu a$	$-a^2 K''_{p,2}\left(\frac{a}{2}\right) + a^2 K''_{p,3}(0)$	(4)
0	0	1	0	0	0	$-K_{p,3}(0)$	(2)
0	0	$\cosh 2\, \mu b$	$\frac{b}{a} \cosh 2\, \mu b$	$\sinh 2\, \mu b$	$\frac{b}{a} \sinh 2\, \mu b$	$-K_{p,3}(b)$	(1)
0	0	$2\, \mu a \sinh 2\, \mu b$	$2\, \mu b \sinh 2\, \mu b + \cosh 2\, \mu b$	$2\, \mu a \cosh 2\, \mu b$	$2\, \mu b \cosh 2\, \mu b + \sinh 2\, \mu b$	$-aK'_{p,3}(b)$	(7)

Equations with numerical values of the coefficients:

$$
\begin{aligned}
7.87981\, T_{1,2} + 3.90805\, a\, T_{4,2} &= -0.0171299\, a^4 \\
43.0417\, T_{1,2} + 29.5124\, a\, T_{4,2} - aT_{2,3} - 5.50680\, T_{3,3} &= 0 \\
238.954\, T_{1,2} + 205.296\, a\, T_{4,2} - 30.3248\, T_{1,3} - 11.0136\, T_{4,3} &= 0 \\
T_{1,3} &= 0. \\
3.65373\, T_{1,3} + 1.30683\, a\, T_{2,3} + 3.51421\, T_{3,3} + 1.25693\, a\, T_{4,3} &= -0.0137780\, a^4 \\
19.3521\, T_{1,3} + 10.5754\, a\, T_{2,3} + 20.1203\, T_{3,3} + 10.7106\, a\, T_{4,3} &= -0.172573\, a^4
\end{aligned}
$$

Solutions

$T_{1,2} = -0.00704369\, a^4$ $\quad T_{1,3} = 0$ $\quad T_{3,3} = +0.00930013\, a^4$

$T_{4,2} = +0.00981898\, a^3$ $\quad T_{2,3} = -0.0646051\, a^3$ $\quad T_{4,3} = +0.030206\, a^3$

TABLE 5.

Equations of table 1 for the plate with one hinge and one end free of section 7.2.3.

Coefficients of the unknowns				known right hand sides	From (...) of table 1
T_1	bT_2	T_3	bT_4		
1	0	0	0	$-K_p$	(1)
0	1	$2\,\mu b$	0	0	(7)
$\cosh 2\,\mu b$	$\cosh 2\,\mu b$	$\sinh 2\,\mu b$	$\sinh 2\,\mu b$	$-K_p$	(1)
$2\,\mu b \sinh 2\,\mu b$	$2\,\mu b \sinh 2\,\mu b + \cosh 2\,\mu b$	$2\,\mu b \cosh 2\,\mu b$	$2\,\mu b \cosh 2\,\mu b + \sinh 2\,\mu b$	0	(7)

With $\mu = 0.98481/b$

$$
\begin{aligned}
T_1 \qquad\qquad\qquad\qquad\qquad\qquad\qquad\qquad\qquad &= -0.066449\,b^4 \\
bT_2 + 1.96960\,T_3 \qquad\qquad\qquad &= 0 \\
3.65366\,T_1 + 3.65366\,bT_2 + 3.51415\,T_3 + 3.51415\,bT_4 &= -0.066449\,b^4 \\
6.92147\,T_1 + 10.5751\,bT_2 + 7.19625\,T_3 + 10.7104\,bT_4 &= 0
\end{aligned}
$$

The solutions are

$$
\begin{aligned}
T_1 &= -0.066449\,b^4 \\
T_2 &= -0.063333\,b^3 \\
T_3 &= 0.032155\,b^4 \\
T_4 &= 0.083870\,b^3
\end{aligned}
$$